



**HAL**  
open science

**Caractérisation de TgZFP2, une nouvelle protéine à motif en doigt de zinc impliquée dans la coordination de la progression du cycle cellulaire du parasite apicomplexe *Toxoplasma gondii***

Ksenia Semenovskaya

► **To cite this version:**

Ksenia Semenovskaya. Caractérisation de TgZFP2, une nouvelle protéine à motif en doigt de zinc impliquée dans la coordination de la progression du cycle cellulaire du parasite apicomplexe *Toxoplasma gondii*. Agricultural sciences. Université Montpellier, 2019. English. NNT : 2019MONTT063 . tel-02650632

**HAL Id: tel-02650632**

**<https://theses.hal.science/tel-02650632>**

Submitted on 29 May 2020

**HAL** is a multi-disciplinary open access archive for the deposit and dissemination of scientific research documents, whether they are published or not. The documents may come from teaching and research institutions in France or abroad, or from public or private research centers.

L'archive ouverte pluridisciplinaire **HAL**, est destinée au dépôt et à la diffusion de documents scientifiques de niveau recherche, publiés ou non, émanant des établissements d'enseignement et de recherche français ou étrangers, des laboratoires publics ou privés.

# THÈSE POUR OBTENIR LE GRADE DE DOCTEUR DE L'UNIVERSITÉ DE MONTPELLIER

En Biologie cellulaire et moléculaire

École doctorale Sciences Chimiques et Biologiques pour la Santé (CBS2)

Unité de recherche UMR 5235 CNRS – LPHI  
Laboratory of Pathogen-Host Interactions

Characterisation of TgZFP2, a novel zinc finger protein  
involved in the coordination of cell cycle progression  
in the apicomplexan parasite *Toxoplasma gondii*

Présentée par Ksenia SEMENOVSKAYA  
Le 13 décembre 2019

Sous la direction de Sébastien BESTEIRO

Devant le jury composé de

Mme Mélanie BONHIVERS, DR2 – CNRS, Université de Bordeaux, France

M. Cyrille BOTTÉ, DR2 - CNRS, Université de Grenoble, France

Mme Catherine BRAUN-BRETON, PR – UM, Université de Montpellier, France

M. Sébastien BESTEIRO, CR – Inserm, Université de Montpellier, France

Rapporteur

Rapporteur

Examineur, Président du jury

Directeur de thèse



UNIVERSITÉ  
DE MONTPELLIER

## Summary

The phylum Apicomplexa encompasses parasitic protists with a complex life cycle that alternates between sexual and asexual replication in different hosts. Apicomplexa are obligate intracellular parasites that display a peculiar organisation of their cell cycle. It consists of a nuclear phase (DNA replication) and a budding phase (daughter cells assembly) that can be uncoupled or coordinated differently, resulting in four distinctive modes of division in the phylum. The simplest of them, endodyogeny, is characteristic for the rapidly proliferating tachyzoite asexual stage of *Toxoplasma gondii* and comprises a single round of DNA replication and subsequent formation of two daughter cells within the mother cell. The regulatory system of endodyogeny is suggested to be physically linked to the parasite's unusual bipartite centrosome, but remains largely unexplored. During this research project I characterized a novel *T. gondii* zinc finger protein named TgZFP2, whose knockdown led to a striking arrest of the parasite cell cycle. While DNA replication proceeded as normally, the budding was affected, resulting in appearance of immature daughters that failed to emerge from the mother cell and often failed to incorporate nuclear material. We have shown that, at the onset of daughter cells assembly, TgZFP2 re-localises from cytoplasmic puncta to the peri-centrosomal region where it persists until the completion of division. TgZFP2 also behaves as a cytoskeleton-associated protein. Though we were unable to identify TgZFP2 molecular partners to decipher the precise molecular mechanisms it is involved in, our data show TgZFP2 is an important regulator of the cell cycle that may have a pleotropic function.

**Key words:** Apicomplexa, cell division, centrosome, *Toxoplasma gondii*, zinc finger protein

## Résumé

Le phylum des Apicomplexes regroupe des parasites protozoaires avec un cycle de vie complexe alternant des réplifications sexuée et asexuée chez différents hôtes. Ce sont des parasites intracellulaires obligatoires qui ont une l'organisation particulière de leur cycle cellulaire. Celui-ci consiste en une phase nucléaire (la répllication de l'ADN) et en une phase de bourgeonnement (l'assemblage des cellules filles) qui peuvent être découplées ou coordonnées différemment, générant quatre modes de division distincts au sein du phylum. Le plus simple d'entre eux, l'endodyogénie, est caractéristique de la forme tachyzoite de *Toxoplasma gondii*, un stade asexué et fortement prolifératif. Lors de ce type de division, il y a un seul tour de répllication de l'ADN avec une formation ultérieure de deux cellules filles dans la cellule mère. Le système de régulation de l'endodyogénie est physiquement lié à un centrosome atypique biparti, cependant il reste largement inexploré. Lors de ce projet de recherche, j'ai caractérisé chez *T. gondii* une nouvelle protéine à motif en doigt de zinc appelée TgZFP2. Interférer avec sa fonction résulte en l'arrêt du cycle cellulaire du parasite. Bien que la répllication de l'ADN se déroule normalement, le bourgeonnement des cellules filles est impacté, donnant naissance à des cellules filles immatures qui ne peuvent pas émerger de la cellule mère et ne parviennent souvent pas à incorporer le matériel nucléaire. Nous avons montré qu'au début de l'assemblage des cellules filles, la protéine TgZFP2 se re-localise depuis des puncta cytoplasmiques vers la région péri-centrosomale, où elle persiste jusqu'à l'achèvement de la division et l'émergence des cellules filles. TgZFP2 présente également des propriétés de protéine associée au cytosquelette. Bien que nous n'ayons pas été en mesure d'identifier les partenaires moléculaires de TgZFP2 pour identifier les mécanismes moléculaires dans lesquels elle est impliquée, nos données montrent que TgZFP2 est un régulateur important de la division cellulaire, potentiellement avec des fonctions multiples.

**Mots-clés:** Apicomplexes, division cellulaire, centrosome, *Toxoplasma gondii*, protéine à doigt de zinc

# **Caractérisation de TgZFP2, une nouvelle protéine à motif en doigt de zinc impliquée dans la coordination de la progression du cycle cellulaire du parasite apicomplexe *Toxoplasma gondii***

Le phylum eucaryote des Apicomplexa comprend plus de 6000 espèces de protozoaires<sup>1</sup> qui sont principalement des parasites. La plupart ont des caractéristiques morphologiques remarquables communes, telles que la présence d'un plaste non photosynthétique appelé apicoplaste et des structures spécialisées occupant la partie antérieure des parasites appelées complexe apical<sup>2</sup>. Beaucoup de ces parasites sont des pathogènes d'importance médicale et vétérinaire. Ils ont un cycle de vie complexe alternant entre une phase de réplication sexuée chez les hôtes définitifs et une phase de réplication asexuée chez des hôtes intermédiaires<sup>3</sup>. L'un des parasites les plus étudiés du phylum, *Toxoplasma gondii*, est l'agent étiologique de la toxoplasmose<sup>4</sup> et peut infecter plus de 350 espèces d'oiseaux et de mammifères, dont les humains<sup>5</sup>. Aujourd'hui, on estime qu'au moins 30% de la population mondiale est infectée par *T. gondii*, ce qui en fait l'un des parasites humains les plus répandus<sup>6</sup>.

Les hôtes définitifs de *T. gondii* sont les félinés (notamment les chats domestiques et sauvages) et le cycle de vie complet de ce parasite se base sur une relation proie-prédateur<sup>7</sup> : la réplication sexuée des parasites se déroule chez des félinés ayant mangé une proie infectée (hôte intermédiaire), entraînant la formation d'oocystes qui sont par la suite excrétés par le féliné dans l'environnement d'où ils peuvent ensuite contaminer d'autres hôtes intermédiaires et perpétuer le cycle<sup>8</sup>. Chez les hôtes intermédiaires ayant ingéré des oocystes infectieux le parasite se multiplie de façon asexuée<sup>5</sup>.

Les humains peuvent notamment être des hôtes intermédiaires pour *T. gondii* et peuvent être infectés par l'une des formes asexuées du parasite : tachyzoïtes à division rapide, bradyzoïtes à division lente contenus dans des kystes tissulaires, ou sporozoïtes contenus dans les oocystes. Une fois dans l'organisme, les bradyzoïtes et les sporozoïtes se transforment en tachyzoïtes ; la prolifération de tachyzoïtes dans différents tissus est responsable des manifestations cliniques de la toxoplasmose<sup>5</sup>. La principale source d'infection par *T. gondii* chez les humains est la transmission alimentaire de bradyzoïtes ou de sporozoïtes<sup>9</sup>.

La transmission verticale du parasite se produit par le passage des tachyzoïtes à travers le placenta d'une mère primo-infectée à un fœtus pendant la grossesse<sup>5</sup>. Chez les personnes immunocompétentes, la toxoplasmose est généralement asymptomatique ou entraîne l'apparition de symptômes pseudo-grippaux non spécifiques qui nécessitent rarement un traitement<sup>6</sup>. Cependant, chez les patients immunodéprimés (par exemple, chez les personnes atteintes du VIH) ou lors de la forme congénitale de la maladie, *T. gondii* peut entraîner des symptômes graves pouvant même entraîner la mort<sup>10,11</sup>.

Pour plusieurs raisons (facilité de manipulations génétiques, propagation *in vitro* rapide,...), le stade tachyzoïte de *T. gondii* est largement utilisé en tant que modèle pour étudier la biologie des parasites apicomplexes<sup>12</sup>. Les tachyzoïtes sont des cellules polarisées en forme de croissant d'environ 6 µm de long et 2 µm de large<sup>13</sup>. Un tachyzoïte possède plusieurs organites typiques des cellules eucaryotes (noyaux, réticulum endoplasmique, appareil de Golgi, mitochondrie,...), tandis que d'autres sont spécifiques des apicomplexes. Ce deuxième groupe comprend les organites de sécrétion (notamment impliqués dans les processus d'attachement et d'invasion des cellules hôtes), l'apicoplaste d'origine endosymbiotique (impliqué dans des voies métaboliques importantes du parasite) et des structures du cytosquelette uniques<sup>13</sup>. Ces dernières comprennent une pellicule tri-membranaire qui couvre la surface de la cellule, ainsi que des éléments situés dans la partie apicale du parasite et contribuant au processus d'invasion. La pellicule est composée de la membrane plasmique et d'un complexe sous-jacent de vésicules aplaties avec leur maillage protéique associé - le complexe membranaire interne (IMC)<sup>14</sup>. L'IMC s'étend sur presque toute la longueur de la tachyzoïte à l'exception des extrémités apicale et basale du parasite<sup>15</sup>. La face cytoplasmique de l'IMC s'associe à des microtubules sous-pelliculaires (MTs) qui s'étendent sur les deux tiers de la longueur du parasite<sup>16</sup>. La pellicule maintient la forme, la polarité et la stabilité structurelle des tachyzoïtes, soutient la motilité des parasites extracellulaires à l'aide du moteur actine-myosine<sup>17</sup>, et joue un rôle important dans l'assemblage des cellules filles pendant la division<sup>18</sup>.

Les tachyzoïtes sont capables d'envahir pratiquement tous les types de cellules nucléées et prolifèrent à l'intérieur d'une vacuole parasitophore. Après plusieurs cycles de division, les tachyzoïtes peuvent sortir activement (egress) de la cellule hôte, qui se rompt, afin d'envahir d'autres cellules hôtes situées à proximité. Ce processus répétitif composé de

3 étapes (invasion, réplication intracellulaire et egress) est connu sous le nom de cycle lytique et permet au parasite de se propager dans des tissus de l'hôte<sup>19</sup>.

La réplication intracellulaire des tachyzoïtes se fait par un mode de division particulier appelé endodyogénie. Ce processus hautement coordonné comprend un cycle de réplication de l'ADN suivi d'une mitose se produisant simultanément avec l'assemblage des cellules filles par bourgeonnement interne<sup>20-22</sup>. C'est le mode de division le plus simple parmi ceux utilisés par les apicomplexes et peut potentiellement servir de modèle pour étudier les trois autres modes de division utilisés par les parasites du phylum<sup>23</sup>. L'organisation spécifique du cycle cellulaire est supposée contribuer à ce phénomène. Ainsi, tous les événements qui se produisent au cours d'une division d'un parasite apicomplexe peuvent être regroupés conceptuellement en deux étapes principales : la phase nucléaire (cycles successifs de réplication de l'ADN et de mitose) et la phase de bourgeonnement (élongation des cellules filles et cytokinèse). Selon les apicomplexes ou les stades de développement parasitaire, elles sont facilement découplées et peuvent être organisées différemment, permettant aux parasites de produire une progéniture en nombre et type appropriés<sup>23,24</sup>.

Le cycle cellulaire des tachyzoïtes de *T. gondii* est limité à une seule phase de croissance et à une seule phase de bourgeonnement, ce qui entraîne la formation de deux cellules filles. Les phases G1 et S du cycle occupent respectivement ≈60% et ≈30% du temps d'un cycle de division (qui dure entre 6 et 8 heures au total), et sont suivies d'une phase M rapide<sup>25</sup>. Typiquement pour les apicomplexes, les tachyzoïtes de *T. gondii* subissent une mitose fermée, lors de laquelle l'enveloppe nucléaire reste pratiquement intacte et le fuseau mitotique y est intégré dans une invagination dédiée appelée le centrocone<sup>22,26,27</sup>. Les chromosomes sont ancrés à la membrane nucléaire dans la région du centrocone, et la connexion entre les chromosomes et le fuseau mitotique est soutenu par les protéines du kinétochore.

La cytokinèse est amorcée à la fin de la phase S et chevauche donc la phase de réplication de l'ADN<sup>25,28</sup>. Au cours de l'endodyogénie, certains organites maternels sont dupliqués et ségrégués dans les cellules filles (p. ex. apicoplaste ou appareil de Golgi), tandis que d'autres sont synthétisés *de novo* (comme les organites de sécrétion ou des éléments du cytosquelette). La duplication des organites est strictement coordonnée avec les dynamiques du centrosome et se déroule dans un ordre invariable : centriole et appareil de Golgi en

premier, apicoplaste en second, noyau et ER en troisième, mitochondrie en quatrième ; les organites de sécrétion sont néosynthétisés. L'assemblage des cytosquelettes des cellules filles est étroitement lié à la dynamique des organelles et dirige la formation des cellules filles<sup>18,29</sup>. Lors de l'émergence de la cellule mère, les filles presque complètes recyclent en partie l'IMC maternelle et terminent leur maturation 2h post-division<sup>30</sup>.

L'endodyogénie est régulée par un mécanisme complexe de facteurs globaux et locaux<sup>23</sup>. Comme pour d'autres eucaryotes, la progression du cycle cellulaire de *T. gondii* est contrôlée à des moments spécifiques du cycle. *T. gondii* conserve 3 points de contrôle typiques chez eucaryotes : la transition G1/S (ou contrôle de l'entrée en phase S), ii) la transition G2/M (contrôle de l'entrée en mitose), et iii) un point de contrôle lié au fuseau mitotique en phase M, empêchant une ségrégation prématurée des chromosomes<sup>31-33</sup>. De plus, *T. gondii* a acquis 2 autres points de contrôle liés au maintien de la structure stœchiométrique d'un centrosome bipartite particulier et à l'assemblage des cellules filles<sup>33</sup>. La progression du cycle cellulaire est très probablement régulée par l'activité des kinases dépendantes de cyclines (CDKs) et donc de leurs partenaires moléculaires, les cyclines<sup>33,34</sup>.

Le centrosome est le coordinateur principal de la progression du cycle cellulaire de *T. gondii*. Il conserve le rôle classique qu'il a chez les eucaryotes, consistant en la formation du fuseau mitotique, mais a acquis également des fonctions supplémentaires liées à l'endodyogénie. Ainsi, il sert aussi de centre organisateur pour l'assemblage des cytosquelettes filles et coordonne la ségrégation des organelles dans les cellules filles<sup>18,35</sup>. Comparativement au centrosome de mammifères, la composition protéique cette structure cellulaire est très probablement différente chez *T. gondii*, bien que sa caractérisation moléculaire n'a commencé à émerger que récemment<sup>36</sup>. Cependant, les études récentes suggèrent que le centrosome de *T. gondii* est composé de deux complexes principaux distincts sur le plan fonctionnel et moléculaire, qui se répliquent séparément<sup>37</sup>. En utilisant des mutants conditionnels, il a été montré que le complexe interne du centrosome contrôle la phase nucléaire du cycle, tandis que le complexe externe régule le processus d'assemblage des cellules filles. Des approches génétiques et des mutants spécifiques ont montré qu'étonnamment, les deux complexes peuvent fonctionner de façon indépendante, car la déconnexion des complexes n'affecte pas leur fonctionnalité<sup>37-39</sup>. En fait c'est en accord avec des études antérieures qui ont démontré, en utilisant des approches pharmaceutiques,

que la réplication de l'ADN et la formation des filles chez *T. gondii* peuvent être facilement découplés. Cela expliquerait comment *T. gondii* pourrait contrôler la flexibilité du cycle cellulaire, une caractéristique des parasites apicomplexes<sup>40,41</sup>.

L'objectif principal de mon travail de thèse était de caractériser une nouvelle protéine de *T. gondii*, précédemment identifiée dans notre laboratoire lors d'une étude protéomique. Cette protéine (www.Toxodb.org numéro d'accès : TGME49\_212260) avait pour seul motif connu un domaine à doigt de zinc annoté qui est notamment également retrouvé dans un autoantigène humain appelé p27 (PFAM PF06677 (<http://pfam.xfam.org/>)). Le domaine en doigt de zinc est, typiquement, une petite sous-unité protéique fonctionnelle pliée indépendamment; sa structure est maintenue par un ion zinc, chélatée par des résidus cystéine (Cys) et d'histidine (His) en positions définies<sup>42,43</sup>. Les liaisons avec l'ion zinc fournissent la structuration stable et permettent d'exposer une boucle d'acides aminés qui peut s'engager dans des interactions intermoléculaires, surtout avec les acides nucléiques (ADN et ARN)<sup>42,44,45</sup>, mais aussi d'autres protéines et des lipides<sup>46-48</sup>. Bien que les protéines à doigt de zinc soient largement répandues et bien caractérisées dans le royaume eucaryote, chez *T. gondii* seulement quelques-unes ont été caractérisées fonctionnellement<sup>49-53</sup>.

La protéine identifiée a été appelée TgZFP2 (pour 'Zinc Finger Protein 2'). Un mutant conditionnel a été généré et, de façon intéressante, la déplétion spécifique de la protéine a montré que TgZFP2 est essentielle à la croissance du parasite : plus précisément, montrait des problèmes de réplication. Par conséquent, l'objectif principal de mon projet de thèse était d'élucider la contribution de TgZFP2 au processus de division cellulaire chez *T. gondii*. Pour atteindre cet objectif, nous avons utilisé plusieurs approches.

Premièrement, nous avons combiné l'utilisation de lignées cellulaires transgéniques et de techniques d'imagerie afin d'élargir la caractérisation du phénotype mutant de TgZFP2 dans les tachyzoïtes. Le mutant conditionnel de TgZFP2 a été complémenté par une version sauvage de TgZFP2 ou celle mutée dans le domaine en doigt de zinc. Par immunofluorescence (IF) l'utilisation de marqueurs du cycle cellulaire a montré que contrairement aux parasites exprimant la copie sauvage de TgZFP2 pour lesquels la formation de cellules filles est parfaitement synchronisée au sein de la même vacuole, lors de la déplétion de TgZFP2, ou de la complémentation d'une version mutée de TgZFP2, la division cellulaire est asynchrone et désordonnée. Les principaux défauts étaient l'initiation multiples de bourgeons internes et

l'émergence de cellules filles incomplètes de leur cellule mère. La réplication de l'ADN n'est par contre pas inhibée en absence de TgZFP2, car le marquage de l'ADN et l'analyse en cytométrie de flux ou par IF a révélé la présence de noyaux multilobés et volumineux chez les parasites. Cependant, la partition des noyaux dans les cellules filles en développement semble être affectée, ce qui a été confirmé par des observations morphologiques en microscopie électronique (ME).

Nous avons étiqueté TgZFP2 afin de pouvoir la localiser par IF. De façon importante, nous avons ainsi pu remarquer que TgZFP2 a une localisation dynamique au cours du cycle cellulaire. Dans les parasites en interphase, TgZFP2 est répartie sous forme de puncta cytoplasmiques. Pendant la division, au début de l'assemblage des cellules filles, TgZFP2 se relocalise dans la région péri-centrosomale et y persiste jusqu'à la fin du processus. Nous avons donc évalué l'impact de la perte de la protéine sur le centrosome : sur son complexe externe (donc le régulateur de la formation des cellules filles) et sur les éléments du pôle fuseau du parasite (protéines du kinétochore et du fuseau mitotique). A l'aide de marqueurs spécifiques de ces compartiments, par IF nous avons obtenu la preuve que la déplétion de TgZFP2 n'affecte pas la duplication du centrosome (car les parasites mutants contiennent un nombre accru de complexes externes et de kinétochores par cellule), ni son association avec les structures mitotiques. Ceci a également été illustré par l'observation ME de parasites n'exprimant plus TgZFP2. Ces parasites présentaient des centrocones/pôles de fuseau normaux, correctement positionnés et associés au centrosome. De plus, la déplétion de TgZFP2 n'a pas causé d'effondrement majeur des microtubules du fuseau mitotique. Enfin, comme le centrosome des tachyzoïtes est responsable du partitionnement de certains organites autres que noyau dans les cellules filles, nous avons par exemple cherché à savoir si l'apicoplaste était correctement ségrégué lors de division. Selon nos résultats, l'apicoplaste était souvent présent et associé au centrosome dans les cellules filles incomplètes émergentes, mais on le trouvait généralement non ségrégué et loin des bourgeons internes dans les cellules syncytiales au phénotype plus prononcé. D'une façon générale, nos données montrent que les parasites n'exprimant plus TgZFP2 n'ont pas de défaut majeur dans la réplication de l'ADN et dans l'initiation de l'assemblage des filles, mais les stades finaux de la mitose sont altérés. Il est intéressant de noter que TgZFP2 présente des propriétés de protéines associées au cytosquelette, ce qui nous a incités à étudier si le cytosquelette des

parasites mutants est affecté par la perte de la protéine. En utilisant les marquages spécifiques de l'IMC et des microtubules par IF, nous avons découvert que la déplétion de TgZFP2 ne cause pas de perturbation majeure du cytosquelette des cellules filles en élongation.

Un domaine en doigt de zinc permet potentiellement à une protéine d'interagir avec plusieurs types de molécules (protéines, acides nucléiques, lipides) et nous avons montré que le domaine Cys<sub>2</sub>-Cys<sup>2</sup> en doigt de zinc est essentiel à la fonction de TgZFP2. Nous supposons donc que des interactions avec d'autres molécules sont cruciales pour le rôle de TgZFP2 dans la coordination de la progression du cycle cellulaire chez les tachyzoïtes. Comme l'analyse phénotypique détaillée n'a pas révélé la fonction moléculaire de TgZFP2, nous avons pensé à découvrir les voies moléculaires dans lesquelles elle est impliquée en identifiant des partenaires interagissant avec elle. Nous pensons que TgZFP2 est moins susceptible d'interagir avec des lipides (car nos expériences d'extraction avec des détergents montrent qu'elle ne s'associe probablement pas aux membranes), ou avec l'ADN (car TgZFP2 semble être exclue du noyau).

Nous avons donc dans un premier temps cherché à identifier des partenaires protéiques. Nous avons appliqué une stratégie d'identification de partenaires protéiques par co-immunoprécipitation couplée à une identification par spectrométrie de masse, réalisée en collaboration avec la plate-forme de protéomique fonctionnelle de Montpellier (<https://www.fpp.cnrs.fr/fr/>). L'expérience a été réalisée deux fois sur des cultures indépendantes et les données des deux séries d'expériences ont été analysées.

Parmi les protéines enrichies dans l'appât par rapport au contrôle et communes aux deux expériences, plusieurs dizaines de candidats ont été identifiés. Nous avons sélectionné en priorité les candidats en fonction de leur annotation et de leur relation possible avec le phénotype du mutant TgZFP2. Nous avons donc étudié des protéines impliquées dans la régulation du cycle cellulaire (comme des kinases ou des cyclines), ou des protéines liées au cytosquelette des parasites.

Nous avons notamment sélectionné une protéine kinase associée au cycle cellulaire (GSK-like, glycogen synthase kinase TGGT1\_265330) et une protéine homologue à la cycline2 (TGGT1\_267580). Pour évaluer l'interaction potentielle des candidats sélectionnés avec TgZFP2, nous avons ajouté une étiquette avec un triple épitope *myc* à chacun de ces candidats

dans le contexte de la souche exprimant déjà TgZFP2 étiquetée et avons procédé à des expériences de co-localisation et de co-immunoprécipitation. Cependant, ces expériences n'ont pas confirmé d'interaction entre TgZFP2 et TgCyclin2 ou TgGSK. Nous avons également étudié un complexe de chaperones dont la fonction est liée au cytosquelette, TgCCT, dont les 8 sous unités ont été retrouvées dans nos analyses protéomiques. Dans les cellules mammifères ce complexe de chaperones est indispensable pour la structuration correcte de l'actine et de la tubuline<sup>54</sup>. De la même manière que pour les candidats liés au cycle cellulaire, nous avons étiqueté 3 sous-unités du complexe (TgCCT1, TgCCT2 et TgCCT5) et avons procédé à des expériences de co-localisation et de co-immunoprécipitation. Encore une fois, nous n'avons pas été en mesure de confirmer une interaction entre TgZFP2 et les sous-unités de TgCCT sélectionnées. Nous avons tenté plusieurs autres approches pour étudier les interactions potentielles entre TgZFP2 et TgCCT. Cependant, une stratégie de double-hybride bactérien (BACTH) n'a pas donné de résultats concluants, tandis que nos tentatives de générer un mutant conditionnel de TgCCT et de comparer le phénotype résultant avec le phénotype de mutant conditionnel de TgZFP2 ont échoué en raison de difficultés techniques.

J'ai également exploré la possibilité que TgZFP2 soit une protéine interagissant avec de l'ARN. Tout d'abord, en utilisant l'approche d'IF, nous avons vérifié si TgZFP2 pouvait être associé aux granules de stress (GS) - un compartiment cellulaire non-membranaire se formant en condition de stress et contenant des ARN non traduits ainsi que des protéines spécifiquement associées<sup>55</sup>. Bien que TgZFP2 semble se relocaliser dans des structures pouvant ressembler à des GS dans les conditions de stress, la nature de ces agrégats n'a pas été confirmée par l'utilisation de marqueurs des GS. J'ai également essayé une stratégie de co-immunoprécipitation TgZFP2/ARN et d'identification des partenaires RNA par séquençage (analyse RIP-seq). Malheureusement, aucun ARN potentiel n'a été identifié par cette approche. En conclusion, nous n'avons obtenu aucune évidence que TgZFP2 peut interagir avec des ARN.

Parmi les autres difficultés rencontrées lors de ce projet de thèse, je n'ai pu réussir à obtenir une version recombinante de la protéine TgZFP2. Avec cette protéine recombinante, nous voulions générer un outil permettant d'étudier les interactions potentielles de la protéine TgZFP2 et d'évaluer la liaison de la protéine avec du zinc. Malgré des multiples

conditions expérimentales que j'ai essayées, la protéine s'est avérée essentiellement insoluble et pas assez pure pour être utilisée dans les essais suivants.

Dans l'ensemble, nos données montrent que TgZFP2 est une protéine essentielle à la progression du cycle cellulaire de *T. gondii* avec potentiellement, des fonctions multiples. Recrutée dynamiquement dans la région péri-centrosomale au cours de l'endodyogénie, cette protéine n'est apparemment pas impliquée dans la duplication des centrosomes ou dans la maintenance structurelle de l'organite, mais a pourtant un rôle crucial de coordination entre la mitose et la biogenèse de cellules filles. En l'absence de TgZFP2, l'émergence et la genèse de cellules filles est bloquée prématurément, alors que de nouveaux cycles de mitose sont réinitiés de façon incontrôlée. Je n'ai malheureusement pas pu déterminer le mécanisme d'action de TgZFP2 au niveau moléculaire, mais ces travaux révèlent qu'il reste encore beaucoup de choses à découvrir sur les protéines associées au centrosome, dont certaines sont potentiellement des acteurs majeurs du contrôle de la prolifération parasitaire.

#### Références :

1. Adl, S. M. *et al.* Diversity, Nomenclature, and Taxonomy of Protists. *Systematic Biology* **56**, 684–689 (2007).
2. Walker, G., Dorrell, R. G., Schlacht, A. & Dacks, J. B. Eukaryotic systematics: a user's guide for cell biologists and parasitologists. *Parasitology* **138**, 1638–1663 (2011).
3. Votýpka, J., Modrý, D., Oborník, M., Šlapeta, J. & Lukeš, J. Apicomplexa. in *Handbook of the Protists* (eds. Archibald, J. M. et al.) 1–58 (Springer International Publishing, 2016).
4. Dardé, M. L., Ajzenberg, D. & Smith, J. Population Structure and Epidemiology of *Toxoplasma gondii*. in *Toxoplasma Gondii* 49–80 (Elsevier, 2007).
5. Robert-Gangneux, F. & Darde, M.-L. Epidemiology of and Diagnostic Strategies for Toxoplasmosis. *Clinical Microbiology Reviews* **25**, 264–296 (2012).
6. Montoya, J. & Liesenfeld, O. Toxoplasmosis. *The Lancet* **363**, 1965–1976 (2004).
7. Tenter AM, Heckeroth AR, Weiss LM. *Toxoplasma gondii*: from animals to humans. *Int J Parasitol*, **30** (12-13) :1217-58 (2000).
8. Gilot-Fromont, E. *et al.* The Life Cycle of *Toxoplasma gondii* in the Natural Environment. in *Toxoplasmosis - Recent Advances* (ed. Djurkovi Djakovi, O.) (InTech, 2012).
9. Jones, J. L. & Dubey, J. P. Foodborne Toxoplasmosis. *Clinical Infectious Diseases* **55**, 845–851 (2012).
10. Hill, D. E., Chirukandoth, S. & Dubey, J. P. Biology and epidemiology of *Toxoplasma gondii* in man and animals. *Anim Health Res Rev* **6**, 41–61 (2005).

11. McAuley, J. B. Congenital Toxoplasmosis. *Journal of the Pediatric Infectious Diseases Society* **3**, S30–S35 (2014).
12. Kim, K. & Weiss, L. M. Toxoplasma gondii: the model apicomplexan. *International Journal for Parasitology* **34**, 423–432 (2004).
13. Dubey, J. P., Lindsay, D. S. & Speer, C. A. Structures of Toxoplasma gondii tachyzoites, bradyzoites, and sporozoites and biology and development of tissue cysts. *Clin. Microbiol. Rev.* **11**, 267–299 (1998).
14. Morrissette, N. S. & Sibley, L. D. Cytoskeleton of Apicomplexan Parasites. *Microbiology and Molecular Biology Reviews* **66**, 21–38 (2002).
15. Porchet, E. & Torpier, G. [Freeze fracture study of Toxoplasma and Sarcocystis infective stages (author's transl)]. *Z Parasitenkd* **54**, 101–124 (1977).
16. Morrissette, N. S., Murray, J. M. & Roos, D. S. Subpellicular microtubules associate with an intramembranous particle lattice in the protozoan parasite Toxoplasma gondii. *J. Cell. Sci.* **110 ( Pt 1)**, 35–42 (1997).
17. Keeley, A. & Soldati, D. The glideosome: a molecular machine powering motility and host-cell invasion by Apicomplexa. *Trends in Cell Biology* **14**, 528–532 (2004).
18. Anderson-White, B. *et al.* Cytoskeleton Assembly in Toxoplasma gondii Cell Division. in *International Review of Cell and Molecular Biology* **298**, 1–31 (Elsevier, 2012).
19. Black, M. W. & Boothroyd, J. C. Lytic Cycle of Toxoplasma gondii. *Microbiology and Molecular Biology Reviews* **64**, 607–623 (2000).
20. Goldman, M., Carver, R. K. & Sulzer, A. J. Reproduction of Toxoplasma gondii by internal budding. *J. Parasitol.* **44**, 161–171 (1958).
21. Ogino, N. & Yoneda, C. The Fine Structure and Mode of Division of Toxoplasma gondii. *Archives of Ophthalmology* **75**, 218–227 (1966).
22. Sheffield, H. G. & Melton, M. L. The Fine Structure and Reproduction of Toxoplasma gondii. *The Journal of Parasitology* **54**, 209 (1968).
23. Francia, M. E. & Striepen, B. Cell division in apicomplexan parasites. *Nature Reviews Microbiology* **12**, 125–136 (2014).
24. Striepen, B., Jordan, C. N., Reiff, S. & van Dooren, G. G. Building the Perfect Parasite: Cell Division in Apicomplexa. *PLoS Pathog* **3**, e78 (2007).
25. Radke, J. R. *et al.* Defining the cell cycle for the tachyzoite stage of Toxoplasma gondii. *Mol. Biochem. Parasitol.* **115**, 165–175 (2001).
26. Dubremetz, J. F. [Genesis of merozoites in the coccidia, Eimeria necatrix. Ultrastructural study]. *J. Protozool.* **22**, 71–84 (1975).
27. Gubbels, M.-J. A MORN-repeat protein is a dynamic component of the Toxoplasma gondii cell division apparatus. *Journal of Cell Science* **119**, 2236–2245 (2006).
28. Radke, J. R. & White, M. W. A cell cycle model for the tachyzoite of Toxoplasma gondii using the Herpes simplex virus thymidine kinase. *Mol. Biochem. Parasitol.* **94**, 237–247 (1998).

29. Nishi, M., Hu, K., Murray, J. M. & Roos, D. S. Organellar dynamics during the cell cycle of *Toxoplasma gondii*. *Journal of Cell Science* **121**, 1559–1568 (2008).
30. Ouologuem, D. T. & Roos, D. S. Dynamics of the *Toxoplasma gondii* inner membrane complex. *Journal of Cell Science* **127**, 3320–3330 (2014).
31. Harashima, H., Dissmeyer, N. & Schnittger, A. Cell cycle control across the eukaryotic kingdom. *Trends in Cell Biology* **23**, 345–356 (2013).
32. Vleugel, M., Hoogendoorn, E., Snel, B. & Kops, G. J. P. L. Evolution and Function of the Mitotic Checkpoint. *Developmental Cell* **23**, 239–250 (2012).
33. Alvarez, C. A. & Suvorova, E. S. Checkpoints of apicomplexan cell division identified in *Toxoplasma gondii*. *PLOS Pathogens* **13**, e1006483 (2017).
34. Morgan, D. O. Cyclin-dependent kinases: engines, clocks, and microprocessors. *Annu. Rev. Cell Dev. Biol.* **13**, 261–291 (1997).
35. Morrissette, N. Targeting *Toxoplasma* Tubules: Tubulin, Microtubules, and Associated Proteins in a Human Pathogen. *Eukaryotic Cell* **14**, 2–12 (2015).
36. Morlon-Guyot, J., Francia, M. E., Dubremetz, J.-F. & Daher, W. Towards a molecular architecture of the centrosome in *Toxoplasma gondii*. *Cytoskeleton* **74**, 55–71 (2017).
37. Suvorova, E. S., Francia, M., Striepen, B. & White, M. W. A Novel Bipartite Centrosome Coordinates the Apicomplexan Cell Cycle. *PLOS Biology* **13**, e1002093 (2015).
38. Courjol, F. & Gissot, M. A coiled-coil protein is required for coordination of karyokinesis and cytokinesis in *Toxoplasma gondii*. *Cellular Microbiology* e12832 (2018).
39. Chen, C.-T. & Gubbels, M.-J. TgCep250 is dynamically processed through the division cycle and is essential for structural integrity of the *Toxoplasma* centrosome. *Molecular Biology of the Cell* **30**, 1160–1169 (2019).
40. Morrissette, N. S. & Sibley, L. D. Disruption of microtubules uncouples budding and nuclear division in *Toxoplasma gondii*. *J. Cell. Sci.* **115**, 1017–1025 (2002).
41. Shaw, M. K., Roos, D. S. & Tilney, L. G. DNA replication and daughter cell budding are not tightly linked in the protozoan parasite *Toxoplasma gondii*. *Microbes Infect.* **3**, 351–362 (2001).
42. Isalan, M. Zinc Fingers. in *Encyclopedia of Biological Chemistry* 575–579 (Elsevier, 2013).
43. Cassandri, M. *et al.* Zinc-finger proteins in health and disease. *Cell Death Discovery* **3**, 17071 (2017).
44. Wolfe, S. A., Nekludova, L. & Pabo, C. O. DNA Recognition by Cys<sub>2</sub> His<sub>2</sub> Zinc Finger Proteins. *Annual Review of Biophysics and Biomolecular Structure* **29**, 183–212 (2000).
45. Hall, T. M. T. Multiple modes of RNA recognition by zinc finger proteins. *Current Opinion in Structural Biology* **15**, 367–373 (2005).
46. Gamsjaeger, R., Liew, C., Loughlin, F., Crossley, M. & Mackay, J. Sticky fingers: zinc-fingers as protein-recognition motifs. *Trends in Biochemical Sciences* **32**, 63–70 (2007).
47. Laity, J. H., Lee, B. M. & Wright, P. E. Zinc finger proteins: new insights into structural and functional diversity. *Curr. Opin. Struct. Biol.* **11**, 39–46 (2001).

48. Stenmark, H. & Aasland, R. FYVE-finger proteins--effectors of an inositol lipid. *J. Cell. Sci.* **112 ( Pt 23)**, 4175–4183 (1999).
49. Mattsson, J. G. & Soldati, D. MPS1: a small, evolutionarily conserved zinc finger protein from the protozoan *Toxoplasma gondii*. *FEMS Microbiology Letters* **180**, 235–239 (1999).
50. Vanchinathan, P., Brewer, J. L., Harb, O. S., Boothroyd, J. C. & Singh, U. Disruption of a Locus Encoding a Nucleolar Zinc Finger Protein Decreases Tachyzoite-to-Bradyzoite Differentiation in *Toxoplasma gondii*. *Infection and Immunity* **73**, 6680–6688 (2005).
51. Daher, W. *et al.* Lipid kinases are essential for apicoplast homeostasis in *Toxoplasma gondii*: Phosphoinositide function in apicoplast biology. *Cellular Microbiology* **17**, 559–578 (2015).
52. Gissot, M. *et al.* An evolutionary conserved zinc finger protein is involved in *Toxoplasma gondii* mRNA nuclear export: A zinc finger protein is involved in mRNA nuclear export. *Cellular Microbiology* **19**, e12644 (2017).
53. Naumov, A. *et al.* The *Toxoplasma* Centrocone Houses Cell Cycle Regulatory Factors. *mBio* **8**, (2017).
54. Yam, A. Y. *et al.* Defining the TRiC/CCT interactome links chaperonin function to stabilization of newly made proteins with complex topologies. *Nature Structural & Molecular Biology* **15**, 1255–1262 (2008).
55. Lirussi, D. & Matrajt, M. RNA granules present only in extracellular *Toxoplasma gondii* increase parasite viability. *Int. J. Biol. Sci.* **7**, 960–967 (2011).

## ACKNOWLEDGMENTS

It was the end of my third year of PhD and it was just another day in the lab. Sunlight was passing through the windows; the noise of a centrifuge was slightly distracting me from reading an article; my cute little toxoplasmas were happily replicating in the depth of their incubator. Absent-mindedly, I looked at my calendar, saw the date of my thesis defence... and the realisation finally hit me: my PhD will be over in several weeks. I could hardly believe it – to be honest, I still cannot. These years were full of everything, from absolutely awful to wonderful and inspiring, and, luckily enough, I was not going through it all alone.

First and foremost, I would like to thank Sébastien Besteiro for his guidance and support and his extraordinary passion for science. You accompanied me from the very beginning to the very end of this project, explaining and directing but also letting me make my own mistakes, encouraging me to be independent, to think, to ask questions and to search for answers. You pushed me to go further, you criticised me without being unfair and you remained positive no matter how many millions of parasites I killed in vain. You taught me that science is a hard work that can, nevertheless, be a great source of inspiration and intellectual fulfilment. Thank you. I could not have a better PhD supervisor.

Thanks to Maryse Lebrun, the first person from Toxoplasma world I've ever talked to and, actually, the one who gave me motivation to apply for a PhD position in the LPHI (DIMNP at the time). Thank you for your consideration, support and scientific feedback during these years. Thanks to Georges Lutfalla for cordially receiving me in the LPHI and being a caring laboratory director.

Many thanks to Mélanie Bonhivers, Cyrille Botté and Catherine Braun-Breton for accepting to be members of the jury, taking their time to read this manuscript and coming to the thesis defence. Thanks to my thesis committee members Mathieu Gissot and Benedicte Delaval for their scientific suggestions and kind encouragement during our meetings, especially the one after my second year of PhD.

I would like to thank all the LPHI and especially team 1, for scientific stimulation and personal help. Indispensable Diana, wise and kind-hearted, always here to share a smile with. Caty, incredibly professional and altruistic. Eleonora who is able to explain absolutely anything about science to anyone (me included). Ever-present Marjo who provides us with necessary

materials and humour. Maude with her curiosity, critical eye and unexpected questions. Jean-François and Laurence who introduced me to a fascinating world of electron microscopy and helped with the analysis. Our former colleagues Wassim and Juliette with their attentiveness and feedback. “Les autophagettes” Maude and Mai who presented me with lifehacks and biomol-hacks. Annabelle who showed me what it means to be strong. Thanks to Margarida, for your support and your ability to change things for good. To Justine, for your jokes and reasonable sister-like advice. To Rakhee, for your deep empathy and kindness during our discussions. To Aude and Sarah - I would not have dared to wish for such great team-members. To Arnault for his good craziness and compassion. To Rania for her comments and hugs. Thanks to Amandine (hope you are doing fine beyond the ocean!) to Kai, Sharon, Rachel and Coralie, for conversations and suggestions. To Michel and Anne who always cheered me up. Thanks to Plasmodium team, Jose Juan, Rafa, Ana-Rita, Diane and Pratima, the lab is not the lab without you. Thanks to Eliane for providing our bacteria with media and us with laboratory equipment.

Thanks to the Bacteriology team, to Anne for helping with BACTH approach, to Leila for her interest in my project, to Marianne for suggestions and antibodies, to Malika for our cosy chats, to Talip for reassuring and fun (and the t-shirt).

Thanks to Yann for the FACS analysis, to Mai for suggestions about my RNA experiments and to Laure for her advice about recombinant proteins. Thanks to Elodie and Vicky for explaining me, over and over, that no, one cannot break a Z2 microscope that easily.

Thanks to Veronique, Nathalie, Gael, Christine for their good mood, organizing skills and administrative help. Thanks to Luc without whom things do not work properly in the lab and the machines do not behave themselves. Special thanks to Christian who saved my Mozart computer from dying 9 times and who generously provided me with Beethoven computer when Mozart finally passed away. Thank you also for the discussions, laughter and music.

I would like to thank the Labex ParafraP 2016 PhD students with whom I shared hopes and fears (and workshops). Your Whatsapp group was a constant source of positive vibes and enthusiastic support. For those who are preparing for the defence – good luck! For everyone – I am sure you will find a path you want to follow.

My second half of PhD was particularly challenging because of my health problems and I feel it only fair to express my gratitude to those who helped me during that period of my life. It would be impossible to mention every single person, however, for there were so many. All my colleagues, all my friends, old and new, even people whose name I will never know - I still remember what each of you have done for me. I was astonished and moved by seeing how much of goodness I was surrounded with. I would like to address several special thanks. To people who helped me the day of the traffic collusion, waiting with me till the ambulance and the police arrived. To the police officers for their professionalism and sympathy. To les pompiers for getting me to hospital as fast as possible – all while listening to my horrible adrenalin-provoked jokes. To the medical team of Service d’Urgence and Chirurgie orthopédique et Traumatologie de l’Hôpital Lapeyronie. My warm thanks to the nurse who tried to convince me that I was not in the hospital but on a tropical island drinking a cocktail. While I did not believe it completely, it still made me laugh a lot. I would especially like to thank my surgeon, Dr. Louis Dagneaux, for his high professionalism. Thanks to Annie Dalle and Martine Nold who provided me with medical help after both operations. Thanks to my physiotherapists, Alexandre Janvier-Bego and Ayodélé Madi, for their assistance during my long recovery and for their positive thinking, patience and great sense of humour. Thanks to those at the University of Montpellier who helped me with fees and administrative procedures. Thanks to Adéline Barthes who guided me through the sea of paperwork.

I would like to thank my Montpellier friends for enlightening my PhD life there and most of all I thank “Les Bibiches” who drove me crazy with laughter, brought me to unexpected places and were ready to give an affectionate kick when necessary. Alexandra, my dear friend, who made my days so much brighter with her jokes, trust and delicious desserts. Hamid, who, while sometimes being unsupportable, supported me all along. Karim, kind and patient and reliable. Adrien with his talks, books and board games. Nico, who presented me with a juggling lesson exactly at the right moment, preventing me from going nuts during the last days of manuscript writing. Thanks to Ihab for music teaching and mentoring, to Julia and Amandine for showing me how to accept emotions and how to love myself and how to deal with it all, for God’s sake. Thanks to my Russian friends Catherine, Kate, Olga and Asya for letting me be honest and vulnerable and encouraging me not to give up. To everyone I did not mention here – I remember everything. I am grateful for you being in my life.

My dearest family, the last lines of these acknowledgements are for you. I sometimes think you were even more stressed about my PhD project progress than I was. My mom, who was always eager to listen for my news and was a source of infinite support. My dad, who took my side in the conflicts and understood my sorrows (and also provided me with a great deal of anecdotes). My brother, who I could always count on. My sister-in-law with her creative spirit and my nephews-cuties. My grandmother, who was able to see a bright side in any situation and took my thesis writing so seriously she actually finished by integrating scientific jargon in her daily vocabulary. All of you were 3000 km away from me, but I never stopped feeling your support. For your love, for you believing in me even when I did not – thank you, thank you, thank you.

# TABLE OF CONTENTS

INTRODUCTION.....	28
<b>CHAPTER 1. The apicomplexan parasite <i>Toxoplasma gondii</i>.....</b>	<b>2</b>
1.1. Apicomplexan parasites: an overview.....	2
1.2. <i>Toxoplasma gondii</i> : an important pathogen of humans and animals.....	4
1.2.1. <i>T. gondii</i> prevalence in human and genotypes.....	4
1.2.2. The <i>T. gondii</i> life cycle.....	5
1.2.3. <i>T. gondii</i> transmission ways.....	7
1.2.4. Clinical manifestations of human toxoplasmosis.....	8
1.2.5. Toxoplasmosis in animals.....	9
1.2.6. Diagnosis, treatment and prevention.....	10
<b>CHAPTER 2. The tachyzoite form of <i>T. gondii</i>.....</b>	<b>12</b>
2.1. Ultrastructure of the tachyzoite.....	12
2.1.1. Conventional organelles.....	13
The nucleus.....	13
The mitochondrion.....	13
The endoplasmic reticulum and the Golgi apparatus.....	13
2.1.2. Apicomplexa-specific organelles.....	14
The secretory organelles: micronemes, rhoptries and dense granules.....	14
The apicoplast.....	15
The cytoskeleton.....	16
2.2. The lytic cycle of tachyzoites.....	18
2.2.1. Egress.....	18
2.2.2. Invasion.....	19
2.2.3. Intracellular replication.....	21
<b>CHAPTER 3. The cytoskeleton of <i>T. gondii</i>.....</b>	<b>22</b>
3.1. The inner membrane complex.....	22
3.2. Microtubules in tachyzoites.....	27
3.2.1. Subpellicular microtubules.....	27
3.3. The cortical cytoskeleton development during <i>T. gondii</i> division.....	28
<b>CHAPTER 4. The cell cycle of <i>T. gondii</i>.....</b>	<b>31</b>
4.1. Cell division in eukaryotes: basic events.....	31
4.2. Cell division in apicomplexan parasites.....	33
4.3. The <i>T. gondii</i> cell cycle.....	36
4.3.1. DNA replication.....	37
4.3.2. Mitosis.....	37
4.3.3. Organellar dynamics and daughter cells assembly.....	39
4.4. Regulation of the endodyogeny process.....	43
4.4.1. Cell-cycle related genes expression in tachyzoites.....	43
4.4.2. Checkpoints and regulatory factors.....	43
4.4.2. The centrosome.....	48
Centrosome structure.....	48
Centrosome regulating factors.....	52

<b>CHAPTER 5. Zinc finger proteins and their roles in <i>T. gondii</i></b> .....	<b>53</b>
<b>Aims of the thesis</b> .....	<b>56</b>
<b>RESULTS</b> .....	<b>58</b>
<b>CHAPTER 1. TgZFP2 functional characterisation</b> .....	<b>59</b>
Introduction .....	59
TgZFP2 is a novel zinc finger protein involved in coordinating mitosis and budding in <i>Toxoplasma</i> .....	60
Conclusion and perspectives.....	109
<b>CHAPTER 2. Identification of TgZFP2 protein binding partners</b> .....	<b>110</b>
2.1. Isolation of proteins interacting with YFP-tagged TgZFP2.....	110
2.2. Selection of the mass-spectrometry identified putative partners .....	111
2.2.1. Selected candidates that could be potential cell cycle regulators. ....	111
2.2.2. Selected candidates that may be potentially important for cytoskeleton homeostasis: the CCT chaperonin complex. ....	114
2.3. TgZFP2 recombinant protein and zinc binding assay .....	123
<b>CHAPTER 3. Identification of TgZFP2 RNA binding partners</b> .....	<b>127</b>
TgZFP2 interactions study: conclusive remarks.....	131
<b>Materials and methods</b> .....	<b>133</b>
Mammalian cell culture .....	133
Parasites maintenance.....	133
Identification of the putative TgZFP2 protein partners .....	133
Identification of the putative TgZFP2 RNA partners .....	138
TgZFP2 recombinant protein production .....	139
Zinc-binding assay.....	141
<b>DISCUSSION</b> .....	<b>142</b>
TgZFP2 and the centrosome.....	143
Could TgZFP2 act as a regulatory factor of endodyogeny? .....	144
TgZFP2 and the cytoskeleton .....	145
Conclusion.....	146
<b>REFERENCES</b> .....	<b>147</b>
<b>ANNEXES</b> .....	<b>173</b>

## LIST OF FIGURES AND TABLES

<b>Figure 1.</b> The diversity of species belonging to the superphylum Alveolata .....	2
<b>Figure 2.</b> The classification of Apicomplexa .....	3
<b>Figure 3.</b> Global status of <i>T. gondii</i> seroprevalence.....	4
<b>Figure 4.</b> <i>T. gondii</i> complete life cycle .....	6
<b>Figure 5.</b> The most common sources of <i>T. gondii</i> infection in humans .....	7
<b>Figure 6.</b> Electron microscopy image of a <i>T. gondii</i> tachyzoite .....	12
<b>Figure 7.</b> Schematic representation of <i>T. gondii</i> secretory organelles .....	14
<b>Figure 8.</b> The schematic representation of the <i>T. gondii</i> cytoskeleton .....	17
<b>Figure 9.</b> The lytic cycle of <i>T. gondii</i> .....	18
<b>Figure 10.</b> Egress of tachyzoites from the host cell .....	19
<b>Figure 11.</b> A model of the tachyzoite's gliding motility and host cell invasion .....	20
<b>Figure 12.</b> <i>T. gondii</i> tachyzoite replication scheme .....	21
<b>Figure 13.</b> Schematic representation of the pellicule in Ciliophora ( <i>T. thermophila</i> ) and in Apicomplexa ( <i>T. gondii</i> tachyzoite) .....	22
<b>Figure 14.</b> IMC morphology in <i>T. gondii</i> assessed by freeze-fracture electron microscopy ....	23
<b>Figure 15.</b> Schematic representation of the IMC structure in a mature <i>T. gondii</i> tachyzoite .	26
<b>Figure 16.</b> Microtubules-based structures in a <i>T. gondii</i> tachyzoite.....	27
<b>Figure 17.</b> Dynamics of the cytoskeleton during the endodyogeny process .....	29
<b>Figure 18.</b> Schematic representation of a conventional eukaryotic cell cycle .....	32
<b>Figure 19.</b> Division modes in apicomplexan parasites .....	34
<b>Figure 20.</b> A bimodal scheme of cell cycle organization in Apicomplexa .....	35
<b>Figure 21.</b> Cell cycle of <i>T. gondii</i> .....	36
<b>Figure 22.</b> Flow cytometry profile of the DNA content of asynchronous tachyzoites.....	37
<b>Figure 23.</b> Schematic representation of the eukaryotic machinery for chromosome segregation .....	37
<b>Figure 24.</b> Closed mitosis of <i>T. gondii</i> .....	39
<b>Figure 25.</b> Morphological events occurring during the replication of a type I strain <i>T. gondii</i> tachyzoite.....	40
<b>Figure 26.</b> Cyclical gene expression during endodyogeny .....	43
<b>Figure 27.</b> Cell cycle checkpoints in a eukaryotic cell .....	44
<b>Figure 28.</b> Distribution of parasite genomic DNA content at permissive (34°C) and restricted (40°C) temperatures for selected temperature-sensitive <i>T. gondii</i> cell cycle mutants .....	45
<b>Figure 29.</b> Checkpoints and cyclin-related kinases required for cell cycle progression in <i>T. gondii</i> .....	47
<b>Figure 30.</b> Structure of the mammalian centrosome.....	48
<b>Figure 31.</b> Structure of the <i>T. gondii</i> centrosome.....	49
<b>Figure 32.</b> A model of <i>T. gondii</i> cell cycle regulation by a bipartite centrosome proposed by Suvorova et al.....	51
<b>Figure 33.</b> Schematic representation of some typical zinc finger domains .....	54

<b>Figure 34.</b> Strategy used for the identification of TgZFP2 putative protein partners .....	110
<b>Figure 35.</b> The investigation of potential interactions between TgZFP2 and cell cycle-related candidates .....	113
<b>Figure 36.</b> TgCCT is a conserved eukaryotic chaperonin complex.....	115
<b>Figure 37.</b> TgCCT is a multimeric complex localising to the cytoplasm of tachyzoites.....	117
<b>Figure 38.</b> The co-immunoprecipitation analysis of potential TgZFP2-TgCCTs interactions..	118
<b>Figure 39.</b> TgCCTs potential interactions with cytoskeleton proteins actin and tubulin .....	119
<b>Figure 40.</b> The principle of BACTH .....	120
<b>Figure 41.</b> $\beta$ -galactosidase assay performed on the <i>E. coli cya<sup>-</sup></i> bacteria with co-expressed TgZFP2 and its potential interacting partners, TgCCT subunits .....	122
<b>Figure 42.</b> TgZFP2 recombinant proteins production. ....	124
<b>Figure 43.</b> Zinc binding assay .....	125
<b>Figure 44.</b> TgZFP2 and the stress granules .....	128
<b>Figure 45.</b> General RIP-seq strategy used for the identification of TgZFP2 putative RNA partners.....	129
<b>Figure 46.</b> TgZFP2 solubility is affected by the formaldehyde cross-linking .....	130
<b>Figure 47.</b> Scheme of our adapted protocol for RIP-seq sample preparation (UV as a cross-linking agent).....	131
<b>Table 1.</b> Selection of putative TgZFP2 protein partners related to the regulation of cell cycle progression .....	112
<b>Table 2.</b> Selection of CCT chaperonin's subunits for studying their potential interactions with the TgZFP2 protein .....	114
<b>Annexe 1.</b> List of identified IMC-related proteins in <i>T. gondii</i> .....	174
<b>Annexe 2.</b> List of <i>T. gondii</i> proteins containing an annotated zinc finger motif .....	177
<b>Annexe 3.</b> List of oligonucleotides used in TgZFP2 characterization study .....	185
<b>Annexe 4.</b> List of oligonucleotides used in study of TgZFP2 potential binding partners .....	186

## ABBREVIATIONS

ABLIM1	Actin-Binding LIM protein 1
AID	auxin-inducible degradation (system)
AMA1	apical membrane antigen 1
Ana2	anastral spindle 2
APR	Apical Polar Ring
Ark	Aurora related kinase
ATG8	Autophagy related protein 8
ATP	adenosine triphosphate
BACTH	Bacterial Adenylate Cyclase Two-Hybrid
BioID	proximity-dependent biotin identification
BSA	Bovine serum albumin
C	Cytokinesis (phase)
cAMP	cyclic adenosine 3'5'-monophosphat
Cas9	CRISPR associated protein 9
CCT	chaperonin-containing tailless (complex)
Cdk	Cyclin-dependent kinase
CDPK	Calcium Dependent Protein Kinase
CEP	Centrosome associated protein
CKI	Cyclin Kinase Inhibitor
c-NAP1	centrosomal Nek2-associated protein 1
CRISPR	Clustered Regularly Interspaced Short Palindromic Repeats
Crk	Cdk-related kinase
Cys	cysteine
DAPI	4',6-diamidino-2-phenylindole
DG	dense granule
DIP13	13 kDa deflagellation-inducible protein
DLC1	Dynein light chain 1 protein
DMEM	Dulbecco's Modified Eagle Medium
DNA	deoxyribonucleic acid
ECR1	NEDD8-activating enzyme E1 catalytic subunit
ER	endoplasmic reticulum

FACS	Fluorescence Activated Cell Sorting
FBS	fetal bovine serum
FISH	fluorescence in situ hybridization
FYVE	Fab, 1YOTB, Vac 1 EEA1 (domain)
G	Gap (phase)
GAP	gliding-associated protein
GAPM	Glideosome-Associated Protein with multiple-Membrane spans
GFP	green fluorescent protein
GRA	dense granules protein
GSK	glycogen synthase kinase
GST	Glutathione S-Transferase
GTPase	Guanosine triphosphatase
HA	Human influenza hemagglutinin
HFF	Human foreskin fibroblasts
His	histidine
HIT	Histidine Triad motif
IFA	Immunofluorescence Assay
Ig	immunoglobulin
IMC	inner membrane complex
IMP	intramembrane particle
IPTG	Isopropyl $\beta$ -D-1-thiogalactopyranoside
ISP	IMC subcompartment protein
ISC	IMC suture component
LB	Lysogeny Broth
LC-MS/MS	liquid chromatography coupled to tandem mass spectrometry
M	Mitosis (phase)
MAP	microtubule-associated protein
MAPK	Mitogen-activated protein kinase
MCS	multicloning site
MIC	Micronemal Protein
MJ	Moving Junction
MMTS	methyl methanethiolsulfonate
MORN1	Morn (membrane occupation and recognition nexus repeat) containing protein 1
MPS1	Monopolar spindle 1 (kinase)

MT	microtubule
MTOC	microtubule-organizing center
Myo	myosin
Nek	NIMA related kinase
Ndc80	nuclear division cycle 80
NIMA	never in mitosis (kinase)
Nuf2	nuclear filament-related 2
OD	optical density
ONPG	ortho-Nitrophenyl- $\beta$ -galactoside
PABP	poly-A binding protein
PAR	4-(2-pyridylazo) resorcinol
PB	processing body
PBS	Phosphate-Buffered Saline
PCM	pericentriolar material
PCR	polymerase chain reaction
PHD	plant homeodomain
PhIL1	photosensitized INA-labeled protein 1
PIKfyve	phosphoinositide kinase containing FYVE-type zinc finger
PLK	Polo-like kinase
PLP1	perforin-like protein 1
PRMT1	Arginine Methyltransferase 1
PV	parasitophorous vacuole
Rab	Ras-associated binding protein
RB	residual body
RING	Really Interesting New Gene
RIP-seq	RNA Immunoprecipitation sequencing
RNA	ribonucleic acid
RON	rhopty neck protein
ROP	rhopty bulb protein
RT	room temperature
S	Synthesis (phase)
SAC	spindle assembly checkpoint
SAG	surface antigen
SAS	Spindle assembly abnormal protein
SFA	striated fiber assembling
Sfi1	suppressor of fil1

SG	stress granule
SPN	subpellicular network
SPM	subpellicular microtubules (proteins)
SSSCA1	Sjogren syndrome/scleroderma autoantigen 1
STIL	SCL-interrupting locus protein
TB	Terrific Broth
TBS	Tris Buffered Saline
TCA	tricarboxylic acid (cycle)
Tet-OFF	tetracycline-off (system)
TFIIIA	Transcription Factor IIIa
Tg	Toxoplasma gondii
TLAP	TrxL1-associating protein
TrxL	Thioredoxin-like protein
TSC	Transverse suture component
WB	western blot
YFP	yellow fluorescent protein
ZFP1	zinc finger protein 1
ZFP2	zinc finger protein 2
ZnF	zinc finger (domain)
ZNF2	zinc finger 2
ZNRD2	Zinc Ribbon Domain containing 2

# **INTRODUCTION**

---

## CHAPTER 1.

### The apicomplexan parasite *Toxoplasma gondii*

---

#### 1.1. Apicomplexan parasites: an overview

The eukaryotic phylum Apicomplexa comprises mostly parasitic protists and encompasses over 6000 described species<sup>1</sup>. Together with two other taxa – diversified but mostly free-living predators Ciliophora<sup>2</sup> and aquatic hetero- and phototrophs Dinoflagellata<sup>3</sup>– it belongs to the superphylum Alveolata (or alveolates)<sup>4,5</sup> (Fig. 1). The notable morphological feature of alveolates, regardless their lifestyle and habitat, is the presence of a set of vesicles (the alveoli) beneath their plasma membrane<sup>6</sup>. Apicomplexa themselves bear several important particular morphological characteristics, including the presence of a non-photosynthetic plastid apicoplast and the development of specialised structures on anterior part of parasites, referred to as an apical complex<sup>6</sup>. The name of the phylum Apicomplexa (from the latin “apex” – top, “complexus” – enfolding) highlights the latter.

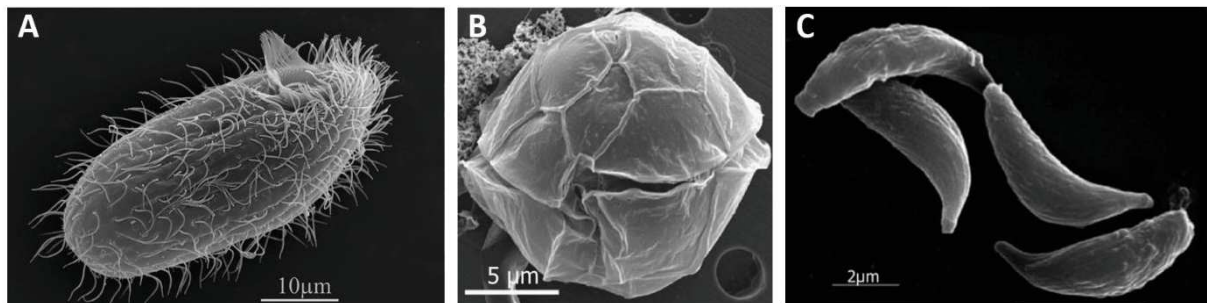


**Figure 1.** The diversity of species belonging to the superphylum Alveolata<sup>7-9</sup>. From left to right: scanning electron microscopy images of (A) a free-living heterotroph of aquatic environments *Tetrahymena thermophila* (phylum Ciliophora), (B) a marine autotroph *Alexandrium tamarense* (phylum Dinoflagellata) known to produce a satotoxin that induces a paralytic shellfish poisoning in humans, and (C) an asexual stage of the parasite *Toxoplasma gondii* (phylum Apicomplexa) responsible for toxoplasmosis in humans and animals.

The Apicomplexa phylum is divided into several sub-groups: Coccidia (coccidians), Gregarinasina (gregarines) and Cryptosporidia, and Hematozoa that include Haemospororida (haemosporidians) and Piroplasmorida (piroplasmids)<sup>10</sup> (Fig. 2). Most comprised species are obligatory intracellular (except for the gregarines) parasites, invading vertebrate and invertebrate animals, both marine and terrestrial. The host preferences, as well as modes of

transmission and cellular tropism vary greatly amongst species. Most Apicomplexa have a complex life cycle that includes the development of sexually replicating forms in so-termed definitive hosts and the asexual proliferation in respective intermediate hosts<sup>11</sup>.

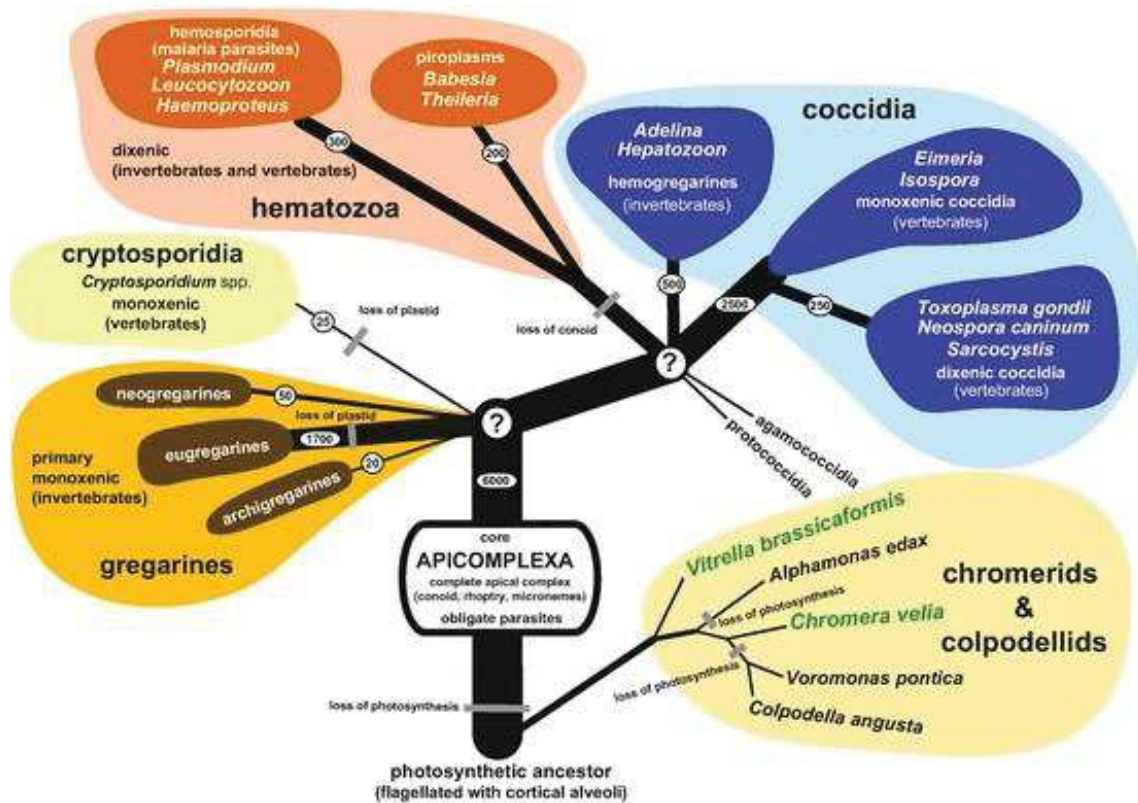


**Figure 2. The classification of Apicomplexa<sup>11</sup>.** The hypothetical tree indicates the principal groups of parasites (coloured) and related non-parasitic taxa, Colpodellids and Chromerids (in beige) that probably emerged from the same photosynthetic ancestor as Apicomplexa. The numbers on branches and the thickness of branches indicate diversity (i.e. named species).

Being pathogens of medical and veterinary importance, apicomplexan parasites have a big impact human life and wellbeing. Most notorious is the case of *Plasmodium* species that cause malaria, one of the deadliest human infectious diseases worldwide, killing about half a million people annually<sup>12</sup>. Cryptosporidiosis, caused by *Cryptosporidium* species, is one of the world's leading cases of intestinal infection in humans and animals, often life-threatening in children and young animals as well as in immunocompromised individuals<sup>13–15</sup>. Bovine tropical theileriosis (caused by *Theileria* species) leads to death of over 1 million cattle in Sub-Saharan Africa per year<sup>16</sup>. Several *Eimeria* species induce coccidiosis in poultry, representing a major case of morbidity and decreased weight gain in chicken and resulting in the severe economic losses to the industry<sup>17</sup>. Some other apicomplexan parasites – like *Neospora caninum* or

*Sarcocystis* spp – provoke abortion in animals, particularly in cattle, which impacts the sector considerably<sup>18</sup>.

Successfully surviving and reproducing, all the listed parasites rely on replication in a restricted range of hosts<sup>16,19–22</sup>. On the contrary, the coccidian pathogen *Toxoplasma* represents a striking example of ubiquitous, world-spread parasite, which is able to invade over 350 host species, including birds and mammals<sup>23</sup>. The only known species, *Toxoplasma gondii*, is the etiological agent of toxoplasmosis<sup>24</sup> and remains, for numerous reasons, one of the most intensively studied parasites of the phylum.

## 1.2. *Toxoplasma gondii*: an important pathogen of humans and animals

### 1.2.1. *T. gondii* prevalence in human and genotypes

*T. gondii* has been discovered over a century ago, in 1908<sup>25–27</sup>, though its importance as the causative agent of human toxoplasmosis remained unknown until 1930<sup>28</sup>. Nowadays it is estimated that at least 30% of global population is infected by *T. gondii* which makes it one of the most prevalent human parasites<sup>29</sup>. This is, however, a mean value, as the percentage of seropositive population differs from country to country, varying between 20% and 60% in Europe for example<sup>30</sup> (Fig. 3). Higher prevalence is generally reported for countries with humid and warm climate; other factors that influence *T. gondii* burden include economic, cultural and social habits of the country, hygienic conditions, dietary habits and the quality of water<sup>23</sup>.

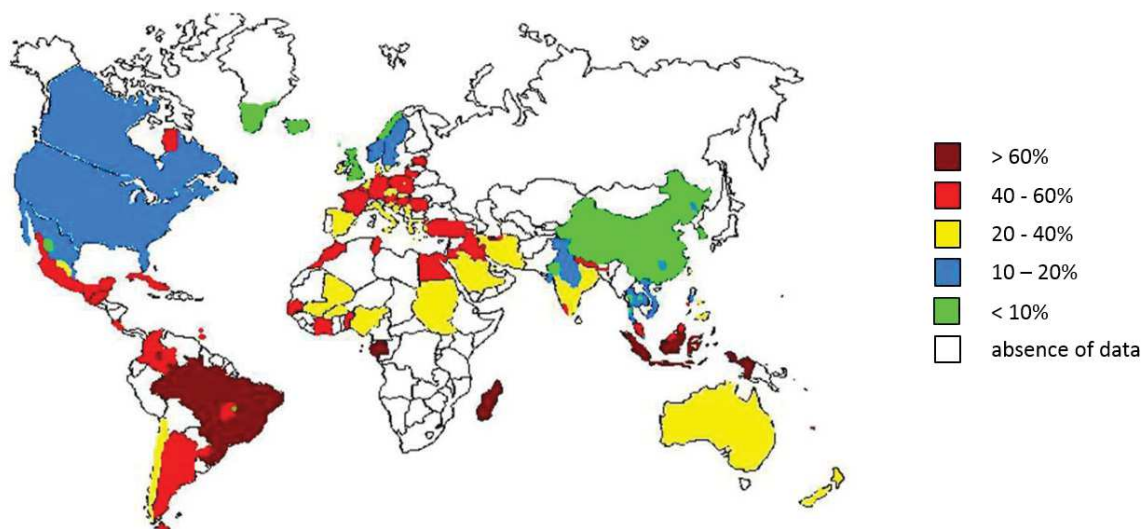


**Figure 3.** Global status of *T. gondii* seroprevalence<sup>30</sup>. Note that the highest prevalence is reported in Latin America and Central Europe. The prevalence is moderate in countries of Southern Europe and is the lowest in North America, Northern Europe and South East Asia.

*T. gondii* exhibits a relatively low genetic diversity and the clinical isolates from humans and animals in USA and Europe were grouped in three main genotypes corresponding to clonal lineages named type I, II and III, with variable virulence in the mouse model (type I is much more virulent than types II and III in mice)<sup>24</sup>. Over 95% of any isolate in these countries fall into one of the listed groups, with a predominancy for type II in humans and animals<sup>31,32</sup>. The majority of isolates from South America, Africa and Asia, however, do not fit in these defined genotypes; only the type III is spread all over the world<sup>24</sup>.

### 1.2.2. The *T. gondii* life cycle

*T. gondii* complete life cycle alternates between sexual reproduction in Felidae (colloquially referred to as the 'cat' family), and the asexual replication in virtually any nucleated cell of warm-blooded vertebrates<sup>33</sup>. The classical life cycle of the parasite relies on the prey-predator relationship (Fig. 4): the felids (domestic and wild-living cats) eat infected prey and host the sexual proliferation of parasites, resulting in the formation of oocysts<sup>34</sup>. A single cat shed with feces more than 100 million oocysts in the environment<sup>35</sup>, and several days after excretion the oocysts become infectious. Once a mammal or a bird ingests infectious (also known as sporulated) oocyst, it becomes an intermediate host in which asexual stages of *T. gondii* proliferate. Noteworthy, as intermediate hosts may prey on each other, and as the transmission of the parasite may occur in mother-to-child manner, *T. gondii* does not necessarily require a sexual development phase in order to propagate in the population<sup>36</sup>.

Humans serve as intermediate hosts for *T. gondii* and may be infected by any of following asexual forms of the parasite: rapidly dividing tachyzoites, slowly dividing bradyzoites enclosed in tissue cysts, or sporozoites preserved inside the sporulated oocyst. Once in the organism, bradyzoites and sporozoites convert into tachyzoites and the proliferation of this stage in different tissues causes the clinical manifestations of toxoplasmosis<sup>23</sup>.

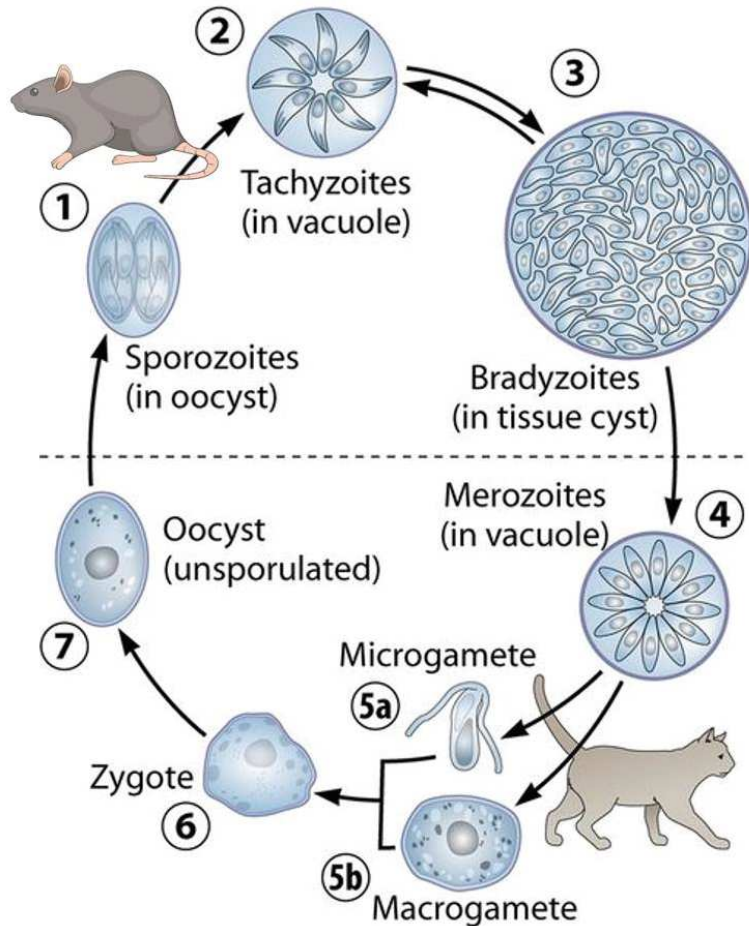


**Figure 4. *T. gondii* complete life cycle<sup>37</sup>.** The development of asexual stages (1-3) of the parasite occurs in intermediate hosts (for example, a rat) while the sexual replication (4-7) that leads to a formation of oocyst happens in a definitive host (a domestic cat on the scheme).

**1.** The oocysts, excreted with the cat's feces become infectious (sporulated) after 1-5 days in the environment and each contains 4 haploid sporozoites. This process of sporulation implies meiotic reduction and morphological changes of the oocyst in presence of oxygen and humidity.

**2.** After the ingestion of the sporulated oocyst by the intermediate host, sporozoites are liberated in the digestive tube, penetrate the intestinal epithelium and differentiate into tachyzoites. They actively proliferate and disseminate throughout the organism.

**3.** The conversion of rapidly replicating tachyzoites to slowly replicating bradyzoites inside tissue cysts happens 7-10 days post-infection. Cysts remain viable for an extended period of time and remain predominantly in muscles and brain tissue of an intermediate host.

**4.** Tissue cysts are ingested by a cat through predation on an intermediate host and the cysts wall is destroyed by gastric enzymes. Liberated bradyzoites settle in the enterocytes and undergo a limited number of asexual replications, which results in the formation of merozoites.

**5.** Merozoites give rise to flagellated male microgametes (**5a**) and female macrogametes (**5b**) between which a sexual replication occurs in the cat's intestines.

**6.** A zygote is formed by fertilization inside cat's enterocytes.

**7.** After the formation of a cyst wall the zygote becomes an unsporulated oocyst. The disruption of the enterocytes liberates the oocysts which are excreted with the cat's feces into the environment. The shedding of oocysts begins 3-7 days after the ingestion of tissue cysts and may continue up to 20 days post-ingestion.

### 1.2.3. *T. gondii* transmission ways

The predominant (although not the only one) source of *T. gondii* infection in humans is the foodborne transmission of bradyzoites or sporozoites (Fig. 5). In this case an individual becomes infected after ingestion of tissue cysts in undercooked meat or after consumption of food or water contaminated by sporulated oocysts<sup>38</sup>. An occasional ingestion of sporulated oocysts may also happen after a contact with contaminated soil or, less frequently, directly from the feline feces<sup>23</sup>. Another way of *T. gondii* horizontal transmission via bradyzoites is the solid-organ transplantation from an infected donor to a non-immunised recipient<sup>39</sup>.

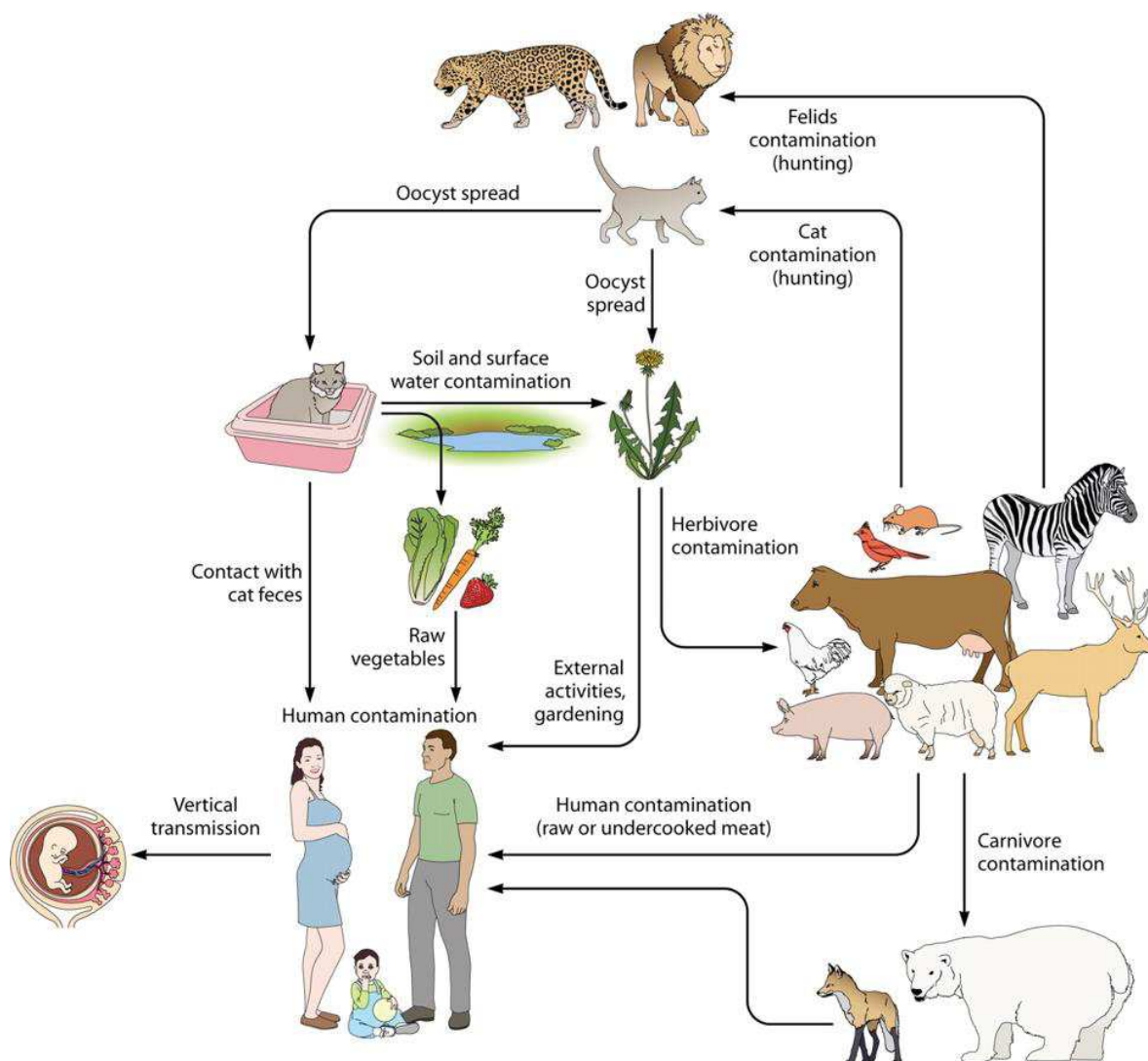


**Figure 5. The most common sources of *T. gondii* infection in humans<sup>23</sup>.**

Horizontal transmission comes from consumption of undercooked or raw meat containing tissue cysts, or via ingestion of sporulated oocysts with food, water, soil particles, or after contact with cat feces. Vertical transmission occurs from infected pregnant woman to fetus. Note that scheme does not include the relatively rare cases of transplantation-related and injection-related *T. gondii* transmission.

The tachyzoite-induced toxoplasmosis is most commonly associated with the congenital form of disease that is caused by the vertical transmission of tachyzoites from an infected mother to a fetus during pregnancy<sup>23</sup>. The existence of foodborne infection by tachyzoites seems possible, while not major: tachyzoites are present in the raw milk of infected animals<sup>40</sup>, and though they were reported to be sensitive to the low pH<sup>41</sup> they could potentially survive in the digestive tube<sup>42</sup>. The tachyzoites may also be transmitted parenterally, through occasional accidental injections in laboratory conditions<sup>43</sup> or, theoretically, via blood transfusions, as they were detected in patients' blood 5 weeks following acute toxoplasmosis<sup>44</sup>.

#### **1.2.4. Clinical manifestations of human toxoplasmosis**

The clinical manifestations of human toxoplasmosis may vary considerably. The development of the disease depends on parasite-related factors, such as the inoculum size and the virulence of the parasite, but also on patient-related factors, like the genetic background, sex, and immunological status of the infected person<sup>29</sup>.

In immunocompetent individuals, toxoplasmosis is generally asymptomatic, or leads to the development of non-specific flu-like symptoms which rarely require treatment<sup>29</sup>. In general, the immune system is able to restrain the development of the parasites, but is unable to eliminate it completely, as *T. gondii* is efficient in crossing biological barriers (e.g. blood-brain, blood-eye) and thus persist in different organs in the form of tissue cysts. The infected patients hence become asymptomatic carriers of *T. gondii* and the latent infection may be reactivated in immunocompromised conditions<sup>23</sup>.

In immunocompromised patients (receiving immuno-suppressing therapy following solid organ or stem cell transplant, or for people with advanced HIV disease), *T. gondii* can initiate severe – and possibly lethal – pathologies<sup>45</sup>. For instance, the reactivation of latent infection usually affects the central nervous system. The clinical manifestations of this process vary from severe headaches in the beginning of infection, to lethargy, ataxia, and coma due to the necrosis of brain tissues at the end of infection<sup>45</sup>. Besides neurological issues, toxoplasmosis in immunocompromised patients can also take the form of pneumonia, or target multiple organs, leading to respiratory failure and haemodynamic abnormalities similar

to a septic shock<sup>29</sup>. Both immunocompromised and immunocompetent patients may develop ocular toxoplasmosis, typically manifesting in the form of retinochoroiditis<sup>46</sup>.

The congenital form of toxoplasmosis is detected once the fetus has been infected by tachyzoites following the primo-infection of a pregnant woman<sup>47</sup>. The transmission of the parasite through placenta stays in tight correlation with the timing of the woman's infection. The placenta is less permeable during the first trimester of pregnancy, thus leading to the passages of parasites only in 10% of reported cases versus 60 to 70% in the third trimester<sup>48</sup>. The severity of the outcomes in the fetus displays an inverse correlation: the earlier the pregnant mother is infected, the more dangerous are the consequences for the fetus (up to abortion). A classical triad of symptoms for congenital toxoplasmosis in newborns includes chorioretinitis, intracranial calcifications, and hydrocephalus<sup>49</sup>.

### **1.2.5. Toxoplasmosis in animals**

Toxoplasmosis is a zoonotic infection; the persistence of *T. gondii* in animals – wild, farm and domestic ones - plays a pivotal role in transmission of the parasite to humans.

*T. gondii* is known to be largely spread in wildlife animals<sup>45</sup>. The propagation of the infection in wild-animal populations is a complex process influenced by a plethora of physical, biological and ecological factors; nevertheless, there is a direct correlation between the presence of felids (which usually have very high seroprevalence) and *T. gondii* seroprevalence in intermediate hosts<sup>23</sup>. Clinical and asymptomatic cases of toxoplasmosis have been reported for carnivorous, omnivorous and herbivorous animals. Noteworthy, asymptomatic toxoplasmosis persists in many species of small mammals, including rats and mice that live in wild, rural and urban environment<sup>45</sup>.

Toxoplasmosis in farm animals, especially in livestock, has an impact on human wellbeing too. The disease in adult animals is generally asymptomatic and is not a veterinary health problem, however the parasite may be transmitted to human via consumption of undercooked meat (notably beef and pork<sup>45</sup>) or raw milk<sup>38</sup>. Besides, congenital toxoplasmosis in livestock may lead to abortion, foetal mummification and neonatal pathologies, and thus causes considerable economic losses to industry<sup>18</sup>.

The domestic animals – especially cats and dogs – are also commonly infected by *T. gondii*. Though toxoplasmosis in these animals is associated with a low morbidity and

mortality, they remain an important reservoir of the parasite in rural and urban environments<sup>34,50</sup>. Clinical toxoplasmosis in dogs is secondary and is initiated by the reactivation of infection in rare context of immunosuppressive therapy; it manifests by neurological, ocular or cutaneous pathologies. Most cats infected with *T. gondii* show no signs of disease, but severe and possibly lethal clinical signs are reported for kittens that acquired infection by vertical transmission. Besides, primo-infection in adult cats could result in appearance of wide range of symptoms, from non-specific to dangerous, associated with acute or generalised toxoplasmosis<sup>50,51</sup>.

### 1.2.6. Diagnosis, treatment and prevention

The diagnosis of *T. gondii* infection relies on the analysis of clinical signs and the assessment of the presence of parasites in the organism. This can be done either indirectly by detection of anti-*T. gondii* antibodies (IgG and IgM) via various serological tests, or directly by detecting DNA (PCR method) or the parasites themselves in biological samples<sup>23,45</sup>. Most commonly, the diagnosis in patients and in animals is based on serological approaches<sup>23,50,52</sup> and is often retrospective. Systematic testing is necessary to determine the immune status of an individual in some specific situations, for instance in pregnant women or in a transplantation setting<sup>23</sup>. While the detection of parasite DNA by PCR is a useful diagnostic approach in humans<sup>23</sup>, it is rarely applied to animals due to the difficulty to extract DNA and concentrate large sample quantities<sup>52</sup>.

Treatment of toxoplasmosis in humans usually includes a combination of pyrimethamine or trimethoprim (inhibitors of dihydrofolate reductase) with sulfonilamides (inhibitors of folic acid synthesis)<sup>29,53</sup>. The vast majority of drugs used in clinical practice against human toxoplasmosis are only effective against the tachyzoite stage and do not completely eradicate infection<sup>53</sup>. It has been demonstrated, however, that several compounds, like guanabenz<sup>54</sup> (commonly used for hypertension treatment) or inhibitors of the calcium-dependent protein kinase 1 (CDPK1)<sup>55</sup>, reduce the number of brain tissue cysts in the murine model. This may offer interesting perspectives for future treatments which are also able to target the bradyzoite stage. As for farm and domestic animals, there is no “golden rule” of toxoplasmosis treatment. Ruminants are treated with antibiotics during pregnancy in order to minimise harmful effects of toxoplasmosis for the fetus<sup>53</sup>, while

the anti-*T. gondii* therapy in cats and dogs includes the combined use of antibiotics (e.g. pyremethamine and sulfonilamides) and symptomatic treatment<sup>51,56</sup>.

The prevention of *T. gondii* infection in human and animals is largely centred around hygiene measures, some of which reduce the risk of consumption of contaminated food and water while the others are aimed to decrease the contamination of the environment with oocysts<sup>53</sup>. Vaccination of human and animals exposed to the risk of *T. gondii* infection could be an effective prophylactic measure. However, with the exception of the Toxovax vaccine for sheep<sup>57</sup>, there is currently no other approved vaccine against animal or human toxoplasmosis<sup>58,59</sup>.

---

## CHAPTER 2. The tachyzoite form of *T. gondii*

---

For several reasons *T. gondii* is an important model to study the biology of apicomplexan parasites. The parasite stage commonly used in the laboratory for this purpose is the tachyzoite. Tachyzoites are amenable to genetic manipulation, can be relatively easily studied by microscopy (for which numerous *T. gondii*-specific sub-cellular markers have been characterised) and, last but not the least, the easy propagation of tachyzoites *in vitro* is highly advantageous for experimentation<sup>60</sup>.

### 2.1. Ultrastructure of the tachyzoite

Tachyzoites are crescent-shaped polarised cells of approximately 6  $\mu\text{m}$  long and 2  $\mu\text{m}$  wide<sup>61</sup> (Fig. 6). A tachyzoite possesses various organelles, some of which are commonly found in eukaryotic cells (such as the nucleus, endoplasmic reticulum, Golgi complex, mitochondrion) while others are Apicomplexa-specific. This second group includes secretory organelles involved in the processes of attachment, invasion and the establishment of the parasite in the host, the endosymbiotic-derived plastid apicoplast and unique cytoskeletal structures.

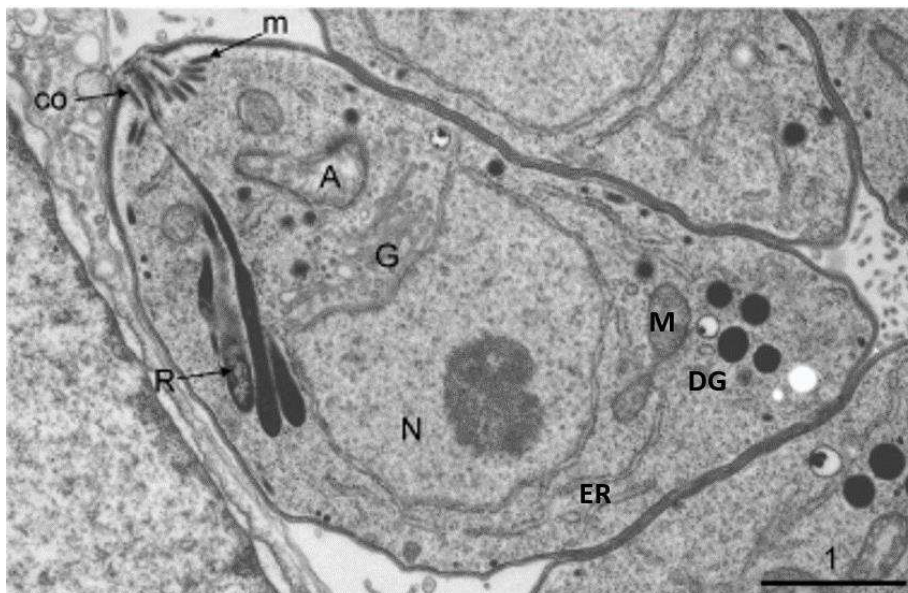


**Figure 6. Electron microscopy image of a *T. gondii* tachyzoite<sup>62</sup>.** The tachyzoite possesses conventional eukaryotic organelles (N=nucleus, G=Golgi, ER=endoplasmic reticulum, M=mitochondrion) and Apicomplexa-specific organelles (A=apicoplast, R=rhoptries, m=micronemes, DG = dense granules). The tachyzoite is a highly polarised cell and has a set of invasion-related organelles (R=rhoptries, m=micronemes) located at the apex, close to a cytoskeletal structure called the conoid (co), as part of a specific apical complex. Scale bar is 1 $\mu\text{m}$ .

### 2.1.1. Conventional organelles

#### ***The nucleus***

Tachyzoites are haploid and their genetic information is concentrated in the nucleus, occupying the central part of the cell, as well as in two endosymbiosis-derived organelles: the mitochondrion and the apicoplast<sup>61</sup>. The nuclear DNA of over 60 Mb is distributed between 13 chromosomes<sup>63</sup> and contains more than 8000 genes<sup>64,65</sup>. A global genetic screen of Sidik et al.<sup>66</sup> provided information on the contribution of each gene for *T. gondii* fitness, but the function of a large part of the proteins encoded by these genes is still unknown.

#### ***The mitochondrion***

In contrast with many eukaryotes, *T. gondii* possess a single lasso-shaped ramified mitochondrion with a severely reduced genome that encodes only for three proteins and for ribosomal RNAs<sup>67–69</sup>. Eukaryotic mitochondria are multifunctional organelles classically considered as the “power stations” of the cell due to their role in producing adenosine triphosphate (ATP) in the tricarboxylic acid (TCA) cycle<sup>70</sup>. *T. gondii* tachyzoites develop in a relatively glucose-rich environment and may survive on the energy supply solely derived from glycolysis<sup>71</sup>. Nevertheless, intracellular tachyzoites actively catabolize host glucose via a canonical TCA cycle<sup>72</sup>. The *T. gondii* mitochondrion is also involved in other pathways, such as pyrimidin and heme biosynthesis<sup>69</sup>, and has been described as essential for parasite survival<sup>72,73</sup>.

Once the tachyzoite is exposed to extracellular conditions, the mitochondrion does not lose its functionality but undergoes morphological changes and retracts from the periphery of the cell where it is normally localised in the intracellular parasites<sup>67,74</sup>. The precise mechanism of these reversible changes is unknown<sup>74</sup>.

#### ***The endoplasmic reticulum and the Golgi apparatus***

The endoplasmic reticulum (ER) and the Golgi apparatus are part of the endomembrane network of *T. gondii* and are responsible for protein trafficking in the cell<sup>75</sup>. The ER is found throughout the cytoplasm but is mainly concentrated on the posterior perinuclear area in such manner that the nuclear envelope provides a considerable part of the ER volume. The single Golgi stack in tachyzoite consists of a limited number of cisternae,

usually from three to five, and is positioned anteriorly to the nucleus, adjusted to the single ER exit site. Protein trafficking from the ER to the Golgi apparatus occurs via the apical end of the nuclear envelope, which thus represents an intermediate compartment between the ER and Golgi apparatus, in contrast to the mammalian cells where ER is dispersed throughout the cytoplasm<sup>75,76</sup>. The biogenesis of Apicomplexa-specific secretory organelles (as well as some cytoskeletal compartments) is thought to be driven by vesicular trafficking from the Golgi stack<sup>75,77</sup>.

### 2.1.2. Apicomplexa-specific organelles

#### *The secretory organelles: micronemes, rhoptries and dense granules*

The apical part of the tachyzoite harbours an assembly of structures involved in the polarised attachment to the host cell and its active, motility-driven invasion by the parasite<sup>61</sup>. The sequential release of specific molecules from morphologically distinct secretory organelles is instrumental for both processes<sup>78</sup>. Amongst these organelles, there are small rod-like micronemes, which are concentrated in the most apical part of the parasite<sup>79</sup>, and club-shaped membrane-bound rhoptries, extended from within the apical tip towards the nucleus<sup>62</sup> (Fig. 7).

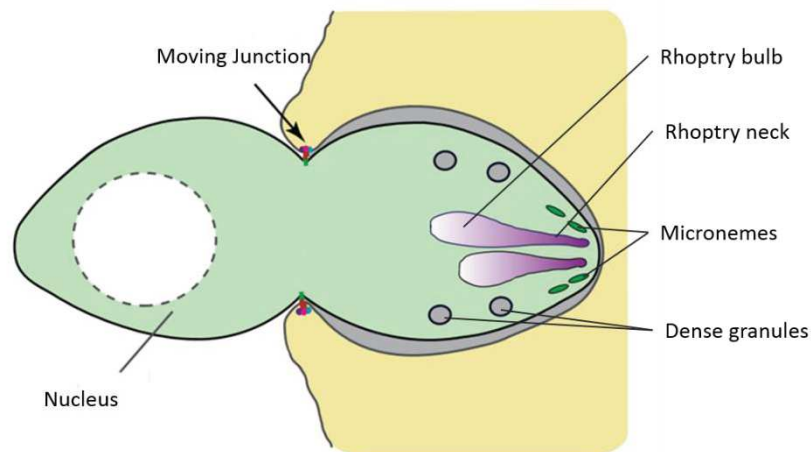


**Figure 7. Schematic representation of *T. gondii* secretory organelles<sup>80</sup> (micronemes, rhoptries and dense granules) and the key Moving Junction structure at the host cell (yellow)/parasite (green) interface during the invasion process.**

The exocytosis of micronemal proteins (MICs) occurs in extracellular tachyzoites as the first step of the invasion process<sup>62</sup>. The MICs are translocated to the tachyzoite plasma membrane and establish a connection with the parasite's actin-myosin motor, thus supporting

tachyzoite's gliding motility; furthermore, the MICs adhesive domains interact with receptors on the surface of the host cell, and participate in the parasite's attachment to it<sup>81</sup>.

The contents of rhoptries are secreted following the initial MICs-mediated attachment step, once the apical part of tachyzoite is in contact with the host cell membrane<sup>82</sup>. The rhoptries contain two distinct sets of proteins segregated either in the anterior part of the organelle, the neck (RONs, the rhoptry neck proteins) or in its posterior part, the bulb (ROPs, rhoptry bulb proteins)<sup>83</sup>. RONs are released first and, together with microneme protein AMA1 (the apical membrane antigen 1) contribute to the formation of a so-called "Moving Junction" (MJ)<sup>84</sup> (Fig. 7). This ring-like structure represents a tight apposition between the parasite's and the host's plasma membranes and, as the tachyzoite propels itself into the host cell, the MJ relocates from the apical tip towards the posterior end of the parasite<sup>85</sup>. Not only the MJ ensures the anchoring for a successful entry of the parasite into the host cell, but it also forms a molecular sieve that likely controls the internalisation of host cell plasma membrane components into the forming parasitophorous vacuole (PV). The PV is a non-phagosomal protective membrane-bound compartment that will eventually contain the intracellular parasite after a successful invasion<sup>85</sup>. ROPs are secreted later on and target either the PV membrane or are injected in the host cell in order to subvert the host cell response towards *T. gondii*<sup>82</sup>.

The third type of tachyzoite secretory organelles is the dense granules (DGs) which can be found throughout the cytosol, but mostly in the posterior end of the parasite. The dense granules proteins (GRAs) are secreted shortly after invasion and play an important role in the formation and modification of the PV for long term establishment of the parasite<sup>86</sup>.

### ***The apicoplast***

The apicoplast is yet another Apicomplexa-specific organelle. This plastid appears as a small ovoid four-membrane compartment positioned anterior to the nucleus of tachyzoites<sup>87</sup> (Fig. 6). Together with the mitochondrion, the apicoplast contains extra-chromosomal DNA (around 35 Kb)<sup>88</sup>. The apicoplast is essential for the survival of tachyzoites: interfering with the organelle function using antibiotics (first shown with bacterial DNA replication machinery inhibitor ciprofloxacin<sup>89</sup>) results in a so-called "delayed death" phenotype. Affected tachyzoites are able to replicate in the host cell, to egress and to reinvade surrounding cells

but then fail to replicate efficiently<sup>90</sup>. This is probably due to an initial ability of parasites to share essential metabolites within the same vacuole in spite of partial apicoplast loss, but individual apicoplast-less parasites are then unable to survive after a new round of invasion<sup>81</sup>.

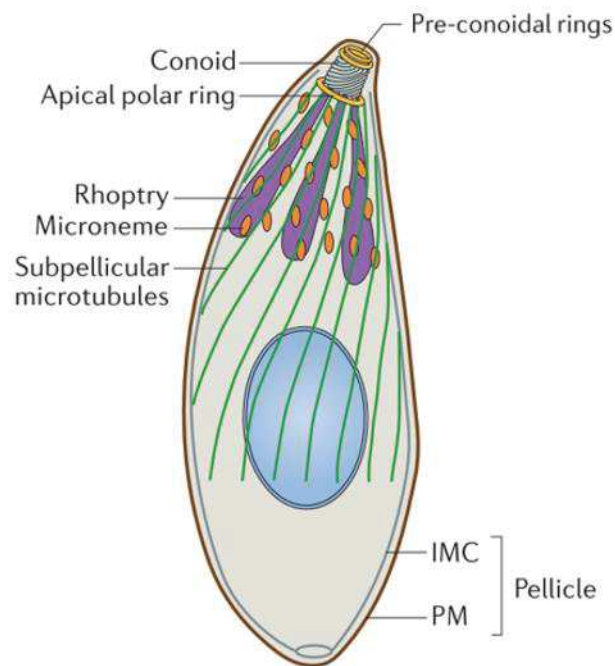
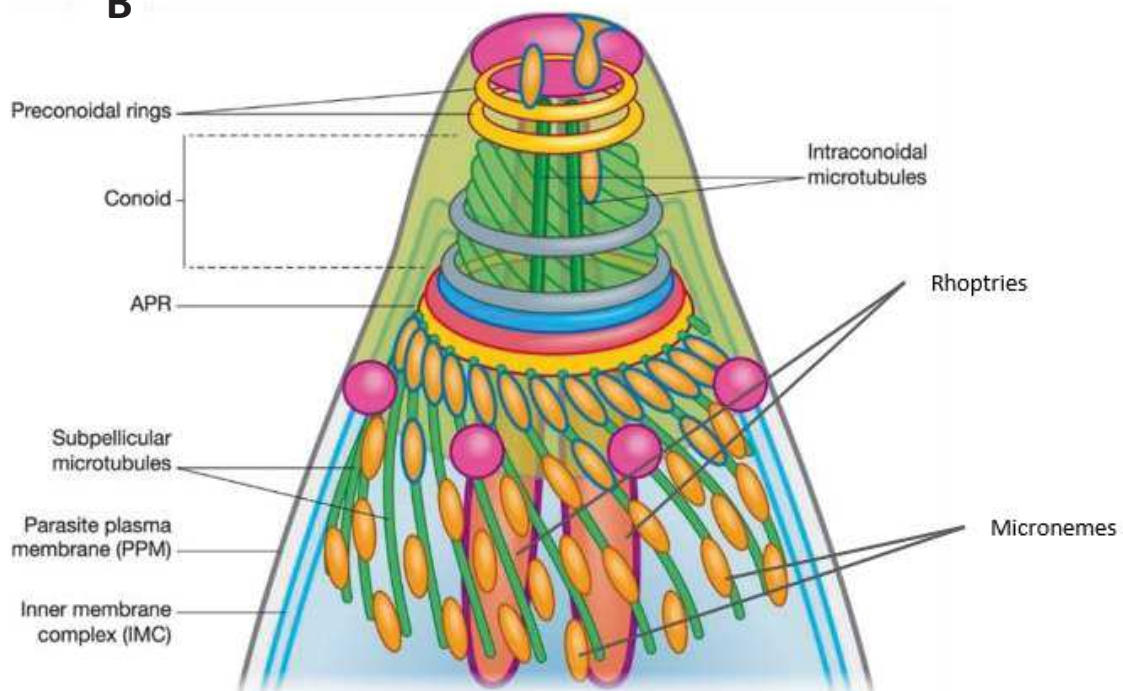
Despite its algal origins<sup>91</sup>, the apicomplexan plastid has lost its photosynthetic ability with the adoption of a parasitic way of life<sup>92</sup>. However, it is involved in several important metabolic pathways and together with the mitochondrion contributes considerably to parasite's metabolic needs<sup>68</sup>. Apicoplast is involved in the biosynthesis of: i) isoprenoid precursors, ii) iron-sulphur complexes, iii) haem (together with the mitochondrion) and iv) fatty acids (essential for the survival of tachyzoites<sup>93</sup>)<sup>68</sup>.

### ***The cytoskeleton***

The cytoskeleton of apicomplexan parasites in general, and of *T. gondii* in particular, represents a mixture of typical eukaryotic traits with phylum-specific features. *T. gondii* shares some basic cytoskeletal components, such as tubulin, actin and myosin, with eukaryotic model organisms. Nevertheless, there is a considerable difference in protein composition and organisation of the cytoskeletal network. Furthermore, the parasite has acquired several peculiar structures, including cytoskeletal elements of the apical complex, as well as a trimembrane pellicle of the cortical cytoskeleton of a tachyzoite<sup>94</sup> (Fig. 8).

The pellicle covers the surface of the tachyzoite and is composed of the plasma membrane and an underlying complex of single membraned flattened vesicles with their associated protein mesh - the Inner Membrane Complex (IMC)<sup>61</sup>. The IMC runs along nearly the entire length of the tachyzoite without completely enclosing the apical and the basal end of the cell<sup>97</sup>. The cytoplasmic face of the IMC associates with underlying subpellicular microtubules (MTs) that expand to the two-thirds of parasite's length<sup>98</sup>. One obvious function of the pellicle consists in maintaining shape, polarity and structural stability of the tachyzoite. It is also linked to the actin-myosin motor and thus supports the glideosome-mediated motility of extracellular parasites<sup>99</sup>. Finally, it plays a role in daughter cells assembly during division<sup>100</sup>.

The parasite's apical complex fills the anterior gap of the IMC<sup>101</sup> and includes rhoptries and micronemes (secretory organelles that were described previously), and cytoskeleton elements<sup>102</sup> that are organised around a structure called the conoid. The conoid is a hollow cone-like structure of 380 nm in diameter and 280 nm in length<sup>103</sup>. It comprises tubulin fibers

**A****B**

**Figure 8. The schematic representation of the *T. gondii* cytoskeleton<sup>95,96</sup>.** (A) General view of the cytoskeleton in a tachyzoite. The pellicle, composed of the plasma membrane (PM) and the inner membrane complex (IMC), is linked to the underlying subpellicular or cortical microtubules and actin-myosin motor (not shown). The cytoskeletal elements of the apical complex are located on the extreme anterior tip of the parasite. (B) The apical complex comprises the cytoskeletal structures (conoid, two preconoidal rings, an apical polar ring (APR) from which originate the subpellicular microtubules, and two intraconoidal microtubules), and the apical secretory organelles: micronemes and rhoptries.

organised in a unique ribbon-like polymer that is quite different from canonical MTs<sup>104</sup>. The conoid is topped by two fibrous preconoidal rings, from which the conoid's fibers originate, and is limited by an apical polar ring (APR) at the bottom. The APR serves a microtubule-organising centre (MTOC) for subpellicular MTs<sup>98,104</sup>. In addition, two short canonical MTs are located inside the conoid<sup>103</sup>. The conoid is a highly dynamic structure capable of calcium-dependent extrusion from/retraction into the APR<sup>105</sup> and plays a role in the motility and invasion of the parasite<sup>105–107</sup>.

## 2.2. The lytic cycle of tachyzoites

While tachyzoites efficiently replicate within virtually any type of nucleated cell, they do not survive outside the host cell for prolonged periods of time. Once their replication inside the host cell is completed, the host cell is ruptured and tachyzoites are exposed to the extracellular environment, they actively invade a new batch of cells and sequentially proliferate within. This repetitive 3 stepped-process of egress, invasion and intracellular replication is known as the lytic cycle of *T. gondii*<sup>108</sup> (Fig. 9).

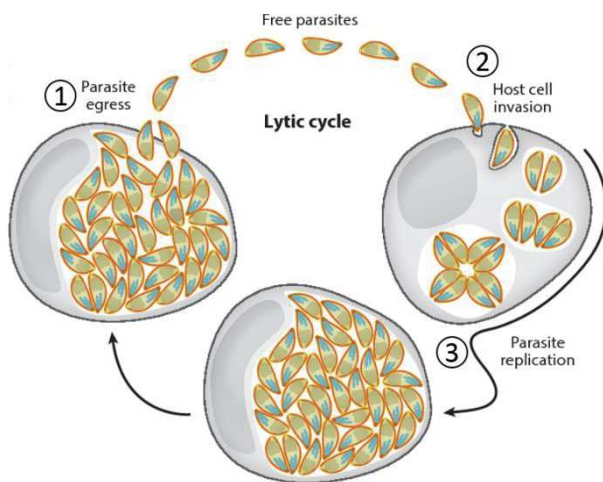


**Figure 9.** The lytic cycle of *T. gondii*<sup>109</sup> includes: (1) the egress of tachyzoites from the host cell; (2) the invasion of the fresh host cells by the highly motile extracellular tachyzoites; (3) the following intracellular replication of the parasite.

### 2.2.1. Egress

Tachyzoites' egress from the host cell is an active process and may be triggered by several factors that go beyond a simple mechanical rupture of the host cell overloaded with replicating parasites<sup>109,110</sup>. Noteworthy, egress is accompanied by a drop of the pH inside the PV and the activation of a Ca<sup>2+</sup> signaling pathway. The increase in the parasite's cytoplasmic Ca<sup>2+</sup> concentration is due to its release from intracellular stocks. Egress is also accompanied by the decrease of the host's cytoplasmic K<sup>+</sup> concentration<sup>109</sup>. Altogether these events allow the secretion of MICs (e.g. the perforin-like protein 1, PLP1, involved in pore formation in the

PV and in the host cell plasma membrane at low pH) and promote the motility of the parasite<sup>111–113</sup>. Thus, during egress ([Fig. 10](#)), tachyzoites push and permeabilise the PV membrane, enter the host cell's cytosol and move towards the periphery of the host cell. In the beginning of the migration, tachyzoites drag the remnants of the PV and of host's ER and eventually lose them when approaching the host cell plasma membrane. The host plasma membrane may reseal following the parasite's passage through it or be lysed instead in case of massive egress<sup>114</sup>.

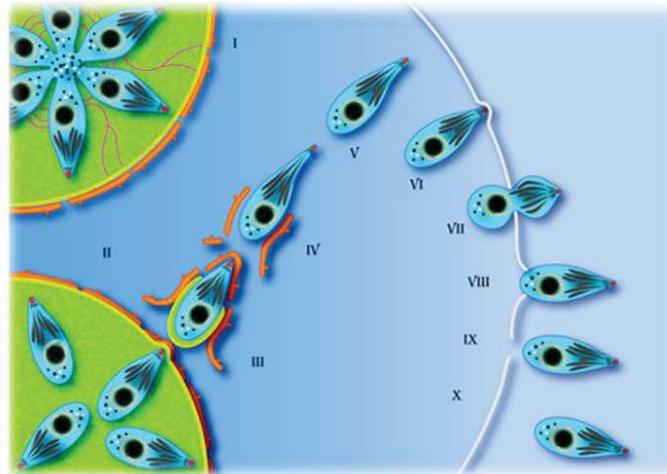


**Figure 10.** *Egress of tachyzoites from the host cell*<sup>114</sup>. When egress is triggered, the intracellular tachyzoites (I) lose their characteristic spatial organization within the parasitophorous vacuole (II) and move out of the PV, dragging it and the host ER on their surface (III). During the migration through the cytosol tachyzoites may change their form, stretching and retracting (IV) and eventually lose the remnants of PV and ER while approaching the host cell plasma membrane (V, VI). During the passage through the host plasma membrane the parasite assumes the shape of hourglass (VII). The successful egress of the parasite (VIII, IX, X) defines its passage to the extracellular form.

### 2.2.2. Invasion

By contrast to the rapidly dividing and non-motile intracellular tachyzoites, non-replicating extracellular tachyzoites actively move in the environment using a specific form of substrate-dependent locomotion that relies on their actin-myosin system. The details of this process known as the gliding motility are shown on the [Fig. 11A](#)<sup>95</sup>.

The initial attachment of the parasite's apical tip to the new host cell is mediated by the interaction between some parasite's surface protein coat (SAGs or surface antigens) and host's proteoglycans. This primary contact is followed by the release of micronemal and rhoptry proteins, and a formation of the MJ<sup>109</sup> ([Fig. 11B](#)). As the MJ is established and the invasion continues, the tachyzoite propels itself into the host cell simultaneously forming

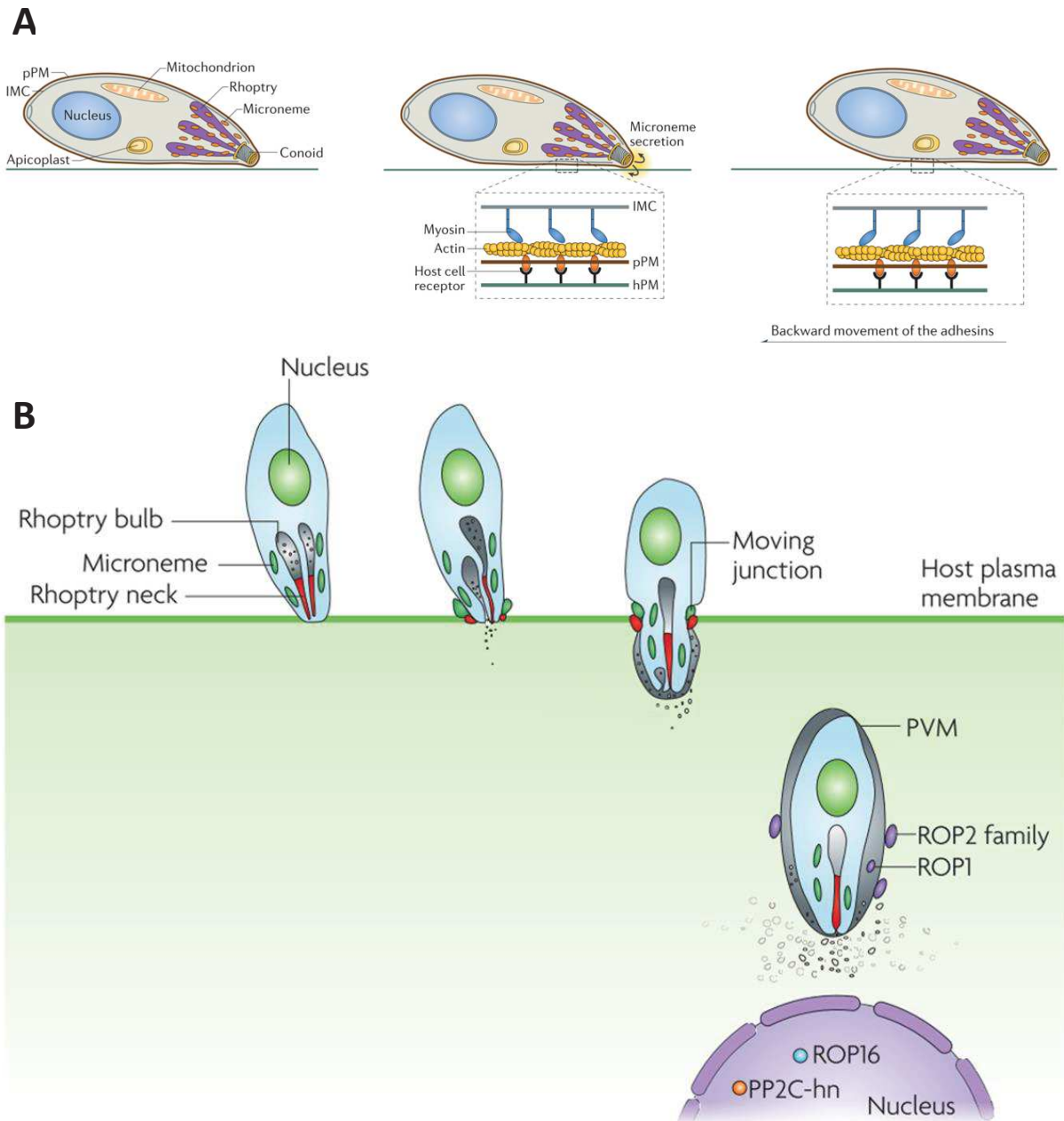


**Figure 11.** A model of the tachyzoite's gliding motility<sup>95</sup> and host cell invasion<sup>82</sup>.

**(A) Gliding motility.** The microneme adhesive proteins (orange) are secreted in the apical tip of the parasite and are embedded in the parasite plasma membrane. They interact with the host cell surface receptors (black). The gliding motility is a result of a backward translocation of the adhesin-receptors complexes; this movement is supported by an actin-myosin system (yellow and blue, respectively) positioned between the parasite's plasma membrane and the inner membrane complex. IMC = inner membrane complex, pPM = parasite plasma membrane, hPM = host plasma membrane.

**(B) Invasion.** From left to right: the attachment of the tachyzoite to the host cell is followed by the release of the content of secretory organelles (see the text), the formation of the Moving Junction by coordinated interaction of AMA1 (microneme protein) with RON2, RON4 and RON5 (rhoptry neck proteins) and the progressive entry of the parasite into the host cell and its incorporation into the forming parasitophorous vacuole. The rhoptry bulb proteins ROP2 and ROP1 target, respectively, the membrane and lumen of PV while ROP16 and PP2C-hn are secreted beyond the PV membrane and target proteins in the host cell nucleus.

the PV by invagination of the host plasma membrane<sup>115</sup>. Invasion, like egress, is a rapid process and may be completed within less than 60 sec following the tachyzoite initial attachment to the host cell<sup>110</sup>.

### 2.2.3. Intracellular replication

The intracellular tachyzoites encapsulated in the PV actively proliferate by a specific mode of division termed endodyogeny. Through this highly coordinated process a single round of DNA replication is followed by the assembly of two daughter cells within the mother cell, which disappears at the very end<sup>116</sup> (Fig. 12). The endodyogeny and its regulation are detailed in Chapter 4.

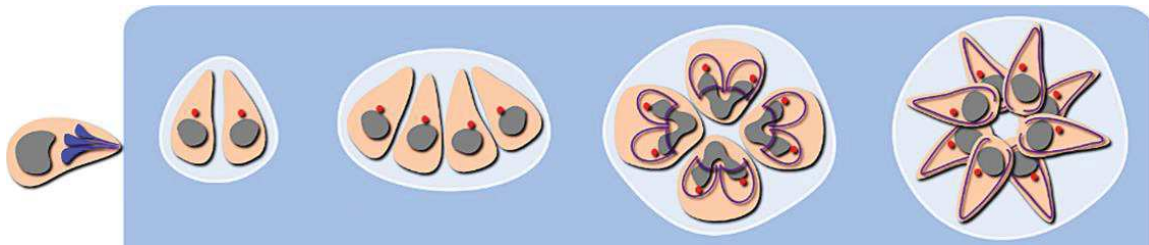


**Figure 12.** *T. gondii* tachyzoite replication scheme<sup>117</sup>. The successive rounds of parasite's division by endodyogeny lead to the rapid accumulation of  $2^n$  parasites inside the parasitophorous vacuole. The nuclei of the cells are indicated in grey, a key regulatory structure of the division process, the centrosome, is in red and the daughter cells, that are forming inside the mother following the DNA duplication, are contoured in violet.

A single round of tachyzoite division takes up to 6 or 8 hours<sup>118</sup>. Parasites within the same PV are tightly synchronised with each other in their replication process, and may accumulate up to 128 cells per PV in *in vitro* conditions<sup>109</sup>. At some point, the egress of tachyzoites is triggered and the lytic cycle is thus complete.

---

## CHAPTER 3. The cytoskeleton of *T. gondii*

---

The pellicle with its system of flattened vesicles (alveoli) underlying the plasma membrane is a trademark of Alveolata protists<sup>6</sup> (Fig. 13). The alveoli support both the structural stability of the cell and its dynamic structures, and are adapted to the particular lifestyles and environments of these protists<sup>119</sup>. For instance, in free-living micropredators ciliates it supports the motility via the anchored cilia whose beating is coordinated by alveoli-linked microtubules; it also serves as calcium storage<sup>120</sup>. A large number of dinoflagellate species developed a rigid protective armour out of their alveoli that contains cellulose or other polysaccharides<sup>121,122</sup>. In Apicomplexa the alveoli system is termed the IMC and structural and motile functions of the pellicle altogether have evolved specific adaptations related to the parasitic lifestyle<sup>94,121,123,124</sup>.

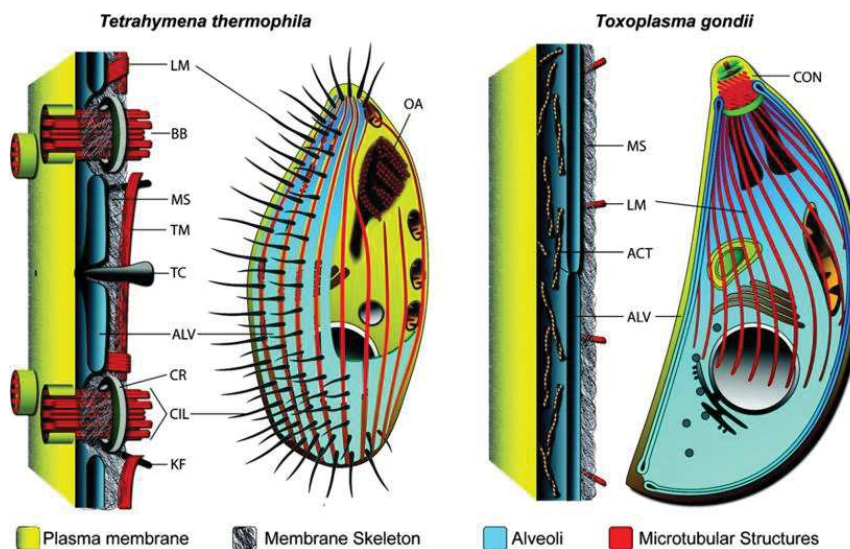


**Figure 13.** Schematic representation of the pellicle in Ciliophora (*T. thermophila*) and in Apicomplexa (*T. gondii* tachyzoite)<sup>119</sup>. The similar pellicular substructures are shown with the same color: the plasma membrane is the outer leaflet (yellow); the underlying alveolar sacs (blue) are associated with longitudinal (LM) and transverse (TM) microtubules (red) and supported by a membrane skeleton (grey). BB = basal body; TC = trichocyst; CR = circumciliary rings; CIL = cilia; KF = kinetodesmal fibers; CON = conoid; ACT = actin filaments.

### 3.1. The inner membrane complex

The IMC in *T. gondii* tachyzoites covers almost the entirety of the parasite and has a conserved characteristic pattern elucidated by freeze fracture electron microscopy<sup>97,98,125</sup> (Fig. 14). On the apical part of the structure lies a single cone-like vesicle of

approximately 1 $\mu$ m (the apical cap); it is followed by three or four longitudinal rows of six rectangular flattened vesicles (plates) that are joined together in a puzzle-like manner (Fig. 15A, C). The longitudinal and the transversal lines at the junctions between the plates are known as sutures. The patchwork of IMC vesicles does not expand above conoid on the apex of the parasite and narrows at the basis to form a turbine-like structure<sup>94</sup>. The apical, the central and the basal sub-compartments of the IMC as well as the longitudinal and transversal sutures hold a distinctive protein composition<sup>100,126–132</sup>.

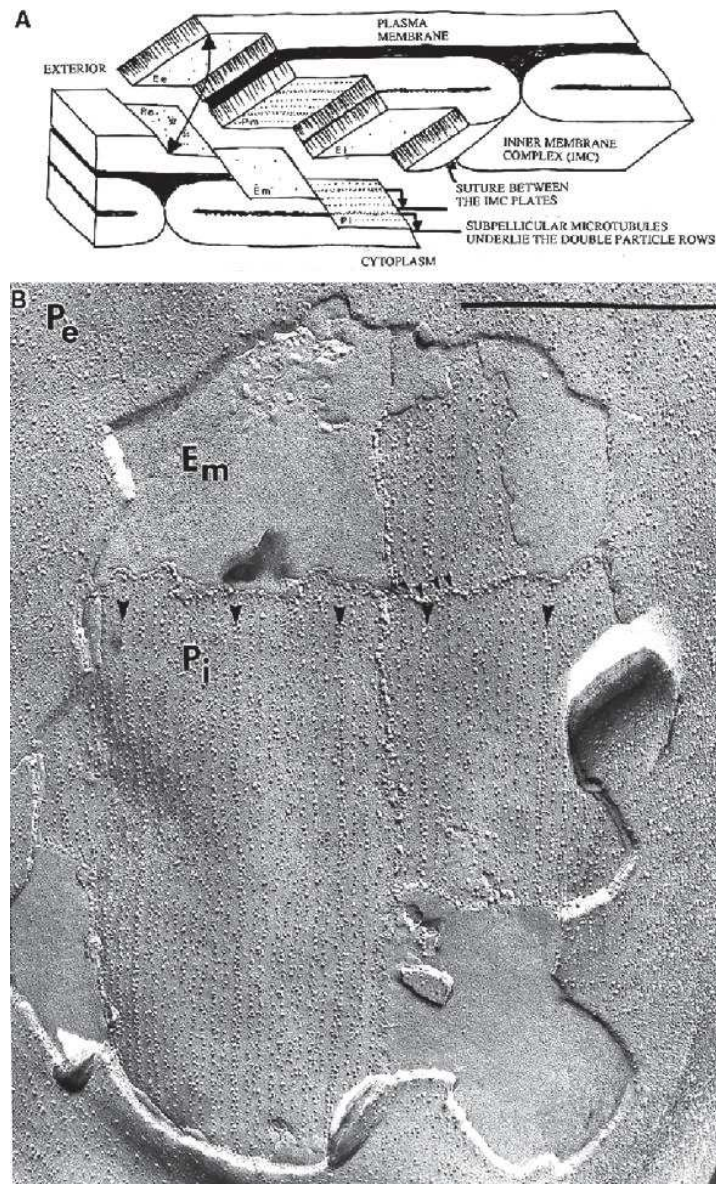


**Figure 14.** IMC morphology in *T. gondii* assessed by freeze-fracture electron microscopy<sup>98</sup>. (A) Freeze-fracture planes of *T. gondii* pellicle comprise three membrane bilayers. Six fracture faces include the P faces adjacent to the protoplasm and the E faces adjacent to the exterior. (B) Freeze-fracture replica of *T. gondii* showing IMP rows in the inner membrane complex. The double IMP rows (thought to overlie the subpellicular microtubules) are indicated by large arrowheads. The sutures between plates are indicated by small arrowheads. e, exterior; m, middle; i, inner. Bar, 0.5  $\mu$ m

On its plasma membrane face the IMC is linked to the actin-myosin motor complex (also called glideosome) responsible for the gliding motility of the parasite and related to the invasion process<sup>133,134</sup> (Fig. 15D).

The cytoplasmic face of the IMC is lined with the mesh of interwoven 8-10nm filaments forming a subpellicular network (SPN) and is linked to the underlying subpellicular MTs<sup>98,101</sup> (Fig. 15B). Within the alveoli, continuous on the entirety of the inner surface of both leaflets there are double and single rows of the intramembrane particles (IMPs) organised with a 32-nm periodicity in concordance with the periodicity of microtubules<sup>98</sup>. The functional significance of these IMPs remains to be described<sup>126</sup>. Their precise arrangement suggests IMPs potential role as connectors between the IMC and subpellicular microtubules-associated proteins (MAPs)<sup>98</sup>; however, the IMPs run the entire length of the parasite contrarily to the MTs and thus could interact with the SPN proteins instead<sup>98</sup>.

For a structure of tremendous importance for all the steps of tachyzoite's lytic cycle, the protein composition of the IMC is still relatively undercharacterised. Nevertheless, a number of recent studies have allowed the identification of several new IMC-associated protein groups in this particular parasite stage.

The IMC-associated proteins are heterogeneously distributed between the subcompartments and the leaflets of the structure (see Annexe 1 for the list of identified proteins), with some amongst them localising directly to the alveoli. For instance, the members of the ISP (for IMC subcompartment proteins) family are detergent-soluble proteins associated with the alveoli membrane via myristoylation and palmytoylation<sup>127,135</sup>. Some of the ISPs are anchored to the entire length of the IMC while the others are specific to the apical cap (like ISP1) or to the central region (like ISP2)<sup>127</sup>. Proteins of the gliding machinery, the GAPs (gliding-associated proteins), namely GAP40<sup>136</sup>, GAP45<sup>133</sup> with its two additional orthologues GAP70<sup>136</sup> and GAP80<sup>137</sup>, and, finally, GAP50<sup>133</sup> are also detergent soluble and connect the IMC plates with the components of the actin-myosin complex.

By contrast to the alveoli membrane-associated proteins, those linked to the SPN are highly resistant to detergent extraction in mature tachyzoites<sup>101,128,130,131,138</sup>. The proteins making up the SPN filaments themselves are termed alveolins or articularin-like proteins or IMC proteins in *T. gondii*. IMC1, 2, 3 and 4 were identified by different approaches in the early

2000s<sup>101,103,139</sup>. Three amongst them carried a series of valine- and proline-rich domains which were later named alveolin repeats and were demonstrated to be conserved throughout the Alveolata<sup>140</sup>. In a systematic study, Anderson-White et al.<sup>128</sup> identified and characterised 14 members of the IMC family that localize on the different sub-compartments of the SPN in mature *T. gondii* tachyzoites or are recruited to the elongating daughter scaffold during parasite division. Furthermore, a proximity-dependent biotin identification (BioID) strategy allowed the identification of novel proteins that reside in the IMC cytoskeleton, thus expanding the family to over 30 members<sup>131</sup>. The tethering of the SPN components to the gliding machinery is likely mediated by members of the GAPM (Glideosome-Associated Protein with multiple-Membrane spans) family of transmembrane proteins, since the GAPMs co-immunoprecipitate with alveolins and with actin-myosin motor to some degree<sup>141</sup>. Apicomplexa-specific family members, such as GAPM1a, GAPM2a and GAPM3, are highly expressed in mature tachyzoites and largely contribute to the parasite's fitness<sup>141,142</sup>. Several other cytoskeletal proteins also interact with the IMC indirectly, including plasma membrane adhesins linked to the gliding machinery<sup>143</sup>, or proteins localised to the apical cap of the IMC (e.g. TgDLC1 for Dynein Light Chain 1 protein)<sup>103</sup>, or detergent insoluble basal proteins, like TgPHL1 (photosensitised INA-labeled protein 1)<sup>144</sup>.

Of note, the molecular composition of the sutures delineating the IMC plates has only started to be identified quite recently<sup>129-132</sup>. Though the first suture-specific protein has been independently characterised by two research groups about 5 years ago<sup>129,130</sup>, two major groups of suture-linked proteins – the ISCs (IMC suture components) and the TSCs (Transverse Suture Components) - have since then been defined by BioID-based approaches<sup>131,132</sup>. Intriguingly, the longitudinal and the transversal sutures are continuously labelled by proteins that associate either with the alveoli membrane or with the underlying cytoskeletal elements of the IMC. The organisation of the sutures as well as the precise anchoring mechanism of these proteins are yet to be identified.

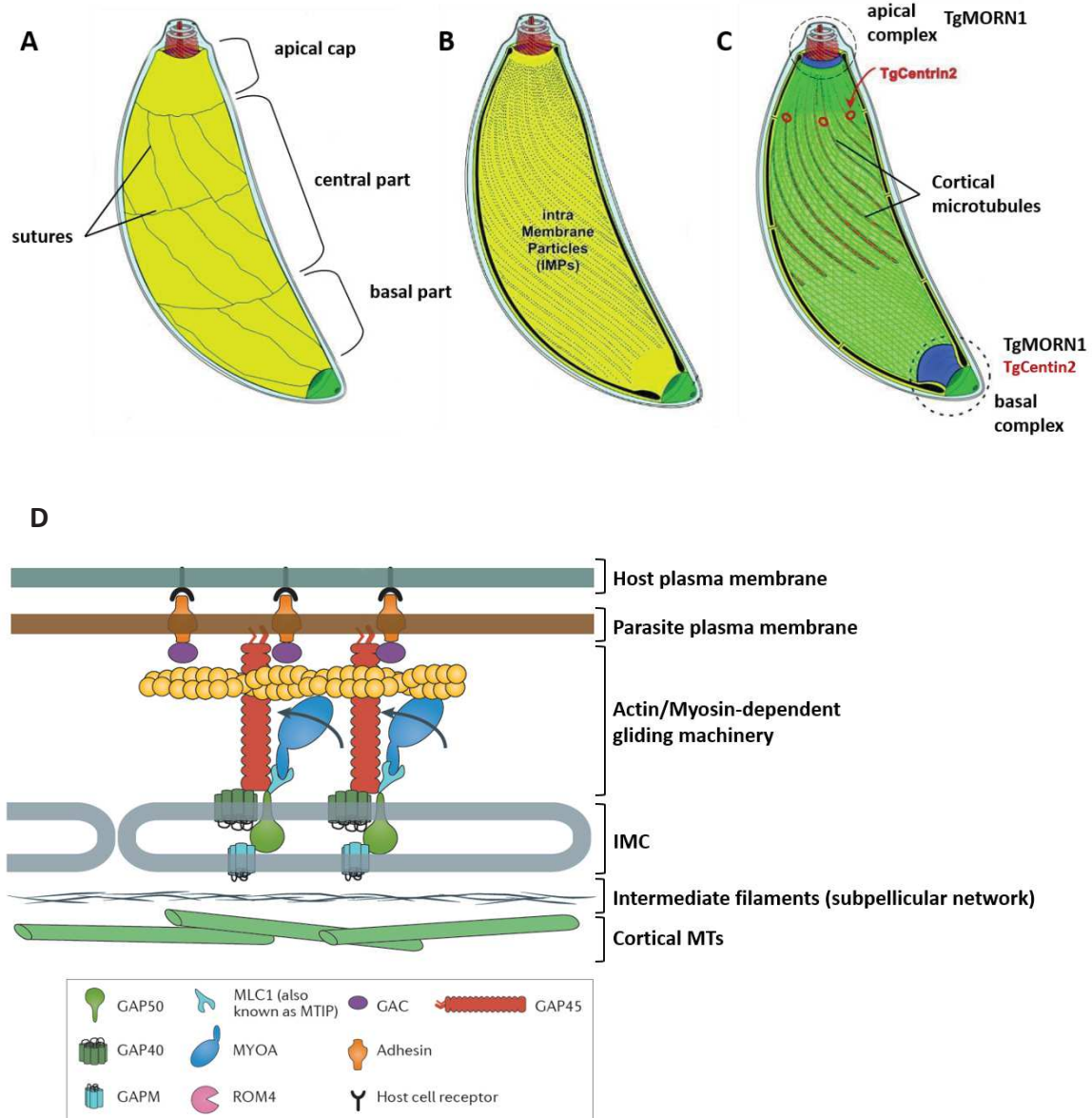


**Figure 15. Schematic representation of the IMC structure in a mature *T. gondii* tachyzoite<sup>95,100</sup>.** (A) IMC is composed of rectangular flattened vesicles underlying the cytoplasm. The different sub-compartments with distinctive protein composition are marked on the scheme. The plasma membrane surface of the IMC is associated with the actin-myosin motor (not shown). (B) The inner surface of the IMC vesicles contains the rows of IMPs arranged in concordance with periodicity of subpellicular MTs. (C) The cytoplasmic surface of the IMC is linked to the meshwork of intermediate filament-like proteins (in green) and the cortical MTs (red lines). The apical complex and the basal complex fills, respectively, the anterior and posterior gaps of the IMC. Both complexes harbor the TgMORN1 and TgCentrin2 proteins. (D) Cross section of the IMC and its associated sub-structures. The glideosome (the machinery mediating *T. gondii* gliding motility) is embedded in the IMC and linked to the plasma membrane.

## 3.2. Microtubules in tachyzoites

MTs are indispensable components in *T. gondii* tachyzoites. Altogether, they contribute to the motility, invasion and replication of the parasite, acting therefore at different steps of the lytic cycle and being essential for parasite survival. There are five reported tubulin-harboring structures in tachyzoites: the mitotic spindle, the centrioles, subpellicular (or cortical) MTs, the conoid, and the intraconoidal MTs<sup>37</sup>. In contrast to other eukaryotic models where the different MT sub-populations are controlled by a single MTOC, the two main subpopulations of MTs, the subpellicular and the spindle MTs have distinct MTOCs in *T. gondii*<sup>145</sup> (Fig. 16). Altogether, there are four MTOCs in the tachyzoite cell, amongst which the APR and the conoid located on the apically in the parasite organise the subpellicular microtubules, while the centrocone and the centrosome are in charge for the mitotic spindle<sup>146</sup>. The current section describes the subpellicular MTs.

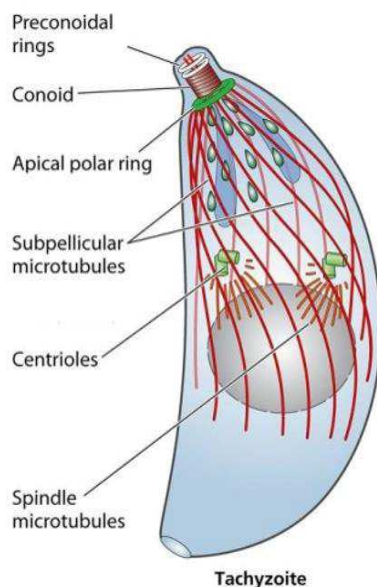


**Figure 16. Microtubules-based structures in a *T. gondii* tachyzoite<sup>37</sup>.**

*Subpellicular MTs cover the 2/3 of the parasite. The apical polar ring is its specific Microtubules-Organising center (MTOC).*

*Spindle microtubules, together with microtubule-based centrioles, are crucial to the cell division process.*

*The apical part of the parasite harbors another microtubular structure, the conoid, located between the apical polar ring (APR) and two preconoidal rings. It contains two intraconoidal microtubules.*

### 3.2.1. Subpellicular microtubules

The subpellicular or cortical MTs constitute the second main component of the cortical cytoskeleton in *T. gondii*. They impose the tachyzoite shape and polarity and play a considerable role in motility and invasion<sup>37</sup>. 22 MTs of  $\sim 5\mu\text{M}$  long<sup>145</sup> originate from the APR – the apical MTOC at the base of the conoid – and extend in left-handed spirals to the two-thirds of the parasite length, just beneath the SPN and the intern leaflet of the IMC (Fig. 15C).

The cortical MTs in *T. gondii* are composed of  $\alpha$ - and  $\beta$ -heterodimers that assemble in a hollow cylinder-like polymer; the slow-growing minus end of the tubules terminates in  $\alpha$ -subunits and is embedded in the APR while the fast-growing plus-end (terminating in  $\beta$ -subunits) remains free in a mature parasite<sup>37</sup>. The *T. gondii* genome encodes three  $\alpha$ - and three  $\beta$ - tubulin isotypes (differing slightly in their amino acid sequence), and their expression levels vary in the tachyzoites, bradyzoites and oocysts stages. The  $\alpha$ 1-  $\beta$ 1-isoforms are suggested to constitute the prominent population of tubulin heterodimers<sup>147</sup>. The  $\alpha$ 1- and  $\beta$ 1-tubulin subunits in *T. gondii* are largely conserved relatively to human cells (>85% identity and >90% similarity)<sup>148</sup>. Additionally to  $\alpha$ - and  $\beta$ -heterodimers, *T. gondii* also possesses a single-copy gene encoding for  $\gamma$ -tubulin related to the centrosome<sup>146</sup>.

MTs in apicomplexan parasites are remarkably stable, resisting to the conditions that typically induce the disassembly of MTs in other eukaryotes (like cold treatment and detergent extraction)<sup>98</sup>. This unusual property could be explained by the tight connection between the IMC scaffold and the MTs network. As mentioned previously, this connexion is thought to be provided by a group of MAP proteins linked to the IMP and organised with the same periodicity. MAPs decorate the MTs in a complex and varied patterns<sup>148</sup> and may be exclusively found on a larger or smaller part of the cortical MTs (like subpellicular MTs proteins SPM1/2, or Thioredoxin-like protein 2, TrxL2, or TLAPs, for TrxL1-associating proteins)<sup>148,149</sup>, or otherwise may localise to both cortical and intraconoid MTs (for example, TrxL1<sup>148,150</sup>). Simple, double and even triple knockout of some MAPs does not lead to any major defect of the cortical MT network, although knockouts of SPM1, TLAP2 and TLAP3 increase the sensitivity of MTs to the detergent treatment. It suggests that MAPs are either not crucial for MTs arrangement, or that their function is highly redundant<sup>94,148–150</sup>.

### **3.3. The cortical cytoskeleton development during *T. gondii* division**

In contrast to mature IMC and subpellicular MTs, the nascent ones are highly dynamic. In fact, their assembly drives the daughter cells formation during the replication of *T. gondii*, a process for which they are clearly essential<sup>100</sup>. In accordance, the disruption of either MTs or the IMC leads to a dysfunctional daughter budding and to several organelles segregation-related defects.

For instance, the inhibition of subpellicular MTs polymerisation (which can be targeted by several drugs<sup>145,151–154</sup>) results in the block of daughter scaffold elongation and in nuclear missegregation<sup>145,151</sup>. *T. gondii* MTs are selectively susceptible to disruption by dinitroanilines, such as oryzalin: upon treatment, productive daughter formation repeatedly fails resulting in an undivided, amorphous mother cell with a polyploid DNA content<sup>145</sup>. Depleting genes encoding for IMC-related proteins (like ISP2) also leads to cell division defects, sometimes coupled with the missegregation of organelles like the apicoplast<sup>127,155</sup>.

At the onset of daughter cells formation, new cytoskeletons assemble within the cytoplasm of the mother cell and elongate rapidly (Fig. 17) in a strictly coordinated manner<sup>156</sup>. Thus, inhibiting cortical MTs polymerisation leads to a lack of functional IMC in progeny<sup>127</sup>. MTs in the daughter cells are *de novo* synthesised. As for the daughters IMC, according to Ouologuem and Roos<sup>157</sup>, its formation involves both neosynthesis and recycling from the mother IMCs at later stages of daughter cell assembly. The biogenesis of the IMC is also tightly associated with vesicular trafficking (clathrin-coated vesicles derived from the ER-Golgi secretory pathway<sup>126</sup> contribute to IMC assembly), and depends on the activity of apicomplexan-specific TgRab11a and TgRab11b small GTPases<sup>158,159</sup>.

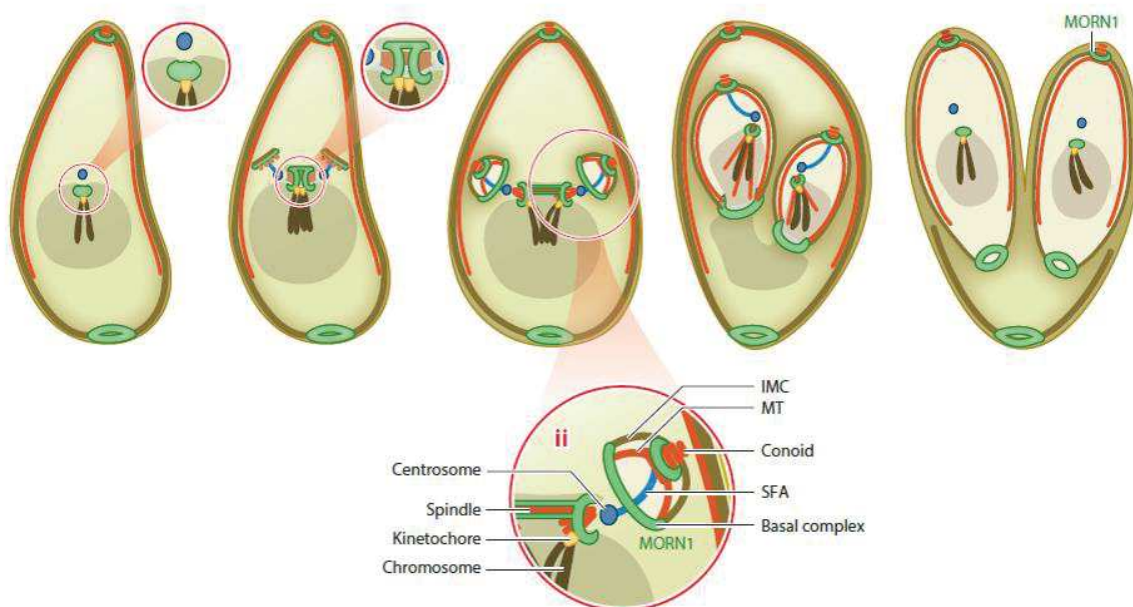


**Figure 17. Dynamics of the cytoskeleton during the endodyogeny process<sup>109</sup>.** Cytoskeletal components assemble in a coordinated fashion during the budding of daughter cells (see text for the details). IMC = inner membrane complex; MT = microtubules; SFA = striated fiber assemblin.

The earliest IMC markers appear shortly after the duplication of the centrosome, when the alveolin IMC15 co-localises with the duplicated centrosome anteriorly to the nucleus<sup>100,128,156</sup>. The assembly of the conoid, intraconoidal MTs and subpellicular MTs also appears shortly after centrosome duplication<sup>103,159</sup>. The alveoli of IMC and the associated protein meshwork develop in parallel with IMC proteins, anchoring into alveoli during the process<sup>100</sup>.

Subsequently to IMC15, a large group of the alveolins, localised centrally and basally to the IMC, are recruited to the forming buds<sup>100,155,156,160</sup>. The appearance of glideosome elements is scheduled early during cytokinesis as well: GAP40 associates with the developing daughters even before IMC1 does<sup>157</sup>.

Once all the early cytoskeleton components are in place, the elongation process starts. TgMORN1 marks the apical end (conoid) and the growing ring-shaped basal end of daughters, the basal complex<sup>103,161</sup> (Fig. 17). When the elongation reaches the posterior border of the IMC apical cap, the elongating cytoskeleton expands beyond the apical cap and the proteins specific to different sub-compartments are recruited<sup>100</sup>. At the midpoint of budding, the basal IMC proteins re-localise towards TgMORN1-labeled basal part of the forming cytoskeleton. This is also the moment when scaffold achieves its widest part : from now on it will begin the cell division-related contraction on its basal end<sup>100</sup>. During elongation, the maternal organelles are progressively segregating into forming daughter cells, including centrosome, Golgi apparatus, apicoplast and nucleus in strict order (see next chapter for details on endodyogeny)<sup>156</sup>.

The late budding is characterised by the nearly complete formation of daughter cytoskeletons and the emergence of daughter parasites from the mother<sup>157</sup>. Importantly, the maternal IMC disassembles at this stage, starting from the apical end<sup>159</sup> and is incorporated into daughter cytoskeletons. Thus, thanks to recycling of the maternal IMC, the progeny IMC continue to expand after their emergence until their complete maturation, acquiring all the cytoskeletal protein markers of mature tachyzoites<sup>157</sup>.

---

## CHAPTER 4. The cell cycle of *T. gondii*

---

### 4.1. Cell division in eukaryotes: basic events

A conventional eukaryotic cell cycle is an invariable sequence of events culminating in duplication of cell's genetic material and production of two identical progeny cells from a single mother<sup>162,163</sup> (Fig. 18A). 4 main stages are distinguished in this process. The Gap 1 (G1), the synthesis (S) and the Gap2 (G2) phases (altogether known as the interphase) are followed by the M phase that encompasses mitosis (or genetic material segregation) and cytokinesis (or partitioning of cytoplasmic components into progeny)<sup>162,163</sup>. In the interphase, the cell conducts its "normal" functioning and prepares itself for division. During the G1, the cell synthesises RNAs and proteins, increases in size and gets ready for DNA replication that occurs at the following S phase. G2 corresponds to the gap between the S phase and the M phase, ensuring DNA replication was correct and the cell is ready to enter mitosis<sup>164</sup>. The complex and highly regulated M phase of the cell cycle is relatively brief and consists in five main steps distinguished by the physical state of the chromosomes: prophase, prometaphase, metaphase, anaphase and telophase<sup>165</sup> (Fig. 18B). The chromosomes segregation and the formation of two new nuclei is accompanied or followed by cytokinesis (C) resulting in the assembly of two daughter cells possessing the same set of organelles and the DNA content as the mother cell<sup>164,166</sup>. Cytokinesis may occur in the form of binary fission (e.g. animal cells, fission yeast) or could be otherwise achieved by budding when the nascent progeny cell outgrows from the mother, gradually increasing in size (e.g. budding yeast)<sup>167</sup>.

During the interphase of each cell cycle, the eukaryotic cell has an opportunity to pursue the chain of events till the progeny formation or to exit the cell cycle in a permanent or reversible manner. The reversible temporary cell cycle arrest is known as the G0 phase (quiescence) and may be induced as a response to extrinsic/intrinsic anti-mitogenic factors<sup>164,168</sup>.

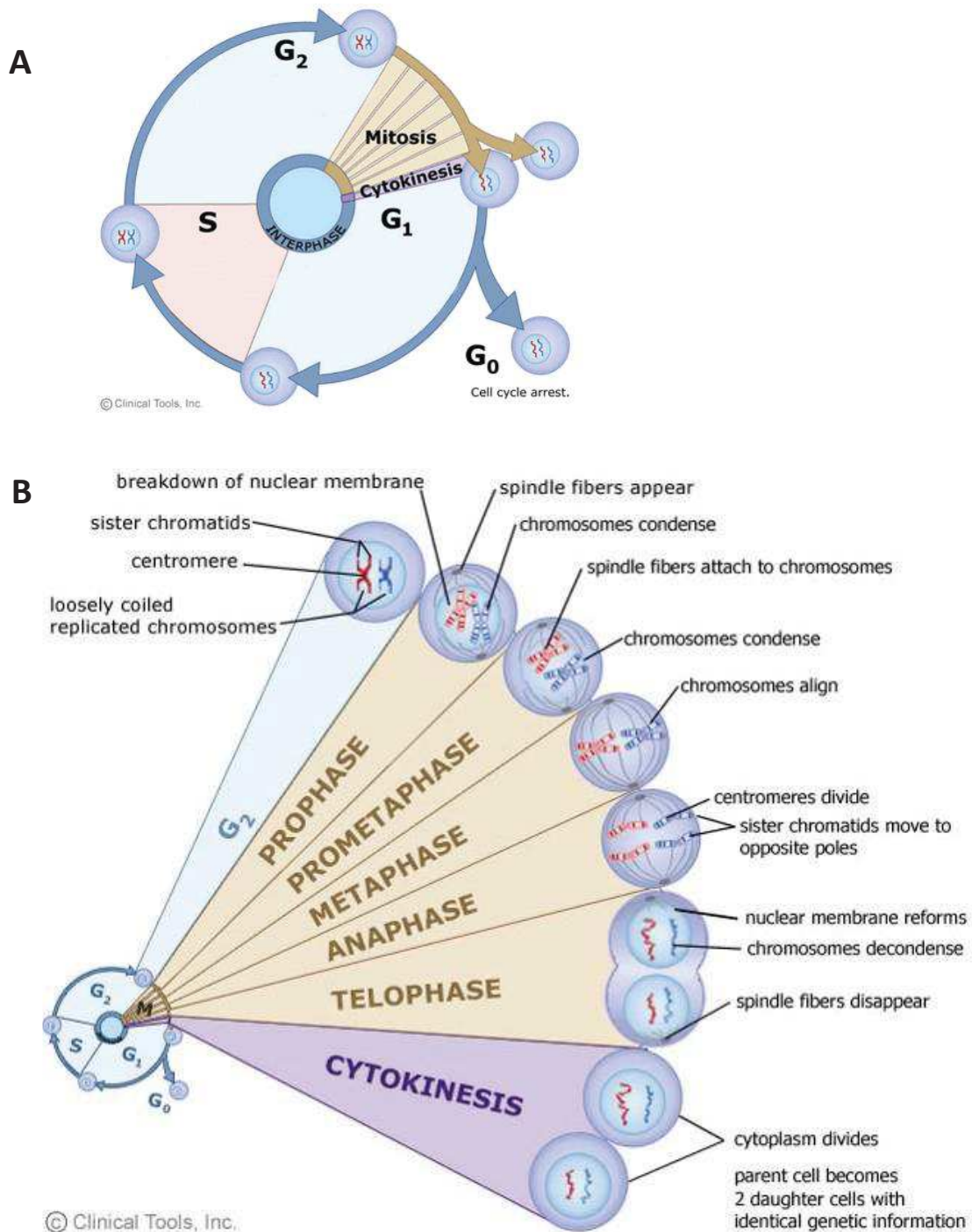


**Figure 18. Schematic representation of a conventional eukaryotic cell cycle<sup>169</sup>.** (A) The main steps of the cell cycle are G<sub>1</sub> phase, S phase, G<sub>2</sub> phase and M phase that includes mitosis and cytokinesis. In some particular instances, a eukaryotic cell can exit its replicative cycle and enter an arrest phase named G<sub>0</sub>. (B) Mitosis consists in five main phases based on the physical state of the chromosomes: prophase, prometaphase, metaphase, anaphase and telophase. Cytokinesis, or the division of the cytoplasm into two identical daughter cells, follows mitosis or occurs simultaneously.

## 4.2. Cell division in apicomplexan parasites

The division of apicomplexan parasites includes the same basic events as the classical model: DNA replication, chromosome segregation with nuclear division and cytokinesis. However, a striking feature of Apicomplexa is their ability to mix and match these basic elements in variable order which contrasts with most of eukaryotic models<sup>117</sup>. For example, during the asexual division of apicomplexan parasite, a round of DNA replication can be followed by daughter cells assembly – or by several other rounds of DNA replication instead<sup>117</sup>. This flexibility in the organisation of division may occur not only between species (e.g. *T. gondii*<sup>170</sup> versus *P. falciparum*<sup>171</sup>), but also within the same parasite at different developmental stages (e.g. *T. gondii* merozoites in cat's intestines may be formed by distinctive modes of division<sup>172</sup>).

Overall, there are four different forms of division, described for the asexual stages of apicomplexan parasites (Fig. 19)<sup>116</sup>. For instance, *T. gondii* tachyzoites undergo only one round of DNA replication which is followed by single mitosis happening simultaneously with daughter budding<sup>116</sup>. This simple but particular mode of division was first observed by light and electron microscopy in the late 1950s - 1960s and was named endodyogeny<sup>173-175</sup> (Fig. 19A). *P. falciparum* and *Eimeria tenella* invasive stages replicate by schizogony<sup>176,177</sup> (Fig. 19B) that includes many rounds of DNA replication and, as a result, a formation of multinucleated syncytium prior to nuclear division and cytokinesis<sup>116</sup>. The nuclei can divide in an asynchronous manner, however the last replication is synchronised and coupled with an assembly of the numerous daughter cells<sup>178</sup>. Another parasite of the phylum, *Sarcocystis neurona*, replicates by a mechanism named endopolygeny<sup>179</sup> (Fig. 19D). It may be considered a variation of schizogony as the parasites undergo five consecutive cycles of chromosomal replication without dividing their nuclei before cytokinesis<sup>179</sup>. Finally, *Theileria spp* has developed a peculiar way to multiply in their host leukocytes. Once inside the host cell, the parasite interferes with its signalling pathways and triggers uncontrolled proliferation of invaded leukocyte. Provoking leukocytes transformation (Fig. 19C) and their immortalisation, *Theileria* divides by co-opting members of the host cell mitotic machinery<sup>180</sup>.

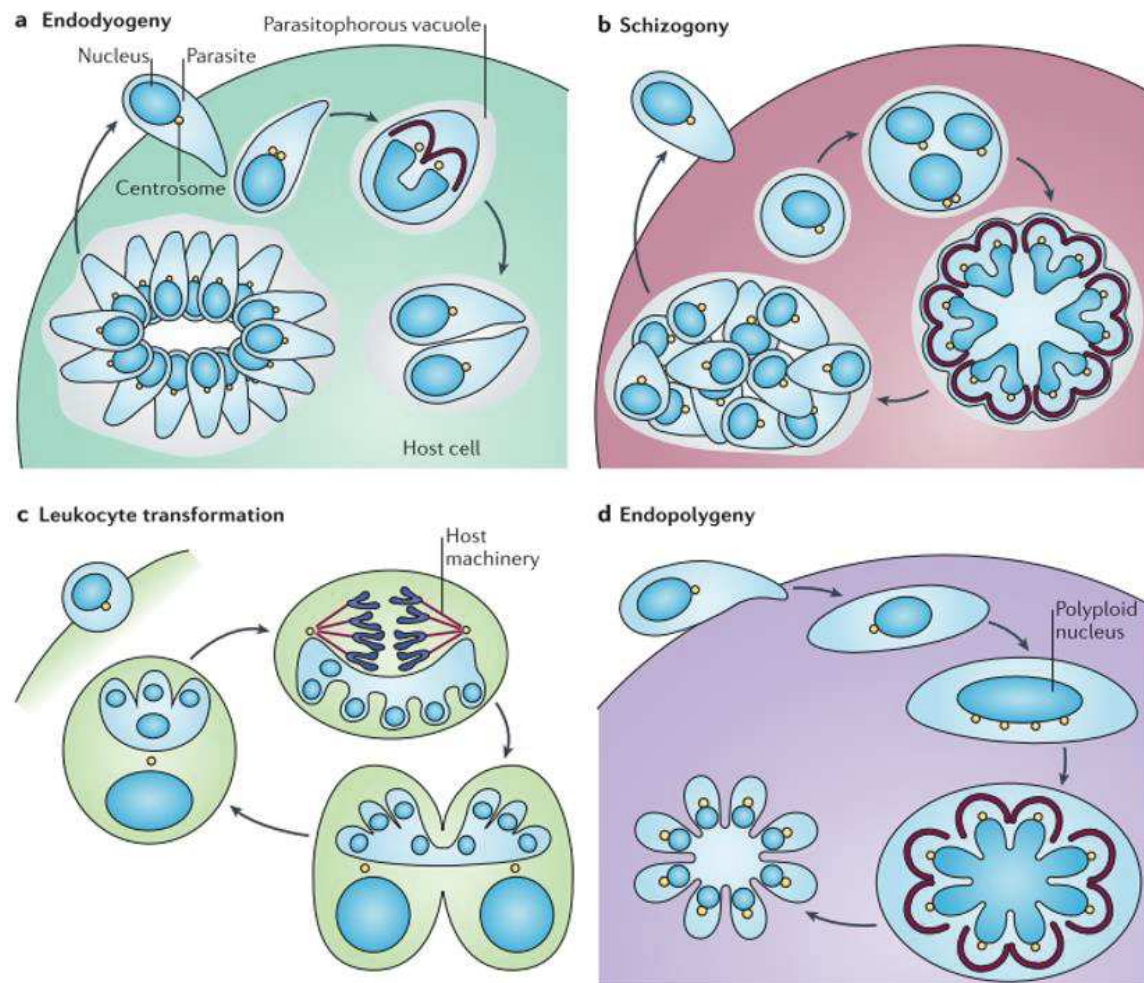


**Figure 19. Division modes in apicomplexan parasites<sup>116</sup>.** (a) *Endodyogeny*. One DNA replication cycle is followed by mitosis and budding. (b) *Schizogeny*. Nucleus undergoes many asynchronous rounds of mitosis, leading to the formation of a syncytium. The last mitosis is synchronous for all nuclei and is coupled with budding. (c) *Leukocyte transformation*. *Theileria* spp invades leukocytes and takes advantage of the host replication machinery for its own proliferation. (d) *Endopolygeny*. There are five consecutive rounds of DNA replication and the formation of a polyploid nucleus, then the final replication coincides with budding.

Despite the diversity of division forms and the remarkable variation in the scale of assembled progeny, the cell cycles of different Apicomplexa share several common fundamental features<sup>116</sup>.

First, all the events that occur during an Apicomplexa division may be conceptually regrouped in two main steps: the growth phase and the budding phase<sup>116</sup> (or the nuclear cycle and the budding cycle as defined by Suvorova et al.<sup>181</sup>). The growth phase consists of parasite's genome amplification by successive rounds of DNA replication and mitosis and comprises S-M-G1 phases (Fig. 19, Fig. 20). Interestingly, the G2 phase of the cell cycle is very brief or absent in Apicomplexa<sup>118,182,183</sup>. The budding phase combines mitosis and cytokinesis (M-C phases). The combination of variable number of growth and budding phases during one cell cycle underlies the diversity of division modes in the parasites.

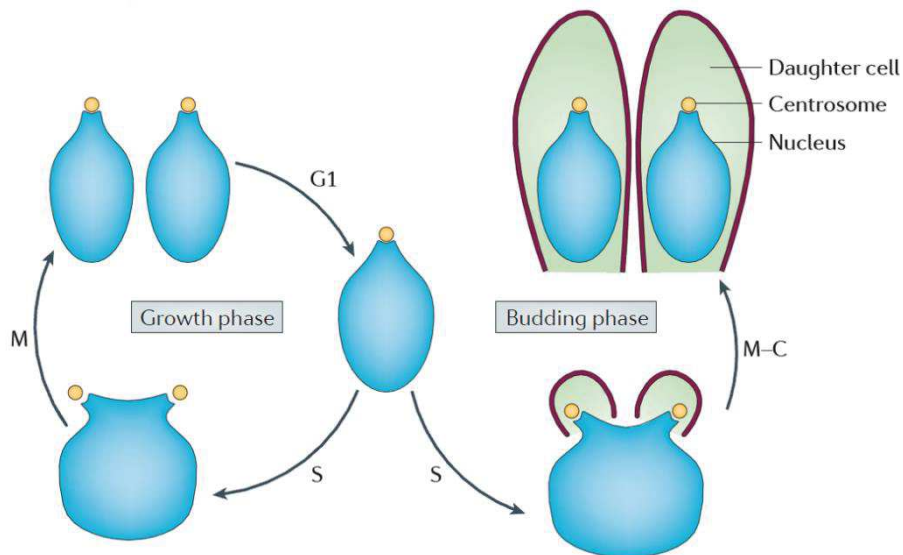


**Figure 20. A bimodal scheme of cell cycle organization in Apicomplexa<sup>116</sup>.**

During the cell cycle, depending on their cell division mode, at the G1/S transition apicomplexan parasites may either i) enter a growth phase (on the left) and proceed to a round of DNA replication or ii) enter a growth phase accompanied by budding phase (on the right); thus the DNA replication and chromosome segregation are synchronised with the assembly of daughter cells by internal budding.

Second, in contrast to most other eukaryotes, Apicomplexa undergo a closed mitosis meaning the nuclear envelope remains mostly intact during the process while chromosome segregation happens inside the nucleus<sup>116</sup>.

Third, as mentioned previously, the formation of daughter cells is achieved by budding, which is a highly organised process guided by self-assembly of cytoskeleton elements<sup>100</sup>.

Last but not the least, a key coordinator of apicomplexan cell cycle progression is the centrosome. Being physically connected to the chromosomes of the nucleus, to several other mother cell organelles and to the MTOC of assembling daughter cells as well, the centrosome ensures the correct positioning and segregation of organelles into the progeny<sup>184</sup>.

### 4.3. The *T. gondii* cell cycle

As stated earlier, the cell cycle of *T. gondii* tachyzoites is restricted to a single growth phase and a single budding phase (Fig. 20) and lasts about 6 to 8h depending on the strain<sup>118</sup> (Fig. 21). Interestingly, the length of the cycle is consistent with the virulence of the strain: it is the shortest for the most virulent and highly replicative type I *T. gondii*<sup>118</sup>. The major G1 and S phases comprise, respectively,  $\approx 60\%$  and  $\approx 30\%$  of the cycle and are followed by short M phase<sup>118</sup>. The cytokinesis is initiated in the late S phase and thus overlaps with DNA replication<sup>118,185</sup>. The non-replicating extracellular tachyzoites correspond, in terms of standard nomenclature, to the G0 state of eukaryotic cells that have exited the cell cycle<sup>186</sup>.

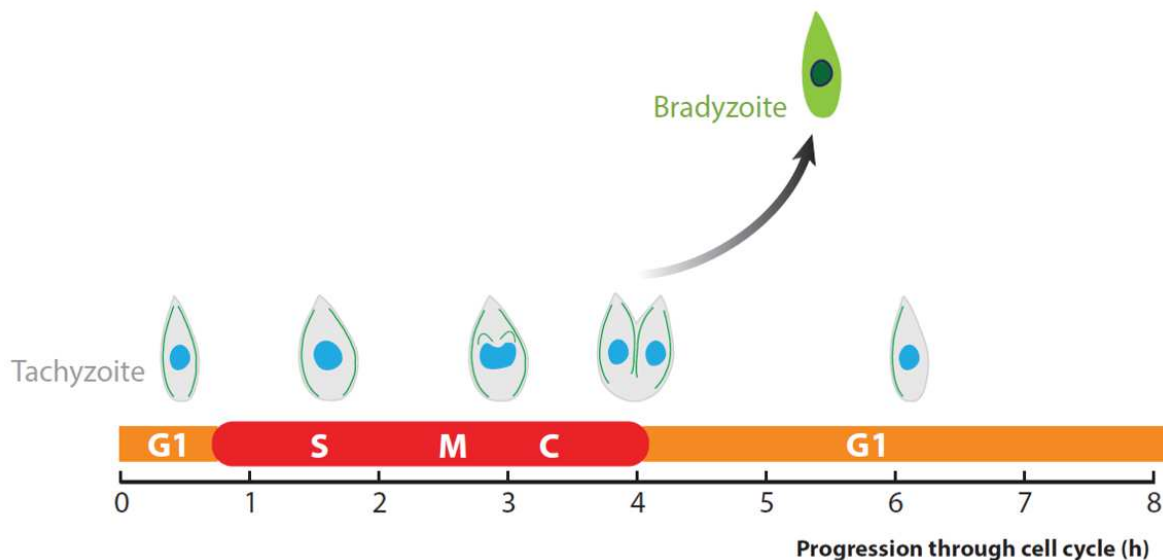


**Figure 21.** Cell cycle of *T. gondii*<sup>186</sup>. The phases of the cycle (G1, S, M and C) are positioned on an approximate time scale. DNA replication occurs in the S phase and is followed by rapid mitosis (M). Cytokinesis (C) is initiated in the late S phase and overlaps with DNA replication.

Note that the length of the cycle depends on the length of G1 phase which is variable in different strains (type I < type III < type II). Bradyzoite-tachyzoite interconversion occurs in late S/M phase. The nucleus of tachyzoite is indicated in blue, the cytoskeleton of the mother and assembling daughter cells are shown in green.

### 4.3.1. DNA replication

DNA replication in *T. gondii* is scheduled for the S phase but pauses once reaching 1.8N content, as accessed by flow cytometry DNA measurements in an asynchronous tachyzoites culture<sup>118</sup> (Fig. 22). The precise reason for this arrest is unknown, nevertheless, the slowdown in the DNA replication appears when the mitotic spindle is assembled and the cytokinesis begins. Taking into account that a true G2 phase is missing in Apicomplexa, the pause at 1.8N might be its functional equivalent<sup>109</sup>. The replication of DNA content seems to be quickly completed after the spindle assembly at the latest<sup>170</sup>.

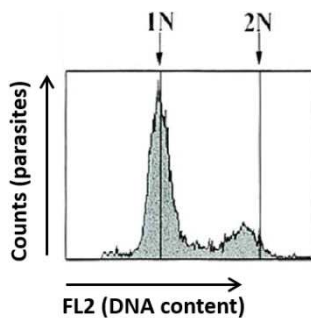


**Figure 22.** Flow cytometry profile of the DNA content of asynchronous tachyzoites<sup>118</sup>. The distribution of the asynchronous population is bimodal, displaying two major peaks that correspond to the G1 and S phases.

### 4.3.2. Mitosis

At the onset of mitosis, the chromosomes of a eukaryotic cell must establish a connection with the mitotic spindle. By that time of the cell cycle, each chromosome is composed of a pair of genetically identical sister chromatids that are joined together at a specialised DNA sequence called the centromere. The chromosome's attachment to the mitotic spindle occurs exactly at its centromeric region upon an assistance of kinetochores, the large protein complexes that are assembled one on each chromatid<sup>165,187</sup> (Fig. 23). Notably, the poles of the mitotic spindle are linked to the duplicated centrosome which is instrumental for the subsequent chromosomes segregation<sup>188</sup>.

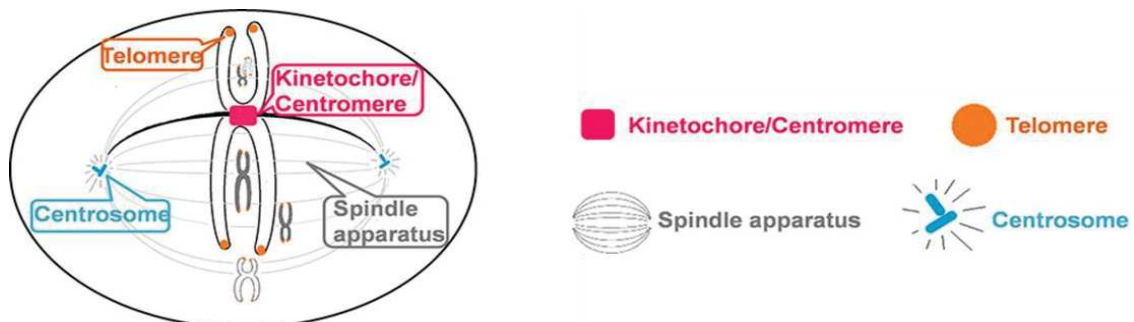


**Figure 23.** Schematic representation of the eukaryotic machinery for chromosome segregation<sup>189</sup>.

Though the segregation process in *T. gondii* is driven by similar centromere-mitotic spindle-centrosome interaction, it also displays several particular features due to the closed mitosis<sup>116</sup> (Fig. 24).

During endodyogeny, the nuclear envelope remains mostly intact and the mitotic spindle is embedded into it in a dedicated electron dense membrane invagination called the centrocone<sup>161,175,190</sup>. While the parasite's spindle MTs assemble in late G1 phase and are retained exclusively during mitosis<sup>191</sup>, the TgMORN1-labeled centrocone persists throughout the cell cycle<sup>161</sup>. Interestingly, the chromosomes are anchored to the centrocone region of nuclear envelope at any point of the tachyzoite cell cycle<sup>192,193</sup>. This peculiar clustering may provide a quick and efficient access of the mitotic spindle (which is typically short<sup>191</sup>) to the chromosomes. Elsewise, it may help to preserve a full set of chromosomes throughout parasite's development<sup>190</sup>. If retained in other Apicomplexa, this could be an important mechanism to ensure a correct genetic inheritance, especially for species with more complicated modes of division that require a formation of a polyploid nucleus<sup>116,193</sup>.

Kinetochores proteins, such as Nuf2 (nuclear filament-related 2) and Ndc80 (nuclear division cycle 80), are conserved in tachyzoites and co-localise with the centromeric regions of the chromosomes throughout the cell cycle<sup>193</sup>. The kinetochore complexes are essential for centromere-mitotic spindle association and are also required for the interaction between the centrocone and the centrosome. Nevertheless, the kinetochore proteins are not involved in chromosome clustering, suggesting a distinctive mechanism for this phenomenon<sup>191,193</sup>.

When the parasite's spindle MTs elongate and drive apart the spindle poles, the centrocone-tunnel structure widens, is perforated and finally separates in two new centrocones with MTs now residing directly in the nucleoplasm and being attached to centromeres<sup>170,116</sup> (Fig. 24). During the next step of mitosis the nucleus assumes a bi-lobed shape and finally undergoes fission, subsequently segregating into nascent daughter buds<sup>156,170</sup>.

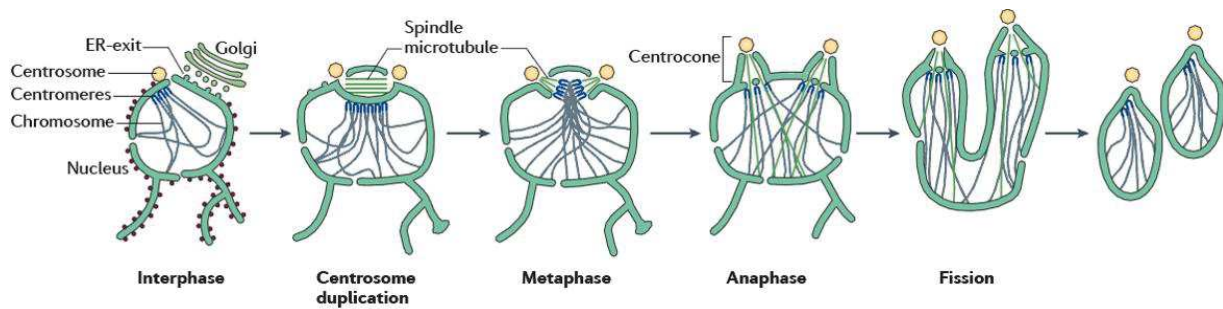
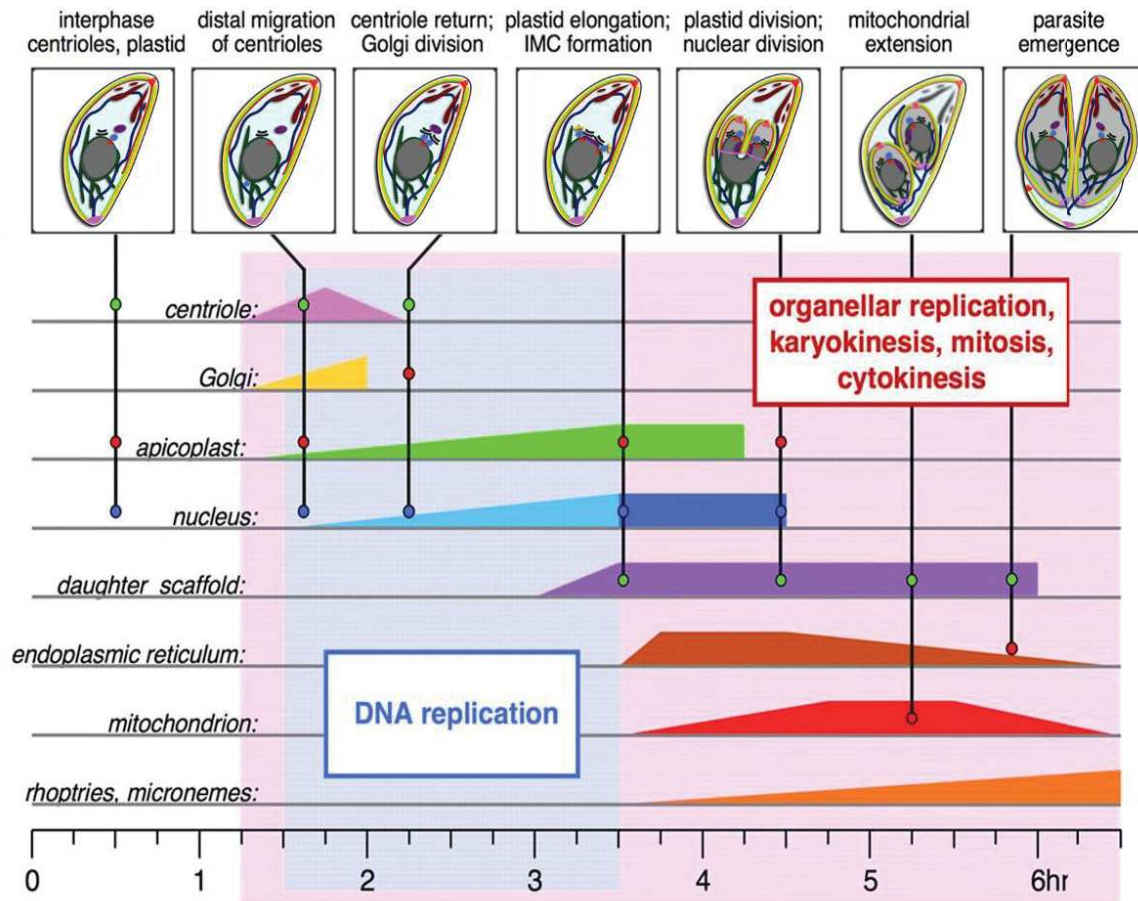


**Figure 24. Closed mitosis of *T. gondii***<sup>116</sup>. The interphase nucleus is a highly organised organelle, with centrosome clustered and tethered to the nuclear envelope. The mitotic spindle resides in the nuclear envelope (centrocone) and establishes a connection with the centromeres of the chromosomes in metaphase. The anaphase nucleus has two centrocones formed at each centrosome. Following the anaphase, the nucleus assumes a bi-lobed shape and undergoes fission and segregation into forming daughter scaffolds.

#### 4.3.3. Organelle dynamics and daughter cells assembly

In order to produce the progeny loaded with a complete set of organelles, *T. gondii* uses a highly coordinated subcellular replication system<sup>156</sup>. During endodyogeny, some maternal organelles are duplicated and/or segregated in forming buds (e.g. the apicoplast or the Golgi apparatus), while the others are synthesised *de novo* (like invasion-related secretory organelles micronemes and rhoptries, or the elements of cytoskeleton). The careful studies of organelles dynamics by time-lapse microscopy revealed that the duplication, the segregation, and the *de novo* synthesis, are organised in agreement with the cell cycle progression and happen in a predefined manner<sup>156</sup> (Fig. 25), in tight coordination with the centrosome dynamics<sup>184</sup>.

The cell cycle-related organelles dynamics start in the G1 phase with the elongation of both the Golgi apparatus and the apicoplast<sup>156,194,195</sup>. At this point of the cell cycle, the Golgi stack, the apicoplast and the centrosomes are localised anteriorly to the nucleus, in close proximity to each other, and one end of the Golgi stack is associated with the centrosome<sup>156,195</sup>. The lateral growth of the Golgi apparatus, however, is followed by the transient detachment of the centrosome and its migration towards the basal end of the nucleus where it duplicates in late G1 phase<sup>191</sup>. The elongation of the ovoid apicoplast and the duplication of its genome coincides with the basal repositioning of the centrosome<sup>156</sup>. Once the centrosome is duplicated, it returns to the apical end of the nucleus at the onset of



Time count (hours:minutes)	Step of the cycle	Events
0 to 1:15	G1 phase	Centriole, Golgi stack and apicoplast are closely associated at the apical end of the nucleus
1:15 to 1:45	First morphological changes	Centriole migrates away from the apical end Golgi stack elongates Apicoplast migrates to juxtannuclear region, associated with mitochondrion, and elongates
1:45 to 3:00	Initial stages of mitotic division	Centriole divides Golgi stack divides Initiation of DNA replication Apicoplast continues to elongate Centriole returns to the apical end and associates with apicoplast
3:00 to 3:30	Establishment of the daughter cytoskeleton	Daughter conoids form Spindle poles and intranuclear spindle form 1.8N DNA content IMC assembly begins Apical ruffling of ER
3:30 to 4:30	Organellar partitioning (early stages)	Daughter IMC elongate Apicoplast partitioned and divides Nucleus partitioned and divides ER partitioned between daughters Initiation of de novo rhoptry and microneme biogenesis Mitochondrion forms branches
4:30 to 6:30	Organellar partitioning (late stages)	Continued partitioning of ER Continued rhoptry and microneme biogenesis Daughter IMC complete Mitochondrion enters daughter scaffolds
6:30	Emergence of daughter parasites	Daughter parasites bud from the mother, picking up plasma membrane Residual material left behind (including waste, ER, mitochondrion, plasma membrane etc.)

**Figure 25. Morphological events occurring during the replication of a type I strain *T. gondii* tachyzoite**<sup>100, 156</sup>.

the G1/S phase and re-associates with the Golgi apparatus (duplicated in late G1 phase)<sup>195</sup>. It re-associates with the apicoplast as well<sup>196</sup>. The function of this TgMyoF-dependent<sup>197</sup> centrosome migration around the nucleus is unclear, but it may have a role in defining the apical-basal polarity of daughter cells<sup>156</sup>.

The initiation of daughters budding is a critical step in the organellar dynamics of dividing tachyzoites. As stated earlier, the budding is driven by the *de novo* assembly of daughter cytoskeletons in an apical-to-basal direction and begins with the formation of daughters conoids in the S phase, shortly after the duplication of the centrosome<sup>100,109,156</sup>. The elongation of the daughters' cortical MTs is strictly coordinated with the simultaneous formation of the daughters' IMC<sup>100</sup>. The full process of cytokinesis, between the appearance of daughter conoids and the complete emergence of daughters from the mother cell, typically takes 1,5h-2h<sup>160</sup> (see Chapter 3 for details on daughter cytoskeletons formation).

As soon as the centrosome duplicates and rotates back to the apical side of the nucleus, a striated fiber assemblin (SFA) emerges from in between two centrioles and connects each daughter conoid to the centrosome<sup>198</sup> (Fig. 17), therefore ensuring the anchoring of the centrosome-connected organelles (nucleus, Golgi stack, apicoplast) in the daughter scaffold<sup>198,199</sup>.

Importantly, the incorporation of organelles into the daughter scaffolds proceeds in a strict invariable order (Fig. 25). The elongating scaffold first encapsulates the centrosome and the Golgi stack<sup>156</sup>. Next comes the turn of the apicoplast. As the cytoskeletons of daughter cells grow, and the centrosome enters the scaffold, the apicoplast is forced to take a U-shape and, finally, is divided in two identical organelles with exactly the same DNA content<sup>156,196,200</sup>. The nucleus segregation follows the one of the apicoplast. As the ER is continuous with the nuclear envelope, its entry and segregation into the daughter scaffolds follows the nucleus and its apical and basal ramifications continue until the completion of endodyogeny<sup>156</sup>.

The rhoptries and micronemes are synthesised *de novo* in the scaffold during the elongation thus their dynamics during division do not depend on the daughter cytoskeleton assembly or the centrosome. The synthesis of these organelles relies on the parasite's endosomal system; the nascent secretory organelles appear in forming daughters before the maternal apically localised rhoptries and micronemes disappear<sup>77,156</sup>.

The mitochondrion segregation into the daughter cells is the very last stage of budding<sup>156,170</sup>. While some division-related morphological changes in the mitochondrion occur as soon as the daughters cytoskeleton assembly begins, the organelle is surprisingly excluded from the developing daughters until they start to emerge from the mother cell<sup>156</sup>. At that moment the mitochondrion, that has previously extended multiple branches, enters the daughters and encircles the nucleus<sup>156</sup>.

During the emergence from the mother cell, the nearly complete daughters (now containing their own sets of organelles) are provided with a plasma membrane. Once the two sets of organelles have been packaged to daughter cells and while these emerge from the mother, the remaining of the mother cell cytoplasm and organelles is left behind in a so called residual body (RB)<sup>156</sup>. The RB establishes during the first round of endodyogeny of an intracellular tachyzoite, and does not disappear during following replications<sup>201</sup>. Although the RB remains largely uncharacterised, it is considered nowadays more than a simple “leftovers-containing” structure. Muniz-Hernandez et al.<sup>202</sup> have shown tachyzoites are interconnected by the RB inside the PV: the RB was thus suggested to support the spatial rosette organisation of tachyzoites in the PV and maybe also metabolites exchange between parasites<sup>81,202</sup>. Furthermore, in a recent study Attias et al.<sup>201</sup> propose that the RB may be a calcium store used by parasites when they egress from the host cell, although that hypothesis requires further investigation.

After the emergence from the mother cell, the progeny parasites remain connected by a narrow cytoplasmic bridge. This connection gradually disappears and the development of daughter cells finishes with the maturation step that follows their exit of the mother cell and lasts for around 2h post-division<sup>156,157</sup>.

## 4.4. Regulation of the endodyogeny process

### 4.4.1. Cell-cycle related genes expression in tachyzoites

Amongst over 8000 *T. gondii* genes<sup>64</sup> more than a third is expressed in a cyclic manner along course of a parasite division cycle<sup>203</sup>. The cell cycle transcripts expression matches one of two major expression waves that correspond either to the G1 or S/MC events. Hence, the G1-subtranscriptome peak is enriched for canonical eukaryotic biosynthetic and metabolic genes while the S/M-subtranscriptome genes encodes for Apicomplexa-specific proteins that are related, for instance, to the cytoskeleton or the invasion machinery<sup>203</sup> (Fig. 26). The identified core set of the conserved cell division cycling genes in *T. gondii* comprises approximately 700 genes that encode for characterised as well as hypothetical proteins<sup>204</sup>.

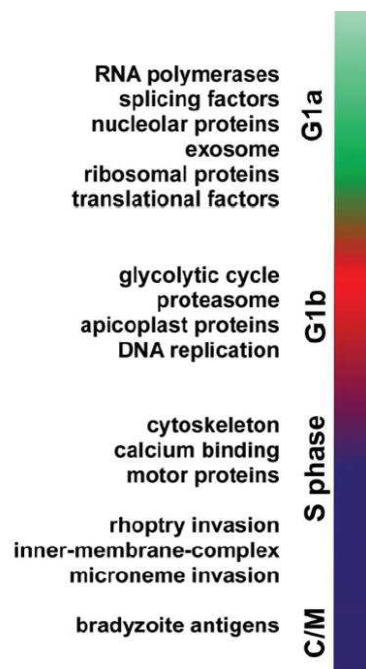


**Figure 26. Cyclical gene expression during endodyogeny<sup>203</sup>.**

### 4.4.2. Checkpoints and regulatory factors

The spatio-temporal organisation of the cell cycle depends on a complex regulation machinery. The progression through the cycle is controlled at specific moments or checkpoints<sup>205</sup> (Fig. 27A). The major checkpoints in eukaryotes are i) the G1/S transition or START checkpoint (controlling the entry into the S phase), ii) the G2/M transition (controlling the entry into mitosis), and iii) a spindle checkpoint in M phase controlling the progression of the cell to the anaphase and preventing premature chromosome segregation (SAC, for

spindle-assembly checkpoint)<sup>205,206</sup>. The G1 and G2 checkpoints are also called the cell size checkpoints and serve to ensure the coordination of the cell size with steps of the cycle and, as a result, to provide each newly forming daughter cell with an appropriate quantity of genetic and organellar material<sup>163</sup>.

The major role in coordination of the cell cycle progression is attributed to the activity of cyclin-dependent kinases (CDKs) and their binding partners, the cyclins<sup>207</sup>. The CDKs constitute a specific class of serine/threonine kinases that phosphorylate protein substrates involved in the cell cycle progression and thus promote the passage through the check-points<sup>163</sup>. As the name implies, the CDKs functioning depends on a presence of a separate cyclin subunit. A cyclin does not have enzymatic activity on its own, but its binding to the CDK allows the enzyme to adopt an active configuration and to undergo a phosphorylation of a key residue in the activation loop<sup>163,208</sup>. The active complex may be inactivated by one of various mechanisms, for instance, via degradation of the cyclin subunit by ubiquitin-mediated proteolysis or via enzyme's association with an inhibitory protein, a CKI (for Cyclin Kinase Inhibitor)<sup>163,208</sup>. In most cases, the expression of the CDKs is constant while the expression of the cyclins oscillates and is coupled to the specific step of the cell cycle they act on<sup>208</sup>.

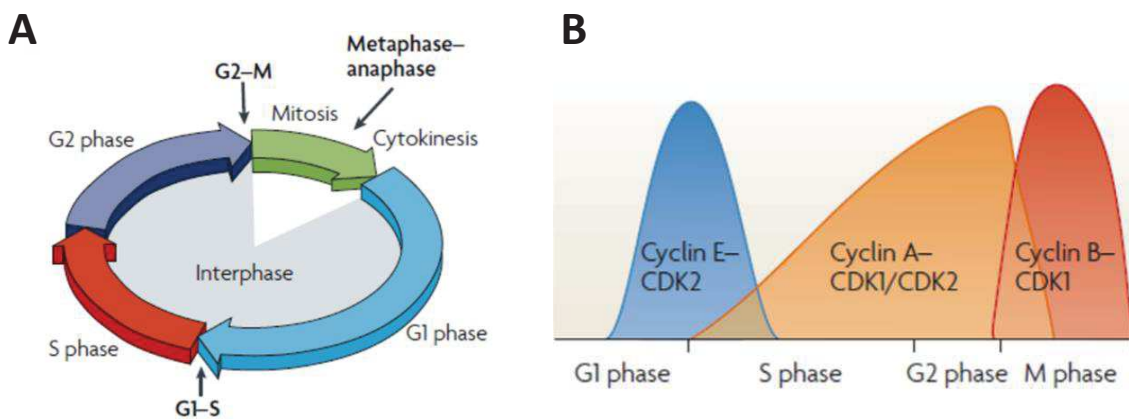


**Figure 27. Cell cycle checkpoints in a eukaryotic cell<sup>208</sup>.** (A) Major checkpoints of a conventional eukaryotic cell cycle. Each checkpoint ensures a completion of one of the key events in the cycle: sufficient cell growth, complete DNA replication and chromosomes' proper attachment of to the spindle poles. Cyclin-dependent kinases (CDKs) trigger the transition through the checkpoints by phosphorylating distinct sets of substrates. (B) The classical model of the cell-cycle regulation. CDK4 and CDK6 with cyclin D control events in early G1 phase (not shown), CDK2/cyclin triggers S phase, CDK1-2/cyclin A ensure the S phase is completed, CDK1/cyclin B acts on mitosis.

Obviously, the division modes and their regulation vary from species to species; nevertheless, there are several key CDK/cyclins pairs involved in the cell cycle progression of

a prototypical eukaryotic cell (Fig. 27B). For instance, the progression through the G1 phase involves CDK4 and CDK6, which are interacting with cyclin D. CDK2, complexed with cyclins E, A and B, governs the progression through the S phase of the cell cycle; it also ensures the correct DNA replication and chromosome segregation during mitosis<sup>205,209</sup>.

A global screening and phenotypic characterisation of temperature sensitive mutants was used in 2008 to isolate various *T. gondii* cell cycle mutants arrested in G1, S phase, or later during the process of budding<sup>210</sup> (Fig. 28). This technique was first used on yeast to functionally characterise important factors governing the cell cycle in a conditional manner<sup>211</sup>. The existence of uncoupling mutants, arrested in specific phases of the cycle, hinted different levels of regulation in *T. gondii* and was lately interpreted as a proof of the multi-factorial control of cell cycle transitions in the parasite<sup>170,212</sup>.

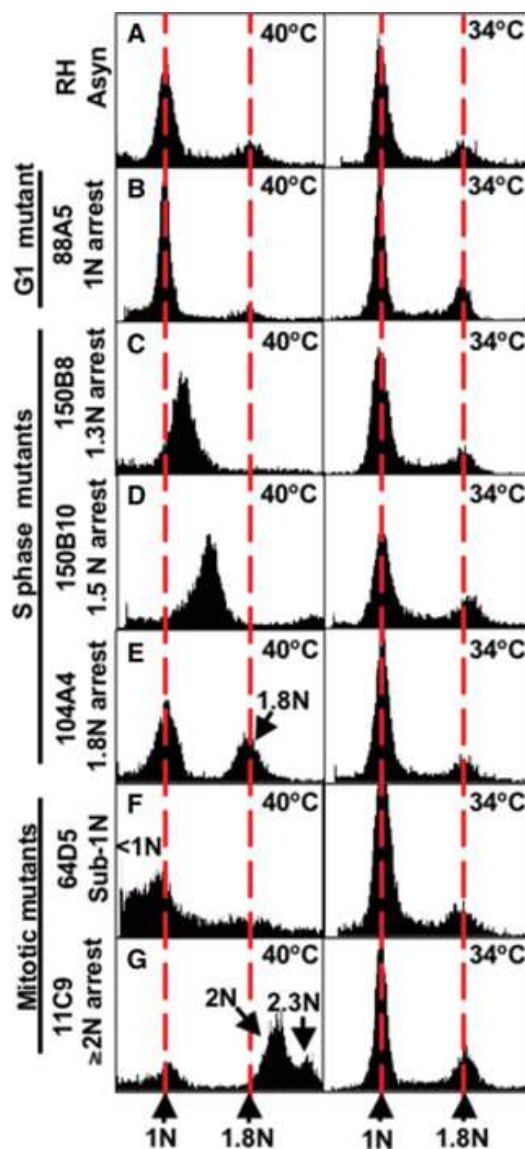


**Figure 28.** Distribution of parasite genomic DNA content at permissive (34°C) and restricted (40°C) temperatures for selected temperature-sensitive *T. gondii* cell cycle mutants<sup>210</sup>.

Red dashed lines reference 1N and 1.8N fluorescence peaks in the asynchronous controls (A). The cell cycle mutants are compared to the asynchronous control (A). The G1 phase mutant 88A5 (B) arrests with a predominant 1N DNA content. The S phase mutants 150B8 (C), 150B10 (D), and 104A4 (E) show altered DNA contents ranged between 1N and 2N. The mis-segregation mutant 64D5 (F) shows significant DNA loss (less than 1N). The mitotic mutant 11C9 arrests with a predominant diploid DNA content (G).

It seems that *T. gondii* retained conserved checkpoints but acquired additional ones due to its peculiar replication; its cell cycle is not orchestrated by the exact same molecular machinery as in model eukaryotic organisms<sup>170,212</sup>. In a systematic mining through the *T. gondii* genome, Alvarez and Suvorova<sup>212</sup> have identified several genes with a kinase domain that included a cyclin-binding sequence, as well as seven (five expressed in tachyzoites) novel cyclin factors (based on the presence of cyclin box and one or several destructive motifs). These regulators have been called CDK-related kinases or Crk (not CDKs, as not all have been linked to a specific cyclin yet) and cyclins, respectively. Interestingly, no canonical eukaryotic cyclins related to type A, B, D or E have been identified, there were instead atypical P-, H-, Y- and L-type factors.

By contrast to some other eukaryotes, which are able to progress through the cell cycle in presence of a single canonical CDK1/2<sup>213</sup>, *T. gondii* tachyzoite requires all five Crks to progress through the cell cycle<sup>212</sup> (Fig. 29). Functional analysis has shown that depletion of TgCrk2 blocks tachyzoites in the G1 phase, and knockdown of TgCrk1, TgCrk4 or TgCrk6 results in extensive mitotic and cytoskeletal defects, while TgCrk5 likely controls the licensing of DNA replication. More precisely, the G1 checkpoint (related to the switch between active replication and dormancy) is controlled by an atypical TgCrk2 kinase-P/U cyclin complex. Low Crk2 activity associates with G1 arrest<sup>214</sup>. Licensing of DNA replication in S phase is likely to be regulated by TgCrk5/ECR1, while TgCrk6 is apparently involved in the control of SAC, marking metaphase-to-anaphase transition<sup>212,215</sup>. Noteworthy, as the G2 phase in the parasites is short or absent, the DNA damage/replication checkpoint, present in higher eukaryotes, is likely absent too<sup>214</sup>.

The two additional checkpoints of *T. gondii* are related to the maintenance of stoichiometric structure of an unusual bipartite centrosome (see next section) and to the assembly of daughter cells with, respectively, TgCrk4 and TgCrk1/cyclin L complex (distantly related to Cdk11 in higher eukaryotes) controlling these events<sup>212,214</sup>. In general, eukaryotic cyclins expression oscillates and that regulates the checkpoint kinases. However, in *T. gondii*, there might be a different level of regulation because several Crks themselves show dynamic expression profiles (TgCrk4, TgCrk6, TgCrk5). This may be in accordance with the fact that some dynamically-expressed TgCrks (TgCrk4 and TgCrk6) lack detectable cyclin partners<sup>212,215</sup>.

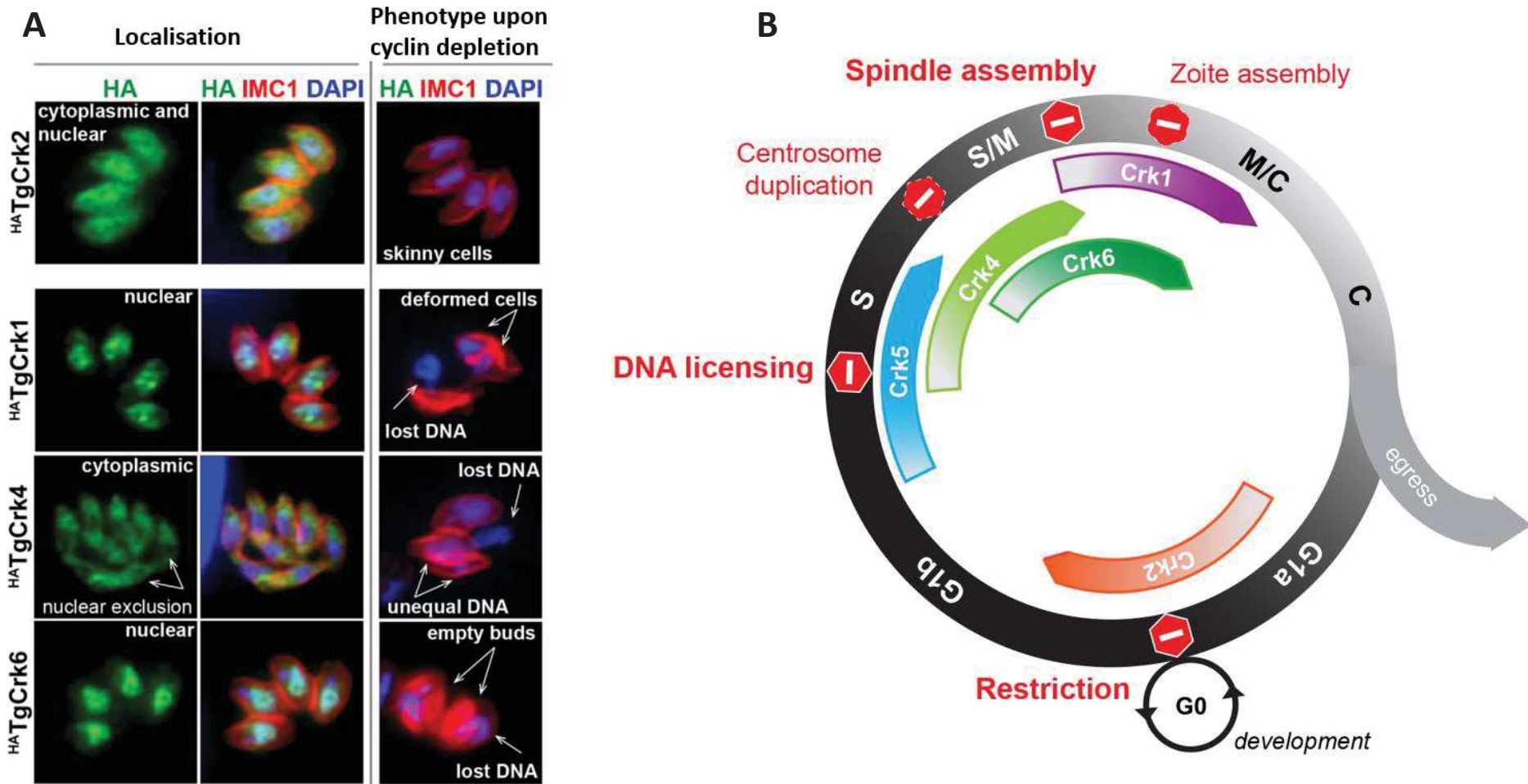


**Figure 29. Checkpoints and cyclin-related kinases required for cell cycle progression in *T. gondii*<sup>212</sup>.** (A) Localisation and functional analysis of TgCrk1, 2, 4 and 6. The down-regulation of TgCrk2 results in growth arrest of morphologically normal parasites, while the knock-down of TgCrk1, 4 and 6 causes the morphological abnormalities, indicated on IFA images. TgCrks are HA-tagged. IMC1 marks the IMC of mother and daughter parasites, the DNA content is marked by DAPI. (B) Summary of putative checkpoints of the tachyzoite cell cycle. Note that *T. gondii* acquired two additional checkpoints related to the centrosome duplication and zoites assembly.

#### 4.4.2. The centrosome

##### *Centrosome structure*

The centrosome in eukaryotic cells is a well-characterised multifunctional organelle<sup>188,216,217</sup>. Though it is involved in numerous processes (e.g. the maintenance of the cell polarity or membrane trafficking), its most recognised function is related to mitosis and consists in coordinating the formation and the maturation of the spindle pole<sup>188</sup>.

The organisation of the centrosome varies amongst species<sup>146</sup>, nevertheless, a classical mammalian centrosome (Fig. 30) is composed of a pair of perpendicularly oriented barrel-shaped centrioles that are surrounded by pericentriolar material (PCM) and held together by a flexible “linker”<sup>188</sup>. The mature centriole, in turn, comprises a cartwheel-like structure on its basal end and two sets of nine appendages on its distal end. The cartwheel self-assembles into a central ring (hub) from which emerge nine filaments (spokes). Each filament is connected to the microtubule triplet. This microtubular composition makes the centriole a polarised structure with a negatively charged basal end<sup>218</sup>. Two centrioles are surrounded by an organised protein network of PCM which composition changes throughout the cell cycle and includes, for instance,  $\gamma$ -tubulin required for the nucleation of microtubules, the cell-cycle regulators and the cell-cycle checkpoints proteins<sup>218,219</sup>. Many centrosomal proteins are of large size (over 150 kDa), and contain coil-coiled domains important for the centrosome assembly. Due to this characteristic composition, the centrosome is suggested to be an instable complex, requiring various chaperonins for its maintenance<sup>188</sup>.

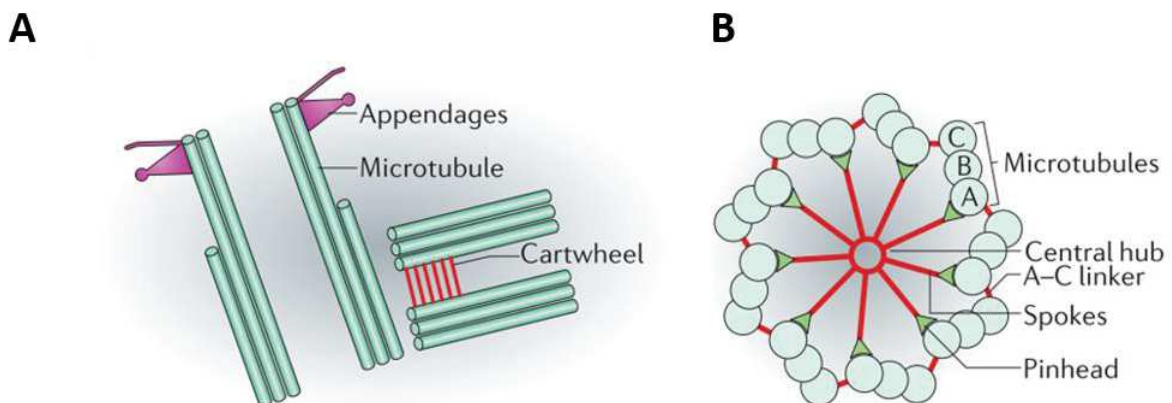


**Figure 30.** Structure of the mammalian centrosome<sup>220</sup>. **(A)** A cut view of a centrosome containing a mature centriole with appendages (on the left) and a pro-centriole, assembling from the cartwheel during division (on the right). **(B)** Centriolar cartwheel viewed from the proximal end. The spokes radiate from the central hub and are attached to the microtubules triplets through pinhead structures.

The centrosome in *T. gondii* retains a role in the mitotic spindle formation<sup>221</sup>, but acquires additional endodyogeny-related functions, thus serving an organising centre for the assembly of the daughter cytoskeletons<sup>100</sup> and coordinating the organelles segregation into forming buds<sup>221</sup>. The *T. gondii* centrosome possesses recognisable centrioles that do not correspond to the conventional triplet formula<sup>94</sup>. Instead, the parasite's centrioles are composed of nine singlet microtubules arranged around a central microtubule, and therefore exhibit a nine plus one singlet organisation (Fig. 31A). Apicomplexan centrioles appear to be shorter than their mammalian counterparts and in *T. gondii*, as well as in *Eimeria spp*, show a parallel and not orthogonal arrangement<sup>94,116,222</sup>. The interphase centrosome in *T. gondii* is positioned in the cytoplasm in proximity to the surface of the nucleus and to the centrocone (Fig. 31B).

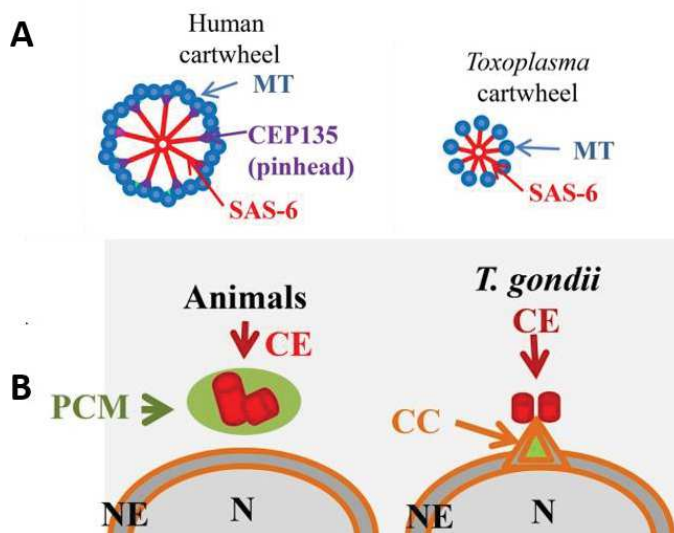


**Figure 31. Structure of the *T. gondii* centrosome**<sup>146</sup>. (A) The top view of the human (on the left) and *T. gondii* (on the right) cartwheel structure of the centriole. In contrast to the human one, the *T. gondii* cartwheel contains 9+1 microtubules. MT = microtubules, CEP135 and SAS-6 are cartwheel proteins. (B) Schematic comparison of the mitotic MTOC organisation in a conventional animal cell and in *T. gondii*. PCM = pericentrosomal matrix; CE = centrosome; CC = centrocone; N = nucleus; NE = nuclear envelope

Comparatively to mammalian centrosome, the protein composition of the organelle in *T. gondii* is poorly characterised. According to sequence homology-based database searches performed recently by Morlon-Guyot et al.<sup>146</sup>, just 30% of genes encoding for mammalian centrosomal proteins are present in the genome of *T. gondii*, which could correlate with the structural difference between mammalian's and parasite's centrosome. For instance, *T. gondii* centriole does not contain an electron-microscopy visible appendage structure; respectively, no orthologues of mammalian appendage-coding genes were found in the annotated parasite's genome<sup>198</sup>. In 2015, Suvorova et al. have identified and localised several *T. gondii* orthologues of canonical centrosomal proteins<sup>181</sup>. Curiously, the results of their study suggested the existence of two functionally distinct replicating core complexes in

the parasite's centrosome, each harbouring a specific set of proteins (Fig. 32). Thus, the outer core localises more distantly from the nucleus and comprises the TgCentrin1/TgSfi1 pair (proteins of centriole's lumen in mammalian cells<sup>218</sup>), TgSAS-6 (a central component of cartwheel<sup>223</sup>),  $\gamma$ -tubulin (a PCM protein<sup>218</sup>) and the regulatory factors, such as the Aurora-related kinase 1, (Ark1, a serine/threonine kinase favouring the centrosome's maturation process<sup>224</sup>). The inner core is closely connected with the centrocone and contains the orthologues of the CEP250/C-Nap protein family (centrosome associated proteins, crucial for centriole duplication and biogenesis<sup>225</sup>)<sup>181</sup>. The family member TgCEP250-Like protein 1 (TgCEP250-L1) appears to be exclusive for the inner core<sup>181,198</sup>. Some other proteins reside on the interphase between the cores and are apparently involved in the maintenance of the centrosome's integrity, as have been shown for the homologue of the human Cep250/c-NAP1, the CEP250 protein<sup>198</sup>, and for the large coil-coiled protein CEP530<sup>226</sup>, both indispensable for the endodyogeny. The inner core was suggested to be surrounded by the PCM containing the centrosome regulatory factors<sup>181</sup>. The specific PCM markers are poorly conserved in *T. gondii* complicating the characterisation of the network; nevertheless, two regulatory factors, the MAPKL-1 (mitogen-activated protein kinase-L1) and the PRMT1 (Arginine Methyltransferase 1), have been confirmed to localise to the PCM<sup>181,227</sup>. Interestingly, the centrosome's cores divide separately, first the inner one and then the outer one, subsequently segregating by pair into each forming daughter parasite<sup>181</sup>.

The hypothesis of the inner and outer core functional specificity<sup>181</sup> was supported by the evaluation of phenotype in temperature-sensitive mutants and transgenic cell lines, deficient in centrosomal proteins<sup>181,198,226</sup>. The defects in the outer core, e.g. when the TgSfi1 protein is depleted, led to a major failure in daughter budding but had no effect on mitosis<sup>181</sup>. Moreover, the physical disconnection of the cores (achieved, for instance, by a conditional knock-down of the CEP250 protein), did not result in a complete disruption of the cores' respective functions, but rather impacted the coordination between the nuclear and the budding cycles (e.g. abnormal partitioning of the nucleus into the nascent daughters)<sup>198</sup>. In line with the described data, the inner core of the centrosome is apparently involved in mitosis and the nuclear cycle, while the outer core is likely to act in the daughter budding process<sup>181</sup>. This also fits with earlier studies which demonstrated, by using specific inhibitors, that DNA replication and daughter budding in *T. gondii* can be easily uncoupled. Indeed, the

inhibition of DNA replication does not completely abolish the initiation of daughter cell budding<sup>198</sup>, and vice versa<sup>145</sup>. The bipartite centrosome model thus provides an explanation on how *T. gondii* could control the cell cycle flexibility, typical for apicomplexan parasites.

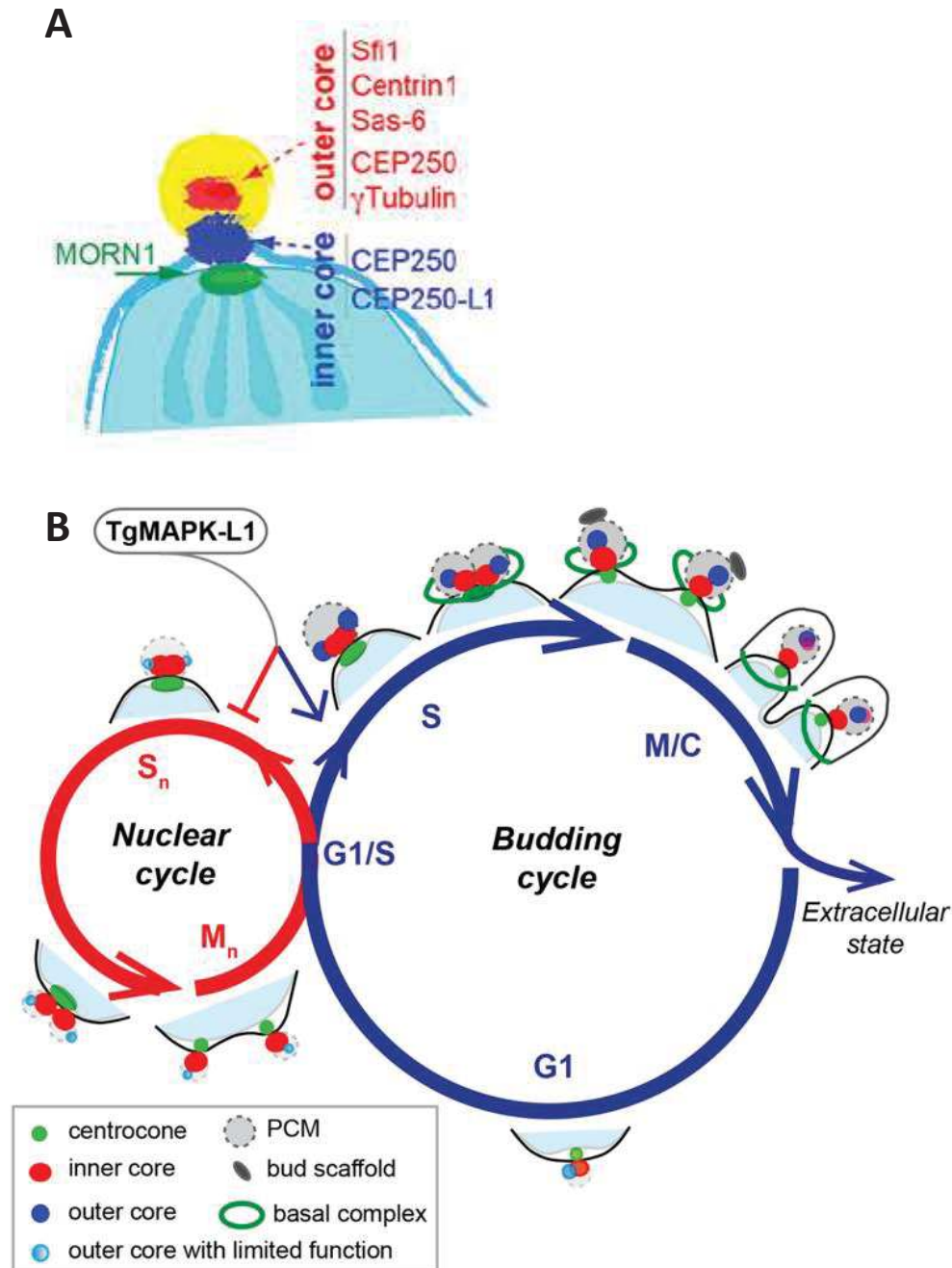


**Figure 32.** A model of *T. gondii* cell cycle regulation by a bipartite centrosome proposed by Suvorova et al.<sup>181</sup> (A) Proteins identified as being part of the centrosome's outer and inner cores. (B) The inner and outer centrosome cores. In the absence of an active outer core, the inner core and the centrocone allow the nucleus to complete DNA replication and mitosis (the nuclear cycle). The mechanisms associated with the outer core control the initiation of the budding cycle.

### ***Centrosome regulating factors***

In mammalian cells, the centrosome duplication process shares the regulators with the DNA duplication and depends on regulatory factors such as Cdk2, Nek2 (NIMA-related kinase 2) and Aurora kinase<sup>116,228</sup>. The centriole biogenesis itself is dependent on the activity of a polo-like kinase, known as PLK4. Polo-like kinase phosphorylates its substrate STIL (SCL-interrupting locus protein), and the phosphorylated STIL can subsequently recruit SAS-6 and initiate the centriole formation<sup>229</sup>.

The data on the regulation of *T. gondii* centrosome biogenesis and division remains patchy<sup>146</sup>. Several homologues of mammalian regulators of the centrosome division, such as Polo-like kinase PLK4 with its substrate STIL, are absent from the *T. gondii* genome. Still, it has been suggested that the centrosomal cycle in *T. gondii* could be under the regulation of CDK2<sup>116</sup>, of NIMA (never in mitosis)-kinases, such as TgNek1 (acts in centrosome splitting)<sup>230</sup>, of Ark3 (plays a role in division)<sup>231</sup> and of CDPK7 (implicated in centrosome positioning)<sup>232</sup>. Furthermore, the functional analysis of two regulatory kinases found in the PCM, namely TgMAPK-L1 and PRMT1, revealed that they ensure the centrosome duplication occurs only once per cell cycle<sup>181,227</sup>.

The depletion of the centrosome regulators results in significant daughter cells budding defects, notably related to the failure of centrosome correct replication. Mutant parasites display a variety of phenotypes, such as a mislocalisation of the centrosome components (TgCDPK7<sup>232</sup>), an uncontrolled centrosome duplication (TgMAPK-L1 and PRMT1<sup>181,227</sup>) or a defect of centrosome segregation into daughter buds (TgNek1<sup>230</sup>). These data highlight that the aforementioned regulators likely act on different substrates and by different mechanisms, although they are not yet identified.

---

## CHAPTER 5.

### Zinc finger proteins and their roles in *T. gondii*

---

The fundamental cellular processes, such as, for instance, cell's growth or division, are tightly regulated by a large number of factors on several levels, from gene transcription to the proteins production and their molecular interactions. Amongst the various regulators of these processes, an important place is occupied by a large group of proteins containing a specific domain termed a "zinc finger". Being one of the most abundant type of domains encoded by the eukaryotic genomes, the zinc fingers are instrumental in mediating diverse molecular interactions<sup>233</sup>.

The zinc finger domain (hereinafter referred to as ZnF) is typically a small functional independently folded protein subunit; its structure is maintained by the metal ion (commonly, zinc), chelated by conserved pair(s) of cysteines (Cys) and histidines (His) at defined positions<sup>234,235</sup>. The classical zinc fingers contain 2Cys and 2His (Cys in one chain and His in the other chain), coordinated by zinc. While the metal ion stabilises the conformation of the structure, it is usually not involved in the domain's function itself. The coordination bonds with the zinc ion provide a stable fold and allow the exposure of a specific amino acids loop that may engage in intermolecular interactions. A single zinc finger protein may contain one or many ZnFs, which can be of different types<sup>236</sup>.

There exist numerous non-classical ZnFs formed by various Cys-His combinations arranged in different manners (Fig. 33). Overall, there are currently 30 types of described ZnFs classified by their domain structure<sup>234,235</sup>. One of the well-characterised group of ZnFs is the Cys<sub>2</sub>-Cys<sub>2</sub> type which includes, in humans, the steroid-hormone receptor family and transcription factors. The first known member of this group - the Transcription Factor IIIa (TFIIIa) - was identified 35 years ago in the *Xenopus laevis* frog<sup>237</sup>. Numerous other ZnF containing proteins have been identified since; they have been described as associated with a wide range of processes including gene transcription, chromatin remodeling, regulation of translation, mRNA trafficking, cytoskeleton organisation, cell adhesion, protein folding and zinc sensing<sup>234</sup>.

The first function classically attributed to ZnF-containing proteins is their interaction with nucleic acids (both DNA and RNA)<sup>234,238,239</sup>. Later on, the ZnFs have also been shown to mediate specific protein-protein interactions, or to be able to bind lipids<sup>236,240,241</sup>. Due to their functions, ZnF-containing proteins localise either to the nucleus of a eukaryotic cell (it is the case for transcription factors or chromatin-remodelling zinc finger proteins), or to its cytoplasm (like members of E3-ubiquitin ligase family), or can be associated to the cytoskeleton (as for the Actin-Binding LIM protein 1, ABLIM1)<sup>235</sup>. The cytoplasmic zinc finger proteins often contain only one or two specific domains, while the nuclear zinc finger proteins frequently possess multiple ZnFs. Interestingly, this may be related to the type of binding molecules and the function of these proteins: it has been suggested that the arrays of fingers are usually required for high-affinity and sequence-specific binding to DNA, whereas in many cases, possessing a single finger may be enough for interacting with proteins<sup>242</sup>.

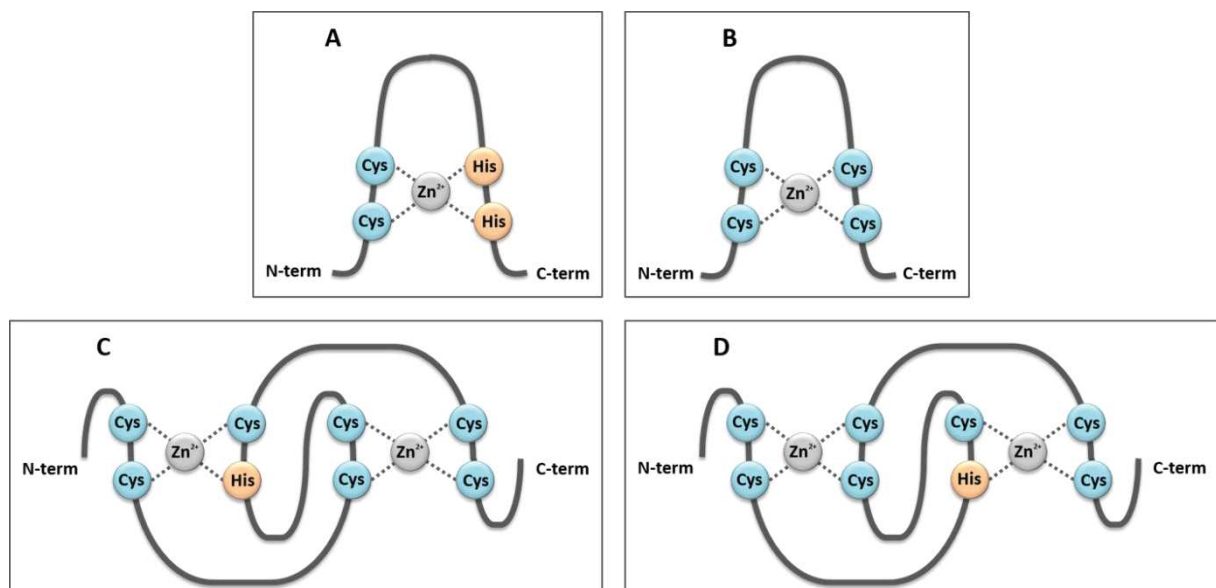


**Figure 33.** Schematic representation of some typical zinc finger domains<sup>235</sup>: the classical Cys<sub>2</sub>-His<sub>2</sub> (A); the Cys<sub>4</sub> (B); the PHD (plant homeodomain) (C) and the RING (Really Interesting New Gene) (D).

Despite the fact that zinc finger proteins are widespread and well-characterised in the eukaryotic kingdom, very little is known about these in *T. gondii*. No common nomenclature for *T. gondii* ZnF-containing proteins exists and very few of such proteins have been functionally characterised.

The first reported protein with a ZnF domain in *T. gondii* was TgMPS1/S27, an evolutionary conserved homologue of a human MPS1 (Monopolar spindle 1) protein with

which it shares 70% of similarity<sup>243</sup>. TgMPS1 has a single Cys<sub>2</sub>-Cys<sub>2</sub> finger; the same domain in human MPS1 resembles those present in the DNA-binding proteins<sup>244</sup>. Nevertheless, the *T. gondii* homologue is cytoplasmic and is suggested to be a multifunctional ribosomal-like protein produced both in tachyzoites and bradyzoites<sup>243</sup>. Another *T. gondii* zinc finger protein is a nucleolar one, named TgZFP1 (for Zinc Finger Protein 1). It has been reported to harbor 3 Cys<sub>2</sub>-HisCys motifs and to be implicated in the initiation of tachyzoites-to-bradyzoites conversion<sup>245</sup>. Daher et al.<sup>246</sup> described TgPIKfyve, a particular toxoplasmic kinase required for the production of phosphoinositides that decorate the outer membrane of the apicoplast. TgPIKfyve contains a FYVE ZnF, involved in lipids binding, and is essential for the parasite fitness, as its depletion disrupts the apicoplast morphology and induces a delayed death phenotype.

Besides the cited examples, *T. gondii* genome also encodes for several Cys<sub>2</sub>-His<sub>2</sub> containing proteins, six of which are conserved in apicomplexan parasites<sup>247</sup>. Amongst the reported proteins, one named TgZNF2 (for Zinc Finger 2) has been functionally characterized by Gissot et al.<sup>247</sup> and appears to be yet another nuclear protein containing non-classical Cys<sub>2</sub>-His<sub>2</sub> domain. In *T. gondii*, this protein has a division-related function and is associated with the mRNA export; TgZNF2 homologues, found in other Apicomplexa, may retain this function.

Lastly, a *T. gondii* ZnF-containing protein named ECR1 (for NEDD8-activating enzyme E1 catalytic subunit) was characterised in the study of Naumov et al.<sup>215</sup>. This coccidian-specific protein has divergent RING and TRAF-Sina-like zinc binding domains that are commonly involved in the ubiquitination pathway<sup>235,248</sup>. Interestingly, ECR1 localises to the centrocone of tachyzoites and is dynamically expressed: first appearing in the early S phase, it reaches the maximal expression in late S phase and is downregulated after the nuclear division<sup>215</sup>. Importantly, it is the only described *T. gondii* ZnF-containing protein with a defined role in regulating the cell cycle progression as, besides interacting with the ubiquitin-mediated protein degradation machinery, it also forms a stable complex with Crk5 and is required for replicating and assembling key mitotic structures<sup>215</sup>.

---

## Aims of the thesis

---

The main objective of the present work was to characterise a novel *T. gondii* zinc finger protein related to the cell cycle progression in tachyzoites. This protein has been identified in our laboratory during the course of the project of M. Lévêque, a previous PhD student. She was studying autophagy (an intracellular degradation system) in *T. gondii* and, more precisely, the autophagy-related protein TgATG8. Along with a potential role in degradative autophagy, this protein has a non-canonical function of maintaining the apicoplast homeostasis<sup>249</sup>. To get insights into the precise molecular function of TgATG8 at the apicoplast, the team attempted a mass-spectrometry identification of TgATG8 putative partners that i) co-immunoprecipitated with GFP-fused TgATG8 or ii) were labeled by BoID (an approach for proximity-labelling of potential partners, adapted to *T. gondii* by Chen et al. in 2015)<sup>131</sup>.

While a number of putative TgATG8-interacting partners has been identified by each of these approaches, only one protein was found in both datasets. This hypothetical protein ([www.Toxodb.org](http://www.Toxodb.org) accession number: TGME49\_212260) had a single annotated ZnF shared with a human protein called 'autoantigen p27' (PFAM (<http://pfam.xfam.org/>) motif database entry: 'Auto\_anti-p27', PF06677). The human p27 (or SSSCA1 for Sjogren syndrome/scleroderma autoantigen 1, or ZNRD2 for Zinc Ribbon Domain containing 2) is known to be one of the antigens targeted in patients suffering from Sjogren Syndrome, a systemic autoimmune disorder that typically affects lacrimal and salivary glands and leads to generalized dryness, musculoskeletal pain and fatigue<sup>250,251</sup>. Although human p27 was initially reported to be recognized by anti-centromere antibodies and suspected to play a role in mitosis<sup>252</sup>, this was not based on firm evidence: this has not been subsequently confirmed, and in fact no study has ever explored its function. Interestingly though, sera from patients with this autoimmune condition widely react with the centrosomes and were historically instrumental in discovering centrosome-associated proteins<sup>253</sup>.

The homology between human p27 and TGME49\_212260 resides mostly in the zinc finger region. In addition, the team could not confirm the association between TGME49\_212260 and TgATG8. However, the team had previously characterized another protein with homology to a Sjögren's syndrome autoantigen, TgDIP13, a pan-eukaryotic coil-coiled protein that, in *T. gondii*, associates with the cytoskeleton<sup>254</sup>.

Overall, we thought it would be worthy pursuing the study of identified uncharacterised protein, and, most interestingly, the protein (that we renamed TgZFP2 for 'Zinc Finger Protein 2') appeared to be essential for parasite growth. More precisely, the phenotype of a conditional mutant cell line that was generated for TgZFP2, seemed to be linked to the parasite replication problem. Therefore, the main goal of my PhD project was to elucidate the contribution of this protein to the cell division process in *T. gondii*. To accomplish this objective, we have used several approaches. First, we combined the use of transgenic cell lines and imagery techniques in order to characterise the mutant phenotype of TgZFP2 in tachyzoites. The results of this study will be presented thereafter in the form of a manuscript (Results, Chapter 1). Second, as it is known that ZnF domains can mediate interactions with a wide variety of molecules, including proteins, nucleic acids and lipids, I also sought to identify the molecular partners of TgZFP2 during my PhD project. We attempted the identification of TgZFP2 protein partners, and I will also present further investigations we carried out on selected candidates, such as members of a chaperonin complex. In addition, I studied the potential interactions of TgZFP2 with RNA molecules. Altogether, these investigations of TgZFP2 putative partners will be presented in their respective chapters 2 and 3 of the thesis results.

# **RESULTS**

---

# CHAPTER 1. TgZFP2 functional characterisation

---

## Introduction

The current chapter describes the functional characterisation of TgZFP2. The initial data on the general role of TgZFP2 in the parasite were obtained before I arrived to the laboratory; they suggested the protein was linked to the tachyzoites' cell cycle progression but gave no further indication on its function. In order to elucidate TgZFP2 importance for endodyogeny and to assess its role in the parasite, we performed a detailed phenotypical study of TgZFP2 conditional knock down tachyzoites.

We have indeed confirmed that interfering with TgZFP2 function has a remarkable effect on tachyzoites cell cycle progression. However, this resulted in a pleiotropic phenotype, rather complicated to dissect, and we did not elucidate TgZFP2 function at the molecular level. With an objective to gain more information on the subject, we complemented this study by a series of analysis on TgZFP2 biochemical properties and localisation using a transgenic cell line with endogenously tagged TgZFP2.

Altogether, TgZFP2 appeared to be a cytoplasmic protein dynamically recruited to the various cellular compartments and, importantly, to the peri-centrosomal region during the parasite's division. Some of data we obtained also highlights the possibility of TgZFP2 potential link with the parasite's cytoskeleton. The functional analysis of TgZFP2 is summarised in the following manuscript entitled "**TgZFP2 is a novel zinc finger protein involved in coordinating mitosis and budding in *Toxoplasma***" (currently in press in *Cellular Microbiology*).

**TgZFP2 is a novel zinc finger protein involved in coordinating mitosis and budding in *Toxoplasma***

Ksenia Semenovskaya<sup>1</sup>, Maude F. Lévêque<sup>1†</sup>, Laurence Berry<sup>1</sup>, Yann Bordat<sup>1</sup>, Jean-François Dubremetz<sup>1</sup>, Maryse Lebrun<sup>1</sup>, Sébastien Besteiro<sup>1\*</sup>

<sup>1</sup>LPHI - Laboratory of Pathogen Host Interactions - UMR5235, CNRS, Université de Montpellier, Montpellier, France

\* For correspondence : Sébastien Besteiro, LPHI-UMR 5235 CNRS, Université de Montpellier, Place Eugène Bataillon, CC107, 34095 Montpellier cedex 5, France

E-mail: [sebastien.besteiro@inserm.fr](mailto:sebastien.besteiro@inserm.fr) ; Tel. +33 4 67 34 14 55; Fax. +33 4 67 14 42 86

**Short title:** A zinc finger protein involved in *Toxoplasma* division

<sup>†</sup> Present address: University Hospital Center (CHU), Department of Parasitology-Myecology, Montpellier, France

## Abstract

Zinc finger proteins (ZFP) are one of the most abundant groups of proteins with a wide range of molecular functions. We have characterised a *Toxoplasma* protein that we named TgZFP2, as it bears a ZF domain conserved in eukaryotes. However, this protein has little homology outside this region and contains no other conserved domain that could hint for a particular function. We thus investigated TgZFP2 function by generating a conditional mutant. We showed that depletion of TgZFP2 leads to a drastic arrest in the parasite cell cycle, and complementation assays demonstrated the ZF domain is essential for TgZFP2 function. More precisely, while replication of the nuclear material is initially essentially unaltered, daughter cell budding is seriously impaired: to a large extent newly formed buds fail to incorporate nuclear material. TgZFP2 is found at the basal complex in extracellular parasites and after invasion, but as the parasites progress into cell division, it relocalises to cytoplasmic punctate structures and, strikingly, accumulates in the peri-centrosomal area at the onset of daughter cell elongation. Centrosomes have emerged as major coordinators of the budding and nuclear cycles in *Toxoplasma* and our study identifies a novel and important component of this machinery.

**Keywords:** Apicomplexa, zinc finger protein, cell division, daughter cell budding, centrosome

## Introduction

Most Apicomplexa are parasites with an obligate intracellular stage at some point of their life cycle. Proliferation of these intracellular stages occurs by invasion of a host cell, followed by multiple rounds of cell division, which will lead to the lysis of the host cell. For example, the tachyzoite form of *Toxoplasma gondii*, the causative agent of toxoplasmosis, multiplies *asexually* within its host cell by repeating a process called endodyogeny, and that accounts for much of the tissue damage associated with the acute phase of the disease (Blader *et al.*, 2015). During endodyogeny, two daughter cells are produced inside a mother cell, whose material either degenerates or is partitioned between the offspring prior to their separation. In contrast, most other apicomplexan parasites undergo division processes producing multiple daughters from a single polyploid mother cell (i.e. called schizogony or endopolygeny). In these modes of division, there are multiple rounds of DNA replication prior to cytokinesis, while during endodyogeny a single round of DNA replication is followed by single mitosis occurring simultaneously with daughter budding (Francia and Striepen, 2014).

*T. gondii* tachyzoites are highly polarised cells that contain, besides a complete set of typical eukaryotic organelles, an apical complex of specialized cytoskeletal structures and secretory organelles (micronemes and rhoptries). They also have an elaborated cytoskeleton comprising a system of flattened vesicles (called the inner membrane complex, IMC) lined underneath the plasmalemma, as well as subpellicular microtubules radiating from an apical ring formed at an early stage of endodyogeny (Morrissette and Sibley, 2002a; Anderson-White *et al.*, 2012). During division, some organelles are synthesized *de novo* (i.e. rhoptries and micronemes), while others are duplicated from a pre-existing one (i.e. the Golgi apparatus, or the non-photosynthetic plastid called the apicoplast). In any case, these parasites possess a highly coordinated subcellular replication system to ensure that each daughter cell acquires a complete complement of organelles in a timely manner (Nishi *et al.*, 2008). Like for other eukaryotes, the tachyzoite cell cycle begins with a biosynthetic gap (G) 1 phase, then chromosomes are replicated in S phase and segregated in mitosis, while the G2 period is either short or absent (Radke *et al.*, 2001). Budding is initiated towards the end of S phase, before the onset of mitosis, when the earliest components of the cytoskeleton begin to assemble near the recently duplicated centrosomes. The IMC provides a scaffold for daughter parasite assembly and organelles are partitioned between these elongating membrane/cytoskeleton scaffolds. At the end of budding, daughter parasites are incorporating components of the mother cell such as

the plasma membrane and part of the IMC (Ouologuem and Roos, 2014), and they finally emerge, leaving only a small residual body behind.

In *T. gondii* tachyzoites DNA replication and nuclear division (nuclear cycle) have to be coordinated with the assembly of daughter scaffold, organelle segregation and cytokinesis (budding cycle) to ensure that a single copy of genetic material, as well as relevant organelles, are properly encapsulated into each daughter cell. The centrosome has been shown to play a central role in coordinating the nuclear and budding cycles, as it is involved in both the nucleation of spindle microtubule and the scaffolding of daughter cells components (Suvorova *et al.*, 2015; White and Suvorova, 2018). Yet, although forward and reverse genetic studies have allowed considerable progress on the identification of molecular actors regulating the *T. gondii* cell cycle (Radke *et al.*, 2000; Gubbels *et al.*, 2008a; Alvarez and Suvorova, 2017), this process remains only partially understood at the mechanistic level.

Zinc fingers (ZFs) are small functional domains that require coordination by at least one zinc ion. Metal binding increases the conformational stability of these small domains, but is typically not directly involved in their function. Residues that participate in coordinating the metal ion are usually Cys and His. The amino acids composing the ZF are folded into loops that can interact with a variety of ligands, including nucleic acids (both DNA and RNA (Wolfe *et al.*, 2000; Hall, 2005)), proteins (Gamsjaeger *et al.*, 2007), and even lipids (Stenmark and Aasland, 1999). These domains are structurally diverse and are present among proteins that perform a broad range of functions in a variety of cellular processes, including DNA replication and repair, transcription and protein translation, signaling and metabolism, as well as cell proliferation (Matthews and Sunde, 2002).

Although ZFs are one of the most common domains found in eukaryotic proteins, very few ZFs proteins have been characterised so far in *Toxoplasma*. One is TgMPS1/S27, a homologue of a human protein called metallopan stimulin (MPS1), a C4 ZF domain-containing member of the S27 family of ribosomal proteins (Mattsson and Soldati, 1999). Acetyltransferases TgMYST-A and -B, that possess an atypical C2HC ZF and a chromodomain, and are part of the histone modifying machinery (Smith *et al.*, 2005). TgECR1 (essential for chromosome replication 1), which contains two divergent ZF domains, is required for replicating and assembling key mitotic structures (Naumov *et al.*, 2017). Another one is TgZFN2, a nuclear C2H2 ZF protein that might be involved in polyA transcript export (Gissot *et al.*, 2017). There are also proteins like TgPYKfyve (Daher *et al.*, 2015), containing a FYVE domain, which is a specific ZF involved in lipid binding. Finally, TgZFP1 is a nucleolar protein

with three CCHC ZF motifs, involved in the conversion of tachyzoites to bradyzoites (Vanchinathan *et al.*, 2005).

Here, we present the characterisation of a novel *Toxoplasma* ZF domain-containing protein that we named TgZFP2. We have shown by conditional depletion of this protein that it is essential for parasite multiplication and survival *in vitro*. More precisely, although TgZFP2-depleted parasites are still able to replicate their DNA content and initiate budding of daughter cells, these fail to fully incorporate nuclear material and to complete emergence from the mother cell. We have thus identified a novel factor which plays an important role in coupling nuclear division and cytokinesis.

## Materials and methods

### Parasites and cells culture

Tachyzoites of the TATi1- $\Delta$ Ku80 (Sheiner *et al.*, 2011a) *T. gondii* strain, as well as derived transgenic parasites generated in this study, were maintained by serial passage in human foreskin fibroblast (HFF, American Type Culture Collection, CRL 1634) cell monolayer grown in Dulbecco's modified Eagle medium (DMEM, Gibco) supplemented with 5% decomplemented fetal bovine serum (Gibco), 2 mM L-glutamine (Gibco) and a cocktail of penicillin-streptomycin (Gibco) at 100  $\mu$ g/mL.

### Bioinformatic analyses

Identification of zinc finger domain-containing proteins in the *T. gondii* genomic database ([www.toxodb.org](http://www.toxodb.org)) was performed searching for zinc finger motifs from the PFAM (<https://pfam.xfam.org/>), the INTERPRO (<https://www.ebi.ac.uk/interpro/>), the SUPERFAMILY ([www.supfam.org/](http://www.supfam.org/)) and the PROSITE (<https://prosite.expasy.org/>) domain databases. See **Table S1** for a list of the specific domains. Sequence alignments of TGGT1\_212260 homologues were performed using the MULTiple Sequence Comparison by Log-Expectation (MUSCLE) algorithm of the Geneious software suite ([www.genious.com](http://www.genious.com)).

### Generation of an HA-tagged TgZFP2 cell line

The ligation independent strategy (Huynh and Carruthers, 2009) was used for C-terminal HA<sub>3</sub>-tagging of TgZFP2. A 1.380 kbp fragment corresponding to the 3' end of *TgZFP2* was amplified by PCR from genomic DNA, with the Phusion polymerase (New England BioLabs) using primers ML1923/ML1924 (primers used in this study are listed on **Table S2**) and inserted in frame with the sequence coding for a triple HA tag, present in the pLIC-HA<sub>3</sub>-CAT plasmid. The resulting vector was linearized with BstXI and 40  $\mu$ g of DNA were transfected into the TATi1-  $\Delta$ Ku80 cell line to allow integration by single homologous recombination, and transgenic parasites of the TgZFP2-HA cell line were selected with chloramphenicol.

In this TgZFP2-HA cell line we also tagged the inner core TgCEP250L1 protein using the ligation independent strategy to add a C-terminal *myc* tag to the corresponding protein. A 1.023 kbp fragment corresponding to the 3' end of *TgCEP250L1* (TGGT1\_290620) was amplified by PCR from genomic DNA, with the Phusion polymerase (New England BioLabs) using primers ML4165/ML4166 and inserted in frame with the sequence coding for a *myc* tag,

present in the pLIC-*myc*-DHFR plasmid. The resulting vector was linearized with *KasI* and 40 µg of DNA were transfected into the TgZFP2-HA cell line to allow integration by single homologous recombination and transgenic parasites of the TgZFP2-HA/ TgCEP250L1-*myc* cell line were selected with pyrimethamine.

### **Generation of conditional knock-down and complemented TgZFP2 cell lines**

The conditional knock-down TgZFP2 cell line (cKD-TgZFP2) was generated based on the Tet-off system using the DHFR-TetO7Sag4 plasmid (Morlon-Guyot *et al.*, 2014). In brief, the 5' region of *TgZFP2* starting with the initiation codon was amplified from genomic DNA by PCR using Q5 polymerase (New England Biolabs) with ML2377/ML2378 primers containing *BglII* and *NotI* restriction sites, respectively. The 977 bp fragment was then inserted into *BglII/NotI* site of the DHFR-TetO7Sag4 plasmid, downstream of the anhydrotetracycline (ATc)-inducible *TetO7Sag4* promoter, obtaining the DHFR-TetO7Sag4-TgZFP2 plasmid. The plasmid was then linearized by *BlpI* digestion and transfected into the TATi1-ΔKu80 cell line containing 3×HA-tagged TgZFP2. Transfected parasites were selected with pyrimethamine at a concentration of 1 µM and cloned by serial limiting dilutions. Correct integration in the positive clones was verified by PCR using primers ML2379/ML2380.

The cKD-TgZFP2 cell line was complemented by the addition of an extra copy of *TgZFP2* put under the dependence of its own promoter at the *uracil phosphoribosyltransferase* (*UPRT*) locus. A 2.5 kbp fragment containing the promoter region of *TgZFP2* was amplified from genomic cDNA with primers ML2630/ML2631 and the fragment was cloned into the *NotI/StuI*-digested pUPRT-TUB-Ty vector (Sheiner *et al.*, 2011a). *TgZFP2* cDNA (1056 bp) was amplified by RT-PCR with primers ML2628/ML2629 and then cloned using *StuI/XmaI* downstream of the promoter fragment to yield the pUPRT-TgZFP2 plasmid.

For complementing with a mutated version of TgZFP2 where cysteines 70 and 73 are replaced by glycine residues, we used the QuikChange site directed mutagenesis kit (Agilent) with primers ML2821/ML2822 using pUPRT-TgZFP2 as a template.

These plasmids were then digested by *KpnI/NcoI* prior to transfection and transgenic parasites were selected using 5-fluorodeoxyuridine to yield the cKD-TgZFP2 comp WT or cKD-TgZFP2 comp mut ZnF cell lines, respectively.

### **Semi-quantitative RT-PCR**

Total mRNAs of freshly egressed extracellular parasites from the TATi1- $\Delta$ Ku80, cKD-TgZFP2, cKD-TgZFP2 comp WT and cKD-TgZFP2 comp mut ZnF cell lines (incubated with or without ATc at 1.5 $\mu$ g/mL for 2 days), were extracted using Nucleospin RNA II Kit (Macherey-Nagel). cDNAs were synthesized with about 800 ng of total RNA per RT-PCR reaction using Superscript II first-strand synthesis system (Invitrogen). Specific *TgZFP2* ML2877/ML2878 primers and, as a control, *Tubulin  $\beta$*  ML841/ML842 primers were used to amplify specific transcripts with the GoTaq DNA polymerase (Promega). PCR was performed with 22 cycles of denaturation (30 s, 95°C), annealing (20 s, 56°C) and elongation (20 s, 72°C).

### **Subcellular fractionation and detergent extraction**

$3 \times 10^7$  TgZFP2-HA tachyzoites were solubilized in 1 ml of Tris HCl 50 mM pH 7.5 and sonicated twice for 30 seconds. Cellular debris were removed by centrifugation at 500 g for 10 minutes. The supernatant was submitted to an ultracentrifugation at 100,000 g for 30 minutes to yield a membrane/cytoskeleton-enriched high speed pellet and high speed supernatant soluble fractions, respectively. The supernatant fraction was TCA-precipitated and extracts were resuspended in SDS-PAGE loading buffer prior to immunoblot analysis.

For assessing protein solubility in various detergents, freshly released parasites were collected by centrifugation at 1,000 g for 10 minutes. These samples were suspended in PBS containing 1% Triton X-100, PBS with 10 mM deoxycholate, or PBS with 1% sodium dodecyl sulfate (SDS) for 15 minutes at room temperature. For immunoblot analysis, samples were centrifuged at 12,000 g for 30 minutes to separate the pellet from the soluble fraction. The latter was acetone-precipitated and both fractions were resuspended in the same volume of loading buffer before being separated by SDS-PAGE and analysed by immunoblot.

### **DNA content analysis by flow cytometry**

Extracellular parasites were fixed in 70% (v/v) ethanol/30% (v/v) PBS for at least overnight at -20°C prior to staining. Following fixation, parasites were pelleted by centrifugation and resuspended at a final concentration of  $5 \times 10^6$  parasites/ml in freshly made 50 mM Tris pH 7.5 buffer with 0.1 mg/ml propidium iodide (Sigma-Aldrich). RNase cocktail was added to the staining solution (200U). The samples were incubated for 30 minutes at room temperature in the dark prior to analysis. Nuclear DNA content was analysed by measuring fluorescence (FL-1) using the 556LP-585/45BP filter of a FACSCANTO flow cytometer

(Becton Dickinson). Fluorescence was collected in linear mode (10,000 events) and the results were analysed and visualised using Cyflogic v1.2.1 (<http://www.cyflogic.com/>).

### **Immunoblot analysis**

Protein extracts from  $10^7$  freshly egressed tachyzoites or from the fractionation assays described above, were separated by SDS-PAGE. Rat monoclonal anti-HA (clone 3F10, Roche) was used to detect tagged TgZFP2. The following antibodies were used as controls: mouse anti- $\alpha$ -tubulin (clone B-5-1-2, Sigma-Aldrich), mouse anti-SAG1 (Couvreur *et al.*, 1988), mouse anti-IMC1 (MAb 45:36; kindly provided by Gary Ward, University of Vermont, USA), rabbit anti-TgIF2 $\alpha$  (Narasimhan *et al.*, 2008), mouse anti-GRA1 (Lecordier *et al.*, 1999), rabbit anti-Eno2 (Dzierszinski *et al.*, 2001).

### **Plaque assays**

Confluent monolayers of HFFs grown in 24-well plates were infected with  $2 \times 10^5$  freshly egressed tachyzoites and incubated with or without ATc (at 1.5  $\mu$ g/ml) for 7 days. Infected cell layer was then fixed in cold methanol (for 1 min) and stained with Giemsa (for 1 min). Images were acquired with an Olympus MVX10 macro zoom microscope equipped with an Olympus XC50 camera. Plaque area measurements were done using ZEN software (Zeiss).

### **Immunofluorescence microscopy**

For immunofluorescence assays (IFA), intracellular tachyzoites grown on coverslips containing HFF monolayers were either fixed for 20 min with 4% (w/v) paraformaldehyde in PBS and permeabilized for 10 min with 0.3% Triton X-100 in PBS, or fixed for 5 minutes in cold methanol (when performing MORN1 and Cen1 staining).

For timecourse analysis of TgZFP2 localization after invasion, freshly egressed parasites were either centrifuged and fixed with 4% (w/v) paraformaldehyde in PBS before and made to adhere onto poly-L-lysine slides for 20 minutes prior to processing for IFA, or synchronized to invade host cells as previously described (Besteiro *et al.*, 2009). Briefly, parasites were sedimented on confluent cells at 4°C and warmed up for invasion for 5 minutes at 37°C. Invasion was either stopped by adding an excess volume of 4% paraformaldehyde in PBS (for subsequent IFA for labelling invading parasites), or extracellular parasites were removed by extensive washes in Hanks' Balanced Salt solution (HBSS, Gibco) and put back at 37°C for various periods of time, prior to fixation and IFA analysis of intracellular parasites.

For morphological analyses of individual cells, parasites were released mechanically by scraping of the HFF monolayer and three consecutive passages through a 25G syringe. Parasites were then centrifuged and fixed with 4% (w/v) paraformaldehyde in PBS before and made to adhere onto poly-L-lysine slides for 20 minutes prior to processing for immunofluorescent labelling.

Slides/coverslips were subsequently blocked with 0.1% (w/v) BSA in PBS. Primary antibodies used (at 1/1000, unless specified) to detect sub-cellular structures were: rabbit anti-CPN60 (Agrawal *et al.*, 2009) or mouse anti-ATRX1 (DeRocher *et al.*, 2008) to label the apicoplast; rabbit polyclonal anti-TgMORN1 (Gubbels *et al.*, 2006); guinea pig anti-Ndc80 (Farrell and Gubbels, 2014); rabbit anti-centrin1 (1/500) (from Iain Cheeseman's laboratory, MIT, USA); mouse anti-myc (Santa Cruz Biotechnology) was used at 1/100 to detect epitope-tagged TgCEP250L1; and rat monoclonal anti-HA antibody (Roche) was used at 1/500 to detect epitope-tagged TgZFP2. For TgEB1 labelling, parasites were transiently transfected with a construct expressing TgEB1-YFP (Chen *et al.*, 2015; Berry *et al.*, 2016). Staining of DNA was performed on fixed cells incubated for 5 min in a 1 µg/ml DAPI solution. All images were acquired at the Montpellier RIO imaging facility from a Zeiss AXIO Imager Z2 epifluorescence microscope equipped with an ORCA-flash 4.0 camera (Hamamatsu) and driven by the ZEN software v2.3 (Zeiss). Adjustments for brightness and contrast were applied uniformly on the entire image. 3D view of Z stacks was performed using the ZEN software using the transparency rendering mode.

For measuring mutant parasites and nuclei areas, images were processed with the ImageJ/Fiji software (Schindelin *et al.*, 2012). Briefly, single plane images were converted to binary and screened with the 'analyze particle' function using the appropriate threshold values (0.5-18 µm<sup>2</sup> for nuclei). At least 100 measurements were made and plotted using the Prism software (Graphpad).

### **Electron microscopy**

Parasites were pre-treated for 24h with ATc, and then used to infect HFF monolayers and grown for an extra 12h in ATc. They were fixed with 2.5% glutaraldehyde in cacodylate buffer 0.1M pH7.4. Coverslips were then processed using a Pelco Biowave pro+ (Ted Pella). Briefly samples were post-fixed in 1% OsO<sub>4</sub> and 2% uranyl acetate, dehydrated in acetonitrile series and embedded in Epon 118 using the following parameters: Glutaraldehyde (150 Watts ON/OFF/ON 1 min cycles); 2 buffer washes (40sec 150 Watts); OsO<sub>4</sub> (150 Watts

ON/OFF/ON/OFF/ON 1 min cycles); 2 water washes.( 40sec 150 Watts); uranyl acetate (100 Watts ON/OFF/ON 1 min cycles); Dehydration (40sec 150 Watts); Resin Infiltration (350 Watts 3 min cycles). Fixation and Infiltration steps were performed under vacuum. Polymerization was performed at 60°C for 48h. 70 nM ultrathin sections were cut with a Leica UC7 ultramicrotome, counterstained with uranyl acetate and lead citrate and observed in a Jeol 1200 EXII transmission electron microscope. All chemicals were from Electron Microscopy Sciences, solvents were from Sigma.

### **Statistical analysis**

Values were expressed as means  $\pm$  standard error of the mean (SEM). Data were analysed for comparison using unpaired Student's t-test with equal variance (homoscedastic) for different samples or paired Student's t-test for similar samples before and after treatment.

## Results

### Identification of a novel putative *T. gondii* ZFP

To evaluate the repertoire of ZFP encoded by the *T. gondii* genome, we conducted a series of motif-based searches in the ToxoDB genomic database ([www.toxodb.org](http://www.toxodb.org)). The search, using canonical motifs from the PFAM, Interpro and Superfamily motif databases retrieved a non-redundant set of 309 proteins (**Table S1**). This means that at least ~3.6% of the nuclear genome-encoded *T. gondii* proteins are potentially ZFP, which is quite considerable. In fact, this is comparable to the ZFP repertoire in mammals, as in humans at least 3% of the genome is supposedly coding for ZFP (Klug, 2010), and in mouse, about 7% of total transcripts are encoding potential ZFP (Ravasi *et al.*, 2003). Although only a fraction of the *T. gondii* ZFPs has a clear predicted function, they are potentially involved in a wide array of important cellular pathways like transcription, translation, signaling and trafficking.

One of these potentially important ZFPs, TGGT1\_212260, drew our attention: it is annotated as containing a domain related to proteins related to human autoimmune disorders called Sjögren's syndrome and scleroderma, for which several autoantigens include cytoskeleton-related proteins (Tuffanelli *et al.*, 1983; Routsias and Tzioufas, 2010). We have previously characterised TgDIP13, a pan-eukaryotic coiled-coil protein with a homology to a Sjögren's syndrome autoantigen that is associated with the *T. gondii* cytoskeleton (Lévêque *et al.*, 2016), and thus decided to investigate TGGT1\_212260 function too.

TGGT1\_212260 contains a domain annotated as 'Sjögren's syndrome/scleroderma autoantigen 1 (Autoantigen p27)' (<https://pfam.xfam.org/family/PF06677>), which is in fact a 4-cysteine ZF motif. Proteins containing this motif, which are found in a wide variety of eukaryotes and also in Archaea, have in fact little homology within the rest of their respective sequences. Even in Apicomplexa, for which homologues of TGGT1\_212260 are found mostly in the coccidia and haematozoa subclasses, the most conserved regions are the single predicted ZF and the C-terminal end (**Figure S1**). Yet, besides the ZF domain, in this protein there is no particular region that would give insights into a specific biological function.

A closer look at the ZF motif of TGGT1\_212260 and its closely-related coccidian homologues (**Figure 1a**) shows the four cysteines around the potential metal-binding site, and the predicted fold of the chain strongly argue for its classification as a zinc ribbon (Krishna, 2003). We thus propose to name TGGT1\_212260 TgZFP2. Interestingly, the small protein domain that is potentially structured around the putative zinc ion would expose a number of

polar and positively-charged amino acids that may be involved in interactions of TgZFP2 with nucleic acids or other proteins (**Figure 1b**).

### **TgZFP2 presents features of a cytoskeleton-associated protein**

To characterise TgZFP2, its corresponding gene was modified at the endogenous locus by single homologous recombination (**Figure 2a**), to express a C-terminal triple haemagglutinin (HA)-tagged version of the protein in *T. gondii* tachyzoites. Transgenic parasites were selected with chloramphenicol and checked for correct integration. Immunoblot analysis showed a main product with an apparent molecular mass close to the expected one (41 kDa), thus likely corresponding to full-length TgZFP2-HA (**Figure 2b**). Immunofluorescence assay (IFA) revealed that this protein localises to punctate structures in the cytoplasm of tachyzoites (**Figure 2c**). Staining patterns were quite similar after formaldehyde or methanol fixation, the only difference being that in methanol fixation conditions only, the protein was sometimes found close to the basal complex, at the end of the elongated IMC, and this was particularly obvious in vacuoles containing single parasites (**Figure 2d**). To further characterise this particular staining pattern, we took freshly egressed parasites that we synchronised for invasion, and we assessed the posterior localisation of TgZFP2 in extracellular, invading and intracellular parasites (**Figure S2**). The posterior staining was present in a majority of extracellular parasites (**Figure S2a, c**), and this was also evidenced by labelling of invading parasites (**Figure S2b**). After invasion, as the intracellular parasites progressed in cell division, the signal became punctate and more evenly distributed in the cell body (**Figure S2a, c**). This shows TgZFP2 has a dynamic localisation during the cell cycle.

In intracellular parasites, TgZFP2 staining appeared largely absent from the nucleus, regardless of the stage of cell cycle progression (**Figure 2c, d**). However, as a large number of ZFPs can bind DNA and are nuclear transcription factors, we sought to investigate more precisely the possibility of a TgZFP2 association with the nucleus. We thus separated cytoplasmic and nuclear fractions from tachyzoites, and the partitioning of TgZFP2-HA was assessed by immunoblotting (**Figure 2e**). Consistent with the IFA data, there was no evidence of presence of TgZFP2-HA in the nuclear fractions.

The localisation of TgZFP2-HA as puncta in the cytoplasm prompted us to investigate its solubility. Upon hypotonic lysis of tachyzoites and ultracentrifugation, a large portion of TgZFP2-HA was found in the insoluble fraction (**Figure 2f**), hinting that it could be associated with the cytoskeleton or with membranes. To further investigate this, we performed detergent

extraction of total tachyzoite proteins and co-fractionation assays (**Figure 2g**). Part of TgZFP2-HA is resistant to extraction with Triton X-100, hinting that it is probably not membrane associated. Only the use of ionic detergents (deoxycholate, sodium dodecyl sulfate) allowed efficient extraction of the protein, suggesting it may be associated with the cytoskeleton instead.

### **TgZFP2 localisation changes during the cell cycle**

The general localisation pattern of TgZFP2 in intracellular parasites (**Figure 2c**) does not seem to correspond to a specific known compartment, but we could see more intense foci in some parasites, which prompted us to scrutinize TgZFP2 localisation together with markers of the cell cycle. In *Toxoplasma* centrosome-associated proteins have been assigned to two main separate cores which are linked to distinct functions (Suvorova *et al.*, 2015): the inner core (IC) is closely associated with the centrocone and drives chromosome segregation, while the outer core (OC) primarily regulating daughter cell budding. We first used centrosomal OC marker Centrin 1 (**Figure 3a**), as well as IMC1 (Mann and Beckers, 2001) to monitor the formation of daughter buds (**Figure 3b**). Strikingly, in mitotic cells TgZFP2 was found by IFA to concentrate as an intense peri-centrosomal signal at the onset of mitosis and daughter cell elongation. This labelling was persisting until emergence of the daughter cells. The TgZFP2 signal appeared distinct from the Centrin 1 signal, yet adjacent to it and often more proximal to the nucleus, suggesting it is not part of the centrosomal OC (**Figure 3a**).

In addition, we looked at TgMORN1, a protein present both at the mitotic spindle poles (centrocones) and the basal complex (Hu *et al.*, 2006; Gubbels *et al.*, 2006). TgMORN1 serves as an additional mitotic marker, as centrocone duplication occurs later than that of centrosomes in the mitotic sequence. We confirmed TgZFP2 is recruited in the peri-centrosomal region after centrocone duplication, and around the time of nuclear separation (**Figure S3**). We could also clearly see TgZFP2 does not co-localize with TgMORN1 present at the centrocone: TgZFP2 appears generally more distal from the nucleus (**Figure S3**). Concerning our previous observation that TgZFP2 might be enriched at the basal complex (**Figure 2d**), it did not appear to be systematically the case during daughter bud elongation, although stainings were occasionally close (**Figure S3**).

As TgZFP2 is neither co-localising with the centrosomal OC nor with the centrocone, we generated a cell line co-expressing tagged TgZFP2 together with tagged IC marker TgCEP250L1 (the IC is intermediate between the OC and the centrocone, to which it is closely associated), and performed co-staining experiments to assess whether or not they co-localise.

The signal corresponding to TgZFP2 was found to be distinct from all three compartments: consistently more apical than the centrocone or the IC, and usually in a basal or lateral position compared with the OC marker (**Figure 3d**). TgZFP2 thus seems to localise at the interface between the centrosomal IC and OC (**Figure 3e**), in a position somewhat similar to the recently characterised protein TgCEP530 (Courjol and Gissot, 2018).

In conclusion, our data suggest TgZFP2 has a dynamic localisation during the cell cycle and may play a specific role related to the centrosome during mitosis.

### Generation of transgenic cell lines

In order to get more insights into TgZFP2 function, we generated a conditional mutant cell line in the TgZFP2-HA-expressing  $\Delta$ Ku80-TATi1 background (Sheiner *et al.*, 2011b). In this TgZFP2 knock-down cell line (cKD-TgZFP2) (**Figure 4a**), the addition of anhydrotetracycline (ATc) can repress *TgZFP2* transcription through a Tet-Off system (Meissner *et al.*, 2001). Several transgenic clones were obtained and subsequent analyzes were performed on two independent clones. As they were found to behave similarly in the first rounds of phenotypic assays we performed, only one will be described in details here. Transgenic parasites were grown for various periods of time in presence of ATc and protein down-regulation was evaluated. Immunoblot analyses of cKD-TgZFP2 parasites (**Figure 4b**) showed a slight overexpression of the protein after promoter replacement. It should be noted that both for the parental cell line and after promoter change (**Figures 2b, 4b**) we detected smaller products, possibly resulting from degradation or maturation processes, and some higher molecular mass products, which might reflect post-translational modifications. However, importantly all these products are specific as they disappear upon ATc treatment: we could show TgZFP2 is already efficiently depleted after one day of ATc treatment and completely undetectable after two days of incubation with the drug (**Figure 4b**). By IFA on cKD-TgZFP2 parasites, we verified that after promoter replacement the HA-tagged TgZFP2 gives a similar staining pattern as when expressed from its native promoter, and confirmed the protein is essentially undetectable after only one day of ATc treatment (**Figure 4c**).

We next generated complemented cell lines by stably integrating in the genome (at the *uracil phosphoribosyl transferase -UPRT-* locus) an additional *TgZFP2* copy expressed under the dependence of its own promoter (**Figure S4a**) or a version mutated on the last two cysteines of the ZF motif (mutated to glycines, **Figure S4b**). The obtained complemented cell lines were named cKD TgZFP2 comp WT, and cKD TgZFP2 comp mut ZnF, respectively. Total RNAs

of the corresponding transgenic parasites, kept in absence or presence of ATc for two days, were extracted for semi-quantitative RT-PCR analyses using primers specific of the transcripts for *TgZFP2*, and for  *$\beta$ -tubulin* as a control. We could show that the transcription of *TgZFP2* is effectively repressed in the conditional knockdown cell line upon addition of ATc, while the completed cell lines exhibits a restored *TgZFP2* transcription level similar to the parental cell line (**Figure S4c**).

### **TgZFP2 is important for cell cycle progression, but not for DNA replication**

To assess the impact of TgZFP2 depletion on the *T. gondii* lytic cycle, a plaque assay was performed. The capacity of the mutant and complemented parasites to produce lysis plaques was analyzed on a host cells monolayer in absence or continuous presence of ATc for 7 days. Depletion of TgZFP2 almost completely impaired plaque formation compared with the cell line complemented with the wild-type copy of TgZFP2 (**Figure 5a**). Interestingly, complementing with the cysteine-mutated version of TgZFP2 did not allow restauration of the parasites ability to form plaques. This shows TgZFP2 is essential for completion of the lytic cycle in host cells, and that the ZF motif is likely crucial for TgZFP2 function. To assess whether this defect the in lytic cycle is due to a replication problem, all cell lines were pre-incubated in ATc for 24h and fixed, or released mechanically and incubated for an additional 24h in ATc prior to parasite counting. No particular delay in cell division was observed in the first 24h, but after a second 24h period of incubation in the presence of ATc we noted an accumulation of vacuoles with fewer parasites in the absence of TgZFP2 (**Figure 5b**). This shows TgZFP2 is important for intracellular parasite replication. Parasites complemented with the cysteine-mutated version of TgZFP2 seem to present slightly different kinetics as they could generate a few vacuoles with up to four parasites, but they were nevertheless completely blocked for further stages of division (**Figure 6b**). Again, this suggests the ZF domain is important for TgZFP2 function.

We then used IFA to assess if TgZFP2 depletion leads to specific morphological defects during cell division. Parasites were kept continuously in the presence of ATc for two days and the formation of daughter buds was monitored using IMC proteins IMC1 and ISP1. Parasites expressing the wild-type copy of TgZFP2 showed perfectly synchronised daughter budding within parasites of the same vacuole (**Figure 6a**), which is the normal situation. In stark contrast, upon depletion of TgZFP2, or when complementing with a mutated ZF version of TgZFP2, cell division appeared largely asynchronous and disordered. The main striking defects were the initiation of multiple internal buddings (leading to more than two daughter cells), and

the emergence of incomplete daughter cells from the mother (**Figure 6a**). However, DAPI staining revealed the presence of multilobed or enlarged nuclei, suggesting DNA replication is not primarily affected, although the final stages mitosis, more precisely partitioning of the nucleus into daughter cells, appears to be. This repeated failure to generate daughter cells results in large amorphous syncytial mother cells with enlarged nuclear material (**Figure 6a**). We assessed the DNA content of these parasites by flow cytometry (**Figure 6b**) and confirmed the lack of TgZFP2 or the expression of a ZF mutant form of the protein, leads to parasites with an increased DNA content, although the presence of mutant parasites with sub-1N DNA was also observed. In conclusion, TgZFP2 appears particularly important for daughter cell generation, while DNA replication is not primarily affected by the depletion of the protein. These results also confirm an intact ZF domain is essential to the cellular function of TgZFP2.

#### **TgZFP2-depleted parasites seem impaired in late stage of mitosis, but not in centrosome duplication**

The phenotypic analysis of cell cycle mutants contained in large vacuoles can be tedious and prone to misinterpretations. We thus decided to release mechanically from the vacuoles parasites incubated continuously for two days in the presence of ATc, to be able to analyse them individually. We could confirm TgZFP2-depleted parasites are heterogenous in size and in nuclear content (**Figure 6c, d**). Consistent with the DNA content analysis we performed by flow cytometry (**Figure 6b**), mutant cells appeared generally larger and contained a larger nucleus, although small cells with little or no visible DNA content ('zoids') were also observed. The presence of large nuclei confirms late stage of mitosis is affected in a substantial part of the population.

We thought one or two consecutive divisions only in the absence of TgZFP2 would also allow obtaining a clearer general picture of the cell division phenotype. Thus we incubated the parasites with ATc for 24 hours, then released them mechanically and made them reinvade and develop into a new host cell for an extra 12 hours only. In these conditions, for the complemented cell line, daughter cells were perfectly synchronised in their budding and their emergence from the mother cell, and were properly incorporating their respective nuclear material (**Figure 6e**). On the other hand, complete depletion of TgZFP2 led to two major defects (**Figure 6e**): i) budding daughter cells tentatively emerging from the mother cell, without fully incorporating their nuclear material, and ii) multiple budding initiations in a syncytial mother cell with an apparent polyploid DNA content. This confirmed our initial observations on parasites grown for two consecutive days in the presence of ATc (**Figure 6a**). Quantitative

phenotypic analysis highlighted that the multiple budding phenotype is the most frequent, and that some cells display both the emergence and budding problems (**Figure 6f**). Multiple internal buds and abortive emergence of daughter cells were also confirmed at the ultrastructural level by electron microscopy (EM) (**Figure 7a**). Internal budding seemed to occur away from the multiple nuclei or from a single multilobed nucleus (often EM does not allow distinguishing between these) (**Figure 7a**). However, daughter cells generally seemed to contain a conoid and seemingly normal sets of *de novo* synthesized secretory organelles such as rhoptries, micronemes or dense granules (**Figure 7a, b**). Strikingly, in cases we could capture elongating daughters in the process of internalising daughter nuclei, we noticed that in TgZFP2-depleted parasites, despite a bona fide association of the nuclear centrocone with the centrosomes, proper budding and internalization of the nucleus in the buds was unlikely to happen due to an early closure of the IMC scaffold (**Figure 7b**, white arrowheads).

In *Toxoplasma*, budding and mitosis are regulated by two unique cores of centrosomal proteins (Suvorova *et al.*, 2015). More generally in eukaryotes, a microtubular spindle originating from the centrosome is formed during mitosis to mediate the segregation of spindle poles and the equal division of the duplicated chromosomes. Thus, the spindle microtubules and the kinetochore, that mediates chromosomes attachment to the spindle (Farrell and Gubbels, 2014), are major organisers of mitosis that work in close association with the centrosome (**Figure 8a**). We first sought to assess the impact of TgZFP2 loss on centrosome OC and kinetochore duplication. On parasites grown for two days in the presence of ATc, we checked for centrosomal OC marker Centrin 1 and kinetochore marker Ndc80 (Farrell and Gubbels, 2014). Upon TgZFP2 depletion, we observed an elevated number of centrosomes or kinetochore clusters per parasite (**Figure 8b, c, d**). It suggests mitotic cycles proceed to some extent in these conditions: a large proportion of mutant parasites contained more than one duplicated centrosome/kinetochore cluster, hinting successive or parallel mitotic cycles had been initiated (**Figure 8b, c**). Consistent with that, when we looked at centrocone marker TgMORN1 (the centrocone houses the spindle pole, **Figure 8a**), we could also see evidence of multiple centrocone duplications in large syncytial TgZFP2-depleted parasites (**Figure S5a**).

Interestingly, EM observations of TgZFP2-depleted parasites revealed several striking examples of “Russian dolls”-like buds embedded within one another (**Figure S6**). This illustrates daughter cell buds that stopped their development, but within which the centrosome initiates a new round of budding, leading to the formation of these structures. It suggests that

in the absence of TgZFP2, while mitosis is blocked the centrioles are still able to duplicate and to initiate a new budding process.

After TgZFP2 depletion, several stray kinetochore clusters or centrosomal OC were observed (**Figure 8b**) and this was quantified. Up to 21% and 17% of stray centrosomes and kinetochores, respectively, were found (**Figure 8e**). Although this indicates TgZFP2 may have some role in coordinating the OC with nuclear structures governing the mitotic cycle, importantly depletion of the protein did not cause a major and systematic disruption of the interaction between these structures. This is also illustrated by the EM observation of TgZFP2-depleted parasites displaying normal centrocones/spindle poles (**Figure 7b, Figure S5b**), which were also correctly positioned and associated with the centrioles (**Figure S5b, b'**).

We further assessed the morphology of the mitotic spindle by using the TgEB1 marker, a protein binding to the spindle microtubules (Chen *et al.*, 2015). As previously published, in control parasites TgEB1 was present in the nucleoplasm of G1 parasites, and then at the onset of mitosis it labelled spindle poles and, finally, fibers that likely represent interpolar spindle microtubules remaining after completion of mitosis (**Figure 8f**). In TgZFP2-depleted parasites, TgEB1 was found essentially at the spindle pole and on spindle microtubules (in 90%±2% of labelled parasites), which is another evidence that these parasites are blocked in mitosis and do not reenter G1. Importantly, not only TgZFP2 depletion did not cause any major collapse of the spindle microtubules, but large syncytial cells showed multiple spindle poles with an extensive TgEB1-labelled network of microtubules (**Figure 8F**), suggesting they may instead fail to disassemble the spindle for mitotic exit.

The centrosome also serves as a scaffold for correct partitioning of organelles besides the nucleus, such as the Golgi apparatus (Hartmann *et al.*, 2006) or the apicoplast (Striepen *et al.*, 2000). Specific co-staining with an apicoplast marker during cell cycle progression confirmed TgZFP2 is closely associated with the organelle as it duplicates and segregates in budding daughter cells (**Figure S7a**). We thus looked for the fate of the apicoplast by following the Atrx1 marker in in TgZFP2-depleted parasites. Co-staining with IMC1 to follow budding (**Figure S7b**), or with Centrin 1 (**Figure S7c**) indicated that the organelle remains generally associated with the centrosomes. However, while it was often present in emerging incomplete daughter cells, it was usually found unsegregated and away from internal buds in larger syncytial cells.

Overall, these data show TgZFP2-depleted parasites do not have a major defect in DNA replication and in initiation of daughter cell budding, but the final stages of mitosis are impaired, as these parasites fail to package their nuclear material correctly into daughter parasites. A primary consequence is that they fail to generate fully formed daughter buds, and longer term consequences include accumulation of masses of nuclear material in the residual mother parasite, as well as later defects in segregation of centrosome-linked organelles.

### **Cytoskeletal components are not drastically affected by TgZFP2 depletion**

Daughter cell budding is driven by the assembly of numerous cytoskeleton components that include the microtubule cytoskeleton, and the IMC with its associated protein meshwork. We assessed whether or not cytoskeletal structures were affected by TgZFP2 depletion. First, we detected no major alteration of the subpellicular microtubules scaffold for intracellularly-developing daughters in the case of syncytial cells with multiple internal budding, or those tentatively emerging as incomplete parasites (**Figure S8a**). We also checked for components of the IMC. Our previous labellings showed IMC1-decorated internal buds in large syncytial mothers (**Figure 6a, e, Figure S7b**), hinting the *de novo* synthesis of the IMC is not completely impaired in the absence of TgZFP2. We also focused on emerging cells, now using both IMC1 as well as GAP45 (Gaskins *et al.*, 2004), a protein related to the gliding machinery of the parasite that does not label daughter cells but gets recruited later to the mature IMC. We could see that, upon TgZFP2 depletion, while tentatively emerging daughter cells were labelled by GAP45 and IMC1, they occasionally showed some discontinuity in the IMC with the remnants of the mother cell (**Figure S8b, c**). This was also confirmed at the ultrastructural level by EM (**Figure S8d**). Post-emergence maturation of the IMC involves salvage and recycling of the maternal IMC (Ouologuem and Roos, 2014), which might be compromised in TgZFP2-depleted parasites. This phenotype, however, may also be secondary, as it could result from a local fragmentation of the mother cell after aborted daughter emergence rather than a major structural defect.

In conclusion, our data show that depletion of TgZFP2 does not seem to cause a major disturbance in early cytoskeletal neogenesis associated with budding, whereas aborted emergence likely alters proper organisation of the IMC.

## Discussion

ZFPs are among the most abundant proteins in eukaryotic genomes. Through a bioinformatics analysis we have identified more than 300 putative ZFPs in *Toxoplasma*, with potentially very diverse cellular functions. However, to this date very few of them have been functionally investigated. The one we chose to characterise, TgZFP2, is a crucial factor for coordinating parasite cell division.

Cell division is a highly regulated process in eukaryotes. It follows an ordered progression of events in which mitosis leads to equal segregation of replicated genomes, and subsequent ingression of a cytokinetic cleavage furrow then partitions the remaining cellular material. In apicomplexan parasites cell division includes a semi-closed mitosis of the nucleus (during which the nuclear envelope remains largely intact), and cytokinesis is achieved by budding, necessitating a coordinated incorporation of organellar and nuclear material in developing daughter cells (Francia and Striepen, 2014). Many apicomplexan parasites can replicate their nuclei without an accompanying cytokinesis, thereby forming multinucleate syncytial cells, until the last round of synchronized mitosis and budding generates multiple daughter cells (a process termed schizogony). *Toxoplasma* tachyzoites use a slightly different process called endodyogeny, where each DNA replication cycle is followed by mitosis and budding. However, blocking DNA replication does not completely abolish initiation of daughter cell budding (Shaw *et al.*, 2001) and inhibiting daughter scaffold formation does not impair DNA replication (Morrissette and Sibley, 2002b). This demonstrates that although they obviously need to be finely coordinated during cell division, mitosis and daughter budding can be easily uncoupled in *Toxoplasma* (Gubbels *et al.*, 2008b).

In many animals, higher fungi and several other eukaryotic lineages, the centrosome plays key roles in the spatio-temporal organization of mitosis and cell division (Ito and Bettencourt-Dias, 2018). Beyond its function as an important microtubule organising centre, this organelle is acting as a general signaling platform for cell cycle regulation. In animal cells for instance, the centrosome is made of a pair of centrioles surrounded by peri-centriolar material made of a dynamic collection of dozens of proteins that includes cell cycle regulators, checkpoint proteins and signalling molecules (Woodruff *et al.*, 2014). In *Toxoplasma*, only a few of these are conserved (Morlon-Guyot *et al.*, 2017), and in fact very few centrosomal proteins have been functionally characterised so far. Recent studies have nevertheless outlined a similar important function for the centrosome as a cell cycle coordination centre (Chen and

Gubbels, 2013; Suvorova *et al.*, 2015; Berry *et al.*, 2016; El Bissati *et al.*, 2016; Courjol and Gissot, 2018; Chen and Gubbels, 2019). Interestingly, *Toxoplasma* centrosome-associated proteins may belong to separate bipartite cores that appear to have distinct functions (Suvorova *et al.*, 2015): the IC is tightly associated with the centrocone and drives chromosome segregation and the mitotic cycle, while the OC controls daughter formation and budding.

Interfering with TgZFP2 function led to the formation of immature daughter buds. TgZFP2-depleted parasites were able to initiate daughter cell budding, with at least partial elongation of accompanying IMC and associated microtubules. In most cases, the elongation of daughter parasites could proceed to a point where *de novo* synthesized organelles such as micronemes were produced (usually a late step of the cell division process (Nishi *et al.*, 2008)) and the apicoplast was often partitioned correctly. However, the resulting parasites generally failed to emerge properly. In fact, the most striking phenotype is that the parasite nucleus was not correctly partitioned into the developing daughters. Tachyzoites were nevertheless able to undergo multiple rounds of DNA replication, centrosome duplication and mitotic spindle formation (evidenced by kinetochore and centrocone duplication –**Figure 8d**, **Figure S5a**-, and normal-looking spindles seen by EM and IFA –**Figure 7b**, **Figure S5b**, **Figure S6c**, **Figure 8f**). Eventually, this led to the formation of abnormal parasite masses, which contained multiple centrin-labeled structures. The parasite nucleus increased greatly in size and became a highly lobed organelle not properly segregated into nascent daughters. A forward genetics screen has identified a number of likewise uncoupled cell division mutants that are blocked in nuclear division but are nevertheless able to re-enter the cell cycle, leading to an increase in centrosomes and nuclear DNA content (Gubbels *et al.*, 2008a). Moreover, this phenotype is somewhat similar to the effects of agents perturbing microtubule dynamics, where cortical microtubules and spindle microtubules can be differentially affected by the drugs (Shaw *et al.*, 2000; Morrisette and Sibley, 2002b). However, in our case both cortical (**Figure S8a, b, c**) and spindle microtubules (**Figure 8f**) showed no sign of major collapse following TgZFP2 depletion, suggesting TgZFP2 function is not directly linked to the microtubular cytoskeleton.

Upon depletion of TgZFP2, the initiation of the mitotic cycle seems unaffected, but nuclear segregation is impaired and the large non-divided nuclei cannot be properly incorporated into developing or emerging buds. At the ultrastructural level, our observations suggest a premature closure of the developing buds encapsulating few, if any, nuclear material (**Figure 7b**, **Figure S5b**). It also shows immature buds nevertheless initiating subsequent rounds of mitosis, leading to the generation of “Russian dolls”-like structures (**Figure S6**).

Thus, coordination between parasite budding and mitosis clearly appears deficient. Breaking the physical connection between mitotic and budding machinery is likely to cause a loss of restriction over nuclear and daughter bud replication. For example, recently characterised mutants for centrosome-associated proteins TgCEP250 (Chen and Gubbels, 2019) and TgCEP530 (Courjol and Gissot, 2018) display a lack of association between the centrosomal IC and OC, that leads to a discoordination between the nuclear and the budding cycles. However, although depletion of TgZFP2 led to some extent to a defect in centrosome association with the spindle pole/kinetochore, in the majority of cells this association was largely preserved (**Figure 8e**). Besides, there is evidence of non-divided nuclear material being pulled out, albeit inefficiently, from the mother cell by emerging daughters (**Figure 6e**, **Figure S5b**, **Figure S8a, c**), again suggesting the connection between the centrosome and the spindle pole is not compromised.

TgZFP2 has a dynamic localisation during the cell cycle: in particular, we have gathered evidence that TgZFP2 accumulates to the peri-centrosomal region during daughter cell elongation, with a particularly strong labelling at the onset of mitosis that persists until daughter cell emergence (**Figure 3**, **Figure S3**, **Figure S7**). Our data thus suggest a centrosome-related function for TgZFP2. Our IFA shows the protein localises between the centrosomal OC and the centrocone/centrosomal IC (**Figure 3d, e**, **Figure S3**), yet as mentioned above it does not seem involved in the physical connection between these structures, as they appear still closely associated in the absence of TgZFP2 (**Figure 8**, **Figure S5b**). Interestingly, some recently-characterised *Toxoplasma* proteins (Courjol and Gissot, 2018; Chen and Gubbels, 2019) were shown to be recruited in a very dynamic fashion to the centrosomal region, and to be located at the interface between the IC/OC, or transiently associated with both of them. This illustrates that the organisation of the peri-centrosomal protein complexes is likely more complex and dynamic than just partitioning into a simple bipartite structure. In mammals centrosomal proteins are also of dynamic nature and many are recruited during the course mitosis to exert a specific function (Woodruff *et al.*, 2014). Of note, SSSCA1 the human protein containing a ZF motif homologous to the one of TgZFP2 is related to a pathology called scleroderma (Muro *et al.*, 1998). Interestingly, although the localisation of this particular human protein has not yet been clearly established, sera from patients with this autoimmune condition react widely with centrosomes and were historically instrumental in discovering centrosome-associated proteins (Tuffanelli *et al.*, 1983).

TgZFP2 also potentially associates with the basal complex, although mostly in extracellular parasites and for a few hours after invasion (**Figure 2d**, **Figure S2**). The protein is generally not detected at the posterior end of actively dividing parasites, but we cannot completely exclude some can persist there. It is thus possible that TgZFP2 has pleiotropic functions during the cell cycle. We noticed that in the absence of the protein, the elongation of the IMC seems to proceed normally to some extent, but the basal complex may play a pivotal role in the early closure of daughter buds and the failed incorporation of the nuclear material that we observed (**Figure 7b**). However, the physical contribution of the IMC elongation, and of the basal complex in particular, to the segregation of the nucleus into daughter buds is currently unknown. Mutants of basal complex proteins such as MORN1 (Heaslip *et al.*, 2010; Lorestani *et al.*, 2010) and the HAD2 phosphatase (Engelberg *et al.*, 2016) are clearly deficient in budding, like TgZFP2-deficient parasites, but usually blocked at later stages of parasite emergence.

In any case, because of its association with cytoskeletal elements such as the centrosome and the basal complex, TgZFP2 is ideally poised to act as a regulator of daughter cell budding. To mediate its function(s), ZgZFP2 likely interacts with other molecules through its ZF domain, which is the only well-defined motif in the protein, and is essential to its function (**Figure 5**, **Figure 6a, b**). Unfortunately, we were unsuccessful in identifying molecular partners of TgZFP2 (not shown). Thus the precise molecular mechanisms by which TgZFP2 contributes to the coordination between mitosis and budding remains to be determined. Although recently there were considerable advances on the comprehension of the molecular basis of apicomplexan cell division (Anderson-White *et al.*, 2012; White and Suvorova, 2018), many regulating factors remain uncharacterised. For instance, the apicomplexan centrosomal proteome is poorly characterised, and as it is likely considerably different from other canonical eukaryotic models (Morlon-Guyot *et al.*, 2017), future studies should concentrate on deciphering its composition. This would most likely provide interesting insights into the intricate cell division regulation process of these divergent eukaryotes.

**Acknowledgements**

We thank C. Beckers, I. Cheeseman, M. Gissot, MJ. Gubbels, B. Striepen, L. Sheiner, D. Soldati-Favre, W. Sullivan and G. Ward for their generous gift of antibodies, plasmids and cell lines. M. Gissot is also gratefully acknowledged for his help with the RNAseq experiments. We thank M. Séveno and the Montpellier Functional Proteomics Platform for the mass spectrometry analysis. We also thank the MRI imaging facility, member of the national infrastructure France-BioImaging supported by the French National Research Agency (ANR-10-INBS-04, «Investments for the future»), for providing access to their microscopes and flow cytometers, as well as the electron microscopy imaging facility of the University of Montpellier. Support from the Inserm (ML and SB are Inserm researchers), the Fondation pour la Recherche Médicale (Equipe EQ20170336725), and the Labex Parafrap (ANR-11-LABX-0024) is also acknowledged. The authors have no conflict of interest to declare.

## References

- Agrawal, S., Dooren, G.G. van, Beatty, W.L., and Striepen, B. (2009) Genetic evidence that an endosymbiont-derived endoplasmic reticulum-associated protein degradation (ERAD) system functions in import of apicoplast proteins. *J Biol Chem* **284**: 33683–33691.
- Alvarez, C.A., and Suvorova, E.S. (2017) Checkpoints of apicomplexan cell division identified in *Toxoplasma gondii*. *PLOS Pathogens* **13**: e1006483.
- Anderson-White, B., Beck, J.R., Chen, C.-T., Meissner, M., Bradley, P.J., and Gubbels, M.-J. (2012) Cytoskeleton Assembly in *Toxoplasma gondii* Cell Division. In *International Review of Cell and Molecular Biology*. Elsevier, pp. 1–31 <http://linkinghub.elsevier.com/retrieve/pii/B9780123943095000018>. Accessed February 3, 2016.
- Berry, L., Chen, C.-T., Reininger, L., Carvalho, T.G., El Hajj, H., Morlon-Guyot, J., *et al.* (2016) The conserved apicomplexan Aurora kinase TgArk3 is involved in endodyogeny, duplication rate and parasite virulence. *Cell Microbiol* **18**: 1106–1120.
- Besteiro, S., Michelin, A., Poncet, J., Dubremetz, J.-F., and Lebrun, M. (2009) Export of a *Toxoplasma gondii* rhoptry neck protein complex at the host cell membrane to form the moving junction during invasion. *PLoS Pathog* **5**: e1000309.
- Blader, I.J., Coleman, B.I., Chen, C.-T., and Gubbels, M.-J. (2015) Lytic cycle of *Toxoplasma gondii* : 15 years Later. *Annual Review of Microbiology* **69**: 463–485.
- Chen, C.-T., and Gubbels, M.-J. (2013) The *Toxoplasma gondii* centrosome is the platform for internal daughter budding as revealed by a Nek1 kinase mutant. *J Cell Sci* **126**: 3344–3355.
- Chen, C.-T., and Gubbels, M.-J. (2019) TgCep250 is dynamically processed through the division cycle and is essential for structural integrity of the *Toxoplasma* centrosome. *MBoC* **30**: 1160–1169.
- Chen, C.-T., Kelly, M., Leon, J. de, Nwagbara, B., Ebbert, P., Ferguson, D.J.P., *et al.* (2015) Compartmentalized *Toxoplasma* EB1 bundles spindle microtubules to secure accurate chromosome segregation. *MBoC* **26**: 4562–4576.
- Courjol, F., and Gissot, M. (2018) A coiled-coil protein is required for coordination of karyokinesis and cytokinesis in *Toxoplasma gondii*. *Cellular Microbiology* **20**: e12832.
- Couvreur, G., Sadak, A., Fortier, B., and Dubremetz, J.F. (1988) Surface antigens of *Toxoplasma gondii*. *Parasitology* **97 ( Pt 1)**: 1–10.
- Daher, W., Morlon-Guyot, J., Sheiner, L., Lentini, G., Berry, L., Tawk, L., *et al.* (2015) Lipid kinases are essential for apicoplast homeostasis in *Toxoplasma gondii*. *Cell Microbiol* **17**: 559–578.
- DeRocher, A.E., Coppens, I., Karnataki, A., Gilbert, L.A., Rome, M.E., Feagin, J.E., *et al.* (2008) A thioredoxin family protein of the apicoplast periphery identifies abundant candidate transport vesicles in *Toxoplasma gondii*. *Eukaryotic Cell* **7**: 1518–1529.
- Dzierszinski, F., Mortuaire, M., Dendouga, N., Popescu, O., and Tomavo, S. (2001) Differential expression of two plant-like enolases with distinct enzymatic and antigenic properties

- during stage conversion of the protozoan parasite *Toxoplasma gondii*. *Journal of Molecular Biology* **309**: 1017–1027.
- El Bissati, K., Suvorova, E.S., Xiao, H., Lucas, O., Upadhyaya, R., Ma, Y., *et al.* (2016) *Toxoplasma gondii* Arginine Methyltransferase 1 (PRMT1) Is Necessary for Centrosome Dynamics during Tachyzoite Cell Division. *mBio* **7**: e02094-15, /mbio/7/1/e02094-15.atom.
- Engelberg, K., Ivey, F.D., Lin, A., Kono, M., Lorestani, A., Faugno-Fusci, D., *et al.* (2016) A MORN1-associated HAD phosphatase in the basal complex is essential for *Toxoplasma gondii* daughter budding. *Cellular Microbiology* **18**: 1153–1171.
- Farrell, M., and Gubbels, M.-J. (2014) The *Toxoplasma gondii* kinetochore is required for centrosome association with the centrocone (spindle pole). *Cell Microbiol* **16**: 78–94.
- Francia, M.E., and Striepen, B. (2014) Cell division in apicomplexan parasites. *Nat Rev Microbiol* **12**: 125–136.
- Gamsjaeger, R., Liew, C.K., Loughlin, F.E., Crossley, M., and Mackay, J.P. (2007) Sticky fingers: zinc-fingers as protein-recognition motifs. *Trends Biochem Sci* **32**: 63–70.
- Gaskins, E., Gilk, S., DeVore, N., Mann, T., Ward, G., and Beckers, C. (2004) Identification of the membrane receptor of a class XIV myosin in *Toxoplasma gondii*. *J Cell Biol* **165**: 383–393.
- Gissot, M., Hovasse, A., Chaloin, L., Schaeffer-Reiss, C., Van Dorsselaer, A., and Tomavo, S. (2017) An evolutionary conserved zinc finger protein is involved in *Toxoplasma gondii* mRNA nuclear export. *Cell Microbiol* **19**.
- Gubbels, M.-J., Lehmann, M., Muthalagi, M., Jerome, M.E., Brooks, C.F., Szatanek, T., *et al.* (2008a) Forward Genetic Analysis of the Apicomplexan Cell Division Cycle in *Toxoplasma gondii*. *PLoS Pathogens* **4**: e36.
- Gubbels, M.-J., Vaishnav, S., Boot, N., Dubremetz, J.F., and Striepen, B. (2006) A MORN-repeat protein is a dynamic component of the *Toxoplasma gondii* cell division apparatus. *Journal of Cell Science* **119**: 2236–2245.
- Gubbels, M.-J., White, M., and Szatanek, T. (2008b) The cell cycle and *Toxoplasma gondii* cell division: tightly knit or loosely stitched? *Int J Parasitol* **38**: 1343–1358.
- Hall, T.M.T. (2005) Multiple modes of RNA recognition by zinc finger proteins. *Curr Opin Struct Biol* **15**: 367–373.
- Hartmann, J., Hu, K., He, C.Y., Pelletier, L., Roos, D.S., and Warren, G. (2006) Golgi and centrosome cycles in *Toxoplasma gondii*. *Mol Biochem Parasitol* **145**: 125–127.
- Heaslip, A.T., Dzierszynski, F., Stein, B., and Hu, K. (2010) TgMORN1 is a key organizer for the basal complex of *Toxoplasma gondii*. *PLoS Pathog* **6**: e1000754.
- Hu, K., Johnson, J., Florens, L., Fraunholz, M., Suravajjala, S., DiLullo, C., *et al.* (2006) Cytoskeletal components of an invasion machine--the apical complex of *Toxoplasma gondii*. *PLoS Pathog* **2**: e13.
- Huynh, M.-H., and Carruthers, V.B. (2009) Tagging of Endogenous Genes in a *Toxoplasma gondii* Strain Lacking Ku80. *Eukaryot Cell* **8**: 530–539.
- Ito, D., and Bettencourt-Dias, M. (2018) Centrosome Remodelling in Evolution. *Cells* **7**: 71.

- Klug, A. (2010) The Discovery of Zinc Fingers and Their Applications in Gene Regulation and Genome Manipulation. *Annual Review of Biochemistry* **79**: 213–231.
- Krishna, S.S. (2003) Structural classification of zinc fingers: survey and summary. *Nucleic Acids Research* **31**: 532–550.
- Recordier, L., Mercier, C., Sibley, L.D., and Cesbron-Delauw, M.F. (1999) Transmembrane insertion of the *Toxoplasma gondii* GRA5 protein occurs after soluble secretion into the host cell. *Mol Biol Cell* **10**: 1277–1287.
- Lévêque, M.F., Berry, L., and Besteiro, S. (2016) An evolutionarily conserved SSNA1/DIP13 homologue is a component of both basal and apical complexes of *Toxoplasma gondii*. *Sci Rep* **6**: 27809.
- Lorestani, A., Sheiner, L., Yang, K., Robertson, S.D., Sahoo, N., Brooks, C.F., *et al.* (2010) A *Toxoplasma* MORN1 null mutant undergoes repeated divisions but is defective in basal assembly, apicoplast division and cytokinesis. *PLoS ONE* **5**: e12302.
- Mann, T., and Beckers, C. (2001) Characterization of the subpellicular network, a filamentous membrane skeletal component in the parasite *Toxoplasma gondii*. *Mol Biochem Parasitol* **115**: 257–268.
- Matthews, J.M., and Sunde, M. (2002) Zinc fingers--folds for many occasions. *IUBMB Life* **54**: 351–355.
- Mattsson, J.G., and Soldati, D. (1999) MPS1: a small, evolutionarily conserved zinc finger protein from the protozoan *Toxoplasma gondii*. *FEMS Microbiology Letters* **180**: 235–239.
- Meissner, M., Brecht, S., Bujard, H., and Soldati, D. (2001) Modulation of myosin A expression by a newly established tetracycline repressor-based inducible system in *Toxoplasma gondii*. *Nucleic Acids Res* **29**: E115.
- Morlon-Guyot, J., Berry, L., Chen, C.-T., Gubbels, M.-J., Lebrun, M., and Daher, W. (2014) The *Toxoplasma gondii* calcium-dependent protein kinase 7 is involved in early steps of parasite division and is crucial for parasite survival. *Cell Microbiol* **16**: 95–114.
- Morlon-Guyot, J., Francia, M.E., Dubremetz, J.-F., and Daher, W. (2017) Towards a molecular architecture of the centrosome in *Toxoplasma gondii*. *Cytoskeleton* **74**: 55–71.
- Morrisette, N.S., and Sibley, L.D. (2002a) Cytoskeleton of apicomplexan parasites. *Microbiol Mol Biol Rev* **66**: 21–38; table of contents.
- Morrisette, N.S., and Sibley, L.D. (2002b) Disruption of microtubules uncouples budding and nuclear division in *Toxoplasma gondii*. *J Cell Sci* **115**: 1017–1025.
- Muro, Y., Yamada, T., Himeno, M., and Sugimoto, K. (1998) cDNA cloning of a novel autoantigen targeted by a minor subset of anti-centromere antibodies. *Clin Exp Immunol* **111**: 372–376.
- Narasimhan, J., Joyce, B.R., Naguleswaran, A., Smith, A.T., Livingston, M.R., Dixon, S.E., *et al.* (2008) Translation regulation by eukaryotic initiation factor-2 kinases in the development of latent cysts in *Toxoplasma gondii*. *J Biol Chem* **283**: 16591–16601.

- Naumov, A., Kratzer, S., Ting, L.-M., Kim, K., Suvorova, E.S., and White, M.W. (2017) The *Toxoplasma centrocone* houses cell cycle regulatory factors. *mBio* **8**: e00579-17, /mbio/8/4/e00579-17.atom.
- Nishi, M., Hu, K., Murray, J.M., and Roos, D.S. (2008) Organellar dynamics during the cell cycle of *Toxoplasma gondii*. *J Cell Sci* **121**: 1559–1568.
- Ouologuem, D.T., and Roos, D.S. (2014) Dynamics of the *Toxoplasma gondii* inner membrane complex. *Journal of cell science* **127**: 3320–30.
- Radke, J.R., Guerini, M.N., and White, M.W. (2000) *Toxoplasma gondii*: Characterization of Temperature-Sensitive Tachyzoite Cell Cycle Mutants. *Experimental Parasitology* **96**: 168–177.
- Radke, J.R., Striepen, B., Guerini, M.N., Jerome, M.E., Roos, D.S., and White, M.W. (2001) Defining the cell cycle for the tachyzoite stage of *Toxoplasma gondii*. *Mol Biochem Parasitol* **115**: 165–175.
- Ravasi, T., Huber, T., Zavolan, M., Forrest, A., Gaasterland, T., Grimmond, S., *et al.* (2003) Systematic characterization of the zinc-finger-containing proteins in the mouse transcriptome. *Genome Res* **13**: 1430–1442.
- Routsias, J.G., and Tzioufas, A.G. (2010) Autoimmune response and target autoantigens in Sjogren's syndrome. *European Journal of Clinical Investigation* **40**: 1026–1036.
- Schindelin, J., Arganda-Carreras, I., Frise, E., Kaynig, V., Longair, M., Pietzsch, T., *et al.* (2012) Fiji: an open-source platform for biological-image analysis. *Nat Methods* **9**: 676–682.
- Shaw, M.K., Compton, H.L., Roos, D.S., and Tilney, L.G. (2000) Microtubules, but not actin filaments, drive daughter cell budding and cell division in *Toxoplasma gondii*. *J Cell Sci* **113 ( Pt 7)**: 1241–1254.
- Shaw, M.K., Roos, D.S., and Tilney, L.G. (2001) DNA replication and daughter cell budding are not tightly linked in the protozoan parasite *Toxoplasma gondii*. *Microbes Infect* **3**: 351–362.
- Sheiner, L., Demerly, J.L., Poulsen, N., Beatty, W.L., Lucas, O., Behnke, M.S., *et al.* (2011a) A Systematic Screen to Discover and Analyze Apicoplast Proteins Identifies a Conserved and Essential Protein Import Factor. *PLoS Pathog* **7** <http://www.ncbi.nlm.nih.gov/pmc/articles/PMC3228799/>. Accessed April 23, 2015.
- Sheiner, L., Demerly, J.L., Poulsen, N., Beatty, W.L., Lucas, O., Behnke, M.S., *et al.* (2011b) A Systematic Screen to Discover and Analyze Apicoplast Proteins Identifies a Conserved and Essential Protein Import Factor. *PLoS Pathog* **7** <http://www.ncbi.nlm.nih.gov/pmc/articles/PMC3228799/>. Accessed April 22, 2015.
- Smith, A.T., Tucker-Samaras, S.D., Fairlamb, A.H., and Sullivan, W.J. (2005) MYST family histone acetyltransferases in the protozoan parasite *Toxoplasma gondii*. *Eukaryotic Cell* **4**: 2057–2065.
- Stenmark, H., and Aasland, R. (1999) FYVE-finger proteins--effectors of an inositol lipid. *J Cell Sci* **112 ( Pt 23)**: 4175–4183.

- Striepen, B., Crawford, M.J., Shaw, M.K., Tilney, L.G., Seeber, F., and Roos, D.S. (2000) The plastid of *Toxoplasma gondii* is divided by association with the centrosomes. *J Cell Biol* **151**: 1423–1434.
- Suvorova, E.S., Francia, M., Striepen, B., and White, M.W. (2015) A novel bipartite centrosome coordinates the apicomplexan cell cycle. *PLoS Biol* **13**: e1002093.
- Tuffanelli, D.L., McKeon, F., Kleinsmith, D.M., Burnham, T.K., and Kirschner, M. (1983) Anticentromere and ant centriole antibodies in the scleroderma spectrum. *Arch Dermatol* **119**: 560–566.
- Vanchinathan, P., Brewer, J.L., Harb, O.S., Boothroyd, J.C., and Singh, U. (2005) Disruption of a locus encoding a nucleolar zinc finger protein decreases tachyzoite-to-bradyzoite differentiation in *Toxoplasma gondii*. *Infect Immun* **73**: 6680–6688.
- White, M.W., and Suvorova, E.S. (2018) Apicomplexa Cell Cycles: Something Old, Borrowed, Lost, and New. *Trends Parasitol* **34**: 759–771.
- Wolfe, S.A., Nekludova, L., and Pabo, C.O. (2000) DNA recognition by Cys2His2 zinc finger proteins. *Annu Rev Biophys Biomol Struct* **29**: 183–212.
- Woodruff, J.B., Wueseke, O., and Hyman, A.A. (2014) Pericentriolar material structure and dynamics. *Philos Trans R Soc Lond, B, Biol Sci* **369**.

## Figure legends

**Figure 1.** TGGT1\_212260/TgZFP2 is a zinc finger protein present in related coccidian parasites. (a) Schematic representation of the zinc finger domain position in protein TGGT1\_212260 from *Toxoplasma gondii*, and alignment of the domain in its homologues from different coccidia species. Asterisks mark the four important cysteine residues of the motif. EupathDB ([www.eupathdb.org](http://www.eupathdb.org)) accession numbers for the homologues are: *Hammondia hammondi* HHA\_212260, *Neospora caninum* NCLIV\_049120, *Besnoitia besnoiti* A0A2A9MJU1, *Eimeria praecox* EPH\_0048600. (b) Schematic representation of the theoretical organisation of the zinc finger domain, positively charged and polar amino acids are highlighted in blue and red, respectively.

**Figure 2.** TgZFP2 localises to cytoplasmic puncta and behaves as a cytoskeleton-associated protein. (a) Schematic representation of the strategy to express triple-HA tagged TgZFP2. (b) Immunoblot analysis of HA-tagged TgZFP2 expression in total parasite extracts. The parental  $\Delta$ Ku80-TATi1 cell line was used as a negative control; SAG1 was used as a loading control. (c) Immunolocalisation of HA-tagged TgZFP2 in intracellular tachyzoites. DNA was stained with DAPI; DIC: differential interference contrast; scale bar is 5  $\mu$ m. parasite shape is outlined on the merged image. (d) TgZFP2 is occasionally seen at the basal complex. Merged images of IFA on methanol-fixed TgZFP2-HA parasites with co-staining between TgZFP2 and either IMC1 (left) or MORN1 (right, parasite shape is outlined). The arrowhead indicates the basal complex at the posterior end of the parasites. DNA was stained with DAPI; scale bar is 2  $\mu$ m. (e) Immunoblot analysis of TgZFP2 partitioning into cytoplasmic and nuclear fractions. The Eno2 nuclear isoform of enolase and the cytoplasmic translation initiation factor TgIF2 $\alpha$  were used as controls. (f) Cellular fractionation after hypotonic/mechanical lysis and ultracentrifugation at 100,000 g, yielding pellet (P100) and supernatant (S100) fractions. Distribution of TgZFP2, membrane-associated protein SAG1 and soluble protein GRA1 was analysed by immunoblot. (g) Parasites were extracted using different detergents and separated into pellet (P) and soluble (S) fraction and analysed by immunoblot. T represent total parasite extracts. IMC1 and tubulin are part of the cytoskeleton, SAG1 is a membrane-associated protein, and TgIF2 $\alpha$  is a soluble cytoplasmic protein.

**Figure 3.** TgZFP2 localises to the peri-centrosomal region during mitosis. Dynamics of TgZFP2 localisation during the cell division process were assessed by IFA using co-staining with centrosomal marker centrin 1 (a) and inner membrane complex protein IMC1 (b). DNA was stained with DAPI; scale bar is 1  $\mu\text{m}$ ; parasite shape is outlined on the merged image; insets show magnifications of selected merged images. (c) Schematic representation of TgZFP2 re-localisation during the different phases of the cell cycle. TgZFP2 is in red, centrosomes are in green, the conoid is in burgundy and the IMC in dark purple. (d) Co-staining of apical TgZFP2 together with Cen1, CEP250L1 and MORN1 as markers of the centrosomal outer core (OC) and inner core (IC) and the centrocone (CC), respectively. MORN1 also labels the basal complex (BC). DNA was stained with DAPI; scale bar is 1  $\mu\text{m}$ ; parasite shape is outlined. (e) Co-staining of TgZFP2 together with markers of the centrosomal sub-domains. DNA was stained with DAPI; scale bar is 0.5  $\mu\text{m}$ . On the right is a magnified 2D view of a volume reconstruction from image stacks, highlighting the relative positions of TgZFP2 and the other centrosomal markers.

**Figure 4.** Genetic knockdown of *TgZFP2*. (a) Schematic representation of the strategy for generating a TgZFP2 conditional mutant in a TATi1-Ku80 $\Delta$  background, by replacement of the endogenous promoter by an ATc-regulated promoter. Clones were obtained after pyrimethamine selection. TetO7: tet operator, DHFR: dihydrofolate reductase selection marker, p*TgSAG4*: SAG4 minimal promoter. (b) Immunoblot analysis of TgZFP2 expression in proteins extracts from TATi1-Ku80 $\Delta$ , cKd-TgZFP2 and parental TgZFP2-HA parasites incubated during up to three days with ATc. SAG1 was used as a loading control. (c) IFA of TgZFP2 conditional depletion. Parasites were grown for one day in the presence of ATc or not and anti-HA antibody was used to detect tagged TgZFP2. DNA was stained with DAPI; DIC: differential interference contrast; scale bar represents 5  $\mu\text{m}$ ; parasite shape is outlined on the merged image.

**Figure 5.** TgZFP2-depleted tachyzoites are deficient in intracellular growth.

(a) Plaque assays were carried out by infecting HFF monolayers with cKD TgZFP2, or parasites complemented with the wild-type or mutant version of the protein. They were grown for 7 days  $\pm$  ATc. Measurements of lysis plaque areas are shown on the right and highlight a significant defect in the lytic cycle when TgZFP2 is depleted or the mutant copy is expressed. AU: arbitrary units. Values are the mean  $\pm$  standard error of the mean for at least 30 plaque measurements, from one representative experiment out of three. \* denotes  $p < 0.001$ , Student's t-test. (b) Intracellular growth of the three cell lines grown in HFF in the presence of ATc for 24h, or subsequently allowed to invade and grow in new HFF cells for an extra 24h in the presence of ATc (24h+24h). Numbers of parasites per vacuole were counted 24h after inoculation. Values are means  $\pm$  SEM for three independent experiments for which 200 vacuoles were counted for each condition.

**Figure 6.** Depletion of TgZFP2 impairs the cell division process. (a) cKD TgZFP2, as well as WT and ZnF mutant complemented parasites were grown for two days in the presence of ATc and IFA was performed with anti-IMC1 and anti-ISP1 antibodies to visualise developing daughter buds. DNA was stained with DAPI; DIC: differential interference contrast; scale bar represents 5  $\mu$ m; parasite shape is outlined on the merged image; insets are magnification of selected merged images. (b) Measurements of the DNA content by flow cytometry in the corresponding cell lines analysed in (a). (c) For morphological observations of the effect of TgZFP2 depletion, parasites were treated for two days in the presence of ATc and then were released mechanically and adhered on poly-lysine slides before being stained with DAPI and observed with a microscope. Scale bar is 5  $\mu$ m. (d) Quantifications of cells (top) and nuclei (bottom) area corresponding to the experimental conditions described in (c). (e) Phenotypic observation of parasites pre-incubated for 24h with ATc, then released mechanically, made to invade new host cells, and grown for an extra 12hr with ATc before IFA. ISP1 and IMC1 were used as IMC markers; DNA was stained with DAPI; scale bar is 2  $\mu$ m. (f) Phenotypic quantification after TgZFP2 depletion (following the experimental conditions described in (e)). On the right are selected examples of the different phenotypes that were identified thanks to DAPI labelling of the DNA (blue) and IMC1 labelling (green).

**Figure 7.** Ultrastructural observations of the consequences of TgZFP2 depletion. cKD TgZFP2 parasites pre-incubated for 24h with ATc, then released mechanically, made to invade new host cells, and grown for an extra 12hr before being processed for EM. (a) TgZFP2-deficient parasite showing a cytoplasmic mass containing four nuclear profiles (N) and five sections through developing tachyzoites, one of which at an early stage of budding (white arrow). (b) TgZFP2-deficient parasite where two developing tachyzoites are at an early stage of elongation (one being already budding: white arrow) and daughter nuclei internalization (following the centrocone –cc- driven by the centriole –ce-, detailed in the enlarged insert), but where the inner membrane complex shows an untimely constriction (arrowheads) likely to impair nuclei entry in the buds. co: conoid. (c) Typical endodyogeny in the complemented cell line: the dividing nucleus is being partitioned between the two elongating daughter tachyzoites within the mother cell and the IMC remains wide open (arrowheads) until the end of the process.

**Figure 8.** Fate of the centrosome and components of the mitotic machinery in TgZFP2-depleted parasites. (a) Schematic representation of the centrosome-linked mitotic machinery in *Toxoplasma*. (b) Co-staining of the centrosome (Cen1) and the kinetochore (Ndc80) in mutant or complemented parasites after two days of ATc treatment. We used maximum intensity projection images after Z-stack acquisition. DNA was stained with DAPI; scale bar represents 5  $\mu\text{m}$ ; parasite shape is outlined. Arrowheads denote cells with supernumerary associations of centrosomes/kinetochore clusters and asterisks highlight cells with stray centrosomes or kinetochores. (c) In cells treated as described in (b) quantification experiments to classify cells containing: one centrosome with one kinetochore cluster (1C1K), two centrosomes with one kinetochore cluster (2C1K), two centrosomes with two kinetochore clusters (2C2K), or an abnormal greater number of centrosomes or kinetochore clusters (>2C or 2K). Data are mean from  $n=4$  experiments  $\pm$ SEM. (d) In cells treated as described in (b), quantification of the average number of centrosomes or kinetochore numbers. Data are mean from  $n=4$  experiments  $\pm$ SEM.  $*p < 0.01$  and  $**p < 0.05$ , Student's t-test. (e) Quantification of the percentage of cells treated as in B) having stray centrosomes or kinetochore clusters. Data are mean from  $n=4$  experiments  $\pm$ SEM.  $*p < 0.01$ , Student's t-test. (f) Complemented or TgZFP2 conditional mutant parasites were transiently transfected to express YFP-tagged spindle marker TgEB1 and incubated for two days in the presence of ATc, before processing for IFA with co-staining for the centrosome (Cen1) and the kinetochore (Ndc80). DNA was stained with DAPI; scale bar represents 5  $\mu\text{m}$ ; parasite shape is outlined on the merged image.

Figure 1.

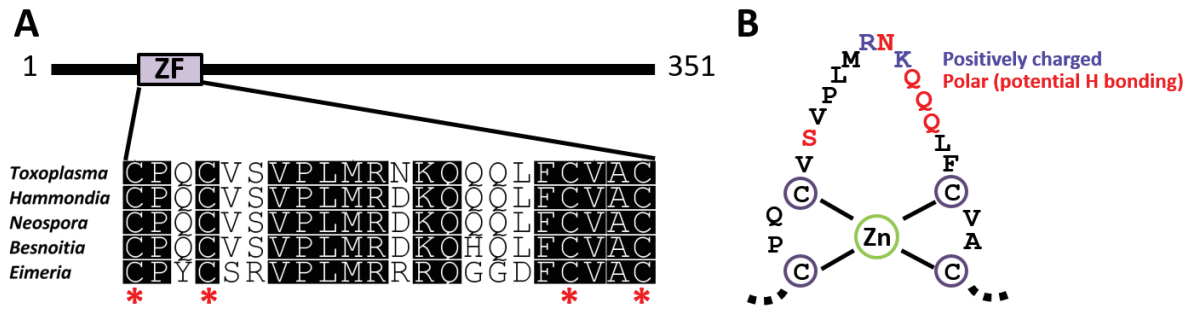


Figure 2.

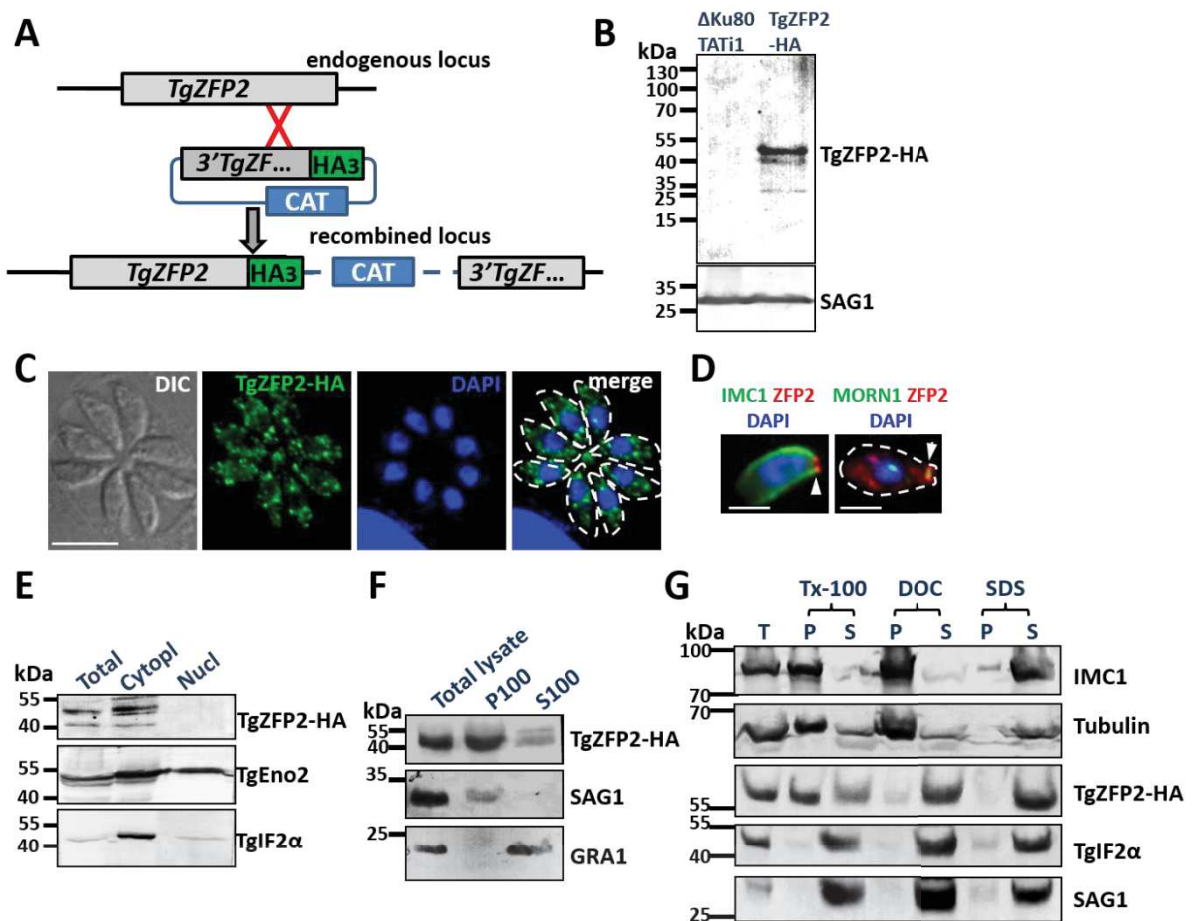


Figure 3.

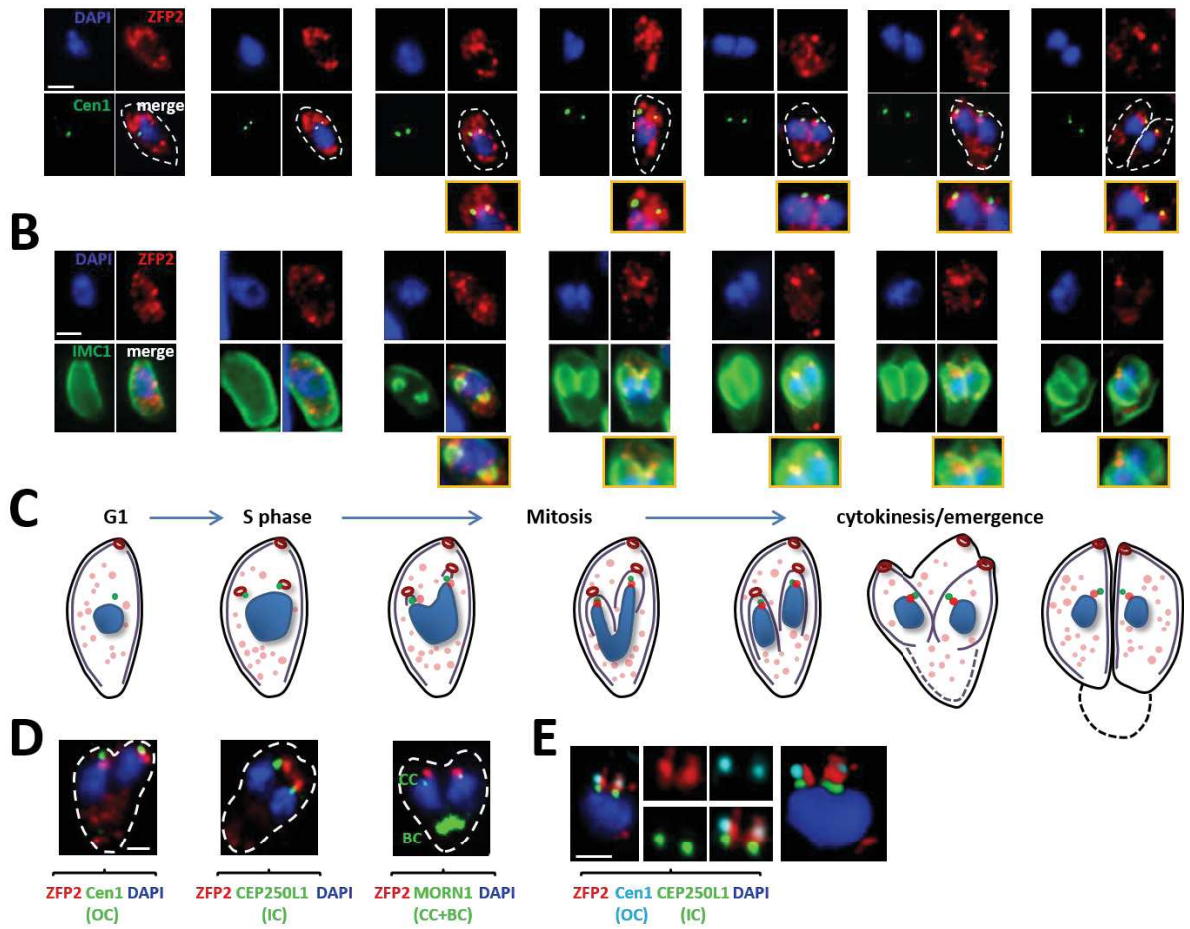


Figure 4.

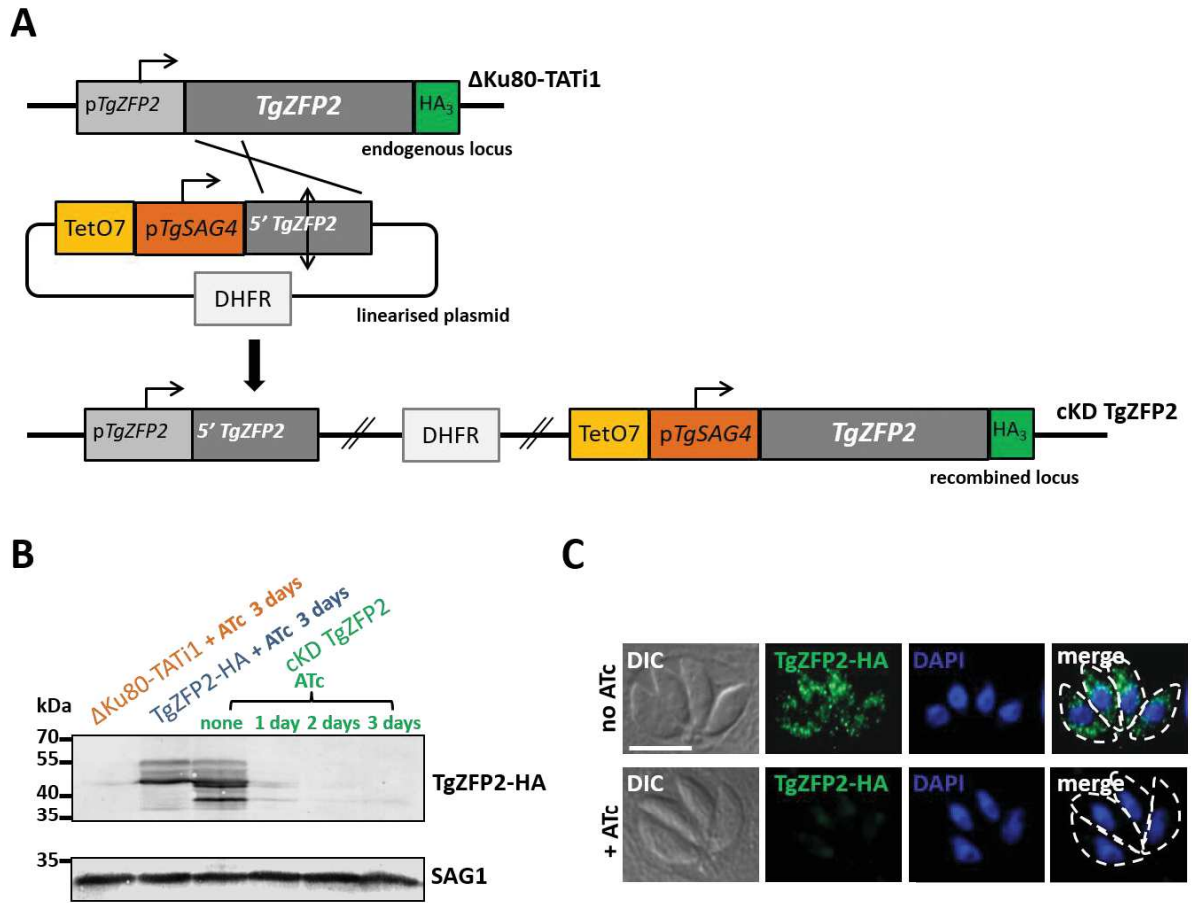
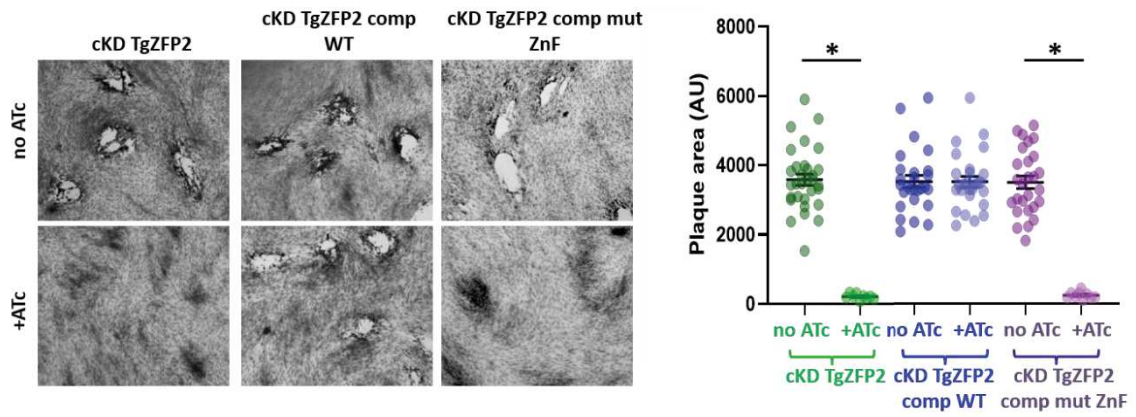


Figure 5.

**A**



**B**

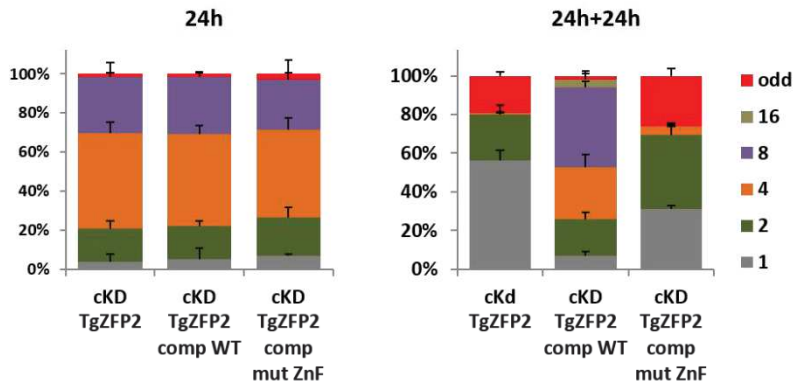


Figure 6.

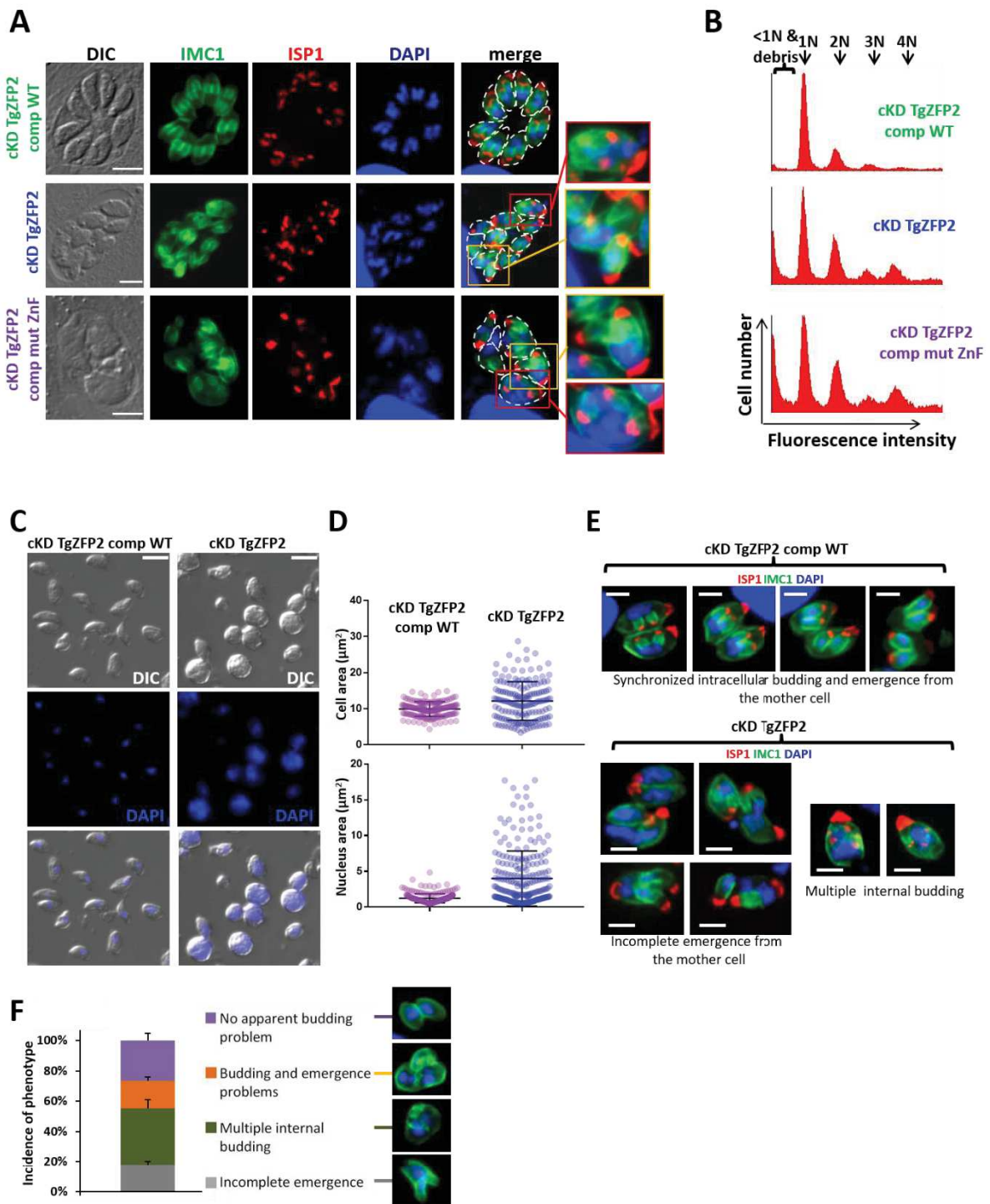


Figure 7.

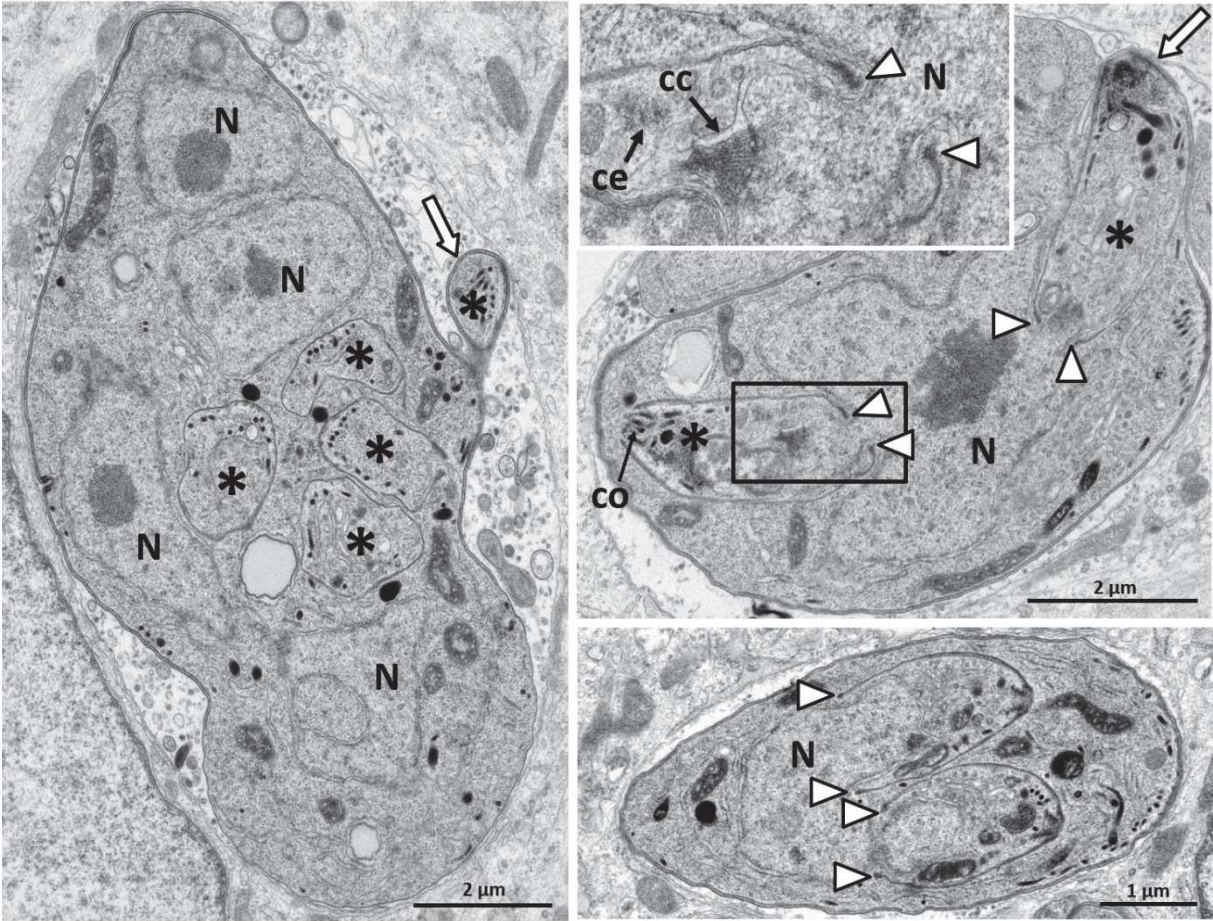
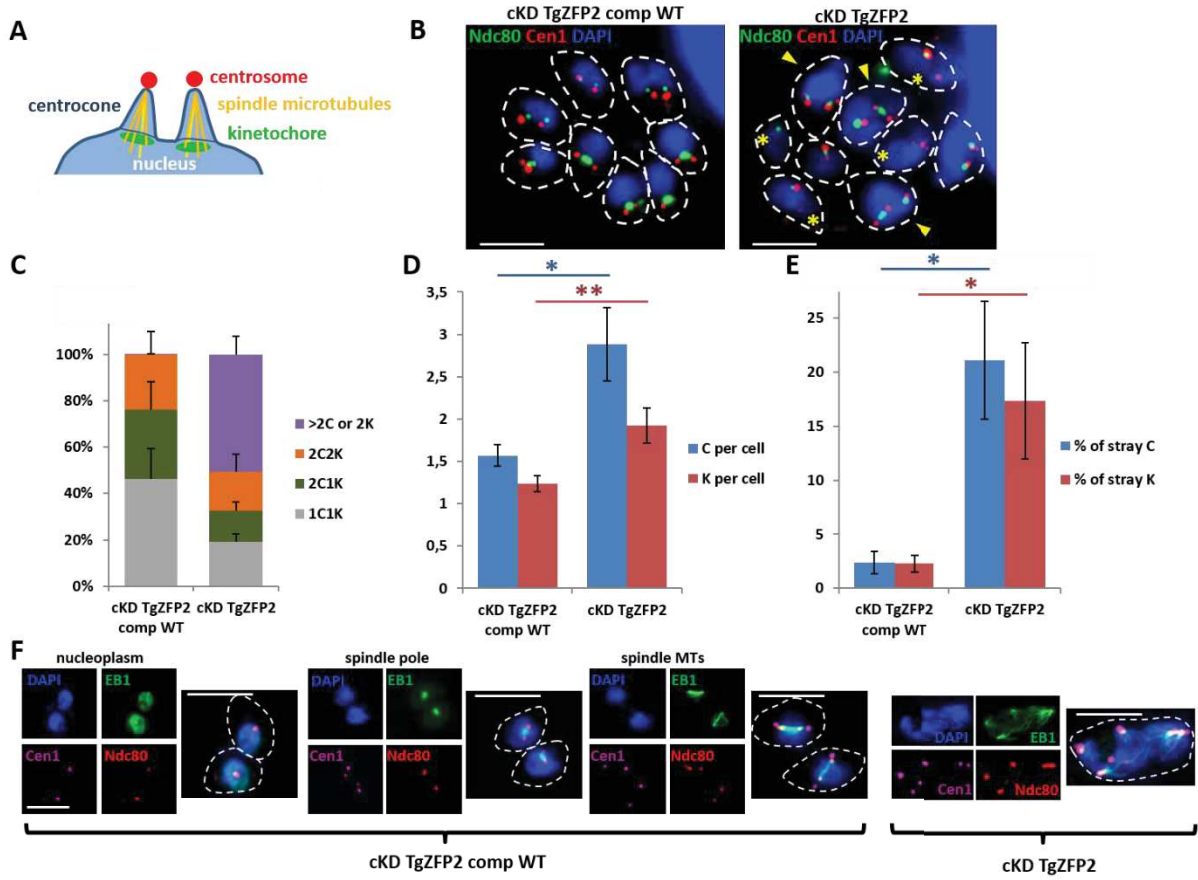
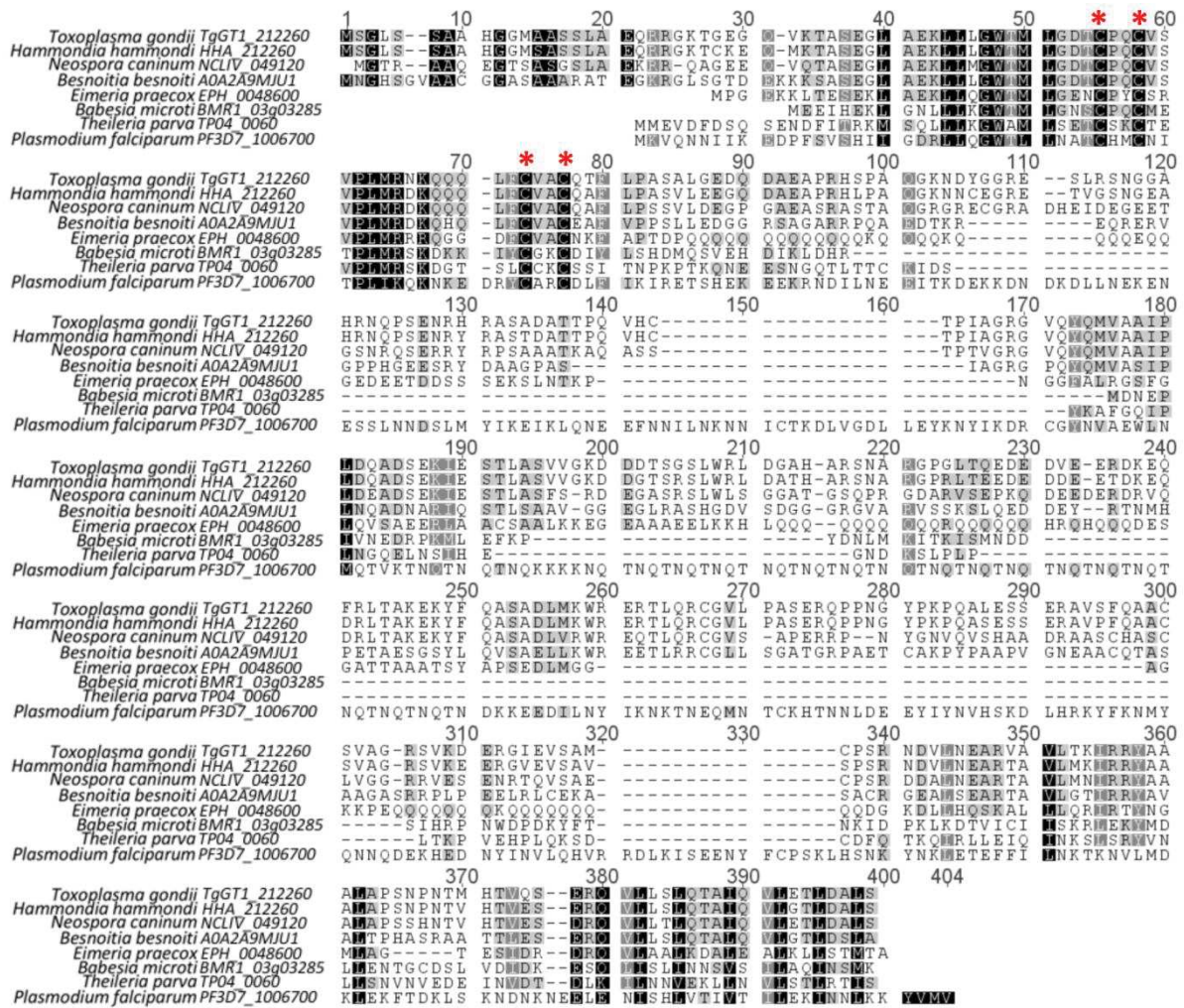


Figure 8.



Supplementary material



**Figure S1.** Alignment of TGGT1\_212260/TgZFP2 and selected apicomplexan homologues. Asterisks denote conserved cysteine residues in the zinc finger domain. [www.eupathdb.org](http://www.eupathdb.org) accession numbers are mentioned. Residues conserved in 100% of the sequences are displayed on a black background, residues conserved in more than 80% of the sequences are displayed on a dark grey background, and residues conserved in more than 60% of the sequences are displayed on a light grey background.

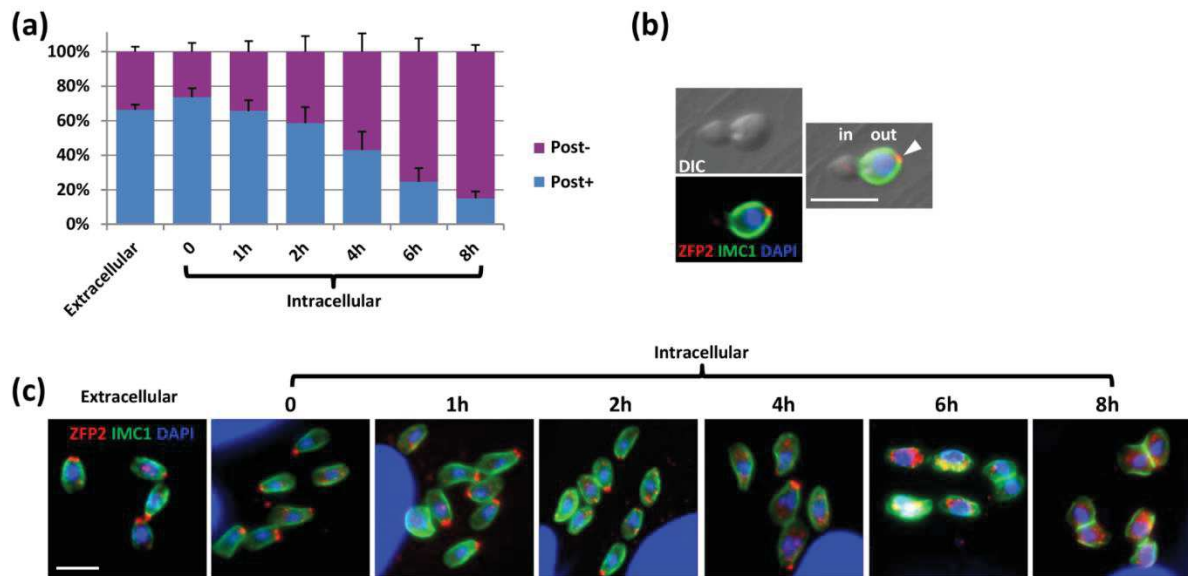


**Figure S2.** TgZFP2 has a dynamic localisation during the cell cycle. (a) Naturally egressed parasites were synchronised for invasion at 4°C and after invasion TgZFP2 localisation was monitored in intracellular parasites as they progressed through cell division. The presence of TgZFP2 as a posterior signal (Post+), versus non-posterior (Post-), was quantified. At least 100 parasites were assessed by timepoint. Data are mean of  $n=3$  independent experiments  $\pm$ SEM. (b) Example of invading parasite with a posterior TgZFP2 signal (arrowhead). DNA was stained with DAPI; DIC: differential interference contrast; scale bar represents 5 μm. (c) Representative examples of TgZFP2 staining for extracellular and intracellular parasites at different timepoints. DNA was stained with DAPI; scale bar represents 5 μm.

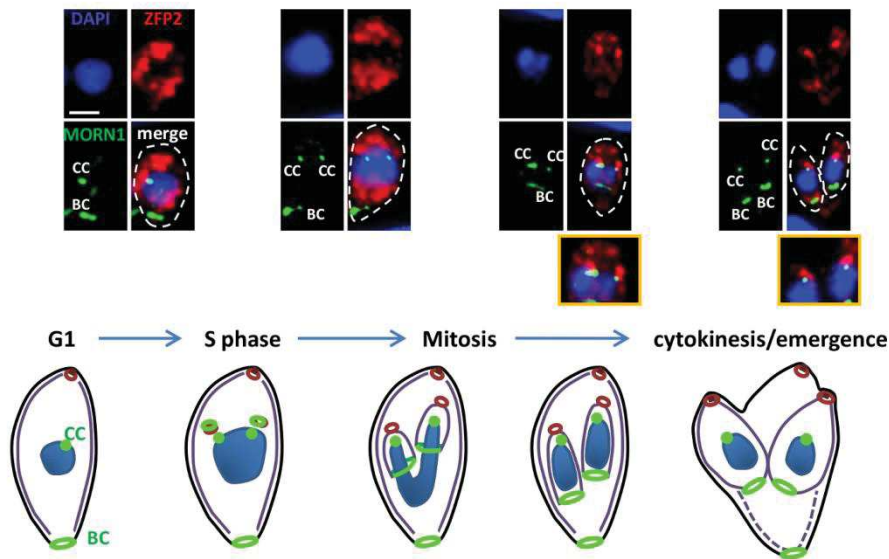


**Figure S3.** TgZFP2 localisation relative to the centrocone shows a close association during mitosis that remains until daughter cell emergence. IFA using co-staining of TgZFP2-HA together with centrocone (CC)/basal complex (BC) marker MORN1. DNA was stained with DAPI; DIC: differential interference contrast; scale bar is 2  $\mu$ m; parasite shape is outlined on merged image; insets show magnifications of selected merged images. Below is a schematic representation of MORN1 localisation during the different phases of the cell cycle (the conoid is in burgundy, the IMC is in dark purple and MORN1 is in green).

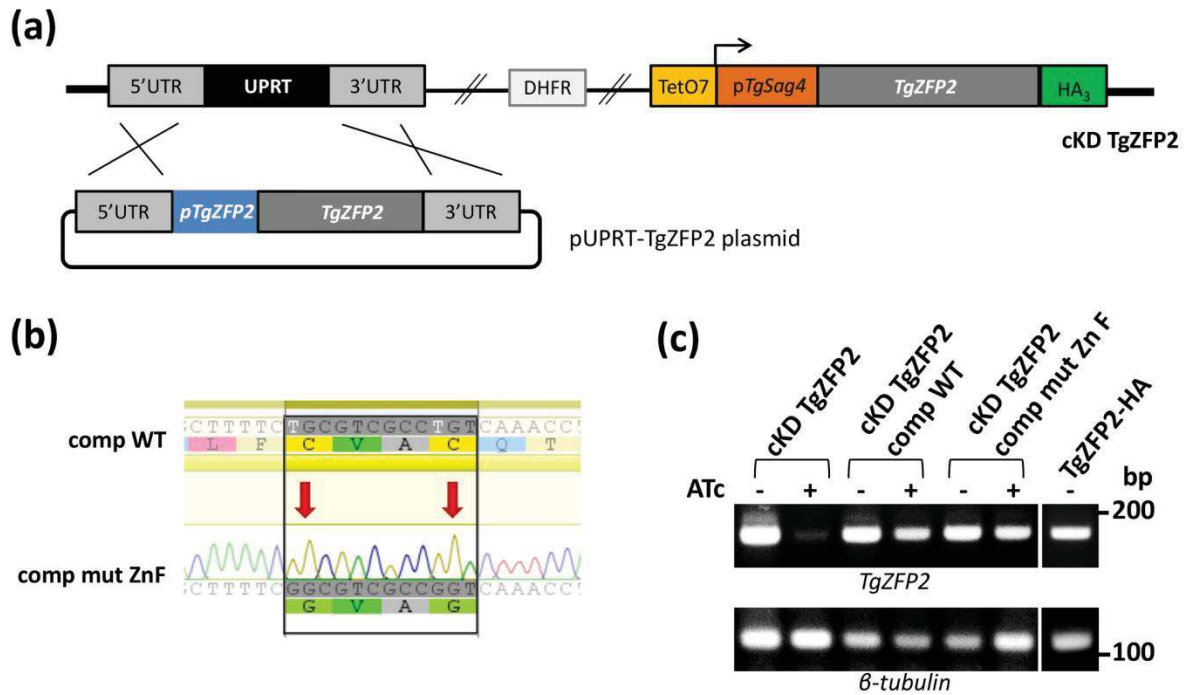


**Figure S4.** Generation of complemented cell lines. (a) Schematic representation of the strategy for complementing the TgZFP2 conditional mutant. The plasmid for expressing an extra copy of TgZFP2 under its own promoter is integrated at the uracil phosphoribosyltransferase (UPRT) locus in the cKD-TgZFP2 cell line. Clones were obtained after 5-Fluoro-2'-deoxyuridine (FUDR) selection. (b) Two versions of the complementation plasmid were used: one containing the wild-type *TgZFP2* cDNA (comp WT), and one obtained by site-directed mutagenesis for expressing a copy of TgZFP2 where the last two cysteines of the zinc finger motif have been replaced by glycines (comp ZnF). (c) Semi-quantitative RT-PCR analysis, using specific *TgZFP2* primers, were performed after RNA extractions of cKD TgZFP2, as well as WT and ZnF mutant complemented parasites and parental cell line TgZFP2-HA, incubated without or with ATc for two days. Transcription of *TgZFP2* is repressed upon addition of ATc but maintained in complemented lines. Specific  $\beta$ -*Tubulin* primers were used as a control.

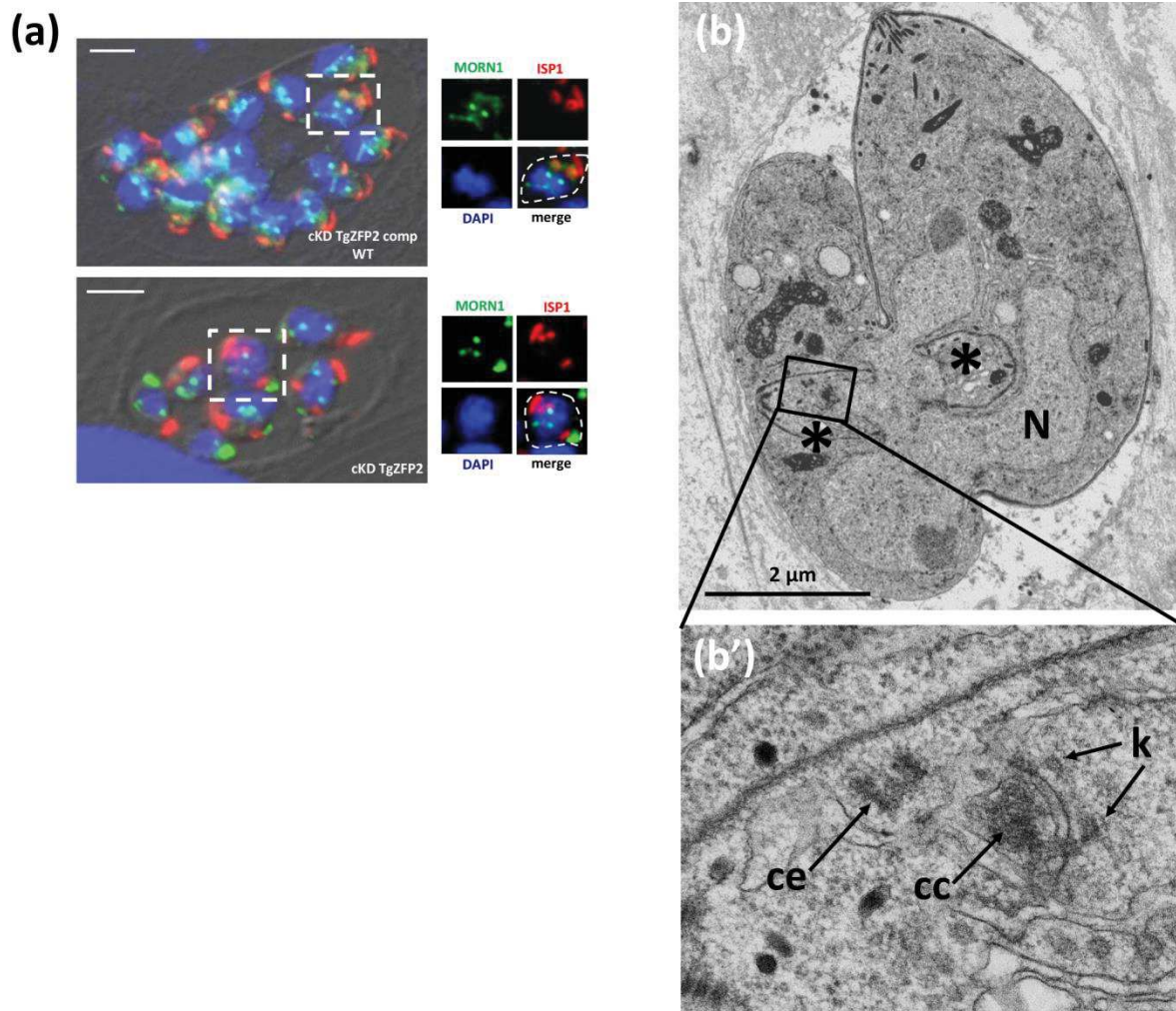


**Figure S5.** Assessing the centrocone/spindle pole upon TgZFP2 depletion. (a) cKD TgZFP2 and WT complemented parasites were grown for two days in the presence of ATc and IFA was performed with anti-MORN1 and anti-ISP1 (to visualise initiation of daughter buds) antibodies. DNA was stained with DAPI; DIC: differential interference contrast; scale bar represents 5 μm; parasite shape is outlined on merged image; insets are magnification of selected merged images. (b) TgZFP2-deficient parasite where two early buds are developing in an abnormal context (a multilobed nucleus –N–, a mother cell on the right connected to a cytoplasmic mass without IMC on the left), and yet showing a perfect interaction between centriole –cen–, centrocone –cc– and kinetochores –k– in the left bud enlarged in the b' insert.

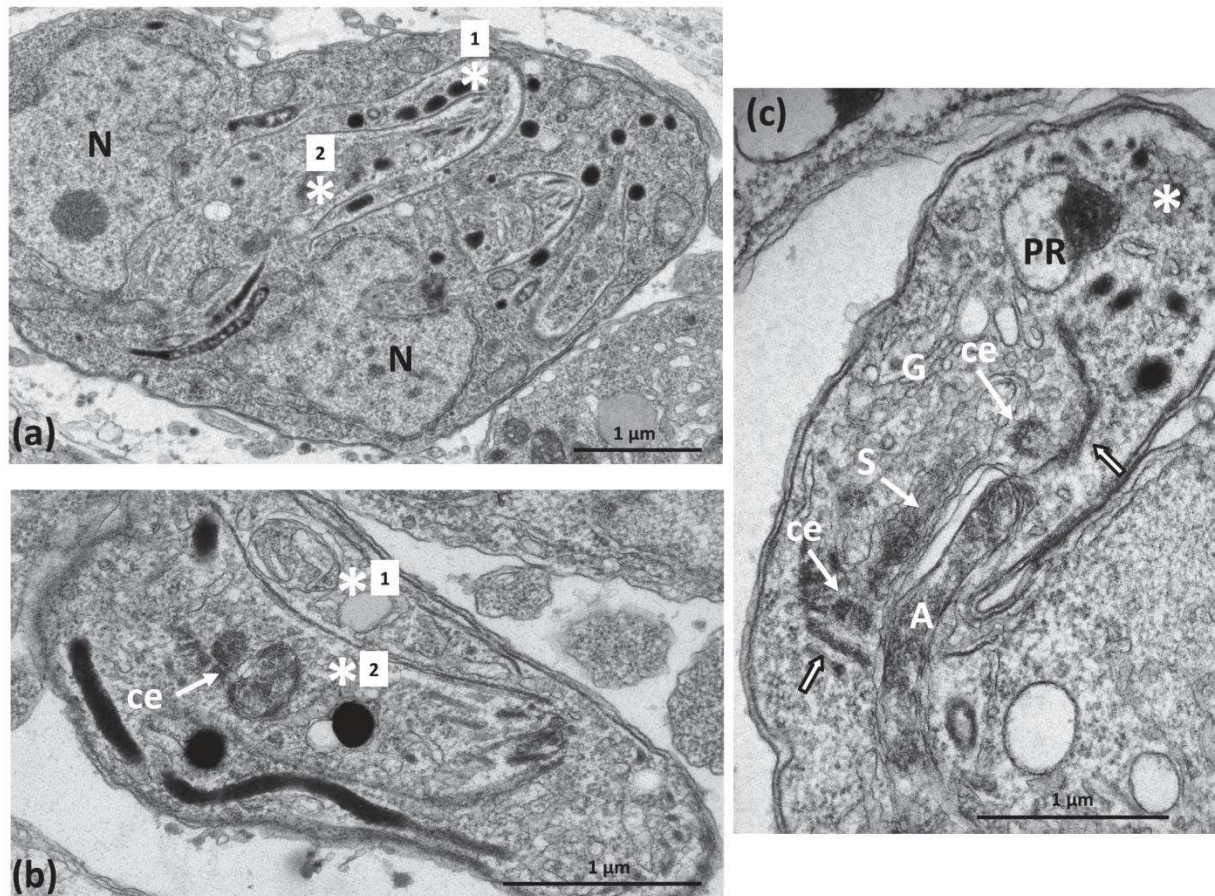


**Figure S6.** Multiple budding initiations in TgZFP2-depleted parasites. (a) TgZFP2-deficient parasite in which a developing bud (asterisk, 2) is growing within another (asterisk 1), in a “Russian doll” fashion suggesting that a new mitosis has started before the first bud could mature and give rise to a fully developed tachyzoite. (b) similar situation in another TgZFP2 deficient parasite, but in a bud that has started to emerge off the mother cytoplasm. A centriole (ce) is found in the younger bud. (c) As in (b), an incompletely formed (containing a pre-rhoptry –PR-) yet tentatively emerging bud (asterisk), displaying an early stage of budding initiation (two white arrows). G: Golgi apparatus; A: apicoplast; S: spindle; ce: centrioles.

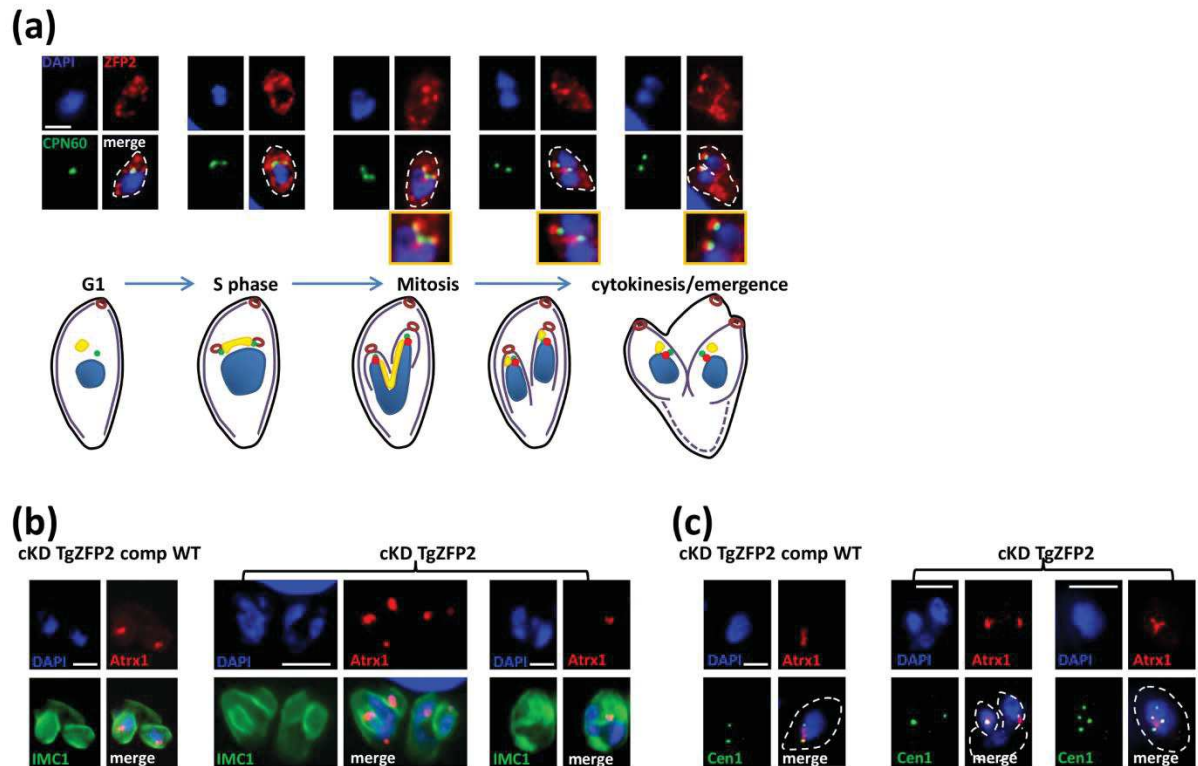


**Figure S7.** Fate of the centrosome-associated apicoplast in TgZFP2-depleted parasites. (a) Co-staining of TgZFP2 with apicoplast marker CPN60 during the different phases of the cell cycle (pictured below; TgZFP2 is in red, centrosomes are in green, the conoid is in burgundy, the IMC in dark purple and the apicoplast in yellow) show close association during mitosis. DNA was stained with DAPI; scale bar is 1  $\mu\text{m}$ ; parasite shape is outlined on the merged image; insets show magnifications of selected merged images. (b) and (c) Effect of TgZFP2 depletion was assessed on apicoplast (labelled with Atrx1) inheritance and replication using co-staining with IMC1 (c) and centrin 1 (d). DNA was stained with DAPI; scale bar is 2  $\mu\text{m}$ . Parasite shape is outlined on the merged image for (d).

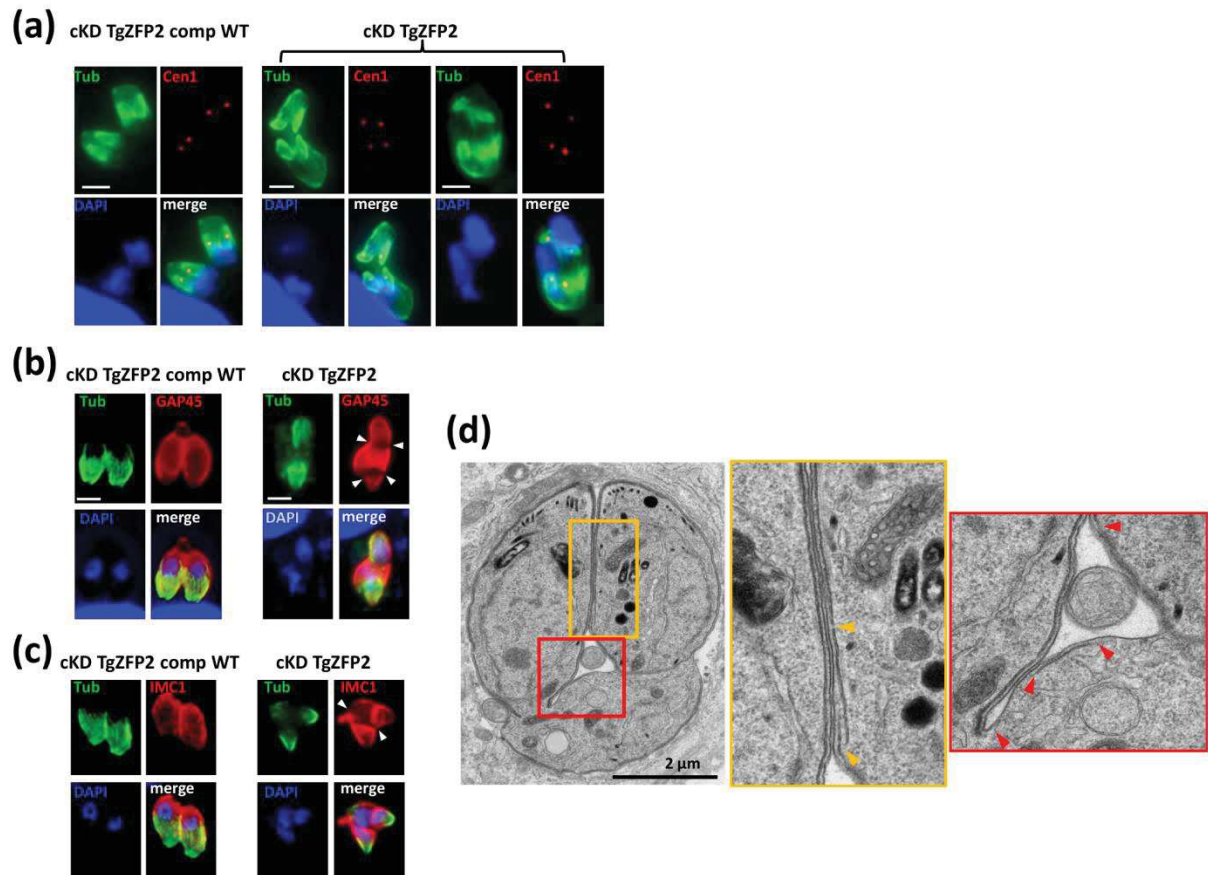


**Figure S8.** Impact of TgZFP2 depletion on the cytoskeleton. (a) cKD TgZFP2 and WT complemented parasites were pre-incubated for 24h with ATc, then released mechanically, made to invade new host cells, and grown for an extra 12hr with ATc before IFA with anti-acetylated tubulin and anti-centrin 1 antibodies; DNA was stained with DAPI; scale bar is 2 μm. (b) Parasites were prepared as described in (a), and IFA was performed with anti-acetylated tubulin and anti-GAP45 antibodies; DNA was stained with DAPI; scale bar is 2 μm. (c) Parasites were prepared as described in (a), and IFA was performed with anti-acetylated tubulin and anti-IMC1 antibodies; DNA was stained with DAPI; scale bar is 2 μm. (d) Ultrastructural analysis showing discontinuity of the IMC in emerging TgZFP2-depleted parasites (arrowheads in magnifications displayed in insets).

## Conclusion and perspectives

Our data demonstrates TgZFP2 importance for the coordinated cell cycle progression in *T. gondii* and suggests this depends on the protein's timely recruitment to the centrosomal region. However, it should be kept in mind that TgZFP2 is a dynamic protein localising to various cellular compartments during the cell cycle, and thus it may have several functions in the course of the parasite's cell cycle. Apart from the ZnF, TgZFP2 has no other region that could hint for a specific function, and in spite of our detailed phenotypic analysis of the TgZFP2 mutant, we could not get insights into the mechanistics of TgZFP2 function at the molecular level. Thus, we decided to focus our attention on the isolation and identification of TgZFP2 potential binding partners with the hope it would provide information on specific cellular pathways this protein belongs to.

We hypothesised the ZnF domain (which we have shown to be crucial for protein's function) may mediate interactions with key molecular partners. ZnFs are known to potentially interact with proteins, lipids or nucleic acids. Our solubility analysis demonstrated TgZFP2 is unlikely to be membrane-associated protein, so we excluded the possibility of its ZnF to mediate an interaction with lipids. The immunofluorescence and cell fragmentation assays have shown TgZFP2 is absent from the nucleus, which suggests TgZFP2 is unlikely to interact with DNA. Consequently, we hypothesised that TgZFP2 could accomplish its role in coordinating cell cycle progression through ZnF-mediated interactions with either other proteins or RNAs. We thus investigated these possibilities and the results of these investigations are described thereafter in Chapters 2 and 3.

---

## CHAPTER 2.

# Identification of TgZFP2 protein binding partners

---

### 2.1. Isolation of proteins interacting with YFP-tagged TgZFP2

We first aimed at investigating the interactions between TgZFP2 and potential protein partners. To address this question, we applied a broad strategy of mass-spectrometry identification of protein candidates after co-immunoprecipitation assays (Fig. 34), performed in collaboration with the Functional Proteomics Platform of Montpellier (<https://www.fpp.cnrs.fr/fr/>). The transgenic cell lines used in the study and the purification conditions had been already set up when I joined the research group. Thus, a cell line expressing TgZFP2 C-terminally-tagged with YFP (TgZFP2-YFP) served as a bait, while a cell line expressing the YFP fused with a short unrelated amino acids sequence was used as a negative control. The negative control was aimed to identify the ‘false positive’ protein candidates that may bound directly to the agarose beads, or have an affinity to the YFP protein. To perform the experiments, we used cultures with a high density of parasites, some of which had already egressed at the time of sample collection. The samples then contained a mix of both intracellularly growing parasites and extracellular parasites. The experiment was done twice on independent cultures and the datasets from both biological replicates were analysed.

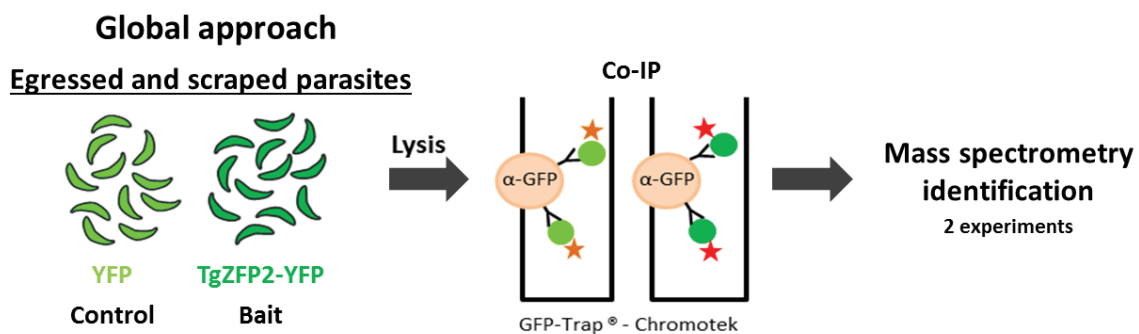


**Figure 34.** Strategy used for the identification of TgZFP2 putative protein partners.

The co-immunoprecipitation of the potential TgZFP2-binding proteins from the lysates of YFP-fused WT (control) and the TgZFP2-YFP (bait) parasites was done on a commercial anti-GFP column. After the confirmation of TgZFP2 binding to the anti-GFP column by Western blotting, the collected proteins were separated on an acrylamide gel. The bands corresponding to the TgZFP2-fraction were cut prior to the digestion of the proteins by trypsin and the subsequent extraction of the peptides for analysis by liquid chromatography coupled to tandem mass spectrometry (LC-MS/MS). In the scheme, light green and dark green dots represent, respectively, the YFP control and the TgZFP2-YFP bait. The red stars correspond to the putative TgZFP2 interacting partners; orange stars correspond to false positive proteins.

## 2.2. Selection of the mass-spectrometry identified putative partners

During the course of analysis, we first selected proteins that were enriched in the TgZFP2-YFP sample over the YFP control in both datasets and, as result, numerous candidates were obtained. Unfortunately, many of the most abundant candidates of one experiment were not ranked as high in the other, hinting there were some experimental or biological discrepancies between the two datasets. We tried to prioritise interesting candidates for further studies, but even when applying stringent criteria for selection, we still obtained a very large number of proteins. For example, if we searched for the candidates that were: 1) present in the two datasets with at least 3 unique peptides and 2) absent in YFP control or enriched by more than 10 fold in bait versus the control, we obtained more than 250 hits. This seriously compromised the possibility of individual experimental verification of each candidate. Moreover, many candidate proteins were uncharacterised and not annotated with functional domains, and we thus had no clue about their function.

We thus tried to prioritise the candidates based on their annotation and their possible relationship with the phenotype of the *TgZFP2* mutant. As we already had an indication that TgZFP2-depleted parasites showed a lack of synchrony between the DNA replication and daughter cells budding and had problems in daughter cell elongation, we were looking especially for proteins involved in the regulation of the cell cycle (like kinases or cyclins), or for proteins linked to the parasites cytoskeleton.

### 2.2.1. Selected candidates that could be potential cell cycle regulators.

Amongst all the potential TgZFP2-interacting proteins, we identified three candidates that could have been involved in regulation of the cell cycle progression and were significantly enriched in bait over control in both experiments ([Table 1](#)). These proteins were annotated as 1) a putative cell-cycle-associated protein kinase (GSK-like, glycogen synthase kinase TGGT1\_265330), 2) a putative HIT (Histidine Triad motif) family protein potentially involved in the cell-cycle regulation (TGGT1\_243580), and 3) a cyclin2 related protein (TGGT1\_267580). Like for TgZFP2 we expected its potential interacting partners pertaining to the same pathway would be essential for parasite fitness. Therefore, we focused on candidates that had a negative fitness score in the Sidik et al. CRISPR-Cas9-based genome-wide screening of *T. gondii*

Description	Gene	Peptides TgZFP2-YFP	Peptides YFP	Phenotype fitness score
<b>Experiment 1</b>				
Putative cell-cycle-associated protein kinase GSK	TGGT1_265330	10	0	-4,12
Putative Hit family protein involved in cell-cycle regulation	TGGT1_243580	1	0	1,19
Cyclin2 related protein	TGGT1_267580	2	0	-2,88
<b>Experiment 2</b>				
Putative cell-cycle-associated protein kinase GSK	TGGT1_265330	13	5	-4,12
Putative Hit family protein involved in cell-cycle regulation	TGGT1_243580	6	0	1,19
Cyclin2 related protein	TGGT1_267580	11	0	-2,88

**Table 1. Selection of putative TgZFP2 protein partners related to the regulation of cell cycle progression.**

genes<sup>66</sup>. Consequently, the study of the HIT domain-containing protein was not pursued as it was probably dispensable for the parasites.

To assess the potential interaction of the selected cell cycle candidates with TgZFP2, we sought to add a triple *myc* tag to each one of these candidates in the TgZFP2-HA3 transgenic cell line background and to proceed with co-localisation and co-immunoprecipitation experiments (Fig. 35).

Based on constructs obtained with the ligation independent cloning method<sup>255</sup>, and through a single recombination event, the sequence coding to a triple *myc* tag was added at the endogenous locus of interest. We successfully obtained stable double-tagged cell lines expressing either TgGSK-*myc*3 or TgCyclin2-*myc*3, together with TgZFP2-HA3 (Fig. 35A). IFA showed that both candidates localised to the cytoplasm of tachyzoites; TgCyclin2 also displayed an additional nuclear localisation (Fig. 35B). Although the cytoplasmic signal corresponding to the candidates did not completely overlap with the TgZFP2 puncta, they still localised in close proximity to each other.

We next performed immunoprecipitation experiments using an anti-*myc* affinity column and could efficiently recover the tagged TgCyclin 2 or TgGSK proteins from lysates of the double-tagged parasites. Revelation with the anti-HA antibody only detected a faint band

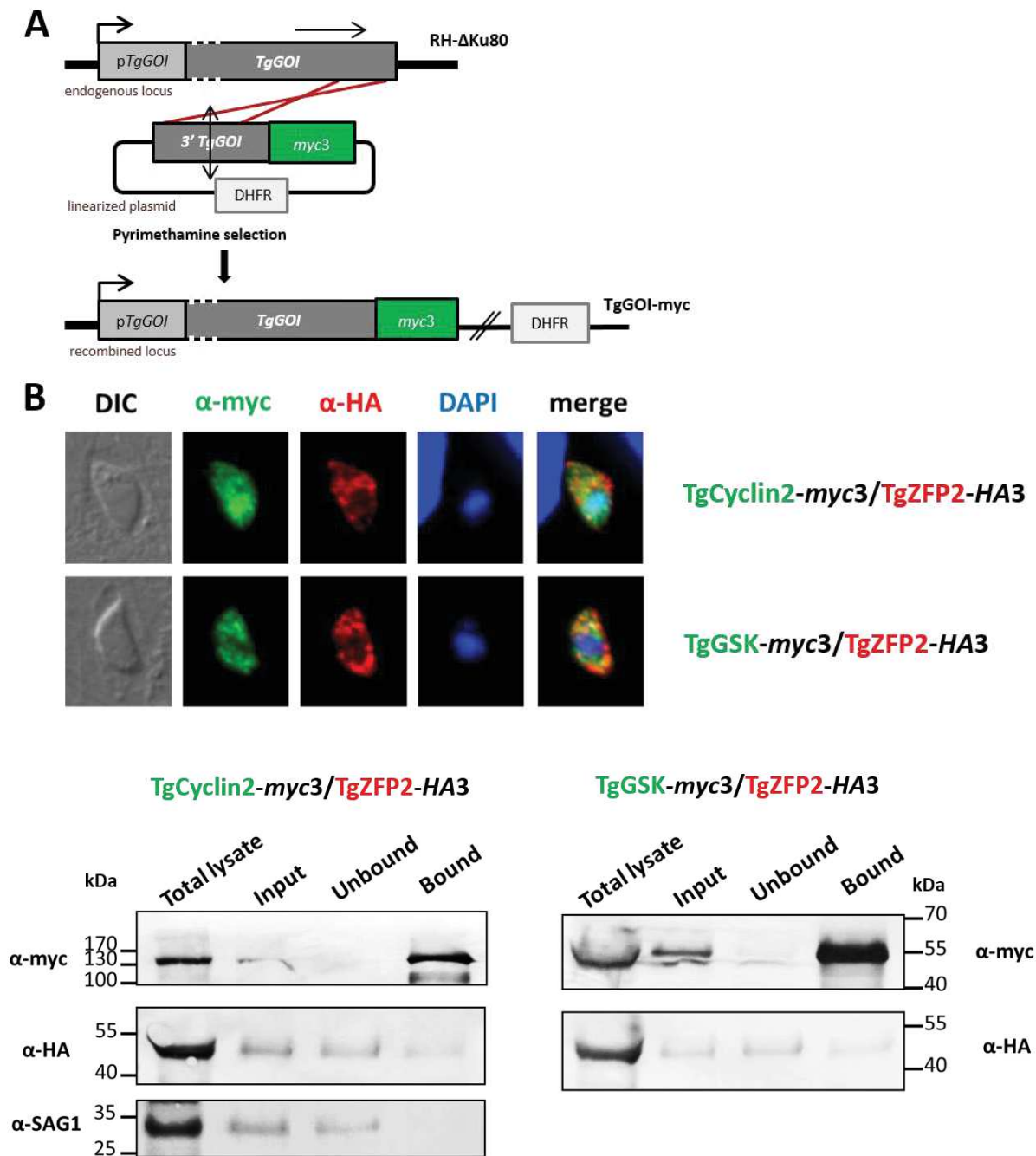


**Figure 35.** The investigation of potential interactions between TgZFP2 and cell cycle-related candidates. (A) The general strategy used for tagging TgGSK and TgCyclin2 with a triple myc tag in a background of TgZFP2-HA3 transgenic cell line. (B) The IFAs show TgCyclin2 localises to the cytoplasm and to the nucleus of tachyzoites while TgGSK displays cytoplasmic localisation. The anti-myc labels cell cycle related candidates, anti-HA labels TgZFP2. The nucleus of the parasites is stained by DAPI. (C) Immunoprecipitation of myc-tagged TgCyclin2 and TgGSK candidates and subsequent immunoblot analysis were used to detect the bound proteins of interest and the potential presence of HA-tagged TgZFP2. SAG1 is an unrelated protein used as a negative control.

corresponding to TgZFP2 in the bound fraction, which, although slightly more intense than the background staining in our negative control (unrelated protein SAG1), did not argue for an enrichment (Fig 35C). Overall, these experiments did not clearly confirm TgCyclin2 or TgGSK was binding partner for TgZFP2.

### 2.2.2. Selected candidates that may be potentially important for cytoskeleton homeostasis: the CCT chaperonin complex.

We decided to go back to the proteomics dataset and identify other putative candidates worth investigating. Strikingly, we noticed that all the 8 subunits of a chaperone complex called ‘chaperonin-containing tailless’ (CCT) were present in our two datasets and were enriched over the YFP control (Table 2). They all have a negative CRISPR score in the Sidik et al fitness screen<sup>66</sup>, suggesting the CCT complex is essential for parasite survival. Interestingly, p27/SSSCA1, the human protein in which TgZFP2 zinc finger motif was first identified, is known to be interacting with several subunits of the CCT complex (Fig. 36A).

Description	Gene	Peptides TgZFP2-YFP	Peptides YFP	Phenotype fitness score
<b>Experiment 1</b>				
CCT1	TGGT1_229990	13	0	-4,96
CCT2	TGGT1_243710	11	0	-4,79
CCT3	TGGT1_205440	7	0	-4,52
CCT4	TGGT1_272910	10	0	-4,41
CCT5	TGGT1_202370	4	0	-6,05
CCT6	TGGT1_318410	6	0	-5,15
CCT7	TGGT1_297500	12	0	-5,99
CCT8	TGGT1_287500	11	0	-4,89
<b>Experiment 2</b>				
CCT1	TGGT1_229990	23	5	-4,96
CCT2	TGGT1_243710	20	8	-4,79
CCT3	TGGT1_205440	19	1	-4,52
CCT4	TGGT1_272910	16	3	-4,41
CCT5	TGGT1_202370	9	1	-6,05
CCT6	TGGT1_318410	12	2	-5,15
CCT7	TGGT1_297500	14	2	-5,99
CCT8	TGGT1_287500	19	1	-4,89

**Table 2.** Selection of CCT chaperonin’s subunits for studying their potential interactions with the TgZFP2 protein. All 8 CCT subunits are enriched in the TgZFP2-YFP bait and are likely essential for parasite fitness. CCT1, CCT2 and CCT5 subunits were selected for further investigation (light blue).

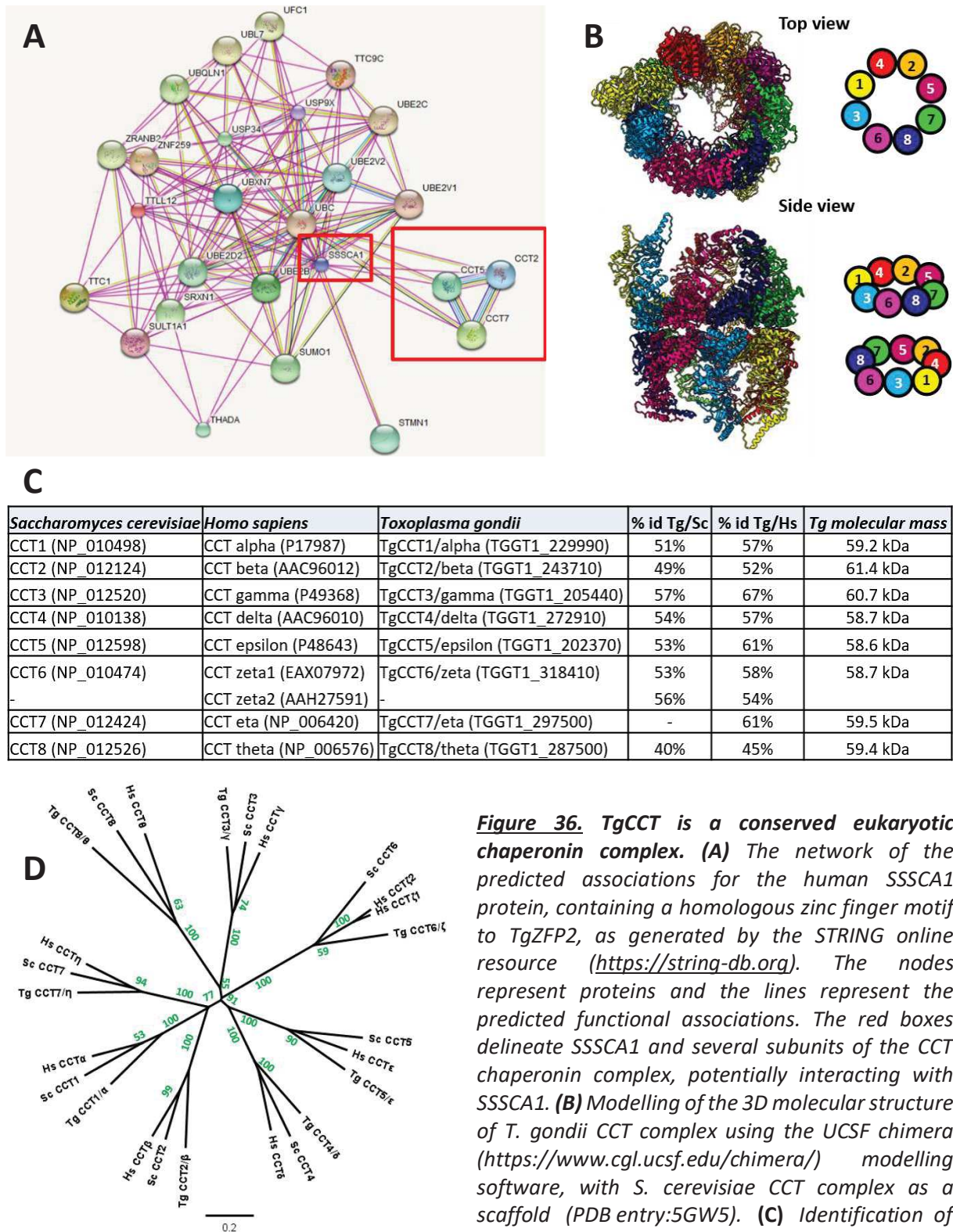


**Figure 36. TgCCT is a conserved eukaryotic chaperonin complex. (A)** The network of the predicted associations for the human SSSCA1 protein, containing a homologous zinc finger motif to TgZFP2, as generated by the STRING online resource (<https://string-db.org>). The nodes represent proteins and the lines represent the predicted functional associations. The red boxes delineate SSSCA1 and several subunits of the CCT chaperonin complex, potentially interacting with SSSCA1. **(B)** Modelling of the 3D molecular structure of *T. gondii* CCT complex using the UCSF chimera (<https://www.cgl.ucsf.edu/chimera/>) modelling software, with *S. cerevisiae* CCT complex as a scaffold (PDB entry:5GW5). **(C)** Identification of

the *T. gondii* homologues of baker's yeast and human CCT subunits using ToxoDB database ([www.toxodb.org](http://www.toxodb.org)). **(D)** Phylogenetic analysis of the CCT subunits from *S. cerevisiae* (Sc), *H. sapiens* (Hs) and *T. gondii* (Tg). Unrooted phylogenetic tree was built using the Neighbor-Joining method with the Geneious software ([www.geneious.com](http://www.geneious.com)). Neighbour-Joining consensus tree support for bootstrap values (% , 200 replicates) are indicated in green. TgCCT contains 8 subunits homologous to the eukaryotic ones and arranged in a similar two-ring manner.

Molecular chaperones are commonly found in the eukaryotic and prokaryotic cells and are known to mediate the proper folding of the proteins and to prevent their aggregation, especially in stress conditions<sup>256</sup>. CCT, for instance, assists the folding of potentially up to 10% of newly translated cytosolic mammalian proteins, amongst which - actin and tubulin<sup>257</sup>. This chaperonin complex is thus intrinsically connected to the cellular processes that rely on the cytoskeleton MTs and actin filaments<sup>258</sup>, and as such plays a pivotal role in cell cycle progression<sup>259</sup>. CCT employs ATP hydrolysis to ensure its function and has a characteristic double-ring structure in which each ring is composed of eight subunits (CCT1 to CCT8) with different substrate specificity, all being essential in yeast<sup>260</sup>. We performed homology searches in the Toxodb.org database and identified homologues of all subunits in the *T. gondii* genome (Fig. 36C). Phylogenetic analysis unambiguously clustered the *T. gondii* subunits with their yeast or human homologue (Fig. 36D). Additionally, our 3D modelling, based on the strong sequence homology with the other eukaryotic CCT subunits, reveals that *T. gondii* CCT likely retains a 16-meric organisation typical for the yeast or human chaperonin (Fig. 36B). We thus hypothesised that CCT complex is likely to have a conserved function in *T. gondii*, and, as it may have a connection with the cytoskeleton and be potentially important for the cell division process, we decided to investigate the possibility of an interaction between TgZFP2 and TgCCT.

In a similar fashion as with the cell cycle-related candidates, we added a C-terminal triple *myc* tag to three selected TgCCT subunits (TgCCT1, TgCCT2 and TgCCT5) (Fig. 37A). After separation on a polyacrylamide gel, tagged proteins were detected at the expected molecular mass by western blot (WB) analysis (Fig. 37B). Interestingly, when run under native conditions, all subunits labelled a similar product of about 1000 kDa that could correspond to the 16-mer complex (the size of each subunit's is ~60kDa), suggesting the predicted oligomeric organisation (Fig. 37C) is probably conserved in *T. gondii*.

The IFAs showed that all three selected TgCCT subunits localised as puncta in the cytoplasm of the parasites and were generally excluded from the nucleus (Fig. 37D). Although the TgCCTs and TgZFP2 signals were generally close in the cytoplasm of tachyzoites, we observed no particular pattern of co-localisation between them (Fig. 37D).

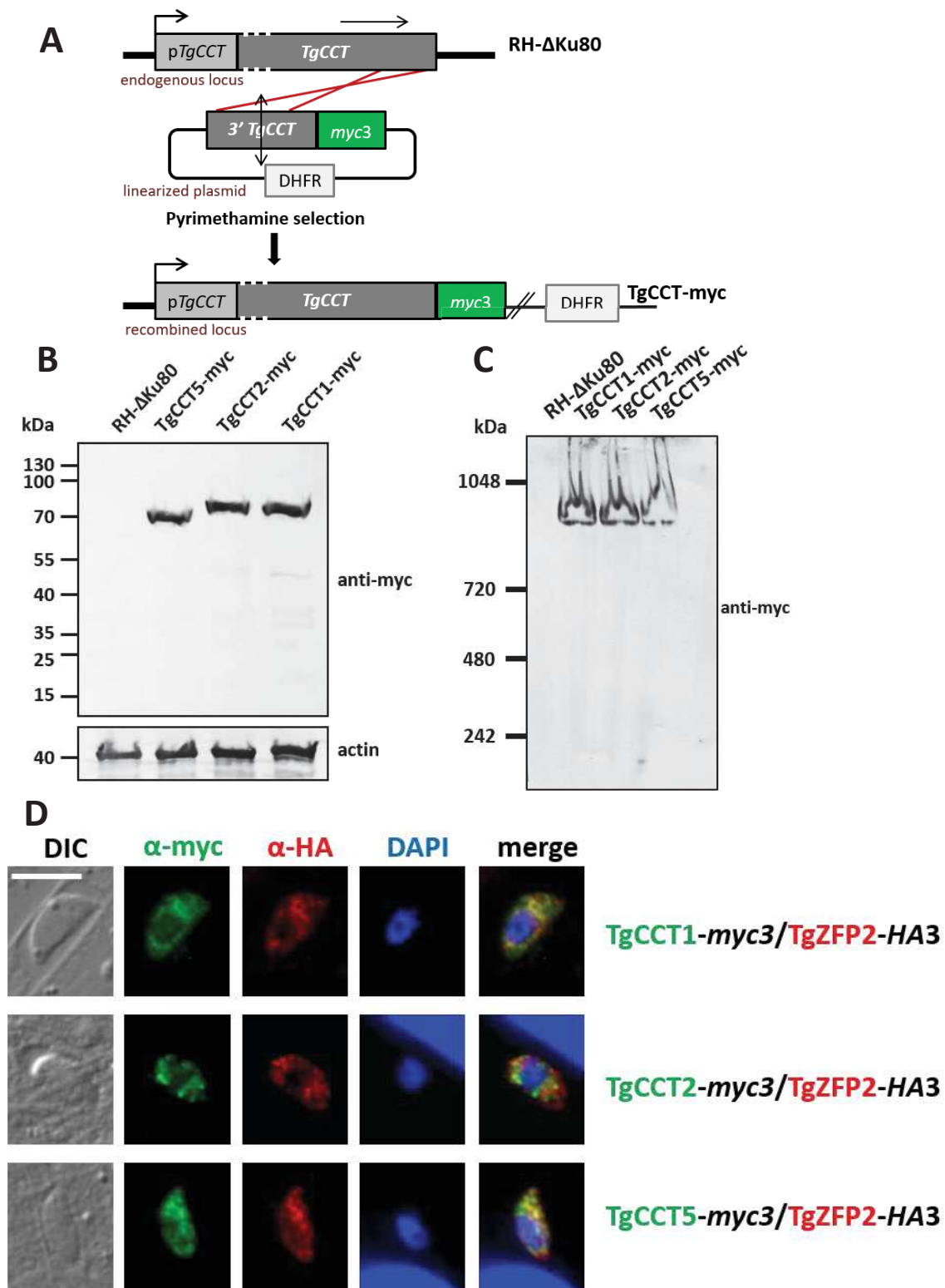


**Figure 37.** *TgCCT* is a multimeric complex localising to the cytoplasm of tachyzoites. **(A)** Strategy for generating myc-tagged *TgCCT* subunits in the *TgZFP2-HA3* transgenic cell line background. **(B)** WB analysis of tagged *TgCCT* subunits in reducing and denaturing conditions. Actin serves as a loading control. **(C)** Western blot analysis of the same cell extracts as in **(B)** after protein separation on a gradient polyacrylamide gel in native conditions. The result suggests the *TgCCT* subunits belong to a large size complex. **(D)** IFAs of the *TgCCT1*, *TgCCT2* and *TgCCT5* sub-units show they localise to the cytoplasm. *TgZFP2* is stained with anti-HA, DNA is stained with DAPI, scale bar is 5  $\mu\text{m}$ .

To gain more insights into the potential interactions between TgCCT and TgZFP2, we performed co-immunoprecipitation assays (Fig. 38). Protein extracts from lysed parasites of all three transgenic cell lines were immunoprecipitated on a commercial anti-*myc* column in order to bind the TgCCT subunits, along with their potential interacting partners (Fig. 38A). As result, all the three TgCCT subunits were successfully bound to the agarose beads; nevertheless, in the corresponding elution fractions, no obvious TgZFP2-specific band was detected for TgCCT1-*myc*3 and TgCCT5-*myc*3 and only a faint TgZFP2-corresponding band was visualised in the TgCCT2-*myc*3. Nevertheless, as CCT is known to interact with a wide range of cytoplasmic proteins in eukaryotes, the interactants would likely have to compete for binding the CCT complex, so only a limited quantity of the chaperonin could potentially bind TgZFP2. We thus tried to perform the reverse immunoprecipitation, purifying TgZFP2-HA3 and assessing if the TgCCT subunits co-immunoprecipitated (Fig. 38B). However, there was no

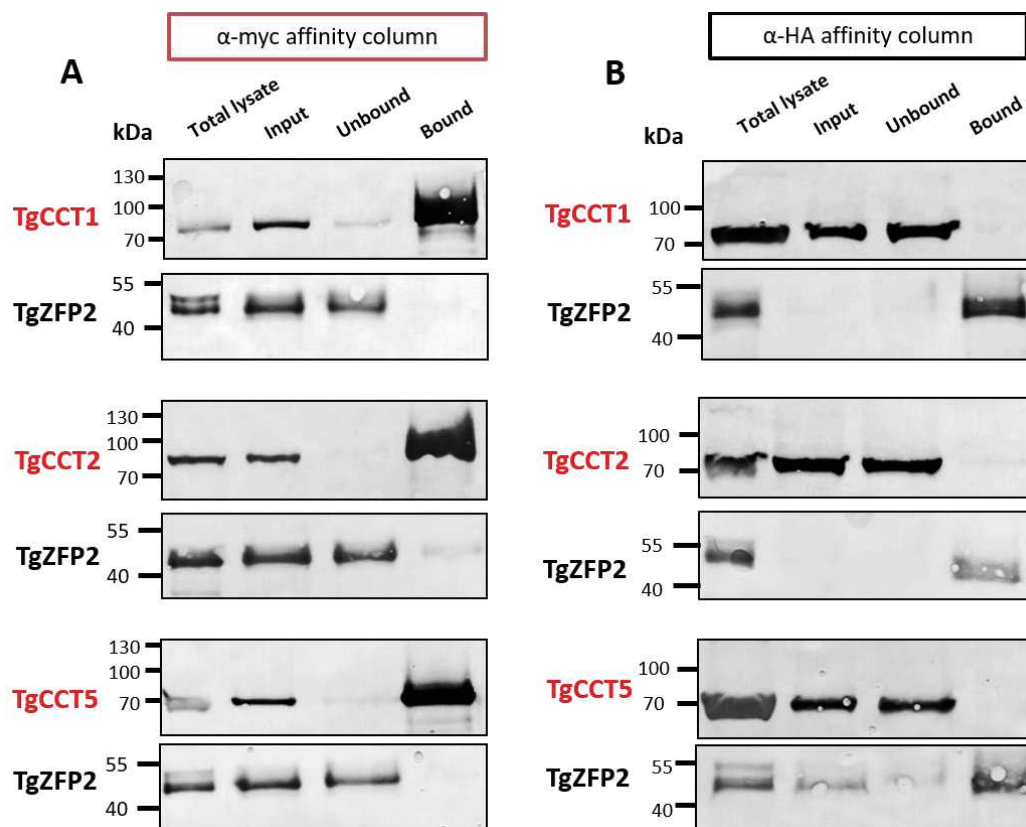


**Figure 38.** The co-immunoprecipitation analysis of potential TgZFP2-TgCCTs interactions. **(A)** Immunoprecipitation of *myc*-tagged TgCCT subunits and subsequent immunoblot analysis to detect the bound proteins of interest and the potential presence of HA-tagged TgZFP2. **(B)** Reverse immunoprecipitation and subsequent immunoblot analysis performed on extracts from the same cell lines using an anti-HA column this time in order to capture HA-tagged TgZFP2. The result of both experiments does not confirm the existence of strong direct interactions between TgZFP2 and TgCCTs.

obvious proof of TgCCT1 and TgCCT5 binding to TgZFP2, while TgCCT2-corresponding band was extremely faint.

We thought we needed a positive control for interacting proteins in the co-immunoprecipitation assay. In mammals, actin and tubulin are obligate substrates of CCT, on which their folding depends. Thus, using the same approach as previously, we immunoprecipitated the TgCCT subunits and investigated whether *T. gondii* actin and tubulin were binding to it (Fig. 39). The experiments showed the presence of considerable amounts of both actin and tubulin in the immunoprecipitated fractions, more with some TgCCT subunits (e.g. TgCCT5) than others (e.g. TgCCT2). Actin and tubulin are very abundant proteins and may thus contaminate fractions, so we immunoprecipitated TgGSK as a negative control aiming to assess the proportion of non-specifically bound actin and tubulin in the immunoprecipitated fraction. Indeed, we could detect actin and tubulin there, albeit in lower amounts than for TgCCT1 and TgCCT5. If anything, it shows that assessing for protein/protein interactions by co-immunoprecipitations when the candidate proteins are not exclusive partners and are expressed in very different amounts is technically challenging.

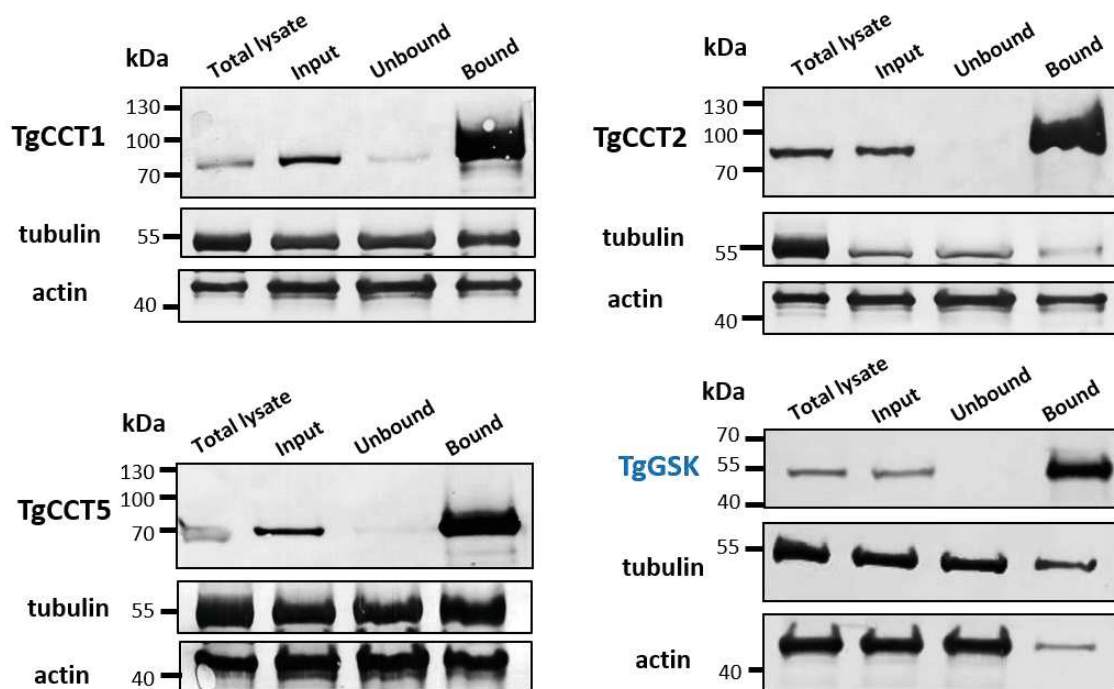


**Figure 39.** *TgCCTs potential interactions with cytoskeleton proteins actin and tubulin.* The immunoprecipitation of myc-tagged TgCCT subunits and subsequent immunoblot analysis were used to detect the bound proteins of interest and the potential presence of *T. gondii* actin and tubulin. TgGSK was used as a negative control to assess for tubulin and actin contamination in the 'bound' fraction.

Consequently, we tried to use a different and complementary approach that would allow assessing direct protein/protein interactions with a limited impact of protein abundance. A team of our institute had implemented a Bacterial Adenylate Cyclase Two-Hybrid (BACTH) system, which we thought could be adequate. The BACTH was initially engineered as an alternative to the yeast two-hybrid system and allows to detect the interactions between prokaryotic as well as between eukaryotic proteins<sup>261</sup>. This technique is based on an interactions-mediated reconstitution of the cyclic adenosine 3'5'-monophosphate (cAMP)-depending regulatory cascade in an *Escherichia coli* *cya*<sup>-</sup> strain via the introduction of a functional adenylate cyclase catalytic domain of *Bordetella pertussis* in the bacteria (Fig. 40). Importantly, the *B. pertussis* adenylate cyclase active domain consists of two subunits, T18 and T25. Once the subunits are co-expressed and brought close together, they interact and it restores the adenylate cyclase activity. The synthesis of cAMP then leads to the expression of a number of genes, including the *lactose* and *maltose* operons<sup>262</sup>. Therefore, if the proteins of interest interact, their fusion to T18 and T25 adenylate cyclase subunits and their subsequent co-expression in the *E. coli* *cya*<sup>-</sup> strain that lacks adenylate cyclase, would allow the bacteria to re-gain its ability to metabolise the lactose and will result in an increase of  $\beta$ -galactosidase activity.

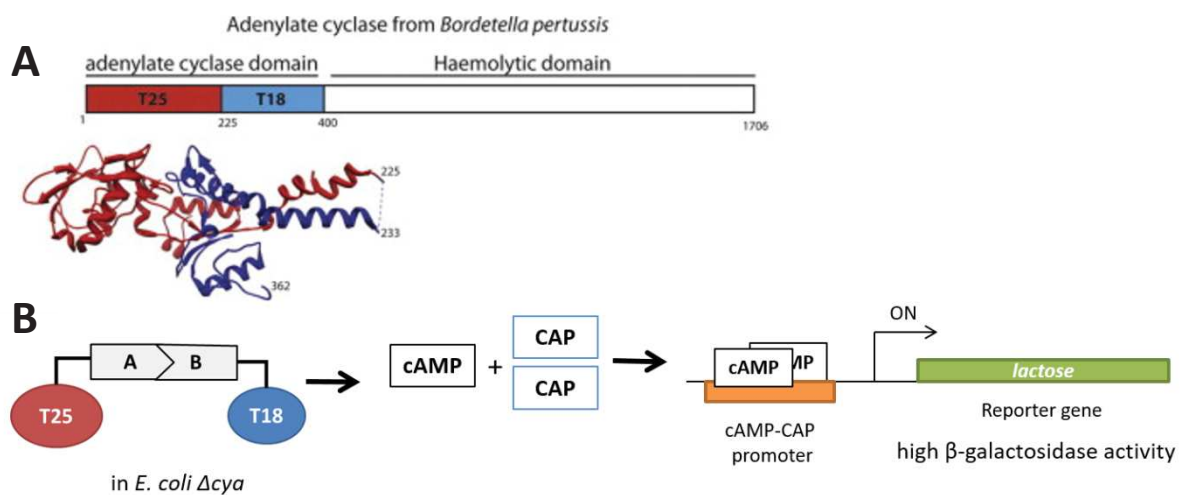


**Figure 40.** The principle of BACTH<sup>262</sup>. (A) The organisation of the adenylate cyclase of *B. pertussis*. The subunits of the adenylate cyclase catalytic domain are shown in red (T25) and in blue (T18). If the domains are physically separated, the activity of the adenylate cyclase is abolished. If the domains interact with each other (B) it leads to the synthesis of cAMP that forms complexes with CAPs (catabolite activator proteins) and binds to the cAMP-CAP promoter of several genes activating their expression. The reporter genes include *lac* and *mal* operon.

To assess the interactions between TgZFP2 and the subunits of TgCCT complex by this method, we first fused TgZFP2 with T18 sub-domain and TgCCT subunits with the T25 sub-domain of adenylate cyclase and co-expressed the pairs of potential binding partners (TgZFP2-TgCCT1, TgZFP2-TgCCT2, TgZFP2-TgCCT5) in *E. coli cya<sup>-</sup>* strain (Fig. 41A). As a result, the transformed bacteria restored their capacity to metabolise lactose. However, quite unfortunately, the co-expression of the TgZFP2-T18 fusion with the empty T25 vector, or of the TgZFP2-T18 fusion only (which were supposedly negative controls), led to an activation of *lactose* operon comparable to that induced by the expression of each of the pairs of potential binding partners. This activation of the *lactose* operon also appeared when the TgZFP2 was expressed in transformed bacteria while fused to the T25 sub-unit (Figure 41B). This was puzzling and raised the possibility that TgZFP2 alone may be able to activate the  $\beta$ -galactosidase activity in bacteria. In any case, this high background activity prevented us to conclude on the validity of the interactions.

As a final attempt to get evidence for potential interactions between TgZFP2 and the TgCCT subunits, we tried to interfere with the function of the TgCCT complex to check if this would lead to a phenotypic convergence with the TgZFP2 mutant. The limitation of this strategy, of course, was a probable generation of mutant parasites with a variety of phenotypes, given the potential pleiotropic function of this chaperonin complex.

We tried several approaches, including generating a conditional knock-down or overexpressing the dominant-negative version of one of the subunits of TgCCT complex. Unfortunately, we were never able to obtain stable transgenic parasites. This may be explained by the importance of this chaperonin complex for parasite viability: as all the approaches we used required changing the promoter (Tet-OFF system) or adding a relatively large C-terminal tag (degron-based mini-AID strategy), that may already have altered the function of the subunit before induction.

In conclusion, in spite of considerable efforts we did not manage to clearly identify protein partners for TgZFP2.

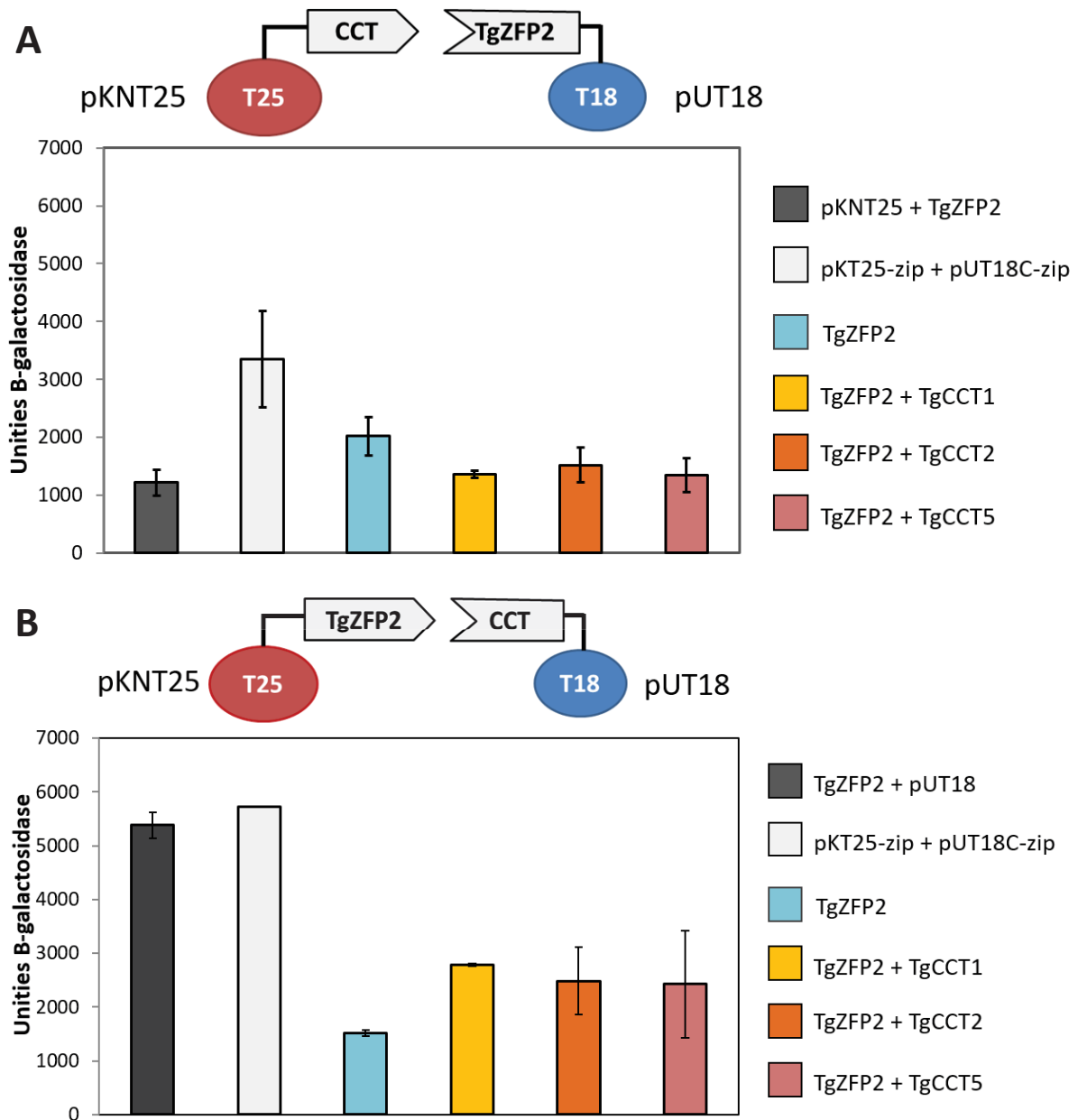


**Figure 41.** *β*-galactosidase assay performed on the *E. coli cya* bacteria with co-expressed TgZFP2 and its potential interacting partners, TgCCT subunits. (A) TgZFP2 is fused to the T18 adenylate-cyclase subdomain while TgCCTs were fused to the T25 subdomain. (B) TgZFP2 is fused to the T25 adenylate-cyclase subdomain while TgCCTs were fused to the T18 subdomain. pKT25-zip and pUT18C-zip constructs represent the positive control (light grey columns) for the assay. Note that the negative controls (black and light blue columns of each figure) show *β*-galactosidase activity. Data are mean from  $n=3$  experiments  $\pm$  standard error.

### 2.3. TgZFP2 recombinant protein and zinc binding assay

We thought the generation of a TgZFP2 recombinant protein would be a valuable tool for studying its potential interactions with proteins and other molecules (e.g. in pull-down or biochemical assay). The endogenously-tagged transgenic cell lines, used during our study, displayed a relatively modest level of TgZFP2 expression and a strategy for overexpressing TgZFP2 in the parasites was unsuccessful. The production of the recombinant protein could help us to overcome this technical difficulty.

We decided to produce a Glutathione S-Transferase (GST)-tagged version of TgZFP2 in *E. coli* and I have generated the constructs allowing the production of the wild type TgZFP2-GST (hereafter TgZFP2-GST WT), as well as the production of the TgZFP2-GST with a mutated zinc finger domain (TgZFP2-GST ZFM) where we have replaced one pair of cysteines by a pair of glycines, similarly to the complemented transgenic cell lines used in the functional studies in parasites (see the manuscript in Chapter 1 of Results).

However useful recombinant proteins are in biological assays, their production may be associated with several problems. For instance, it might be impaired by expression or solubility issues<sup>263</sup>. This is what happened for the TgZFP2-GST proteins, which, while being successfully produced in the bacteria, were almost completely insoluble ([Fig. 42A](#)).

In many cases, the recombinant proteins can be produced in high amounts by the bacteria but end up in an unfolded form accumulating in so called 'inclusion bodies'<sup>264</sup>. A change in protein production conditions may sometimes lead to, at least, partial solubilisation of the produced protein. I thus tried to optimise the protocol by step-by-step changes in each of the conditions, but to no avail. I tried adjusting the concentration of the inducer, lowering the growth temperature of the bacterial culture, changing the type of culture medium, or strain of bacteria, or, finally, the time of induction (see Materials and methods for details), but it did not allow me to circumvent the solubility problem. We thus decided to solubilise the protein post-expression by adding urea to the bacterial extracts, allowing the purification to proceed ([Fig. 42B](#)). After purification, urea was progressively removed by several sequential dialyses against series of buffers with decreasing urea concentrations, with the hope to recover a soluble and properly folded protein. A quantification of TgZFP2-GST WT and TgZFP2-GST ZFM obtained after dialysis was

performed with Coomassie staining after separation on a polyacrylamide gel in the presence of a protein standard. It allowed us only to estimate the concentration of the proteins. Of note, the extracts were not completely pure, but hoping that our proteins of interest were properly folded we proceeded with the assays we wanted to perform.

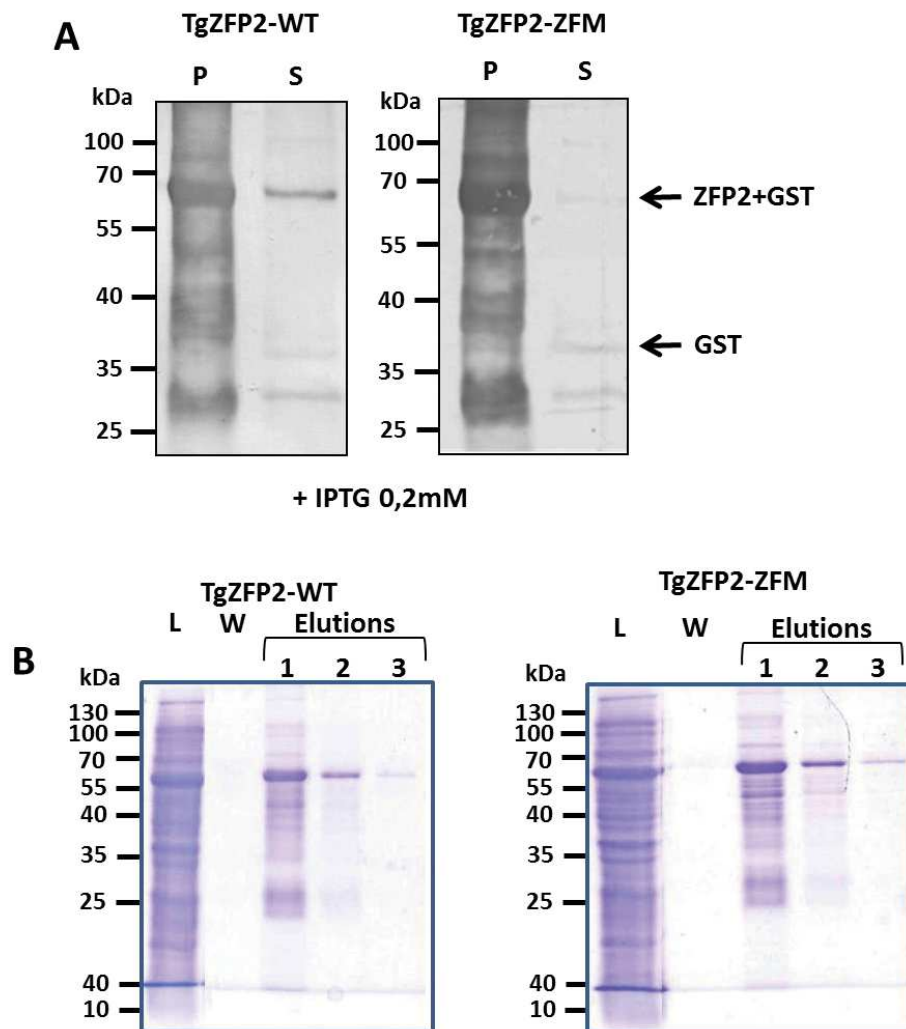


**Figure 42. TgZFP2 recombinant proteins production.** (A) WB analysis of soluble (supernatant, S) and insoluble (pellet, P) fractions of lysed bacterial extracts of *E. coli* expressing recombinant TgZFP-GST WT and TgZFP2-GST ZFM. Proteins of expected size are produced, but are mostly insoluble. IPTG: Isopropyl  $\beta$ -D-1-thiogalactopyranoside (inducer). (B) Coomassie staining of protein extracts from the purification process for the TgZFP-GST WT and TgZFP2-GST ZFM proteins after their solubilisation in urea. L: total lysate after induction; W: wash fraction; 1, 2, 3: sequential elution fractions.

In most studies the 'zinc finger protein' denomination is based on the identification of a particular amino acid motif resembling a typical, already characterised, ZnF. Very few studies actually verify whether these domains can accommodate a zinc molecule. We thought we could try to achieve this with a recombinant version of TgZFP2 (with zinc finger mutated version serving as a negative control). The principle of measuring the zinc content is based on

a spectroscopic method, with methyl methanethiolsulfonate (MMTS) as the cysteine modifier, and 4-(2-pyridylazo) resorcinol (PAR) as a zinc sensitive probe<sup>265</sup>. The PAR is known to bind the free zinc, forming a Zn-(PAR)<sub>2</sub> complex. This reaction is associated with an increase of sample's absorbance at 500 nm ( $A_{500}$ ). Based on this principle, for our assay, we first added MMTS to the eluted recombinant proteins in estimated concentrations in order to release zinc from its bound state, and then added the PAR, monitoring the  $A_{500}$  throughout the assay. The resulting measurements were plotted on curve for further zinc quantification by comparing it to a standard curve I generated with known amounts of zinc (Fig. 43A).

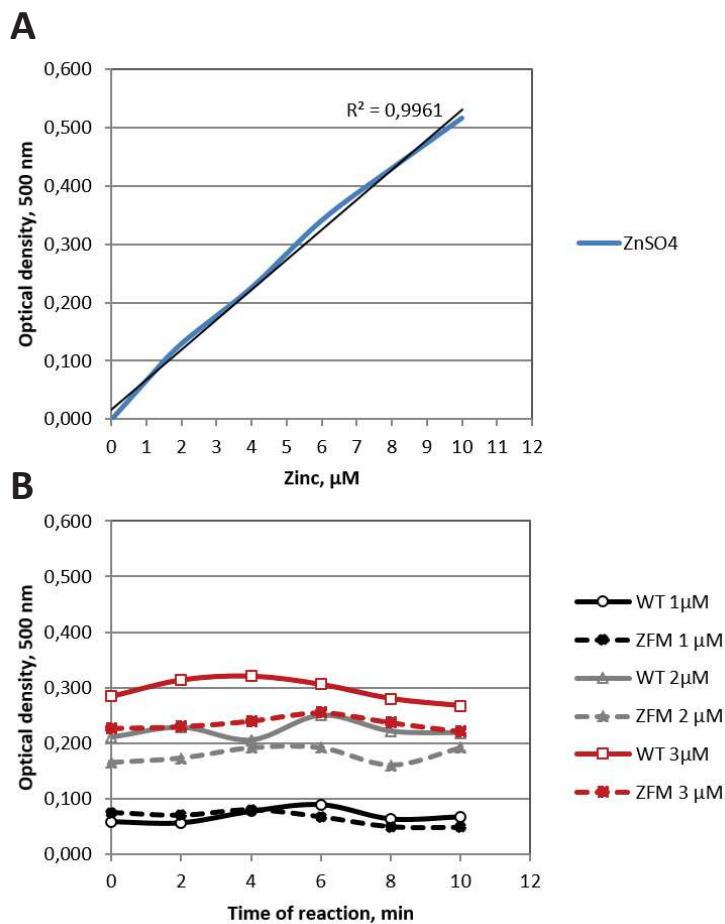


**Figure 43. Zinc binding assay.**

**(A)** Standard curve of zinc ion release was generated using 1 $\mu\text{M}$ , 2 $\mu\text{M}$ , 4 $\mu\text{M}$ , 6 $\mu\text{M}$ , 8 $\mu\text{M}$  and 10 $\mu\text{M}$  of ZnSO<sub>4</sub>. **(B)** The representative experiment of measurements of zinc ion release from TgZFP2-GST WT and TgZFP2-GST ZFM proteins done with estimated concentrations of 1, 2 and 3  $\mu\text{M}$ . The initial solutions of recombinant proteins contained 50 $\mu\text{M}$  of PAR and measurements of the optical density were monitored for 10 min after the addition of the cysteine modifier (MMTS) and the beginning of the PAR+Zn reaction.

Increasing the amount of recombinant protein extract led to an increase in  $A_{500}$ , but, quite unexpectedly, there was very little difference between the results obtained with the TgZFP2-GST ZFM negative control and the TgZFP2-GST WT protein (Fig. 43B). Moreover, the incubation of both proteins with the cysteine modifier did not lead to an important increase of the absorbance. The absorbance of each sample was, however, clearly different from that of the negative control (bovine serum albumin used in same concentrations, not shown). There might be a residual presence of zinc ions in the fraction containing our protein

of interest, or zinc could originate from the other proteins eluted together with the recombinant proteins.

Altogether, the production of recombinant TgZFP2-GST proteins turned out to be difficult to implement. TgZFP2 is not produced as a soluble protein by *E. coli* and the purification in denaturing conditions/renaturation might not generate optimally folded proteins. Moreover, other residual proteins remained in the elution fractions after purification of TgZFP2-GSTs, and the process would thus benefit from an additional chromatography purification step (e.g. by size exclusion chromatography). However, due to time limitation, I had to give up trying to optimise the production of these recombinant proteins in order to focus on another part of the project.

---

## CHAPTER 3. Identification of TgZFP2 RNA binding partners

---

A majority of zinc finger-containing proteins use this motif to bind nucleic acids. Though many of them exhibit DNA-binding properties and are involved in transcription, there are several zinc finger proteins capable of binding RNA and involved, for instance, in the regulation of mRNA stability and processing<sup>240</sup>. The commonly known RNA-related ZnFs are classical Cys<sub>2</sub>-His<sub>2</sub> or Cys-Cys-Cys-His<sup>266,267</sup>; nevertheless, Cys<sub>2</sub>-Cys<sub>2</sub> motif is also defined as a potential RNA-binding one, like in the human splicing factor ZNF265<sup>267,268</sup>. Taking into account the cytoplasmic localisation of TgZFP2 and the impact that mRNA homeostasis could clearly have on cell cycle regulation, we tried to explore the potential RNA-binding properties of TgZFP2.

One of the simplest ways to get insights into the TgZFP2-RNAs putative association was to check this protein's presence in RNA granules, which are important participants of the post-transcriptional regulation of gene expression in living cell<sup>269</sup>. The eukaryotic RNA granules are aggregates that belong to cellular non-membrane bound compartments. As their name implies, they contain translationally inactive mRNAs (along with a specific set of proteins)<sup>270</sup>. The processing bodies (PB) together with the stress granules (SG) represent two conserved ubiquitous classes of RNA granules<sup>271</sup> (Fig. 44A). The PB contain the mRNAs associated with transcription repressors and are known to harbour the RNA decay machinery, thus participating in mRNAs decapping and degradation. The SG, in turn, are formed with the mRNAs stalled in the initiation of translation and also contain the translation initiation machinery that allows to trigger the translation of specific mRNAs in response to stress<sup>272</sup>. The SGs can be differentiated from PBs by using specific protein markers such as the poly-A binding proteins (PABP) that PB lack<sup>273</sup>. In *T. gondii* the SG-like mRNAs aggregates were identified in extracellular tachyzoites; their formation can be induced experimentally in a specific high potassium buffer that mimics the ionic composition of host cell cytosol (conditions parasites encounter as they egress from the host to become extracellular)<sup>273</sup>.

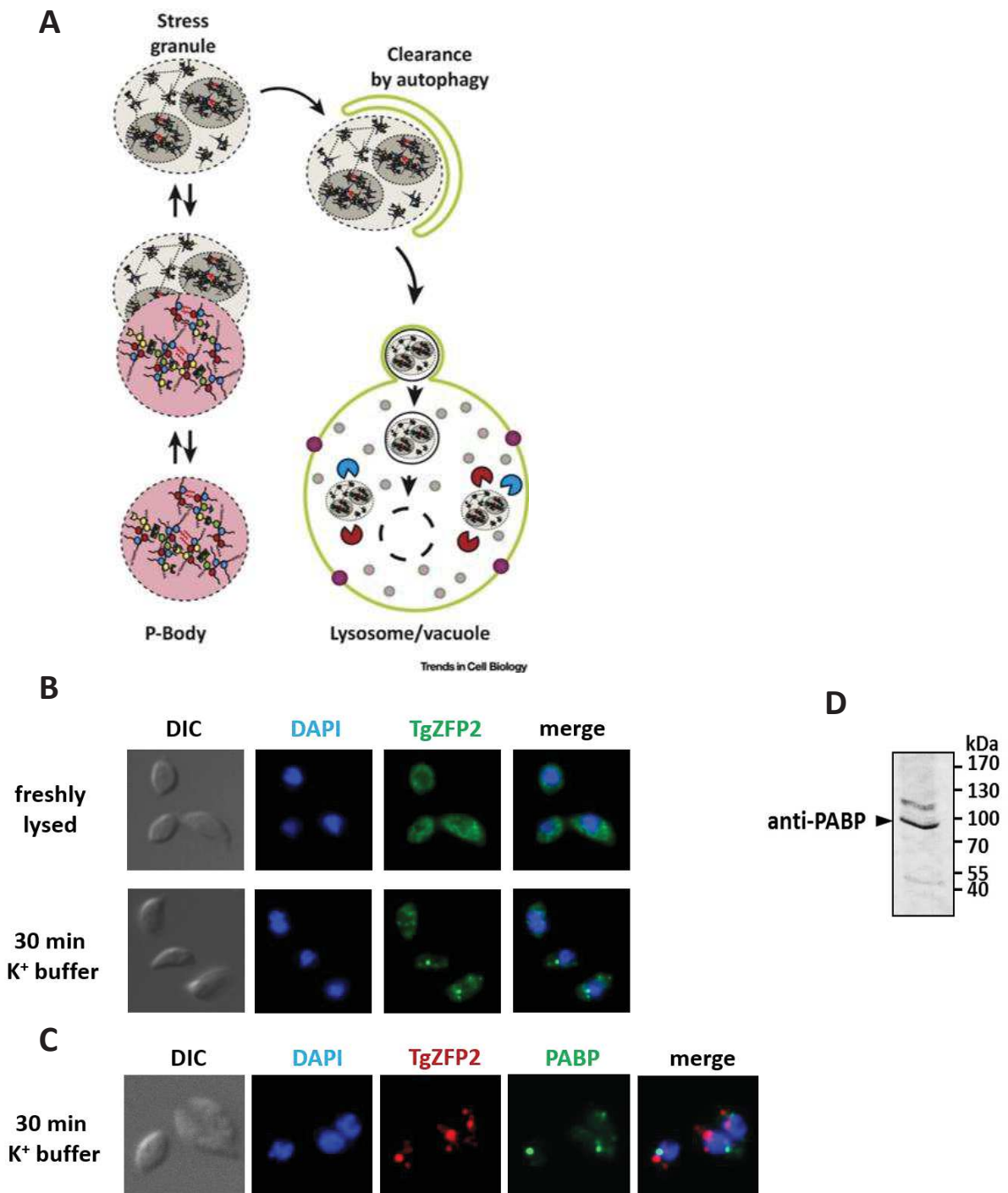


**Figure 44. TgZFP2 and the stress granules.** (A) The SGs contain untranslated mRNAs<sup>272</sup>. They are dynamic structures that can interact with the processing bodies (P-bodies), exchange components with cytoplasm and be subjected to autophagy. (B) Once the tachyzoites are exposed to conditions mimicking host cell ionic composition, TgZFP2 re-localises in agglomerates resembling the stress granules. However, (C) these agglomerates are distinctive from the SGs that are marked by the anti-PABP mouse antibody. On the images, TgZFP2 is stained with anti-HA antibody, DNA content is labelled by DAPI. (D) Validation by immunoblot of the anti-PABP antibody. Although originally raised against mouse PABP, in *T. gondii* extracts this reagent recognises a protein with the expected molecular mass for TgPABP (82 kDa).

We checked whether TgZFP2 re-localised to SG-like structures in stress conditions. For this purpose, we performed IFAs on extracellular parasites placed into high potassium buffer (Fig. 44B,C). Quite strikingly, in these parasites TgZFP2 accumulated to intensely labelled punctate cytoplasmic structures not visible in the freshly egressed tachyzoites, which may represent protein aggregates. However, when co-stained with anti-PABP antibodies, these TgZFP2 aggregates did not co-localise with the SG. This did not completely rule out that TgZFP2 could interact with RNAs, for instance, in a different subpopulation of granules that are not PABP-positive. This hypothesis could be tested by a co-staining of TgZFP2 with more generally labelled mRNAs-containing granules via an RNA-FISH approach. However, due to time constraints and other priorities in the project, I did not finalise the optimisation and the implementation of this strategy.

Another way of assessing the TgZFP2 potential binding to RNAs was to use the RIP-seq (RNA immunoprecipitation and sequencing) approach described and successfully applied in *T. gondii* tachyzoites by Gissot et al.<sup>274</sup>. With this method, RNA-protein complexes are co-immunoprecipitated with antibodies targeted to the protein of interest. After RNase digestion, the RNAs protected by their binding to the protein, are extracted and reverse-transcribed to cDNA. Deep sequencing of cDNA then allows the identification of protein-bound RNAs. We applied this technique to our cell line expressing HA-tagged TgZFP2, as well as to a RH Tati  $\Delta ku80$  control parental cell line (Fig. 45). This part of the study has been done in collaboration with the team of Mathieu Gissot at the Lille Pasteur Institute: I generated the RNA samples that were sent to Lille for further processing.

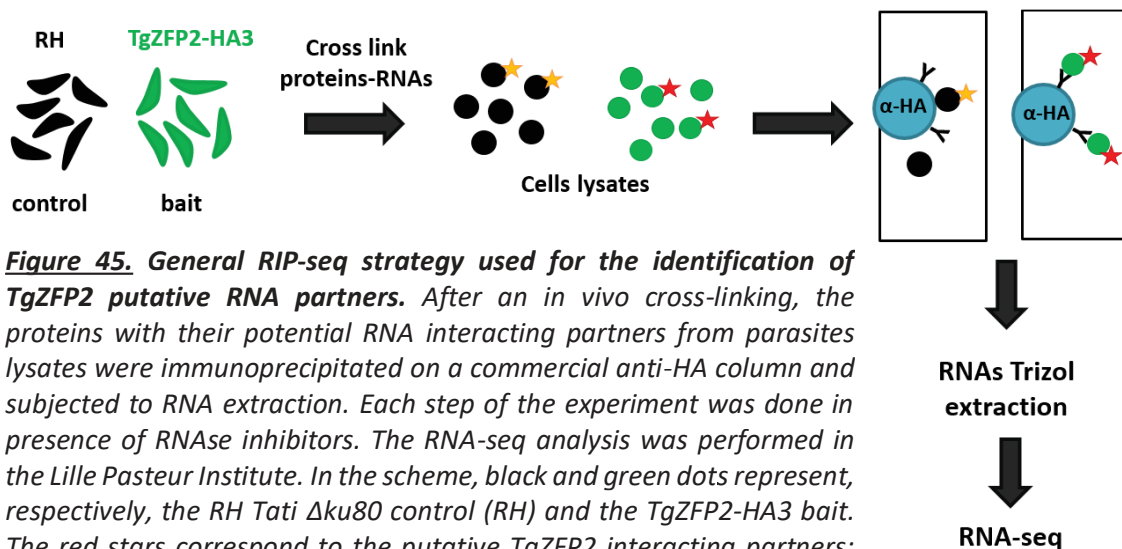


**Figure 45.** General RIP-seq strategy used for the identification of TgZFP2 putative RNA partners. After an *in vivo* cross-linking, the proteins with their potential RNA interacting partners from parasites lysates were immunoprecipitated on a commercial anti-HA column and subjected to RNA extraction. Each step of the experiment was done in presence of RNase inhibitors. The RNA-seq analysis was performed in the Lille Pasteur Institute. In the scheme, black and green dots represent, respectively, the RH Tati  $\Delta ku80$  control (RH) and the TgZFP2-HA3 bait. The red stars correspond to the putative TgZFP2 interacting partners; orange stars correspond to false positive partners.

The classical protocol of RNA-seq includes a compulsory cross-linking step destined to stabilise the association between the protein of interest and the RNAs *in vivo*. Unfortunately, in our case this step proved particularly cumbersome. TgZFP2 is already only partially soluble in normal immunoprecipitation conditions (i.e. using small amounts of non-ionic detergent), but the cross-link by formaldehyde rendered the solubilisation of the protein by detergents completely inefficient and prevented subsequent co-immunoprecipitation (Fig. 46A). As we suspected TgZFP2 to be associated with cytoskeletal structures (see manuscript in Chapter 1 of Results), it is possible that formaldehyde cross-linking prevented the release of the protein from the cytoskeletal fraction.

The change of the cross-linking method from formaldehyde to short wave UV irradiation (Fig. 47) allowed us to resolve this technical difficulty and to, at least, succeed in solubilising and immunoprecipitating TgZFP2-HA3 (Fig. 46B).

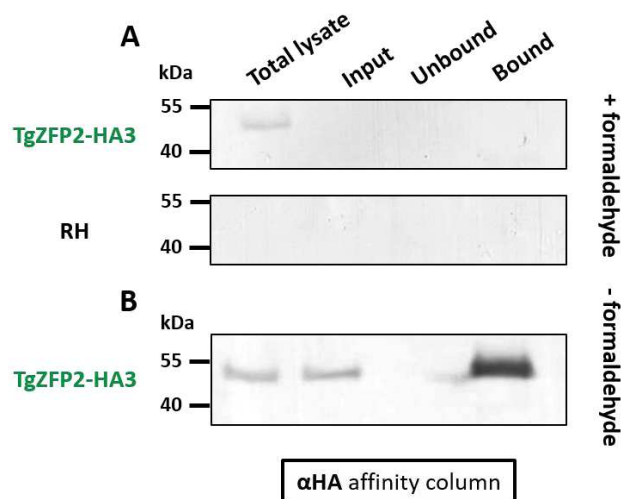


**Figure 46. TgZFP2 solubility is affected by the formaldehyde cross-linking.** (A) WB analysis of fractions from the anti-HA immunoprecipitation of TgZFP2 shows the protein is not solubilised (absent from the soluble extracts loaded on the column, 'Input') and thus cannot be purified in the RIP-seq experiment after formaldehyde cross-linking. (B) In absence of formaldehyde crosslinking, soluble TgZFP2 is successfully immunoprecipitated on the anti-HA commercial column and can be subsequently purified.

The experiment was performed three times on independent intracellular cultures and, in the end, the amount of extracted RNAs was considerably low ( $\leq 5$  ng/ $\mu$ l). More worryingly, there was no significant difference in RNA quantity between the TgZFP2 and the control samples. The yield of this sort of experiments is typically low (as only minute amount of RNAs binds to the protein of interest), hence, assuming we were close to the limit of detection, we decided to proceed with subsequent steps of RNA-seq. Unfortunately, our collaborators could not amplify enough cDNA from collected samples and, regrettably, no TgZFP2 interacting RNAs were isolated in these series of experiments. We efficiently recovered our protein through immunoprecipitation, but the negative result could be due to sub-optimal sample

preparation, as RNAs are very labile and can be easily degraded. The other possibility, of course, would be that TgZFP2 does not interact with RNAs. We cannot definitely rule out TgZFP2 has RNA-binding properties, but neither our IFAs of RNA granules nor our RIP-seq experiments would strongly support any evidence of TgZFP2-RNAs interactions.

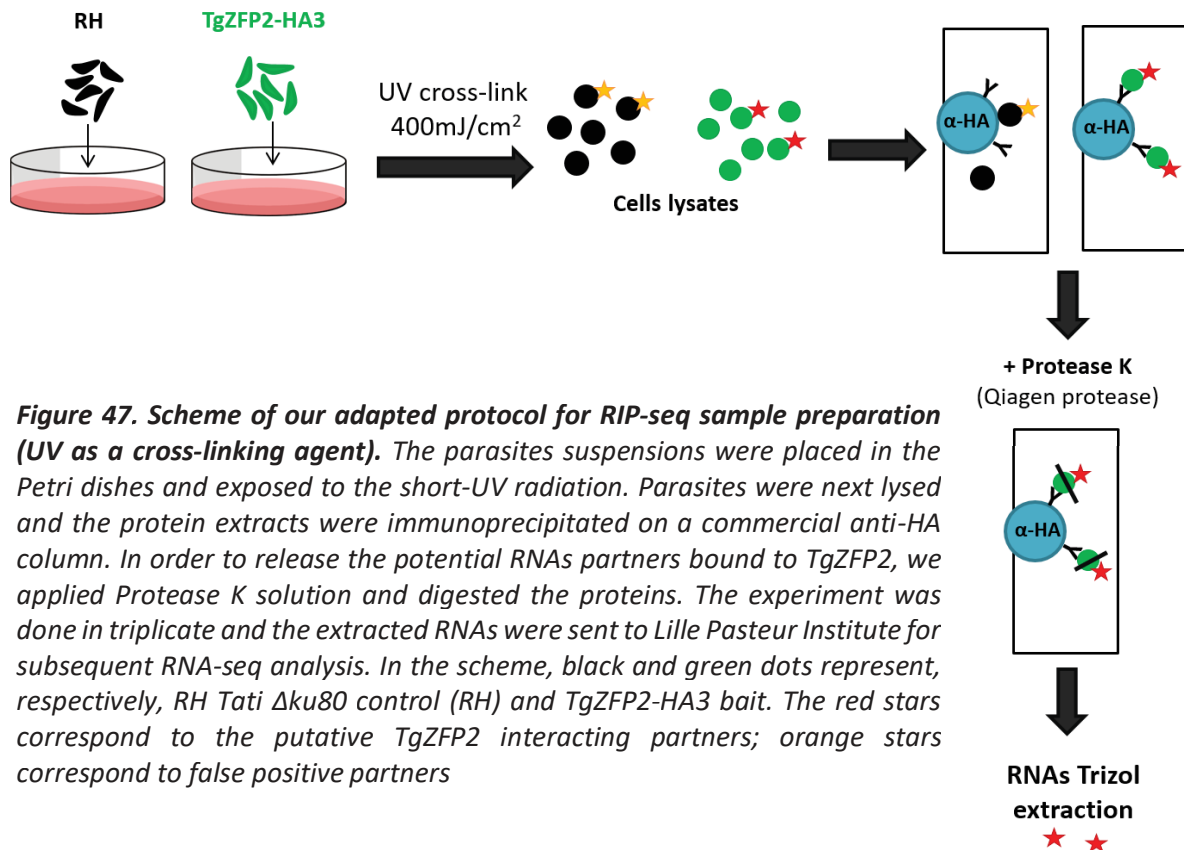


**Figure 47. Scheme of our adapted protocol for RIP-seq sample preparation (UV as a cross-linking agent).** The parasites suspensions were placed in the Petri dishes and exposed to the short-UV radiation. Parasites were next lysed and the protein extracts were immunoprecipitated on a commercial anti-HA column. In order to release the potential RNAs partners bound to TgZFP2, we applied Protease K solution and digested the proteins. The experiment was done in triplicate and the extracted RNAs were sent to Lille Pasteur Institute for subsequent RNA-seq analysis. In the scheme, black and green dots represent, respectively, RH Tati  $\Delta ku80$  control (RH) and TgZFP2-HA3 bait. The red stars correspond to the putative TgZFP2 interacting partners; orange stars correspond to false positive partners

### TgZFP2 interactions study: conclusive remarks

The study of potential TgZFP2 binding partners was a challenging part of my PhD project. The broad mass spectrometry strategy used to select putative TgZFP2-interacting proteins revealed a large list of candidates, from which we selectively targeted those potentially associated with the regulation of the cell cycle progression or linked to the cytoskeleton of tachyzoites. Disappointedly, none of the selected cell-cycle related putative partners (TgGSK and TgCyclin2-related protein) had shown a strong direct interaction with TgZFP2 in co-immunoprecipitation study. CCT, a chaperonin complex involved in cytoskeletal homeostasis<sup>257</sup>, and whose homologue in human cells potentially interacts with a SSSCA1 protein bearing a zinc finger motif similar to TgZFP2's, seemed to be another candidate worthy of investigation. TgCCT was enriched in both mass spectrometry experiments. However,

despite the use of a variety of approaches we implemented to assess the potential TgZFP2-TgCCT interactions, we were unable to confirm the existence of direct link between TgZFP2 and the three selected subunits of TgCCT. Human CCT (as well as TgCCT) has a complex two-ring-like structure<sup>260</sup> and is composed of eight distinctive subunits, each of them having a substrate specificity<sup>275</sup>. Hence, there remains a possibility that TgZFP2 may interact with TgCCT subunit(s) other than selected for our study. Of note, a subunit of the CCT complex was reported to localise in the centrosome region in mammals, in a specific cell cycle phase or in stress conditions<sup>276,277</sup>. As TgZFP2 is dynamically recruited to the peri-centrosomal region and, apparently, interacts with molecular partners there, this raises the possibility of a transient interaction between TgZFP2 and subunits of the TgCCT complex. We have seen a global co-immunoprecipitation strategy failed to clearly identify TgZFP2 partners, so further studies would be required for this. Strategies, alternative to co-immunoprecipitation include proximity labelling-based approaches<sup>278</sup>, but the dynamics of TgZFP2 and potentially transient interactions with partners during the cell cycle may render this difficult to implement. A two-hybrid approach, which is less biased by protein abundance and allows mapping the regions of interactions, may be useful to overcome some of the difficulties we experienced.

---

## Materials and methods

---

### Mammalian cell culture

#### 1. Human foreskin fibroblasts

Human foreskin fibroblasts (HFF), from the American Type Culture Collection, CRL 1634, were cultivated at 37°C in a humidified atmosphere containing 5% CO<sub>2</sub> using Dulbecco's modified Eagle medium (DMEM, Gibco) supplemented with 10% decompemented fetal bovine serum (FBS, Gibco), 2 mM glutamine and a cocktail of penicillin-streptomycin (Gibco) at 100 µg/mL.

#### 2. Vero cells

Vero cells (cell line established from kidney epithelial cells of African green monkey) were cultivated at 37°C in a humidified atmosphere containing 5% CO<sub>2</sub> using DMEM (Gibco) supplemented with 3% FBS, 2 mM glutamine and a cocktail of penicillin-streptomycin at 100 µg/mL.

### Parasites maintenance

Tachyzoites of the RH TATi1-ΔKu80 *T. gondii* strain<sup>279</sup> and derived transgenic parasites were maintained by serial passage on HFFs monolayer grown in DMEM (Gibco) supplemented with 5% FBS (Gibco), 2 mM L-glutamine (Gibco) and a cocktail of penicillin-streptomycin (Gibco) at 100 µg/mL.

### Identification of the putative TgZFP2 protein partners

#### 1. Mass spectrometry

The cell lines used in the experiment - YFP and TgZFP2-YFP – were grown in Vero cells. Four 175cm<sup>2</sup> flasks of Vero cells were infected with transgenic TgZFP2-YFP parasites, while one 175cm<sup>2</sup> flask was infected by YFP parasites to obtain about the same amount of the respective proteins to bind to the affinity purification column.

After two days of parasite replication, naturally egressed parasites were collected and Vero cells were scrapped and syringed through a 25-gauge needle to collect intracellular parasites as well. A total of ~1.5x10<sup>9</sup> (for YFP) and ~3x10<sup>9</sup> (for TgZFP2-YFP-expressing

strain) tachyzoites were lysed by successive freeze/thaw cycles (in liquid nitrogen and at 40°C) in 500 µL lysis buffer (50 mM Tris-HCl pH 7.5, 150 mM NaCl, 1% Triton Tx-100, 0,1% SDS 0.5 mM EDTA and a EDTA-free Protease Inhibitor Cocktail (Roche)) and incubated for 2 h at 4°C on a rotating wheel. Following the incubation, the lysates were centrifuged three times at 1500 g for 15 min to remove non-lysed parasites and the supernatants were collected after each centrifugation. After the final centrifugation, the supernatants were diluted to the half in washing buffer (50 mM Tris-HCl pH 7.5, 150 mM NaCl, 0.5 mM EDTA and a EDTA-free Protease Inhibitor Cocktail (Roche)) and the samples were incubated for 4 hours at 4°C with 50 µL GFP-Trap magnetic agarose beads (Chromotek) previously equilibrated in the same buffer. Following the incubation, the samples were washed three times in washing buffer and eluted in 50 µL of Laemmli loading buffer and subjected to WB analysis prior to peptide digestion by trypsin and mass spectrometry analysis.

Eluted proteins were separated on 10% acrylamide gels, stained overnight with colloidal Coomassie blue, and cut in 5 fractions. Following reduction and alkylation with 10 mM DTT and 55 mM iodoacetic acid, samples were digested overnight by 600 ng of trypsin proteases at room temperature (RT) under agitation. Peptides were then extracted in 5% formic acid and analyzed by liquid chromatography coupled to tandem mass spectrometry (LC-MS/MS) using an Orbitrap ELITE mass spectrometer (Thermo Fisher Scientific, PPM proteomic platform, IGF, Montpellier). Peptides which were found to be abundant in the TgZFP2-YFP fractions and essentially absent from the control fractions were considered for selecting protein candidates. Two independent experiments were conducted in order to select the putative protein interactive candidates.

## **2. Generation of *myc*-tagged cell cycle related candidates parasites**

The ligation independent cloning strategy<sup>255</sup> was used to tag GSK kinase (TGGT1\_265330) and Cyclin2 related protein (TGGT1\_267580) at their C-term with a triple *myc* tag, in the TgZFP2-*HA3* transgenic cell line background. The fragments of 1.5 kb were amplified using: i) the Phusion High-Fidelity DNA Polymerase (New England BioLabs) for TgGSK with ML2933/ML2934 primers and ii) the Q5 High-Fidelity DNA Polymerase (New England BioLabs) with ML2949/ML2938 primers for TgCyclin2. The amplified fragments were inserted in frame with the *myc3* tag-coding sequence present in the pLIC-*myc3*-DHFR plasmid using T4 DNA ligase (New England BioLabs). The resulting vectors were linearized with NsiI (TgGSK) or

NcoI enzymes (TgCyclin2) and 50 µg of DNA were transfected into the TgZFP2-*HA3* transgenic cell line to allow the integration by single homologous recombination.

### **3. Generation of doubly-tagged TgCCTs-*myc3*/TgZFP2-*HA3* cell lines.**

The ligation independent cloning strategy<sup>255</sup> was used to tag TgCCT1 (TGGT1\_229990), TgCCT2 (TGGT1\_243710) and TgCCT5 (TGGT1\_202370) at their 3' with the triple *myc* tag in the background of TgZFP2-*HA3* transgenic cell line. The fragments of 1,7kb, 1,7 kb and 1,6 kb corresponding, respectively, to the 5' of the genes coding for TgCCT 1,2 and 5 subunits, have been amplified using: i) the Phusion High-Fidelity DNA Polymerase (New England BioLabs) with primers ML2989/ ML2990 for TgCCT1 and ii) the Q5 High-Fidelity DNA Polymerase (New England BioLabs) with primers ML2991/ML2992 and ML2993/2994 for TgCCT2 and TgCCT5, respectively. The amplified fragments were inserted in frame with the *myc3* tag-coding sequence present in the pLIC-*myc3*-DHFR plasmid using T4 DNA ligase (New England BioLabs). The resulting vectors have been linearised with, respectively, ApaI, NcoI and AsiSI and 50 µg of DNA were transfected into the TgZFP2-*HA3* transgenic cell line to allow the integration by single homologous recombination.

### **4. The immunofluorescent microscopy**

For the immunofluorescence assays (IFA) tachyzoites were grown in HFF monolayers on coverslips for 24h. The intracellular parasites were fixed with 4% (w/v) paraformaldehyde in 1X Phosphate-Buffered Saline (PBS) for 20 min. After 3 washes in PBS the cells were permeabilised with 0.3% triton in PBS for 10 min, washed thrice and subsequently blocked with 0,1% (w/v) Bovine serum albumin (BSA) in PBS for 15 min. Primary antibodies used to visualize the proteins and sub-cellular structures were: rat monoclonal anti-*HA* antibody (Roche) at 1/500 dilution to detect epitope-tagged TgZFP2; mouse monoclonal anti-*myc* antibody (Dominique Soldati-Favre laboratory, Switzerland) at a 1/10 dilution to detect *myc*-tagged protein candidates TgGSK, TgCyclin2, TgCCT1, TgCCT2 and TgCCT5. Staining of DNA was performed by a 5 min incubation of fixed cells in a 1 µg/ml 4',6-diamidino-2-phenylindole (DAPI) solution. Slides were mounted with Shandon Immu-Mount (Thermo Scientific).

All images were acquired at the Montpellier RIO imaging facility from a Zeiss AXIO Imager Z2 epifluorescence microscope equipped with an ORCA-flash 4.0 camera

(Hammamatsu) and driven by the ZEN software (Zeiss). Adjustments for brightness and contrast were applied uniformly on the entire image.

## 5. Immunoprecipitation assays

For each transgenic cell line a 175 cm<sup>2</sup> flask of HFF cells was infected. After two days of parasites replication, the parasites were collected and lysed by successive freeze/thaw cycles (in liquid nitrogen and at 40°C) in 500 µL lysis buffer (50 mM Tris-HCl pH 7.5, 150 mM NaCl, 0.5% Triton Tx-100, 0.5 mM EDTA and a EDTA-free Protease Inhibitor Cocktail (Roche)) and incubated at 4°C on a rotating wheel for 1 h. The lysates were then centrifuged three times at 1,500 g, 4°C, for 15 min to remove non-lysed parasites and supernatants were collected after each centrifugation. Following the 1/2 dilution in 500 µL washing buffer (10 mM Tris-HCl pH 7.5, 150 mM NaCl, 0.5 mM EDTA and a EDTA-free Protease Inhibitor Cocktail (Roche)), samples were incubated for 4 h at 4°C with 20 µL of magnetic agarose Myc-Trap beads (Chromotek) previously equilibrated in the same buffer or with 40 µL of anti-HA beads (Roche), also equilibrated. Beads were washed three times in washing buffer and bound proteins were eluted in 30 µL of Laemmli loading buffer, separated by SDS-PAGE and subjected to WB analysis. TgGSK, TgCyclin2, TgCCT1, TgCCT2 and TgCCT5 were revealed with anti-myc mouse monoclonal antibodies (Dominique Soldati-Favre laboratory, Switzerland) at a 1/10 dilution. TgZFP2 was revealed with anti-HA antibodies (Roche) at a 1/1000 dilution. Actin and tubulin were revealed with, respectively, anti-actin mouse monoclonal antibodies (Dominique Soldati-Favre laboratory, Switzerland) at a 1/25 dilution and with anti-tubulin mouse monoclonal antibodies (clone B-5-1-2, Sigma-Aldrich) at a 1/4000 dilution. SAG1 was revealed with anti-SAG1 rabbit antibodies<sup>280</sup> at a 1/2000 dilution.

## 6. Native gel assay

The parasites collected after 48h of growth on a 25 cm<sup>2</sup> HFF flask (approx. 30 x 10<sup>6</sup> parasites) were resuspended in 10 µL of Tris-Glycine Native Sample Buffer (2X) and separated in native state on NuPAGE Tris-Acetate Mini Gel 3-8% (Invitrogen) along with NativeMark Unstained Protein Standard 20-1200kDa (Invitrogen). Following 3 h of migration at 120 V, the proteins were transferred on a PVDF membrane overnight at 4°C (17 mA) and subjected to WB analysis. The TgCCT1, TgCCT2 and TgCCT5 were revealed with anti-myc mouse

monoclonal antibodies (Dominique Soldati-Favre laboratory, Switzerland). The marker was revealed separately with Colloidal Gold Total Protein Stain (Bio-Rad).

## 7. BACTH (bacterial two-hybrid system)

The BACTH approach included i) the fusion of the protein binding partners to the sub-domains of the *B. pertussis* CyaA in two separate plasmids; ii) the co-expression of the two plasmids in *E. coli cya<sup>-</sup>* background; iii) the measurement of  $\beta$ -galactosidase activity in liquid bacteria cultures.

i) To fuse the putative interacting protein partners to the sub-units of the *B. pertussis* adenylate cyclase catalytic domains, we used two following plasmids:

- the low copy pKNT25 plasmid that encodes the T25 fragment (corresponding to the first 224 amino acids of CyaA) expressed under the transcriptional control of a *lac* promoter that is fused in frame downstream of a multicloning site (MCS).
- the high copy pUT18 plasmid that encodes the T18 fragment (amino acids 225 to 399 of CyaA) expressed under the transcriptional control of a *lac* promoter that is fused in frame downstream of a MCS.

Full length TgZFP2 (1.1 kb) and TgCCT1 (1,7 kb), TgCCT2 (1,7 kb), TgCCT5 (1,6 kb) were amplified by PCR from cDNA of RH TATi  $\Delta$ Ku80 parasites with the Q5 High-Fidelity DNA Polymerase (New England BioLabs) using respective primers: ML3092/ML3093, ML3094/ML3095, ML3096/ML3097 and ML3098/ML3099 containing HindIII/BamHI restriction sites. The amplified fragments were inserted in frame into the MCS of the pKNT25 and pUT18 plasmids using T4 DNA ligase (New England BioLabs). The amplification of the plasmids was done in Top10 competent bacteria (for TgCCT subunits) and in Stellar™ Competent Cells, Clontech (for TgZFP2) according to the protocol. The bacteria were cultivated in liquid Lysogeny Broth (LB) media supplemented with 100  $\mu$ g/ml of ampicillin (for pUT18 constructs) or 50  $\mu$ g/ml of kanamycin (for pKNT25 constructs).

ii) The generated constructs were co-expressed in the chimio-competent non-reverting adenylate cyclase deficient *E. coli cya<sup>-</sup>* reporter strain, BTH101. To check the activation of the *lactose* operon, bacteria were cultivated at 30°C overnight on LB agar Petri dishes supplemented with 100  $\mu$ g/ml of X-gal, 100  $\mu$ g/ml of ampicillin and 50  $\mu$ g/ml of kanamycin. The blue coloured colonies were considered positive.

iii) To perform the  $\beta$ -galactosidase assay, the transformed BTH101 were cultivated overnight at 30°C in 1 ml of LB media supplemented with 100  $\mu$ g/ml of IPTG, 100  $\mu$ g/ml of ampicillin and 50  $\mu$ g/ml of kanamycin. The OD<sub>600</sub> of 1/3 diluted cultures was measured (so that it would be between 0.28 and 0.7), and the cultures were diluted 1/10 in Z buffer (1 ml total volume). The bacteria were then lysed by the addition of 20  $\mu$ l of 0.1% SDS and 40  $\mu$ l of CHCl<sub>3</sub> and rapid vortexing.

The colorimetric reaction was initiated at RT by the addition of 200  $\mu$ l of 4 mg/ml ortho-Nitrophenyl- $\beta$ -galactoside (ONPG) at 30°C. The time required for the appearance of yellow colour (t) was noted and the reaction was arrested by the addition of 500  $\mu$ l of 1M Na<sub>2</sub>CO<sub>3</sub> and the following T decrease to 4°C. Finally, the OD<sub>550</sub> and OD<sub>420</sub> were measured and the  $\beta$ -galactosidase activity was calculated using the formula:

$$U \beta\text{-gal} = 1000 \times [ DO_{420} - (1.75 \times DO_{550}) ] / 0.1 \times t \times DO_{600}$$

## Identification of the putative TgZFP2 RNA partners

### 1. RNA granules detection

The induction of the RNA granules formation in tachyzoites and their visualisation were described by Lirussi and Matrajt<sup>273</sup> and Gissot et al.<sup>274</sup>. The extracellular TgZFP2-HA3 tachyzoites were incubated in [K<sup>+</sup>] buffer ((pH 7.2): 142 mM KCl, 5 mM NaCl, 2 mM EGTA, 5 mM MgCl<sub>2</sub>, 25 mM Hepes-KOH, 1 mg/ml BSA) for 1 h as described, then collected and settled on poly-lysine slides. The IFAs were done as described above. The RNA granules were visualised with mouse monoclonal anti-mouse PABP antibody (Santa Cruz) at a 1/1000 dilution. The rat monoclonal anti-HA antibody (Roche) at a 1/500 dilution was used to detect TgZFP2. DNA was detected by DAPI staining.

### 2. RNA immunoprecipitation

The protocol was based on the one described by Gissot et al.<sup>274</sup>. The experiment was performed using the TgZFP2-HA3 transgenic cell line as bait and RH Tati  $\Delta$ ku80 cell line as control. All the solutions used in the experiment were prepared in RNase-free water and supplemented with RNase-OUT (Invitrogen) at a concentration of 40 U/ml.

Tachyzoites were grown for 48 h on HFF monolayers in 175 cm<sup>2</sup> flasks and the intracellular tachyzoites from 4 (RH $\Delta$ ku80 line) or 5 (TgZFP2-HA3 line) flasks were harvested for the experiment by scraping, passing thrice through 25-gauge needle and subsequent centrifugation. To separate the tachyzoites from HFF cells debris, the cell pellets were

resuspended in ice-cold TBS solution and filtered. 450 to 500 x 10<sup>6</sup> parasites were typically obtained after filtration.

The protein-RNAs complexes were cross-linked by ultra-violet radiation *in vivo*. Briefly, the parasites suspension was placed in a 150 mm Petri dish and irradiated with short UVs (254 nm) at 400 mJ/cm<sup>2</sup> in a Bio-Link 254 nm irradiator (BLX, 1184-0520). The cells were then collected, washed in PBS solution and pelleted in a 1.5 ml tube at 4°C by centrifugation.

The parasites pellets were lysed by successive freeze/thaw cycles (in liquid nitrogen and at 30°C) in 1 ml of lysis buffer (50 mM Tris-HCl pH 7,5; 0.5 mM EDTA, 150 mM NaCl; 1% triton) supplemented with a EDTA-free Protease Inhibitor Cocktail (Roche) and subsequently incubated at 4°C on a rotating wheel for 1 - 1,5 h. Following a 1/2 dilution in washing buffer (50 mM Tris-HCl pH 7.5, 0.5 mM EDTA, 150 mM NaCl and a EDTA-free Protease Inhibitor Cocktail (Roche)), samples were incubated for 4 h at 4°C with Pierce anti-HA magnetic beads (ThermoScientific Ref 88836) previously equilibrated in the same buffer (60 µl of beads per 500 x 10<sup>6</sup> parasites).

The proteins were then degraded by a Protease K treatment (Fisher, 50 µg per sample) for 1 h at 55°C. The supernatants were collected and the RNAs were eluted with 300 µl of TRIzol LS according to the manufacturer instructions.

WB analysis was performed at each step of the immunoprecipitation to control the presence of the TgZFP2 protein.

The samples collected from three independent experiments were frozen at -80°C and sent to the Pasteur Institute in Lille for RNA-seq analysis.

## **TgZFP2 recombinant protein production**

### **1. Generation of the TgZFP2-GST constructs**

In order to generate a wild type TgZFP2-GST construction (TgZFP2-GST WT), a full-length TgZFP2 cDNA fragment 1.1 kb was amplified from pUT18-TgZFP2 vector DNA using the Q5 High-Fidelity DNA Polymerase (New England BioLabs) and ML3151/ML3152 primers. The amplified fragment was subcloned in competent bacteria using TOPO TA Cloning Kit (Invitrogen) according to the manufacturer's instructions, and the TgZFP2-TOPO construct was then digested by BahHI/XhoI enzymes (New England BioLabs). The resulting DNA fragment was inserted in frame into the MCS of the pGEX-4T-3 plasmid using T4 DNA ligase (New England BioLabs) and amplified in Top10 competent bacteria.

In order to generate a zinc finger-mutated TgZFP2-GST construction (TgZFP2-GST ZFM) we used the pUPRT-TgZFP2 ZFM plasmid as a template for PCR (See Materials and Methods section in Chapter 1, Results). The resulting DNA fragment of approximately 1.1 kb was inserted by T4 ligation in frame into the MCS of the pGEX-4T-3 plasmid using BahHI/XhoI enzymes (New England BioLabs) and amplified in Top10 competent bacteria.

## **2. Recombinant proteins production**

The production of recombinant proteins was induced by 0.2 mM of IPTG in *E. coli BL21* bacteria, cultivated in liquid LB media supplemented with 100 µg/ml of ampicillin at 37°C. In summary, bacteria pre-cultures were incubated overnight and diluted to 1/5 in LB ampicillin media and incubated at vigorous shaking until the OD<sub>600</sub> reached a minimum of 1.0<sup>281</sup>. The induction of recombinant proteins production was done by 0.2mM IPTG (Sigma-Aldrich) for 1 h at 37°C. The bacteria were collected by centrifugation and the pellets were frozen at -20°C.

During the optimization of the protocol, the following conditions have been tested:

- Bacteria strains: *E. coli BL21* and *E. coli C41*
- Temperature of cultivation: 37°C and 16°C, overnight
- Culturing media: liquid LB or TB (Terrific Broth), supplemented as above
- IPTG concentrations: 0.1 mM, 0.2 mM
- Induction time: 0.5 h, 1 h, 3 h.

## **3. Recombinant proteins preparation**

The preparation of insoluble TgZFP2-GST proteins was performed according to Rebay and Fehon<sup>281</sup>. The bacteria pellets were resuspended in 10 ml of phosphate-BME buffer (supplemented with 0.5 mg/ml of lysozyme) and lysed by successive freeze/thaw cycles (5 min freeze in liquid nitrogen/rapid thaw at 65°C) followed by 3 x 20 sec sonication on ice, in presence of 6 M urea. The protein extracts were collected by centrifugation at 12000 g for 10 min at 4°C.

Urea was gradually removed by 3 sequential dialyses using Spectrum<sup>TM</sup> Spectra/Por<sup>TM</sup> Dialysis Membrane Tubing (MWCO 6-8000) against the following solutions: 1X PBS containing 3 M urea; 1X PBS containing 1 M urea; 1X PBS. Each dialysis was performed at 4°C for at least 3 h. The precipitate formed after the last dialysis was pelleted by centrifugation at 12000 g for 10 min at 4°C and the soluble part containing GST-fused TgZFP2 proteins was recovered and

subsequently incubated with hydrated glutathione agarose beads (Sigma-Aldrich) for 2 h at 4°C with rocking. The beads were collected by brief centrifugation and washed thrice in 1X PBS.

The elution of proteins was done in freshly prepared elution buffer for GST (Tris-HCl pH 8.8 supplemented with 6.25 mg/ml glutathione). The eluted proteins were kept at -20°C.

### **Zinc-binding assay**

The PAR metal-binding assay was used to assess the zinc ion presence in the TgZFP2 recombinant protein samples<sup>265,282</sup>. For the assay, the TgZFP2-GST WT and TgZFP2-GST ZFM recombinant proteins were prepared according to the protocol described above. Importantly, the initial steps of the protocol (induction of the recombinant proteins production and the proteins preparation until the first dialysis) were conducted in presence of 20  $\mu\text{M}$  of  $\text{ZnSO}_4$  and the last two dialyses were conducted in presence of 10  $\mu\text{M}$  of  $\text{ZnSO}_4$ . The recombinant proteins quantity after elution was estimated by their separation in the field of electrophoresis on the Coomassie gel compared to the known quantities of BSA. 1  $\mu\text{M}$ , 2  $\mu\text{M}$  and 3  $\mu\text{M}$  of TgZFP2-GST WT and TgZFP2-GST ZFM in reaction buffer containing 50 mM Tris-HCl pH 7 and 200 mM NaCl were used for the assay. The PAR metal chelator (Acros Organics) was added to each sample to 50  $\mu\text{M}/\text{ml}$  final concentration. After 20 min incubation, the MMTS (Acros Organics) was added to each sample and the absorbance of the samples at 500 nm was measured for 10 min.

# **DISCUSSION**

## DISCUSSION

The phylum Apicomplexa comprises species that evolved from free-living organisms into intracellular parasites and adapted typical eukaryotic traits to their lifestyle<sup>214</sup>. As such, and because of their importance as medical and veterinary pathogens, apicomplexan parasites are intensively studied. Still, our knowledge about many of their fundamental cellular processes, such as division, remains incomplete. Though the morphological events of the apicomplexan cell cycle have long been described and later regrouped in two main steps (according to the evidence gathered by functional genomics and drug-based approaches)<sup>116</sup>, the complex regulatory system underlying this process remains mostly uncharacterised. We know that the cell cycle progression in parasites should be controlled by a complex machinery, including the centrosome as the main coordinator<sup>184</sup>, the cyclin-dependent kinases regulating a number of checkpoints<sup>212</sup>, and structural elements, such as daughter cytoskeletons, that play a pivotal role in the formation of the progeny<sup>100</sup>. Nevertheless, while many proteins are likely essential for cell cycle progression, only a handful of them have seen their function elucidated at the molecular level in these parasites.

The main objective of my PhD was to explore the function of a novel *T. gondii* protein with a single putative predicted ZnF, which depletion resulted in severe division problems in tachyzoites. This protein, that we named TgZFP2, appears to be important for the coordination of nuclear and budding cycles in dividing parasites. However, despite the various approaches we applied during the study, we were unable to define the precise molecular mechanism behind the complex phenotype induced in TgZFP2 mutant parasites. The lack of information on the homologues of the protein in other organisms together with the lack of information on the molecular actors of the cell cycle progression in *T. gondii* added to the technical difficulties we encountered during the study. The hypotheses on possible roles for TgZFP2 are therefore based essentially on our localisation and phenotypic studies.

### **TgZFP2 and the centrosome**

In a very fitting way with the necessity to coordinate budding and nuclear cycles in *T. gondii*, its centrosome has been suggested to contain two core structures<sup>181</sup>. The inner core, which constitutes a spindle pole together with the mitotic spindle-holding centrocone in the dividing parasites<sup>214</sup>, appears to be in charge of the nuclear cycle by directing the mitosis. The outer core with its centrioles, in turn, is apparently responsible for the coordination of

## DISCUSSION

the budding cycle and the correct formation of daughter scaffold<sup>181</sup>. The structures are interconnected and function together with a surrounding protein matrix of dynamic composition<sup>184</sup>.

We have gathered evidence that TgZFP2 is accumulated as puncta in the peri-centrosomal region at the onset of mitosis and persists there until the completion of division. However, it does not seem to localise to the outer core, to the inner core or to the centrocone. Instead, TgZFP2 is recruited at the interface between the inner and outer cores, raising a most evident question as to whether or not the protein may be required for the maintenance of structural integrity between the centrosomal cores or for their duplication. However, it seems not to be the case because in the absence of TgZFP2 the duplication of the cores and their association remains largely unaffected.

In addition to the above, the depletion of TgZFP2 does not inhibit the function of both cores in regulating the nuclear and budding cycles. The nucleation of spindle MTs, driven by the centrosomes, seems mostly unaffected in the mutant parasites. Moreover, cycles of DNA replication seem to be properly initiated. The segregation of nuclear material into dividing mutant parasites, however, is not accurate, leading sometimes to the appearance of anucleated cells ('zoids') on the one hand, and big syncytial cells accumulating large nuclei on the other. The reason of this particular defect remains unclear, but we can put forward a few hypotheses as to how TgZFP2 may act upon the coordination between budding and mitosis.

### **Could TgZFP2 act as a regulatory factor of endodyogeny?**

Importantly, centrosomal protein complexes do not only contain molecules needed for assembly, duplication or maturation of the centrioles, they also harbour regulatory factors of cell cycle progression<sup>146,283</sup>. Thus, TgZFP2 particular positioning and timing of recruitment also make it a potential candidate for acting upon the regulation of the cell cycle.

Typically, the main actors in the regulation of cell cycle progression are specific kinases (CDKs) and their cyclin binding partners<sup>163</sup>. Once a cyclin is bound to a related CDK, it activates the enzyme and also directs it to target effectors; this, in turn, promotes progression through cell cycle checkpoints. The kinase/cyclin regulation system is conserved in *T. gondii*, even if it likely evolved to fit this eukaryote's specific mode of division<sup>214</sup>. TgZFP2-depleted parasites not only show a lack of coordination between mitosis and budding, but they look, in fact, as

## DISCUSSION

being continuously in a mitotic state. They reinitiate the amplification of their DNA content, they show a stable establishment of the mitotic spindle, they go on duplicating their centrosomal machinery, and they proceed to the formation of the next progeny before previous buds are completed. Clearly, this type of phenotype could be related to an alteration of a cyclin-dependent regulation, but unfortunately, we did not obtain any evidence of TgZFP2 interaction with kinases or cyclins.

### **TgZFP2 and the cytoskeleton**

During our studies, we assessed TgZFP2 detergent extraction properties and gathered evidence that this protein could be associated with the cytoskeleton of the parasites. Along the same line, when exposed to formaldehyde cross-linking, TgZFP2 became essentially insoluble, indicating once again a possible association with cytoskeletal elements, that would be consolidated by the cross-linking.

The centrosome is, by all means, indispensable to cytoskeletal structures as it drives both nuclear segregation (i.e. mitotic spindle) and daughter cell elongation (i.e. cortical MTs)<sup>116</sup>. Moreover, various studies have reported that disruption of the cytoskeleton is linked to a disorganised division in *T. gondii* tachyzoites<sup>127,145,151–155</sup>. Interestingly, the TgZFP2 mutant phenotype was associated with a defect in daughter cells formation and nuclear segregation without affecting the replication of DNA, quite similarly as when some drugs targeting the MT cytoskeleton are used<sup>145</sup>. However, in our case neither cortical nor spindle MTs seemed to be primarily affected by TgZFP2 depletion. Yet, preparations of cortical cytoskeletons upon detergent extraction of TgZFP2-depleted parasites have shown they were slightly shorter than in the control cell lines (data not shown). This confirms there was a problem in the later steps of budding leading to the generation of shorter buds, but does not imply TgZFP2 is acting on the MTs of the cytoskeleton. In fact, when we performed IFAs on detergent-extracted parasites, we could not detect any association of TgZFP2 with cortical MTs.

Interestingly though, in extracellular parasites and in parasites that freshly invaded host cells, TgZFP2 is found at the posterior end where the cytoskeletal structure called the 'basal complex' is located. The basal complex is important for tapering of the nascent daughter buds toward their posterior end and for completion of budding<sup>100</sup>. This could provide an interesting possibility for TgZFP2 function because in absence of the protein the elongating

## DISCUSSION

daughters' IMCs seem to close prematurely, before complete integration of the nuclear material. However, at this stage TgZFP2 is usually not found at the posterior end of developing daughters, which prevents us from clearly establishing the direct involvement of TgZFP2 in the process. The protein might be present there in undetectable amounts at this particular stage of budding, so we cannot exclude it is not one of the functions of the protein. To which extent the elongation of the IMC is playing a role in the encapsulation of DNA into forming buds is also currently unknown, but it is likely a regulated and coordinated process.

## Conclusion

Studying TgZFP2 role was rendered difficult by the absence of known functional domains and the very dynamic localisation of this protein. The complex localisation pattern of TgZFP2 hints it may have pleiotropic function at different moments of the cell cycle. Yet, our careful observations have demonstrated it gets recruited in a timely manner, at the onset of mitosis, to the peri-centrosomal region, where it is ideally positioned to act on cell division. Recent years have seen the classification of *T. gondii* centrosome-associated proteins in two functionally distinct cores, but, if anything, our data show there are important regulators that may be associated with, but not be a part of, centrosomal cores. This highlights the lack of knowledge about the centrosome-associated proteins in *T. gondii* in general. Taking into account that diverging eukaryotes, like Apicomplexa, probably had to evolve specific machineries to control their peculiar cell cycle, it is not surprising that bioinformatics analyses have shown the typical mammalian pericentriolar markers are poorly conserved in *T. gondii*<sup>181</sup>. Thus it would be particularly interesting to initiate proteomic studies to characterise the composition of *T. gondii* centrosome-associated proteins and novel cell cycle-regulating proteins, using for instance spatial proteomics approaches. Protein correlation profiling, implemented by Andersen et al. was used to characterise proteins associated with the human centrosome<sup>284,285</sup>. Interestingly, Localisation of Organelle Proteins by Isotope Tagging (LOPIT), a method well suited for the simultaneous identification of proteins associated with subcellular structures from complex biological mixtures, has been recently adapted to *T. gondii*<sup>286</sup> and will probably be very informative. Several of these proteins and regulatory factors in *T. gondii* will likely have potentially interesting and vital functions, some of which may even be leveraged for designing novel therapeutic strategies against these parasites.

## **REFERENCES**

## REFERENCES

1. Adl, S. M. *et al.* Diversity, Nomenclature, and Taxonomy of Protists. *Systematic Biology* **56**, 684–689 (2007).
2. Clamp, J. C. & Lynn, D. H. Investigating the biodiversity of ciliates in the ‘Age of Integration’. *European Journal of Protistology* **61**, 314–322 (2017).
3. Taylor, F. J. R., Hoppenrath, M. & Saldarriaga, J. F. Dinoflagellate diversity and distribution. *Biodivers Conserv* **17**, 407–418 (2008).
4. Levine, N. D. *et al.* A newly revised classification of the protozoa. *J. Protozool.* **27**, 37–58 (1980).
5. Adl, S. M. *et al.* The New Higher Level Classification of Eukaryotes with Emphasis on the Taxonomy of Protists. *J Eukaryotic Microbiology* **52**, 399–451 (2005).
6. Walker, G., Dorrell, R. G., Schlacht, A. & Dacks, J. B. Eukaryotic systematics: a user’s guide for cell biologists and parasitologists. *Parasitology* **138**, 1638–1663 (2011).
7. Aswati Subramanian. Save the Last Dance for Me. A scanning electron microscope image of *Tetrahymena thermophila*. (2009). <http://miamioh.edu/news/media/1588.jpg>
8. Borkman, D. G., Smayda, T. J., Schwarz, E. N., Flewelling, L. J. & Tomas, C. R. Recurrent vernal presence of the toxic *Alexandrium tamarense*/*Alexandrium fundyense* (Dinoflagellata) species complex in Narragansett Bay, USA. *Harmful Algae* **32**, 73–80 (2014).
9. del Carmen, M. G., Calvo, L. C. & Mondragón, R. Induction of conoid extrusion is associated to MIC secretion in *Toxoplasma gondii* tachyzoites. in *European Microscopy Congress 2016: Proceedings* (ed. European Microscopy Society) 242–243 (Wiley-VCH Verlag GmbH & Co. KGaA, 2016).
10. Adl, S. M. *et al.* The Revised Classification of Eukaryotes. *J. Eukaryot. Microbiol.* **59**, 429–514 (2012).
11. Votýpka, J., Modrý, D., Oborník, M., Šlapeta, J. & Lukeš, J. Apicomplexa. in *Handbook of the Protists* (eds. Archibald, J. M. *et al.*) 1–58 (Springer International Publishing, 2016).
12. WHO - World Malaria report 2018 (2018). <https://www.who.int/malaria/publications/world-malaria-report-2018/report/en/>

## REFERENCES

13. Shrivastava, A. K., Kumar, S., Smith, W. A. & Sahu, P. S. Revisiting the global problem of cryptosporidiosis and recommendations. *Trop Parasitol* **7**, 8–17 (2017).
14. Pumipuntu, N. & Piratae, S. Cryptosporidiosis: A zoonotic disease concern. *Vet World* **11**, 681–686 (2018).
15. Hunter, P. R. & Nichols, G. Epidemiology and Clinical Features of Cryptosporidium Infection in Immunocompromised Patients. *Clinical Microbiology Reviews* **15**, 145–154 (2002).
16. Morrison, W. I. The aetiology, pathogenesis and control of theileriosis in domestic animals. *Rev. - Off. Int. Epizoot.* **34**, 599–611 (2015).
17. Blake, D. P. & Tomley, F. M. Securing poultry production from the ever-present Eimeria challenge. *Trends in Parasitology* **30**, 12–19 (2014).
18. Shaapan, R. M. The common zoonotic protozoal diseases causing abortion. *Journal of Parasitic Diseases* **40**, 1116–1129 (2016).
19. Rathore, D. *et al.* Molecular Mechanism of Host Specificity in *Plasmodium falciparum* Infection: ROLE OF CIRCUMSPOROZOITE PROTEIN. *J. Biol. Chem.* **278**, 40905–40910 (2003).
20. Allen, P. C. & Fetterer, R. H. Recent Advances in Biology and Immunobiology of Eimeria Species and in Diagnosis and Control of Infection with These Coccidian Parasites of Poultry. *Clinical Microbiology Reviews* **15**, 58–65 (2002).
21. McAllister, M. M. *et al.* Rapid communication. *International Journal for Parasitology* **28**, 1473–1479 (1998).
22. Fayer, R. Sarcocystis spp. in Human Infections. *Clinical Microbiology Reviews* **17**, 894–902 (2004).
23. Robert-Gangneux, F. & Darde, M.-L. Epidemiology of and Diagnostic Strategies for Toxoplasmosis. *Clinical Microbiology Reviews* **25**, 264–296 (2012).
24. Dardé, M. L., Ajzenberg, D. & Smith, J. Population Structure and Epidemiology of Toxoplasma gondii. in *Toxoplasma Gondii* 49–80 (Elsevier, 2007).

## REFERENCES

25. Nicolle, C. & Manceaux, L. Sur une infection á corps de Leishman (ou organismes voisins) du gondi. 369 (1908).
26. Splendore, A. Un nuovo protozoa parassita de' conigli. incontrato nelle lesioni anatomiche d'une malattia che ricorda in molti punti il Kala-azar dell' uomo. Nota preliminare pel. 109–112.
27. Nicolle, C. & Manceaux, L. Nicolle, C., Manceaux, L., 1909. Sur un protozoaire nouveau du gondi. 369–372 (1909).
28. Dubey, J. P. The History of *Toxoplasma gondii* —The First 100 Years. *Journal of Eukaryotic Microbiology* **55**, 467–475 (2008).
29. Montoya, J. & Liesenfeld, O. Toxoplasmosis. *The Lancet* **363**, 1965–1976 (2004).
30. Pappas, G., Roussos, N. & Falagas, M. E. Toxoplasmosis snapshots: Global status of *Toxoplasma gondii* seroprevalence and implications for pregnancy and congenital toxoplasmosis. *International Journal for Parasitology* **39**, 1385–1394 (2009).
31. Howe, D. K. & Sibley, L. D. *Toxoplasma gondii* Comprises Three Clonal Lineages: Correlation of Parasite Genotype with Human Disease. *Journal of Infectious Diseases* **172**, 1561–1566 (1995).
32. Schlüter, D. *et al.* Animals are key to human toxoplasmosis. *International Journal of Medical Microbiology* **304**, 917–929 (2014).
33. Tenter AM, Heckeroth AR, Weiss LM. *Toxoplasma gondii*: from animals to humans. *Int J Parasitol*
34. Gilot-Fromont, E. *et al.* The Life Cycle of *Toxoplasma gondii* in the Natural Environment. in *Toxoplasmosis - Recent Advances* (ed. Djurkovi Djakovi, O.) (InTech, 2012).
35. Dabritz, H. A. *et al.* Detection of *Toxoplasma gondii* -like oocysts in cat feces and estimates of the environmental oocyst burden. *Journal of the American Veterinary Medical Association* **231**, 1676–1684 (2007).
36. Worth, A. R., Lymbery, A. J. & Thompson, R. C. A. Adaptive host manipulation by *Toxoplasma gondii*: fact or fiction? *Trends in Parasitology* **29**, 150–155 (2013).

## REFERENCES

37. Morrissette, N. Targeting Toxoplasma Tubules: Tubulin, Microtubules, and Associated Proteins in a Human Pathogen. *Eukaryotic Cell* **14**, 2–12 (2015).
38. Jones, J. L. & Dubey, J. P. Foodborne Toxoplasmosis. *Clinical Infectious Diseases* **55**, 845–851 (2012).
39. Morris, M. I., Fischer, S. A. & Ison, M. G. Infections Transmitted by Transplantation. *Infectious Disease Clinics of North America* **24**, 497–514 (2010).
40. Dehkordi, F. S., Haghghi Borujeni, M. R., Rahimi, E. & Abdizadeh, R. Detection of *Toxoplasma gondii* in Raw Caprine, Ovine, Buffalo, Bovine, and Camel Milk Using Cell Cultivation, Cat Bioassay, Capture ELISA, and PCR Methods in Iran. *Foodborne Pathogens and Disease* **10**, 120–125 (2013).
41. Dubey, J. P. Re-examination of resistance of *Toxoplasma gondii* tachyzoites and bradyzoites to pepsin and trypsin digestion. *Parasitology* **116 ( Pt 1)**, 43–50 (1998).
42. Koethe, M., Schade, C., Fehlhaber, K. & Ludewig, M. Survival of *Toxoplasma gondii* tachyzoites in simulated gastric fluid and cow's milk. *Veterinary Parasitology* **233**, 111–114 (2017).
43. Herwaldt, B. L. Laboratory-Acquired Parasitic Infections from Accidental Exposures. *Clinical Microbiology Reviews* **14**, 659–688 (2001).
44. Guy, E. C. & Joynson, D. H. M. Potential of the Polymerase Chain Reaction in the Diagnosis of Active *Toxoplasma* Infection by Detection of Parasite in Blood. *Journal of Infectious Diseases* **172**, 319–322 (1995).
45. Hill, D. E., Chirukandoth, S. & Dubey, J. P. Biology and epidemiology of *Toxoplasma gondii* in man and animals. *Anim Health Res Rev* **6**, 41–61 (2005).
46. Furtado, J., Smith, J., Belfort, R., Gattey, D. & Winthrop, K. Toxoplasmosis: A global threat. *Journal of Global Infectious Diseases* **3**, 281 (2011).
47. Hampton, M. M. Congenital Toxoplasmosis: A Review. *Neonatal Network* **34**, 274–278 (2015).
48. Dunn, D. *et al.* Mother-to-child transmission of toxoplasmosis: risk estimates for clinical counselling. *The Lancet* **353**, 1829–1833 (1999).

## REFERENCES

49. McAuley, J. B. Congenital Toxoplasmosis. *Journal of the Pediatric Infectious Diseases Society* **3**, S30–S35 (2014).
50. Calero-Bernal, R. & Gennari, S. M. Clinical Toxoplasmosis in Dogs and Cats: An Update. *Frontiers in Veterinary Science* **6**, 54 (2019).
51. Dubey, J. P., Lindsay, D. S. & Lappin, M. R. Toxoplasmosis and Other Intestinal Coccidial Infections in Cats and Dogs. *Veterinary Clinics of North America: Small Animal Practice* **39**, 1009–1034 (2009).
52. Cenci-Goga, B. T., Rossitto, P. V., Sechi, P., McCrindle, C. M. E. & Cullor, J. S. Toxoplasma in Animals, Food, and Humans: An Old Parasite of New Concern. *Foodborne Pathogens and Disease* **8**, 751–762 (2011).
53. Dunay, I. R., Gajurel, K., Dhakal, R., Liesenfeld, O. & Montoya, J. G. Treatment of Toxoplasmosis: Historical Perspective, Animal Models, and Current Clinical Practice. *Clinical Microbiology Reviews* **31**, (2018).
54. Benmerzouga, I. *et al.* Guanabenz Repurposed as an Antiparasitic with Activity against Acute and Latent Toxoplasmosis. *Antimicrob. Agents Chemother.* **59**, 6939–6945 (2015).
55. Vidadala, R. S. R. *et al.* Development of an Orally Available and Central Nervous System (CNS) Penetrant *Toxoplasma gondii* Calcium-Dependent Protein Kinase 1 (*Tg* CDPK1) Inhibitor with Minimal Human Ether-a-go-go-Related Gene (hERG) Activity for the Treatment of *Toxoplasmosis*. *J. Med. Chem.* **59**, 6531–6546 (2016).
56. Elmore, S. A. *et al.* *Toxoplasma gondii*: epidemiology, feline clinical aspects, and prevention. *Trends in Parasitology* **26**, 190–196 (2010).
57. Buxton, D. Toxoplasmosis: the first commercial vaccine. *Parasitol. Today (Regul. Ed.)* **9**, 335–337 (1993).
58. Hiszczyńska-Sawicka, E., Gatkowska, J. M., Grzybowski, M. M. & Długońska, H. Veterinary vaccines against toxoplasmosis. *Parasitology* **141**, 1365–1378 (2014).

## REFERENCES

59. Zhang, N.-Z., Chen, J., Wang, M., Petersen, E. & Zhu, X.-Q. Vaccines against *Toxoplasma gondii* : new developments and perspectives. *Expert Review of Vaccines* **12**, 1287–1299 (2013).
60. Kim, K. & Weiss, L. M. *Toxoplasma gondii*: the model apicomplexan. *International Journal for Parasitology* **34**, 423–432 (2004).
61. Dubey, J. P., Lindsay, D. S. & Speer, C. A. Structures of *Toxoplasma gondii* tachyzoites, bradyzoites, and sporozoites and biology and development of tissue cysts. *Clin. Microbiol. Rev.* **11**, 267–299 (1998).
62. Dubremetz, J. F. Rhoptries are major players in *Toxoplasma gondii* invasion and host cell interaction. *Cellular Microbiology* **9**, 841–848 (2007).
63. Bunnik, E. M. *et al.* Comparative 3D genome organization in apicomplexan parasites. *Proc Natl Acad Sci USA* **116**, 3183–3192 (2019).
64. Lau, Y.-L. *et al.* Deciphering the Draft Genome of *Toxoplasma gondii* RH Strain. *PLOS ONE* **11**, e0157901 (2016).
65. Khan, A. Composite genome map and recombination parameters derived from three archetypal lineages of *Toxoplasma gondii*. *Nucleic Acids Research* **33**, 2980–2992 (2005).
66. Sidik, S. M. *et al.* A Genome-wide CRISPR Screen in *Toxoplasma* Identifies Essential Apicomplexan Genes. *Cell* **166**, 1423-1435.e12 (2016).
67. Melo, E. J. L., Attias, M. & De Souza, W. The Single Mitochondrion of Tachyzoites of *Toxoplasma gondii*. *Journal of Structural Biology* **130**, 27–33 (2000).
68. Sheiner, L., Vaidya, A. B. & McFadden, G. I. The metabolic roles of the endosymbiotic organelles of *Toxoplasma* and *Plasmodium* spp. *Current Opinion in Microbiology* **16**, 452–458 (2013).
69. Seeber, F., Limenitakis, J. & Soldati-Favre, D. Apicomplexan mitochondrial metabolism: a story of gains, losses and retentions. *Trends in Parasitology* **24**, 468–478 (2008).
70. Focusing on mitochondrial form and function. *Nat Cell Biol* **20**, 735–735 (2018).
71. Seeber, F. & Steinfeldler, S. Recent advances in understanding apicomplexan parasites. *F1000Res* **5**, 1369 (2016).

## REFERENCES

72. MacRae, J. I. *et al.* Mitochondrial Metabolism of Glucose and Glutamine Is Required for Intracellular Growth of *Toxoplasma gondii*. *Cell Host & Microbe* **12**, 682–692 (2012).
73. Jacot, D., Waller, R. F., Soldati-Favre, D., MacPherson, D. A. & MacRae, J. I. Apicomplexan Energy Metabolism: Carbon Source Promiscuity and the Quiescence Hyperbole. *Trends in Parasitology* **32**, 56–70 (2016).
74. Ovcariikova, J., Lemgruber, L., Stilger, K. L., Sullivan, W. J. & Sheiner, L. Mitochondrial behaviour throughout the lytic cycle of *Toxoplasma gondii*. *Scientific Reports* **7**, 42746 (2017).
75. Sheiner, L. & Soldati-Favre, D. Protein Trafficking inside *Toxoplasma gondii*. *Traffic* **9**, 636–646 (2008).
76. Joiner, K. A. & Roos, D. S. Secretory traffic in the eukaryotic parasite *Toxoplasma gondii*: less is more. *The Journal of Cell Biology* **157**, 557–563 (2002).
77. Venugopal, K. & Marion, S. Secretory organelle trafficking in *Toxoplasma gondii*: A long story for a short travel. *International Journal of Medical Microbiology* **308**, 751–760 (2018).
78. Gubbels, M.-J. & Duraisingh, M. T. Evolution of apicomplexan secretory organelles. *International Journal for Parasitology* **42**, 1071–1081 (2012).
79. Carruthers, V. B. & Tomley, F. M. Microneme proteins in apicomplexans. *Subcell. Biochem.* **47**, 33–45 (2008).
80. Tyler, J. S., Trecek, M. & Boothroyd, J. C. Focus on the ringleader: the role of AMA1 in apicomplexan invasion and replication. *Trends in Parasitology* **27**, 410–420 (2011).
81. Fréna, K. *et al.* Myosin-dependent cell-cell communication controls synchronicity of division in acute and chronic stages of *Toxoplasma gondii*. *Nature Communications* **8**, 15710 (2017).
82. Boothroyd, J. C. & Dubremetz, J.-F. Kiss and spit: the dual roles of *Toxoplasma* rhoptries. *Nature Reviews Microbiology* **6**, 79–88 (2008).
83. Bradley, P. J. *et al.* Proteomic Analysis of Rhoptry Organelles Reveals Many Novel Constituents for Host-Parasite Interactions in *Toxoplasma gondii*. *J. Biol. Chem.* **280**, 34245–34258 (2005).

## REFERENCES

84. Mordue, D. G., Desai, N., Dustin, M. & Sibley, L. D. Invasion by *Toxoplasma gondii* establishes a moving junction that selectively excludes host cell plasma membrane proteins on the basis of their membrane anchoring. *J. Exp. Med.* **190**, 1783–1792 (1999).
85. Besteiro, S., Dubremetz, J.-F. & Lebrun, M. The moving junction of apicomplexan parasites: a key structure for invasion: The moving junction of apicomplexan parasites. *Cellular Microbiology* **13**, 797–805 (2011).
86. Mercier, C., Adjogble, K. D. Z., Däubener, W. & Delauw, M.-F.-C. Dense granules: Are they key organelles to help understand the parasitophorous vacuole of all apicomplexa parasites? *International Journal for Parasitology* **35**, 829–849 (2005).
87. McFadden, G. I. The apicoplast. *Protoplasma* **248**, 641–650 (2011).
88. Köhler, S. *et al.* A plastid of probable green algal origin in Apicomplexan parasites. *Science* **275**, 1485–1489 (1997).
89. Fichera, M. E. & Roos, D. S. A plastid organelle as a drug target in apicomplexan parasites. *Nature* **390**, 407–409 (1997).
90. Fichera, M. E., Bhopale, M. K. & Roos, D. S. In vitro assays elucidate peculiar kinetics of clindamycin action against *Toxoplasma gondii*. *Antimicrob. Agents Chemother.* **39**, 1530–1537 (1995).
91. Moore, R. B. *et al.* A photosynthetic alveolate closely related to apicomplexan parasites. *Nature* **451**, 959–963 (2008).
92. van Dooren, G. G. & Striepen, B. The Algal Past and Parasite Present of the Apicoplast. *Annual Review of Microbiology* **67**, 271–289 (2013).
93. Mazumdar, J., H. Wilson, E., Masek, K., A. Hunter, C. & Striepen, B. Apicoplast fatty acid synthesis is essential for organelle biogenesis and parasite survival in *Toxoplasma gondii*. *Proceedings of the National Academy of Sciences* **103**, 13192–13197 (2006).
94. Morrissette, N. S. & Sibley, L. D. Cytoskeleton of Apicomplexan Parasites. *Microbiology and Molecular Biology Reviews* **66**, 21–38 (2002).

## REFERENCES

95. Frénal, K., Dubremetz, J.-F., Lebrun, M. & Soldati-Favre, D. Gliding motility powers invasion and egress in Apicomplexa. *Nat Rev Micro* **15**, 645–660 (2017).
96. Dubois, D. J. & Soldati-Favre, D. Biogenesis and secretion of micronemes in *Toxoplasma gondii*. *Cellular Microbiology* e13018 (2019).
97. Porchet, E. & Torpier, G. [Freeze fracture study of *Toxoplasma* and *Sarcocystis* infective stages (author's transl)]. *Z Parasitenkd* **54**, 101–124 (1977).
98. Morrissette, N. S., Murray, J. M. & Roos, D. S. Subpellicular microtubules associate with an intramembranous particle lattice in the protozoan parasite *Toxoplasma gondii*. *J. Cell. Sci.* **110** (Pt 1), 35–42 (1997).
99. Keeley, A. & Soldati, D. The glideosome: a molecular machine powering motility and host-cell invasion by Apicomplexa. *Trends in Cell Biology* **14**, 528–532 (2004).
100. Anderson-White, B. *et al.* Cytoskeleton Assembly in *Toxoplasma gondii* Cell Division. in *International Review of Cell and Molecular Biology* **298**, 1–31 (Elsevier, 2012).
101. Mann, T. & Beckers, C. Characterization of the subpellicular network, a filamentous membrane skeletal component in the parasite *Toxoplasma gondii*. *Mol. Biochem. Parasitol.* **115**, 257–268 (2001).
102. Katris, N. J. *et al.* The Apical Complex Provides a Regulated Gateway for Secretion of Invasion Factors in *Toxoplasma*. *PLoS Pathog* **10**, e1004074 (2014).
103. Hu, K. *et al.* Cytoskeletal Components of an Invasion Machine—The Apical Complex of *Toxoplasma gondii*. *PLoS Pathogens* **2**, e13 (2006).
104. Hu, K., Roos, D. S. & Murray, J. M. A novel polymer of tubulin forms the conoid of *Toxoplasma gondii*. *The Journal of Cell Biology* **156**, 1039–1050 (2002).
105. Mondragon, R. & Frixione, E. Ca<sup>2+</sup>-dependence of conoid extrusion in *Toxoplasma gondii* tachyzoites. *J. Eukaryot. Microbiol.* **43**, 120–127 (1996).
106. Graindorge, A. *et al.* The Conoid Associated Motor MyoH Is Indispensable for *Toxoplasma gondii* Entry and Exit from Host Cells. *PLOS Pathogens* **12**, e1005388 (2016).

## REFERENCES

107. Santos, J. M., Lebrun, M., Daher, W., Soldati, D. & Dubremetz, J.-F. Apicomplexan cytoskeleton and motors: Key regulators in morphogenesis, cell division, transport and motility. *International Journal for Parasitology* **39**, 153–162 (2009).
108. Black, M. W. & Boothroyd, J. C. Lytic Cycle of *Toxoplasma gondii*. *Microbiology and Molecular Biology Reviews* **64**, 607–623 (2000).
109. Blader, I. J., Coleman, B. I., Chen, C.-T. & Gubbels, M.-J. Lytic Cycle of *Toxoplasma gondii* : 15 Years Later. *Annual Review of Microbiology* **69**, 463–485 (2015).
110. Hoff, E. F. & Carruthers, V. B. Is *Toxoplasma* egress the first step in invasion? *Trends in Parasitology* **18**, 251–255 (2002).
111. Moudy, R., Manning, T. J. & Beckers, C. J. The Loss of Cytoplasmic Potassium upon Host Cell Breakdown Triggers Egress of *Toxoplasma gondii*. *J. Biol. Chem.* **276**, 41492–41501 (2001).
112. Roiko, M. S., Svezhova, N. & Carruthers, V. B. Acidification Activates *Toxoplasma gondii* Motility and Egress by Enhancing Protein Secretion and Cytolytic Activity. *PLoS Pathog* **10**, e1004488 (2014).
113. Kafsack, B. F. C. *et al.* Rapid Membrane Disruption by a Perforin-Like Protein Facilitates Parasite Exit from Host Cells. *Science* **323**, 530–533 (2009).
114. Caldas, L. & de Souza, W. A Window to *Toxoplasma gondii* Egress. *Pathogens* **7**, 69 (2018).
115. Clough, B. & Frickel, E.-M. The *Toxoplasma* Parasitophorous Vacuole: An Evolving Host–Parasite Frontier. *Trends in Parasitology* **33**, 473–488 (2017).
116. Francia, M. E. & Striepen, B. Cell division in apicomplexan parasites. *Nature Reviews Microbiology* **12**, 125–136 (2014).
117. Striepen, B., Jordan, C. N., Reiff, S. & van Dooren, G. G. Building the Perfect Parasite: Cell Division in Apicomplexa. *PLoS Pathogens* **3**, e78 (2007).
118. Radke, J. R. *et al.* Defining the cell cycle for the tachyzoite stage of *Toxoplasma gondii*. *Mol. Biochem. Parasitol.* **115**, 165–175 (2001).

## REFERENCES

119. Gould, S. B. *et al.* Ciliate Pellicular Proteome Identifies Novel Protein Families with Characteristic Repeat Motifs That Are Common to Alveolates. *Molecular Biology and Evolution* **28**, 1319–1331 (2011).
120. Frankel, J. Chapter 2 Cell Biology of *Tetrahymena thermophila*. in *Methods in Cell Biology* **62**, 27–125 (Elsevier, 1999).
121. Lee, R. E. & Kugrens, P. Relationship between the flagellates and the ciliates. *Microbiol. Rev.* **56**, 529–542 (1992).
122. Hackett, J. D., Anderson, D. M., Erdner, D. L. & Bhattacharya, D. Dinoflagellates: a remarkable evolutionary experiment. *Am. J. Bot.* **91**, 1523–1534 (2004).
123. Allen, R. D. Fine structure of membranous and microfibrillar systems in the cortex of *Paramecium caudatum*. *J. Cell Biol.* **49**, 1–20 (1971).
124. Kono, M., Prusty, D., Parkinson, J. & Gilberger, T. W. The apicomplexan inner membrane complex. *Front Biosci (Landmark Ed)* **18**, 982–992 (2013).
125. Dubremetz, J. F. & Torpier, G. Freeze fracture study of the pellicle of an eimerian sporozoite (Protozoa, Coccidia). *J. Ultrastruct. Res.* **62**, 94–109 (1978).
126. Harding, C. R. & Meissner, M. The inner membrane complex through development of *Toxoplasma gondii* and *Plasmodium*: The IMC in *Plasmodium* and *Toxoplasma*. *Cell Microbiol* **16**, 632–641 (2014).
127. Beck, J. R. *et al.* A novel family of *Toxoplasma* IMC proteins displays a hierarchical organization and functions in coordinating parasite division. *PLoS Pathog.* **6**, e1001094 (2010).
128. Anderson-White, B. R. *et al.* A family of intermediate filament-like proteins is sequentially assembled into the cytoskeleton of *Toxoplasma gondii*: IMC proteins in *Toxoplasma* cell division. *Cellular Microbiology* **13**, 18–31 (2011).
129. Tilley, L. D., Krishnamurthy, S., Westwood, N. J. & Ward, G. E. Identification of TgCBAP, a Novel Cytoskeletal Protein that Localizes to Three Distinct Subcompartments of the *Toxoplasma gondii* Pellicle. *PLoS ONE* **9**, e98492 (2014).

## REFERENCES

130. Lentini, G. *et al.* Identification and characterization of *Toxoplasma* SIP, a conserved apicomplexan cytoskeleton protein involved in maintaining the shape, motility and virulence of the parasite: Cytoskeleton protein associated with the IMC edges. *Cellular Microbiology* **17**, 62–78 (2015).
131. Chen, A. L. *et al.* Novel Components of the Toxoplasma Inner Membrane Complex Revealed by BioID. *mBio* **6**, (2015).
132. Chen, A. L. *et al.* Novel insights into the composition and function of the *Toxoplasma* IMC sutures: IMC sutures composition and function. *Cellular Microbiology* **19**, e12678 (2017).
133. Gaskins, E. *et al.* Identification of the membrane receptor of a class XIV myosin in *Toxoplasma gondii*. *The Journal of Cell Biology* **165**, 383–393 (2004).
134. Dobrowolski, J. M., Carruthers, V. B. & Sibley, L. D. Participation of myosin in gliding motility and host cell invasion by *Toxoplasma gondii*. *Mol. Microbiol.* **26**, 163–173 (1997).
135. Fung, C., Beck, J. R., Robertson, S. D., Gubbels, M.-J. & Bradley, P. J. Toxoplasma ISP4 is a central IMC Sub-compartment Protein whose localization depends on palmitoylation but not myristoylation. *Molecular and Biochemical Parasitology* **184**, 99–108 (2012).
136. FrénaI, K. *et al.* Functional Dissection of the Apicomplexan Glideosome Molecular Architecture. *Cell Host & Microbe* **8**, 343–357 (2010).
137. FrénaI, K., Marq, J.-B., Jacot, D., Polonais, V. & Soldati-Favre, D. Plasticity between MyoC- and MyoA-Glideosomes: An Example of Functional Compensation in *Toxoplasma gondii* Invasion. *PLoS Pathogens* **10**, e1004504 (2014).
138. Lemgruber, L., Kloetzel, J. A., Souza, W. de & Vommoro, R. C. *Toxoplasma gondii*: further studies on the subpellicular network. *Mem. Inst. Oswaldo Cruz* **104**, 706–709 (2009).
139. Gubbels, M.-J., Wieffer, M. & Striepen, B. Fluorescent protein tagging in *Toxoplasma gondii*: identification of a novel inner membrane complex component conserved among Apicomplexa. *Molecular and Biochemical Parasitology* **137**, 99–110 (2004).

## REFERENCES

140. Gould, S. B., Tham, W.-H., Cowman, A. F., McFadden, G. I. & Waller, R. F. Alveolins, a New Family of Cortical Proteins that Define the Protist Infrakingdom Alveolata. *Molecular Biology and Evolution* **25**, 1219–1230 (2008).
141. Bullen, H. E. *et al.* A Novel Family of Apicomplexan Glideosome-associated Proteins with an Inner Membrane-anchoring Role. *Journal of Biological Chemistry* **284**, 25353–25363 (2009).
142. Harding, C. R. *et al.* Alveolar proteins stabilize cortical microtubules in *Toxoplasma gondii*. *Nature Communications* **10**, (2019).
143. Boucher, L. E. & Bosch, J. The apicomplexan glideosome and adhesins – Structures and function. *Journal of Structural Biology* **190**, 93–114 (2015).
144. Gilk, S. D. *et al.* Identification of PHIL1, a Novel Cytoskeletal Protein of the *Toxoplasma gondii* Pellicle, through Photosensitized Labeling with 5-[<sup>125</sup>I]Iodonaphthalene-1-Azide. *Eukaryotic Cell* **5**, 1622–1634 (2006).
145. Morrissette, N. S. & Sibley, L. D. Disruption of microtubules uncouples budding and nuclear division in *Toxoplasma gondii*. *J. Cell. Sci.* **115**, 1017–1025 (2002).
146. Morlon-Guyot, J., Francia, M. E., Dubremetz, J.-F. & Daher, W. Towards a molecular architecture of the centrosome in *Toxoplasma gondii*. *Cytoskeleton* **74**, 55–71 (2017).
147. Ma, C. *et al.* Secondary mutations correct fitness defects in *Toxoplasma gondii* with dinitroaniline resistance mutations. *Genetics* **180**, 845–856 (2008).
148. Liu, J. *et al.* An ensemble of specifically targeted proteins stabilizes cortical microtubules in the human parasite *Toxoplasma gondii*. *Molecular Biology of the Cell* **27**, 549–571 (2016).
149. Tran, J. Q., Li, C., Chyan, A., Chung, L. & Morrissette, N. S. SPM1 Stabilizes Subpellicular Microtubules in *Toxoplasma gondii*. *Eukaryotic Cell* **11**, 206–216 (2012).
150. Liu, J. *et al.* Novel Thioredoxin-Like Proteins Are Components of a Protein Complex Coating the Cortical Microtubules of *Toxoplasma gondii*. *Eukaryotic Cell* **12**, 1588–1599 (2013).

## REFERENCES

151. Shaw, M. K., Compton, H. L., Roos, D. S. & Tilney, L. G. Microtubules, but not actin filaments, drive daughter cell budding and cell division in *Toxoplasma gondii*. *J. Cell. Sci.* **113 ( Pt 7)**, 1241–1254 (2000).
152. Barkhuff, W. D. *et al.* Targeted Disruption of TgPHL1 in *Toxoplasma gondii* Results in Altered Parasite Morphology and Fitness. *PLoS ONE* **6**, e23977 (2011).
153. Stokkermans, T. J. W. *et al.* Inhibition of *Toxoplasma gondii* Replication by Dinitroaniline Herbicides. *Experimental Parasitology* **84**, 355–370 (1996).
154. Morrissette, N. S., Mitra, A., Sept, D. & Sibley, L. D. Dinitroanilines Bind  $\alpha$ -Tubulin to Disrupt Microtubules. *MBoC* **15**, 1960–1968 (2004).
155. Dubey, R. *et al.* Differential Roles for Inner Membrane Complex Proteins across *Toxoplasma gondii* and *Sarcocystis neurona* Development. *mSphere* **2**, (2017).
156. Nishi, M., Hu, K., Murray, J. M. & Roos, D. S. Organellar dynamics during the cell cycle of *Toxoplasma gondii*. *Journal of Cell Science* **121**, 1559–1568 (2008).
157. Ouologuem, D. T. & Roos, D. S. Dynamics of the *Toxoplasma gondii* inner membrane complex. *Journal of Cell Science* **127**, 3320–3330 (2014).
158. Agop-Nersesian, C. *et al.* Rab11A-Controlled Assembly of the Inner Membrane Complex Is Required for Completion of Apicomplexan Cytokinesis. *PLoS Pathogens* **5**, e1000270 (2009).
159. Agop-Nersesian, C. *et al.* Biogenesis of the Inner Membrane Complex Is Dependent on Vesicular Transport by the Alveolate Specific GTPase Rab11B. *PLoS Pathogens* **6**, e1001029 (2010).
160. Hu, K. *et al.* Daughter Cell Assembly in the Protozoan Parasite *Toxoplasma gondii*. *MBoC* **13**, 593–606 (2002).
161. Gubbels, M.-J. A MORN-repeat protein is a dynamic component of the *Toxoplasma gondii* cell division apparatus. *Journal of Cell Science* **119**, 2236–2245 (2006).
162. Schafer, K. A. The Cell Cycle: A Review. *Vet Pathol* **35**, 461–478 (1998).
163. Barnum, K. J. & O’Connell, M. J. Cell Cycle Regulation by Checkpoints. in *Cell Cycle Control* (eds. Noguchi, E. & Gadaleta, M. C.) **1170**, 29–40 (Springer New York, 2014).

## REFERENCES

164. Tessema, M., Lehmann, U. & Kreipe, H. Cell cycle and no end. *Virchows Archiv* **444**, 313–323 (2004).
165. McIntosh, J. R. Mitosis. *Cold Spring Harb Perspect Biol* **8**, a023218 (2016).
166. O'Connor, C. Mitosis and Cell division. 188 (2008).
167. Guertin, D. A., Trautmann, S. & McCollum, D. Cytokinesis in Eukaryotes. *Microbiology and Molecular Biology Reviews* **66**, 155–178 (2002).
168. Mohammad, K., Dakik, P., Medkour, Y., Mitrofanova, D. & Titorenko, V. I. Quiescence Entry, Maintenance, and Exit in Adult Stem Cells. *IJMS* **20**, 2158 (2019).
169. Virtual Genetics Education Centre. The Cell Cycle, Mitosis and Meiosis.  
<https://www2.le.ac.uk/projects/vgec/highereducation/topics/cellcycle-mitosis-meiosis>
170. Gubbels, M.-J., White, M. & Szatanek, T. The cell cycle and *Toxoplasma gondii* cell division: Tightly knit or loosely stitched? *International Journal for Parasitology* **38**, 1343–1358 (2008).
171. Gerald, N., Mahajan, B. & Kumar, S. Mitosis in the Human Malaria Parasite *Plasmodium falciparum*. *Eukaryotic Cell* **10**, 474–482 (2011).
172. Speer, C. A. & Dubey, J. P. Ultrastructural differentiation of *Toxoplasma gondii* schizonts (types B to E) and gamonts in the intestines of cats fed bradyzoites. *International Journal for Parasitology* **35**, 193–206 (2005).
173. Goldman, M., Carver, R. K. & Sulzer, A. J. Reproduction of *Toxoplasma gondii* by internal budding. *J. Parasitol.* **44**, 161–171 (1958).
174. Ogino, N. & Yoneda, C. The Fine Structure and Mode of Division of *Toxoplasma gondii*. *Archives of Ophthalmology* **75**, 218–227 (1966).
175. Sheffield, H. G. & Melton, M. L. The Fine Structure and Reproduction of *Toxoplasma gondii*. *The Journal of Parasitology* **54**, 209 (1968).
176. Arnot, D. E. & Gull, K. The *Plasmodium* cell-cycle: facts and questions. *Ann Trop Med Parasitol* **92**, 361–365 (1998).

## REFERENCES

177. Strout, R. G. & Ouellette, C. A. Schizogony and gametogony of *Eimeria tenella* in cell cultures. *Am. J. Vet. Res.* **31**, 911–918 (1970).
178. Read, M., Sherwin, T., Holloway, S. P., Gull, K. & Hyde, J. E. Microtubular organization visualized by immunofluorescence microscopy during erythrocytic schizogony in *Plasmodium falciparum* and investigation of post-translational modifications of parasite tubulin. *Parasitology* **106 (Pt 3)**, 223–232 (1993).
179. Vaishnava, S. Plastid segregation and cell division in the apicomplexan parasite *Sarcocystis neurona*. *Journal of Cell Science* **118**, 3397–3407 (2005).
180. Dobbelaere, D. A. & Küenzi, P. The strategies of the *Theileria* parasite: a new twist in host–pathogen interactions. *Current Opinion in Immunology* **16**, 524–530 (2004).
181. Suvorova, E. S., Francia, M., Striepen, B. & White, M. W. A Novel Bipartite Centrosome Coordinates the Apicomplexan Cell Cycle. *PLOS Biology* **13**, e1002093 (2015).
182. Irvin, A. D., Ocamo, J. G. R. & Spooner, P. R. Cycle of bovine lymphoblastoid cells parasitised by *Theileria parva*. *Research in Veterinary Science* **33**, 298–304 (1982).
183. Arnot, D. E., Ronander, E. & Bengtsson, D. C. The progression of the intra-erythrocytic cell cycle of *Plasmodium falciparum* and the role of the centriolar plaques in asynchronous mitotic division during schizogony. *International Journal for Parasitology* **41**, 71–80 (2011).
184. Chen, C.-T. & Gubbels, M.-J. Apicomplexan cell cycle flexibility: centrosome controls the clutch. *Trends in Parasitology* **31**, 229–230 (2015).
185. Radke, J. R. & White, M. W. A cell cycle model for the tachyzoite of *Toxoplasma gondii* using the Herpes simplex virus thymidine kinase. *Mol. Biochem. Parasitol.* **94**, 237–247 (1998).
186. Kim, K. The Epigenome, Cell Cycle, and Development in *Toxoplasma*. *Annual Review of Microbiology* **72**, 479–499 (2018).
187. Monda, J. K. & Cheeseman, I. M. The kinetochore–microtubule interface at a glance. *Journal of Cell Science* **131**, jcs214577 (2018).

## REFERENCES

188. Vertii, A., Hehnlly, H. & Doxsey, S. The Centrosome, a Multitalented Renaissance Organelle. *Cold Spring Harb Perspect Biol* **8**, a025049 (2016).
189. Huang, Z. *et al.* MiCroKiTS 4.0: a database of midbody, centrosome, kinetochore, telomere and spindle. *Nucleic Acids Research* **43**, D328–D334 (2015).
190. Dubremetz, J. F. [Genesis of merozoites in the coccidia, *Eimeria necatrix*. Ultrastructural study]. *J. Protozool.* **22**, 71–84 (1975).
191. Chen, C.-T. *et al.* Compartmentalized *Toxoplasma* EB1 bundles spindle microtubules to secure accurate chromosome segregation. *Molecular Biology of the Cell* **26**, 4562–4576 (2015).
192. Brooks, C. F. *et al.* *Toxoplasma gondii* sequesters centromeres to a specific nuclear region throughout the cell cycle. *Proceedings of the National Academy of Sciences* **108**, 3767–3772 (2011).
193. Farrell, M. & Gubbels, M.-J. The *Toxoplasma gondii* kinetochore is required for centrosome association with the centrocone (spindle pole): *Toxoplasma* Nuf2 essential for nuclear partitioning. *Cellular Microbiology* **16**, 78–94 (2014).
194. Pelletier, L. *et al.* Golgi biogenesis in *Toxoplasma gondii*. *Nature* **418**, 548–552 (2002).
195. Hartmann, J. *et al.* Golgi and centrosome cycles in *Toxoplasma gondii*. *Molecular and Biochemical Parasitology* **145**, 125–127 (2006).
196. Striepen, B. *et al.* The plastid of *Toxoplasma gondii* is divided by association with the centrosomes. *J. Cell Biol.* **151**, 1423–1434 (2000).
197. Jacot, D., Daher, W. & Soldati-Favre, D. *Toxoplasma gondii* myosin F, an essential motor for centrosomes positioning and apicoplast inheritance. *The EMBO Journal* **32**, 1702–1716 (2013).
198. Chen, C.-T. & Gubbels, M.-J. TgCep250 is dynamically processed through the division cycle and essential for structural integrity of the *Toxoplasma* centrosome. *MBoC* **30** (10), 1129-1244 (2019).
199. Francia, M. E. *et al.* Cell Division in Apicomplexan Parasites Is Organized by a Homolog of the Striated Rootlet Fiber of Algal Flagella. *PLoS Biology* **10**, e1001444 (2012).

## REFERENCES

200. Seeber, F., Feagin, J. E. & Parsons, M. The Apicoplast and Mitochondrion of *Toxoplasma gondii*. in *Toxoplasma Gondii* 297–350 (Elsevier, 2014).
201. Attias, M., Miranda, K. & De Souza, W. Development and fate of the residual body of *Toxoplasma gondii*. *Experimental Parasitology* **196**, 1–11 (2019).
202. Muñiz-Hernández, S. *et al.* Contribution of the Residual Body in the Spatial Organization of *Toxoplasma gondii* Tachyzoites within the Parasitophorous Vacuole. *Journal of Biomedicine and Biotechnology* **2011**, 1–11 (2011).
203. Behnke, M. S. *et al.* Coordinated Progression through Two Subtranscriptomes Underlies the Tachyzoite Cycle of *Toxoplasma gondii*. *PLoS ONE* **5**, e12354 (2010).
204. Butler, C. L. *et al.* Identifying Novel Cell Cycle Proteins in Apicomplexa Parasites through Co-Expression Decision Analysis. *PLoS ONE* **9**, e97625 (2014).
205. Harashima, H., Dissmeyer, N. & Schnittger, A. Cell cycle control across the eukaryotic kingdom. *Trends in Cell Biology* **23**, 345–356 (2013).
206. Vleugel, M., Hoogendoorn, E., Snel, B. & Kops, G. J. P. L. Evolution and Function of the Mitotic Checkpoint. *Developmental Cell* **23**, 239–250 (2012).
207. Morgan, D. O. Cyclin-dependent kinases: engines, clocks, and microprocessors. *Annu. Rev. Cell Dev. Biol.* **13**, 261–291 (1997).
208. Hochegger, H., Takeda, S. & Hunt, T. Cyclin-dependent kinases and cell-cycle transitions: does one fit all? *Nat Rev Mol Cell Biol* **9**, 910–916 (2008).
209. Malumbres, M. & Barbacid, M. Mammalian cyclin-dependent kinases. *Trends in Biochemical Sciences* **30**, 630–641 (2005).
210. Gubbels, M.-J. *et al.* Forward Genetic Analysis of the Apicomplexan Cell Division Cycle in *Toxoplasma gondii*. *PLoS Pathogens* **4**, e36 (2008).
211. Nurse, P. Cyclin dependent kinases and cell cycle control (nobel lecture). *ChemBiochem* **3**, 596–603 (2002).

## REFERENCES

212. Alvarez, C. A. & Suvorova, E. S. Checkpoints of apicomplexan cell division identified in *Toxoplasma gondii*. *PLOS Pathogens* **13**, e1006483 (2017).
213. Santamaría, D. *et al.* Cdk1 is sufficient to drive the mammalian cell cycle. *Nature* **448**, 811–815 (2007).
214. White, M. W. & Suvorova, E. S. Apicomplexa Cell Cycles: Something Old, Borrowed, Lost, and New. *Trends in Parasitology* **34**, 759–771 (2018).
215. Naumov, A. *et al.* The *Toxoplasma* Centrocone Houses Cell Cycle Regulatory Factors. *mBio* **8**, (2017).
216. Bornens, M. The Centrosome in Cells and Organisms. *Science* **335**, 422–426 (2012).
217. Conduit, P. T., Wainman, A. & Raff, J. W. Centrosome function and assembly in animal cells. *Nature Reviews Molecular Cell Biology* **16**, 611 (2015).
218. Winey, M. & O’Toole, E. Centriole structure. *Philosophical Transactions of the Royal Society B: Biological Sciences* **369**, 20130457–20130457 (2014).
219. Teixido-Travesa, N., Roig, J. & Luders, J. The where, when and how of microtubule nucleation - one ring to rule them all. *Journal of Cell Science* **125**, 4445–4456 (2012).
220. Gönczy, P. Towards a molecular architecture of centriole assembly. *Nature Reviews Molecular Cell Biology* **13**, 425 (2012).
221. Morrissette, N. Targeting *Toxoplasma* Tubules: Tubulin, Microtubules, and Associated Proteins in a Human Pathogen. *Eukaryotic Cell* **14**, 2–12 (2015).
222. Dubremetz, J. F. [Ultrastructural study of schizogonic mitosis in the coccidian, *Eimeria necatrix* (Johnson 1930)]. *J. Ultrastruct. Res.* **42**, 354–376 (1973).
223. Hirono, M. Cartwheel assembly. *Philosophical Transactions of the Royal Society B: Biological Sciences* **369**, 20130458–20130458 (2014).
224. Willems, E. *et al.* The functional diversity of Aurora kinases: a comprehensive review. *Cell Div* **13**, 7 (2018).

## REFERENCES

225. Kumar, A., Rajendran, V., Sethumadhavan, R. & Purohit, R. CEP proteins: the knights of centrosome dynasty. *Protoplasma* **250**, 965–983 (2013).
226. Courjol, F. & Gissot, M. A coiled-coil protein is required for coordination of karyokinesis and cytokinesis in *Toxoplasma gondii*. *Cellular Microbiology* e12832 (2018). doi:10.1111/cmi.12832
227. El Bissati, K. *et al.* *Toxoplasma gondii* Arginine Methyltransferase 1 (PRMT1) Is Necessary for Centrosome Dynamics during Tachyzoite Cell Division. *mBio* **7**, (2016).
228. Fu, J., Hagan, I. M. & Glover, D. M. The Centrosome and Its Duplication Cycle. *Cold Spring Harbor Perspectives in Biology* **7**, a015800 (2015).
229. Moyer, T. C., Clutario, K. M., Lambrus, B. G., Daggubati, V. & Holland, A. J. Binding of STIL to Plk4 activates kinase activity to promote centriole assembly. *The Journal of Cell Biology* **209**, 863–878 (2015).
230. Chen, C.-T. & Gubbels, M.-J. The *Toxoplasma gondii* centrosome is the platform for internal daughter budding as revealed by a Nek1 kinase mutant. *Journal of Cell Science* **126**, 3344–3355 (2013).
231. Berry, L. *et al.* The conserved apicomplexan Aurora kinase TgArk3 is involved in endodyogeny, duplication rate and parasite virulence: Apicomplexan Aurora kinases. *Cellular Microbiology* **18**, 1106–1120 (2016).
232. Morlon-Guyot, J. *et al.* The *Toxoplasma gondii* calcium-dependent protein kinase 7 is involved in early steps of parasite division and is crucial for parasite survival: Functional dissection of *T. gondii* CDPK7 protein. *Cell Microbiol* **16**, 95–114 (2014).
233. Klug, A. The Discovery of Zinc Fingers and Their Applications in Gene Regulation and Genome Manipulation. *Annual Review of Biochemistry* **79**, 213–231 (2010).
234. Isalan, M. Zinc Fingers. in *Encyclopedia of Biological Chemistry* 575–579 (Elsevier, 2013).
235. Cassandri, M. *et al.* Zinc-finger proteins in health and disease. *Cell Death Discovery* **3**, 17071 (2017).

## REFERENCES

236. Gamsjaeger, R., Liew, C., Loughlin, F., Crossley, M. & Mackay, J. Sticky fingers: zinc-fingers as protein-recognition motifs. *Trends in Biochemical Sciences* **32**, 63–70 (2007).
237. Miller, J., McLachlan, A. D. & Klug, A. Repetitive zinc-binding domains in the protein transcription factor IIIA from *Xenopus* oocytes. *EMBO J.* **4**, 1609–1614 (1985).
238. Wolfe, S. A., Nekludova, L. & Pabo, C. O. DNA Recognition by Cys<sub>2</sub> His<sub>2</sub> Zinc Finger Proteins. *Annual Review of Biophysics and Biomolecular Structure* **29**, 183–212 (2000).
239. Hall, T. M. T. Multiple modes of RNA recognition by zinc finger proteins. *Current Opinion in Structural Biology* **15**, 367–373 (2005).
240. Laity, J. H., Lee, B. M. & Wright, P. E. Zinc finger proteins: new insights into structural and functional diversity. *Curr. Opin. Struct. Biol.* **11**, 39–46 (2001).
241. Stenmark, H. & Aasland, R. FYVE-finger proteins--effectors of an inositol lipid. *J. Cell. Sci.* **112** (Pt 23), 4175–4183 (1999).
242. Mackay, J. P. & Crossley, M. Zinc fingers are sticking together. *Trends Biochem. Sci.* **23**, 1–4 (1998).
243. Mattsson, J. G. & Soldati, D. MPS1: a small, evolutionarily conserved zinc finger protein from the protozoan *Toxoplasma gondii*. *FEMS Microbiology Letters* **180**, 235–239 (1999).
244. Fernandez-Pol, J. A., Klos, D. J. & Hamilton, P. D. A growth factor-inducible gene encodes a novel nuclear protein with zinc finger structure. *J. Biol. Chem.* **268**, 21198–21204 (1993).
245. Vanchinathan, P., Brewer, J. L., Harb, O. S., Boothroyd, J. C. & Singh, U. Disruption of a Locus Encoding a Nucleolar Zinc Finger Protein Decreases Tachyzoite-to-Bradyzoite Differentiation in *Toxoplasma gondii*. *Infection and Immunity* **73**, 6680–6688 (2005).
246. Daher, W. *et al.* Lipid kinases are essential for apicoplast homeostasis in *Toxoplasma gondii*: Phosphoinositide function in apicoplast biology. *Cellular Microbiology* **17**, 559–578 (2015).
247. Gissot, M. *et al.* An evolutionary conserved zinc finger protein is involved in *Toxoplasma gondii* mRNA nuclear export: A zinc finger protein is involved in mRNA nuclear export. *Cellular Microbiology* **19**, e12644 (2017).

## REFERENCES

248. Xie, P. TRAF molecules in cell signaling and in human diseases. *Journal of Molecular Signaling* **8**, 7 (2013).
249. Lévêque, M. F. *et al.* Autophagy-Related Protein ATG8 Has a Noncanonical Function for Apicoplast Inheritance in *Toxoplasma gondii*. *mBio* **6**, e01446-15 (2015).
250. Routsias, J. G. & Tzioufas, A. G. Autoimmune response and target autoantigens in Sjogren's syndrome: AUTOIMMUNE RESPONSE IN SJOGREN'S SYNDROME. *European Journal of Clinical Investigation* **40**, 1026–1036 (2010).
251. Mavragani, C. P. & Moutsopoulos, H. M. Sjögren's Syndrome. *Annual Review of Pathology: Mechanisms of Disease* **9**, 273–285 (2014).
252. Muro, Yamada, Himeno & Sugimoto. cDNA cloning of a novel autoantigen targeted by a minor subset of anti-centromere antibodies. *Clinical and Experimental Immunology* **111**, 372–376 (1998).
253. Tuffanelli, D. L. Anticentromere and Anticentriole Antibodies in the Scleroderma Spectrum. *Arch Dermatol* **119**, 560 (1983).
254. Lévêque, M. F., Berry, L. & Besteiro, S. An evolutionarily conserved SSNA1/DIP13 homologue is a component of both basal and apical complexes of *Toxoplasma gondii*. *Sci Rep* **6**, 27809 (2016).
255. Huynh, M.-H. & Carruthers, V. B. Tagging of Endogenous Genes in a *Toxoplasma gondii* Strain Lacking Ku80. *Eukaryotic Cell* **8**, 530–539 (2009).
256. Kim, Y. E., Hipp, M. S., Bracher, A., Hayer-Hartl, M. & Ulrich Hartl, F. Molecular Chaperone Functions in Protein Folding and Proteostasis. *Annu. Rev. Biochem.* **82**, 323–355 (2013).
257. Yam, A. Y. *et al.* Defining the TRiC/CCT interactome links chaperonin function to stabilization of newly made proteins with complex topologies. *Nature Structural & Molecular Biology* **15**, 1255–1262 (2008).
258. Vallin, J. & Grantham, J. The role of the molecular chaperone CCT in protein folding and mediation of cytoskeleton-associated processes: implications for cancer cell biology. *Cell Stress and Chaperones* **24**, 17–27 (2019).

## REFERENCES

259. Brackley, K. I. & Grantham, J. Activities of the chaperonin containing TCP-1 (CCT): implications for cell cycle progression and cytoskeletal organisation. *Cell Stress and Chaperones* **14**, 23–31 (2009).
260. Leitner, A. *et al.* The Molecular Architecture of the Eukaryotic Chaperonin TRiC/CCT. *Structure* **20**, 814–825 (2012).
261. Karimova, G., Pidoux, J., Ullmann, A. & Ladant, D. A bacterial two-hybrid system based on a reconstituted signal transduction pathway. *Proceedings of the National Academy of Sciences* **95**, 5752–5756 (1998).
262. Battesti, A. & Bouveret, E. The bacterial two-hybrid system based on adenylate cyclase reconstitution in *Escherichia coli*. *Methods* **58**, 325–334 (2012).
263. Gräslund, S. *et al.* Protein production and purification. *Nature Methods* **5**, 135–146 (2008).
264. García-Fruitós, E. Inclusion bodies: a new concept. *Microb Cell Fact* **9**, 80 (2010).
265. Hunt, J. B., Neece, S. H. & Ginsburg, A. The use of 4-(2-pyridylazo) resorcinol in studies of zinc release from *Escherichia coli* aspartate transcarbamoylase. *Analytical Biochemistry* **146**, 150–157 (1985).
266. Font, J. & Mackay, J. P. Beyond DNA: Zinc Finger Domains as RNA-Binding Modules. in *Engineered Zinc Finger Proteins* (eds. Mackay, J. P. & Segal, D. J.) **649**, 479–491 (Humana Press, 2010).
267. Darby, M. K. RNA Binding by Single Zinc Fingers. in *Zinc Finger Proteins* (eds. Iuchi, S. & Kuldell, N.) 66–75 (Springer US, 2005).
268. Plambeck, C. A. *et al.* The Structure of the Zinc Finger Domain from Human Splicing Factor ZNF265 Fold. *Journal of Biological Chemistry* **278**, 22805–22811 (2003).
269. Anderson, P. & Kedersha, N. RNA granules: post-transcriptional and epigenetic modulators of gene expression. *Nature Reviews Molecular Cell Biology* **10**, 430–436 (2009).
270. Anderson, P. & Kedersha, N. RNA granules. *J Cell Biol* **172**, 803–808 (2006).

## REFERENCES

271. Thomas, M. G., Loschi, M., Desbats, M. A. & Boccaccio, G. L. RNA granules: The good, the bad and the ugly. *Cellular Signalling* **23**, 324–334 (2011).
272. Protter, D. S. W. & Parker, R. Principles and Properties of Stress Granules. *Trends in Cell Biology* **26**, 668–679 (2016).
273. Lirussi, D. & Matrajt, M. RNA granules present only in extracellular toxoplasma gondii increase parasite viability. *Int. J. Biol. Sci.* **7**, 960–967 (2011).
274. Gissot, M. *et al.* Toxoplasma gondii Alba Proteins Are Involved in Translational Control of Gene Expression. *Journal of Molecular Biology* **425**, 1287–1301 (2013).
275. Joachimiak, L. A., Walzthoeni, T., Liu, C. W., Aebersold, R. & Frydman, J. The Structural Basis of Substrate Recognition by the Eukaryotic Chaperonin TRiC/CCT. *Cell* **159**, 1042–1055 (2014).
276. Brown, C. R., Hong-Brown, L. Q., Doxsey, S. J. & Welch, W. J. Molecular Chaperones and the Centrosome: A ROLE FOR HSP 73 IN CENTROSOMAL REPAIR FOLLOWING HEAT SHOCK TREATMENT. *J. Biol. Chem.* **271**, 833–840 (1996).
277. Brown, C. R., Doxsey, S. J., Hong-Brown, L. Q., Martin, R. L. & Welch, W. J. Molecular Chaperones and the Centrosome: A ROLE FOR TCP-1 IN MICROTUBULE NUCLEATION. *J. Biol. Chem.* **271**, 824–832 (1996).
278. Trinkle-Mulcahy, L. Recent advances in proximity-based labeling methods for interactome mapping. *F1000Res* **8**, 135 (2019).
279. Fox, B. A., Ristuccia, J. G., Gigley, J. P. & Bzik, D. J. Efficient Gene Replacements in Toxoplasma gondii Strains Deficient for Nonhomologous End Joining. *Eukaryotic Cell* **8**, 520–529 (2009).
280. Couvreur, G., Sadak, A., Fortier, B. & Dubremetz, J. F. Surface antigens of *Toxoplasma gondii*. *Parasitology* **97**, 1–10 (1988).
281. Rebay, I. & Fehon, R. G. Preparation of Insoluble GST Fusion Proteins. *Cold Spring Harbor Protocols* **2009**, pdb.prot4997-pdb.prot4997 (2009).

## REFERENCES

282. Säbel, C. E., Shepherd, J. L. & Siemann, S. A direct spectrophotometric method for the simultaneous determination of zinc and cobalt in metalloproteins using 4-(2-pyridylazo)resorcinol. *Analytical Biochemistry* **391**, 74–76 (2009).
283. Doxsey, S., Zimmerman, W. & Mikule, K. Centrosome control of the cell cycle. *Trends in Cell Biology* **15**, 303–311 (2005).
284. Andersen, J. S. *et al.* Proteomic characterization of the human centrosome by protein correlation profiling. *Nature* **426**, 570–574 (2003).
285. Foster, L. J. *et al.* A Mammalian Organelle Map by Protein Correlation Profiling. *Cell* **125**, 187–199 (2006).
286. Barylyuk, K. *et al.* Global mapping of protein subcellular location in apicomplexans: the parasite as we've never seen it before. *Access Microbiology* **1**, (2019).

# **ANNEXES**

***Annexe 1. List of identified IMC-related proteins in T. gondii***

ToxoDB gene identifier	Name	Localisation	Maternal IMC	Daughter IMC	Association with IMC alveoli	References
<b>IMC Sub-compartment Protein (ISPs)</b>						
TgGT1_260820	ISP1	Apical cap	Yes	Yes	Membrane (acylation)	Beck et al., 2010 <sup>127</sup>
TgGT1_237820	ISP2	Center	Yes	Yes	Membrane (acylation)	Beck et al., 2010
TgGT1_316540	ISP3	Center/base	Yes	Yes	Membrane (acylation)	Beck et al., 2010
TgGT1_205480	ISP4	Center	Yes	Yes	Membrane (acylation)	Fung et al., 2012 <sup>135</sup>
<b>Alveolins (IMC proteins)</b>						
TgME49_231640	IMC1	Center	Yes	Yes	Cytoskeletal	Mann et al., 2001 <sup>101</sup>
TgME49_216000	IMC3	Center	Yes	Yes	Cytoskeletal	Anderson-White et al., 2011 <sup>128</sup>
TgME49_231630	IMC4	Center	Yes	Yes	Cytoskeletal	Anderson-White et al., 2011
TgME49_224530	IMC5	Base	Yes	No	Cytoskeletal	Anderson-White et al., 2011
TgME49_220270	IMC6	Center	Yes	Yes	Cytoskeletal	Anderson-White et al., 2011
TgME49_222220	IMC 7	Center	Yes	No	Cytoskeletal	Anderson-White et al., 2011
TgME49_224520	IMC8	Base	Yes	No	Cytoskeletal	Anderson-White et al., 2011
TgME49_226220	IMC9	Base	Yes	No	Cytoskeletal	Anderson-White et al., 2011
TgME49_230210	IMC10	Center	Yes	Yes	Cytoskeletal	Anderson-White et al., 2011
TgME49_239770	IMC11	Apical cap/base	-	-	Cytoskeletal	Anderson-White et al., 2011
TGME49_248700	IMC12	Center	Yes	NO	Cytoskeletal	Anderson-White et al., 2011
TgME49_253470	IMC13	Base	Yes	No	Cytoskeletal	Anderson-White et al., 2011
TgME49_260540	IMC14	Center	Yes	No	Cytoskeletal	Anderson-White et al., 2011
TgME49_275670	IMC15	Integral	Yes	Yes	Cytoskeletal	Anderson-White et al., 2011
TgGT1_286580	IMC17	Center/base	Yes	No	Cytoskeletal	Chen et al., 2015 <sup>131</sup>
TgGT1_295360	IMC18	Center/base	Yes	No	Cytoskeletal	Chen et al., 2015
TgGT1_217510	IMC19	Center/base	Yes	Yes	Cytoskeletal	Chen et al., 2015
TgGT1_271930	IMC20	Center/base	Yes	No	Cytoskeletal	Chen et al., 2015
TgGT1_232030	IMC21	Center/base	Yes	No	Membrane	Chen et al., 2015
TgGT1_316340	IMC22	Center/base	Yes	No	Cytoskeletal	Chen et al., 2015
TgGT1_304670	IMC23	Center/base	Yes	Yes	Cytoskeletal	Chen et al., 2015
TgGT1_258470	IMC24	Center/base	Yes	No	Cytoskeletal	Chen et al., 2015
TgGT1_315750	IMC26	Center/base	Yes	-	-	Chen et al., 2017 <sup>132</sup>

## ANNEXES

ToxoDB gene identifier	Name	Localisation	Maternal IMC	Daughter IMC	Association with IMC alveoli	References
TgGT1_259630	IMC27	Center/base	Yes	-	-	Chen et al., 2017
TgGT1_239400	IMC28	Integral	Yes	-	-	Chen et al., 2017
TgGT1_243200	IMC29	-	No	Yes	-	Chen et al., 2017
<b>Apical cap proteins (ACs)</b>						
TgGT1_311480	AC1	Apical cap	Yes	Yes	Membrane	Chen et al., 2015
TgGT1_250820	AC2	Apical cap	Yes	Yes	Cytoskeletal	Chen et al., 2015
TgGT1_308860	AC3	Apical cap	Yes	Yes	Cytoskeletal	Chen et al., 2015
TgGT1_214880	AC4	Apical cap	Yes	Yes	Cytoskeletal	Chen et al., 2015
TgGT1_235380	AC5	Apical cap	Yes	Yes	Cytoskeletal	Chen et al., 2015
TgGT1_251850	AC6	Apical cap	Yes	Yes	Membrane	Chen et al., 2015
TgGT1_225690	AC7	Apical cap	Yes	Yes	Cytoskeletal	Chen et al., 2015
TgGT1_229640	AC8	Apical cap	Yes	-	-	Chen et al., 2017
TgGT1_246950	AC9	Apical cap	Yes	-	-	Chen et al., 2017
<b>Suture proteins (ISCs)</b>						
TgGT1_235340	ISC1	Transverse and longitudinal sutures	Yes	Yes	Cytoskeletal	Chen et al., 2015
TgGT1_219170	ISC2	Transverse and longitudinal sutures	Yes	Yes	Membrane	Chen et al., 2015
TgGT1_220930	ISC3	Transverse and longitudinal sutures	Yes	Yes	Membrane	Chen et al., 2015
TgGT1_305930	ISC4	Transverse and longitudinal sutures	Yes	Yes	Cytoskeletal	Chen et al., 2015
TgGT1_202930	ISC5	Transverse and longitudinal sutures	Yes	-	Cytoskeletal	Chen et al., 2017
TgGT1_267620	ISC6	Transverse and longitudinal sutures	Yes	-	Membrane	Chen et al., 2017
<b>Suture proteins (TSCs)</b>						
TgME49_267500	CBAP/SIP/TSC1	Transverse sutures	Yes	Yes	Cytoskeletal	Lentini et al., 2015 <sup>130</sup> , Tilley et al., 2014 <sup>129</sup>
TgGT1_239800	TSC2	Transverse sutures	Yes	-	Cytoskeletal	Chen et al., 2017

## ANNEXES

ToxoDB gene identifier	Name	Localisation	Maternal IMC	Daughter IMC	Association with IMC alveoli	References
TgGT1_230850	TSC3	Transverse sutures	Yes	-	Cytoskeletal	Chen et al., 2017
TgGT1_272520	TSC4	Transverse sutures	Yes	-	Cytoskeletal	Chen et al., 2017
TgGT1_232260	TSC5	Transverse sutures	Yes	-	Membrane	Chen et al., 2017
TgGT1_294340	TSC6	Transverse sutures	Yes	-	Membrane	Chen et al., 2017
<b>Glideosome Associated Proteins (GAPMs)</b>						
TgME49_202500	GAPM1a	Center	Yes	Yes	Integral alveoli membrane protein	Bullen et al., 2009 <sup>141</sup> ; Harding et al., 2019 <sup>142</sup>
TgME49_202510	GAPM1b	Center	Yes	-	Integral alveoli membrane protein	Bullen et al., 2009
TgME49_219270	GAPM2a	Center	Yes	-	Integral alveoli membrane protein	Bullen et al., 2009
TgME49_206690	GAPM2b	Center	Yes	-	Integral alveoli membrane protein	Bullen et al., 2009
TgME49_271970	GAPM3	Center	Yes	Yes	Integral alveoli membrane protein	Bullen et al., 2009
<b>Glideosome Proteins (GAPs)</b>						
TgME49_249850	GAP40	Integral	Yes	Yes	Integral alveoli membrane protein	Frénal et al., 2010 <sup>136</sup>
TgME49_219320	GAP50	Integral	Yes	Yes	Integral alveoli membrane protein	Gaskins at al., 2004 <sup>133</sup>
TgME49_223940	GAP45	Center	Yes	Yes	acylation	Gaskins at al., 2004
TgME49_233030	GAP70	Apical cap	Yes	No	acylation	Frénal et al., 2010 <sup>136</sup>
TgME49_246940	GAP80	Basis	Yes	Yes	acylation	Frénal et al., 2014 <sup>137</sup>

***Annexe 2. List of T. gondii proteins containing an annotated zinc finger motif***

Gene ID	Product Description	<i>T. gondii</i> RH CRISPR score
TGGT1_201200	zinc finger (CCCH type) motif-containing protein	-3.11
TGGT1_201220	zinc finger protein	-5.4
TGGT1_201250	putative histone lysine methyltransferase, SET	0.48
TGGT1_202490	AP2 domain transcription factor AP2VIIa-7	-2.76
TGGT1_202690	DNA-directed RNA polymerase II RPB9	-2.89
TGGT1_202840	FHA domain-containing protein	-3.54
TGGT1_202900	zinc finger (CCCH type) motif-containing protein	0.89
TGGT1_203320	zinc finger in N-recognin protein	-2.09
TGGT1_203510	zinc finger, C3HC4 type (RING finger) domain-containing protein	-0.46
TGGT1_203630	ribosomal protein RPL44+B11	-4.1
TGGT1_203830	FHA domain-containing protein	-0.44
TGGT1_204140	PHD-finger domain-containing protein	-4.89
TGGT1_205460	AN1 family Zinc finger domain-containing protein	1.61
TGGT1_205600	zinc finger, C3HC4 type (RING finger) domain-containing protein	-0.36
TGGT1_206330	PHD-finger domain-containing protein	-0.95
TGGT1_206650	zinc finger, c2h2 type domain-containing protein	0.56
TGGT1_207760	DnaJ C terminal region domain-containing protein	-3.41
TGGT1_207900	transcription initiation factor TFIIIB	-4.73
TGGT1_208200	PHD-finger domain-containing protein	-4.65
TGGT1_209260	putative cytochrome c oxidase subunit	-3.07
TGGT1_209770	putative helicase	-4.09
TGGT1_211670	S1 RNA binding domain-containing protein	0.72
TGGT1_212220	hypothetical protein	-4.91
TGGT1_212260	Sjogren's syndrome/scleroderma autoantigen 1 (Autoantigen p27) protein	-4.5
TGGT1_212840	HIT zinc finger protein	-4.75
TGGT1_213020	hypothetical protein	-1.31
TGGT1_213400	zinc finger (CCCH type) motif-containing protein	-0.94
TGGT1_213550	DHHC zinc finger domain-containing protein	-0.5
TGGT1_213660	zinc finger (CCCH type) motif-containing protein	0.32
TGGT1_213690	ring box protein 1 family protein	-4.21
TGGT1_213870	UBA/TS-N domain-containing protein	-4.83
TGGT1_213900	regulator of chromosome condensation RCC1	-5.48
TGGT1_215390	putative TIM10 family protein	-1.92
TGGT1_215440	WWE domain-containing protein	1.43
TGGT1_215640	zinc finger, C3HC4 type (RING finger) domain-containing protein	-3.46
TGGT1_216490	hypothetical protein	-0.86
TGGT1_216840	hypothetical protein	-0.55
TGGT1_217050	ADA2-A transcriptional co-activator SAGA component	-4.55
TGGT1_217220	zinc finger, C3HC4 type (RING finger) domain-containing protein	-4.34
TGGT1_217570	TgMPS1/ribosomal protein RPS27	-3
TGGT1_217870	DHHC zinc finger domain-containing protein	0.47
TGGT1_218300	zinc finger (CCCH type) motif-containing protein	1.21

## ANNEXES

Gene ID	Product Description	<i>T. gondii</i> RH CRISPR score
TGGT1_218358	TgZFP1, zinc knuckle domain-containing protein	-2.35
TGGT1_218362	zinc finger protein	1.83
TGGT1_218570	Nin one binding (NOB1) Zn-ribbon family protein	-4.79
TGGT1_218930	BTB/POZ domain-containing protein	0.71
TGGT1_219120	zinc finger (CCCH type) motif-containing protein	2.32
TGGT1_219150	zinc finger, zz type domain-containing protein	-4.1
TGGT1_219300	ran binding protein	0.11
TGGT1_219640	hypothetical protein	-0.83
TGGT1_219670	zinc finger (CCCH type) motif-containing protein	0.63
TGGT1_220570	hypothetical protein	0.68
TGGT1_221200A	CW-type Zinc Finger protein	-1.34
TGGT1_221910	AN1 family Zinc finger domain-containing protein	-2.38
TGGT1_221950	putative spliceosome-associated protein	-6
TGGT1_221980	U1 zinc finger protein	-2.25
TGGT1_223130	hypothetical protein	-1.72
TGGT1_223570	hypothetical protein	-3.13
TGGT1_223668	LYAR-type C2HC zinc finger protein	0.52
TGGT1_223880	zinc finger, C3HC4 type (RING finger) domain-containing protein	-2.25
TGGT1_224260	PHD-finger domain-containing protein	-5.13
TGGT1_224290	DHHC zinc finger domain-containing protein	-3.68
TGGT1_224310	DHHC zinc finger domain-containing protein	-0.02
TGGT1_224630	zinc finger (CCCH type) motif-containing protein	1.07
TGGT1_224900	putative adenylate kinase	-4.02
TGGT1_225310	putative ARF1-directed GTPase-activating protein	0.89
TGGT1_225890	hypothetical protein	-4.63
TGGT1_226050	hypothetical protein	0.13
TGGT1_226240	putative bud site selection protein	-3.33
TGGT1_226310	zinc finger (CCCH type) motif-containing protein	1.1
TGGT1_226440	SWI2/SNF2-containing protein RAD16	-0.56
TGGT1_226510	Sec23/Sec24 trunk domain-containing protein	-4.28
TGGT1_226560	zinc finger (CCCH type) motif-containing protein	-4.2
TGGT1_226640	putative zinc binding protein	-0.35
TGGT1_226740	zinc finger, C3HC4 type (RING finger) domain-containing protein	1.4
TGGT1_226780	zinc finger, C3HC4 type (RING finger) domain-containing protein	-0.15
TGGT1_226810	histone lysine methyltransferase SET1	-3.7
TGGT1_227020	histone deacetylase SIR2	0.87
TGGT1_227870	Tim10/DDP family zinc finger superfamily protein	-1.38
TGGT1_228000	putative splicing factor 3A subunit 2	-3.87
TGGT1_228070	hypothetical protein	-4.21
TGGT1_228080	dihydrouridine synthase (dus) protein	0.26
TGGT1_228220	MYND finger domain-containing protein	0.81
TGGT1_228670	hypothetical protein	-2.85
TGGT1_228990	zinc finger (CCCH type) motif-containing protein	0.99
TGGT1_229160	DHHC zinc finger domain-containing protein	-1.38

## ANNEXES

Gene ID	Product Description	<i>T. gondii</i> RH CRISPR score
TGGT1_229440	zinc finger, C3HC4 type (RING finger) domain-containing protein	0.07
TGGT1_230440	CHY zinc finger domain-containing protein	-2.49
TGGT1_230890	PHD-finger domain-containing protein	-5.53
TGGT1_231010	general transcription factor IIE polypeptide 1 GTF2E1	-3.5
TGGT1_231930	hypothetical protein	-1.24
TGGT1_232160	zinc finger, C3HC4 type (RING finger) domain-containing protein	-1.52
TGGT1_232240	hypothetical protein	-5.42
TGGT1_232370	CW-type Zinc Finger protein	-0.62
TGGT1_232510	hypothetical protein	-1.38
TGGT1_233920	zinc finger, C3HC4 type (RING finger) domain-containing protein	0.09
TGGT1_234460	hypothetical protein	1.16
TGGT1_234900	PHD-finger domain-containing protein	-4.45
TGGT1_235540	putative eukaryotic initiation factor-2 beta	-5.6
TGGT1_235550	PHD-finger domain-containing protein	-0.61
TGGT1_235980	ARIADNE family protein	0.49
TGGT1_236270	hypothetical protein	-0.72
TGGT1_236640	zinc finger, C3HC4 type (RING finger) domain-containing protein	0.61
TGGT1_236780	zinc finger, C3HC4 type (RING finger) domain-containing protein	-0.67
TGGT1_236840	putative zinc finger (C-x8-C-x5-C-x3-H)-2	-3.3
TGGT1_236850	hypothetical protein	-1.7
TGGT1_236910	putative U2 snRNP auxiliary factor	-3.26
TGGT1_236970	SWI2/SNF2-containing PHD finger protein	-1.93
TGGT1_237870	FYVE zinc finger domain-containing protein	-1.4
TGGT1_238080	hypothetical protein	-4.42
TGGT1_238510	hypothetical protein	-4.38
TGGT1_239070	hypothetical protein	-0.59
TGGT1_239250	putative diacylglycerol kinase	-2.74
TGGT1_239330	ribosomal protein RPL37	-4.25
TGGT1_239410	hypothetical protein	-3.68
TGGT1_240300	zinc finger domain, LSD1 subclass domain-containing protein	-0.55
TGGT1_242090	zinc finger (CCCH type) motif-containing protein	-0.36
TGGT1_242320	B-box zinc finger domain-containing protein	-3.14
TGGT1_242415	histone lysine-specific demethylase	-2.58
TGGT1_244120	hypothetical protein	-0.72
TGGT1_244610	zinc finger, C3HC4 type (RING finger) domain-containing protein	-0.89
TGGT1_244650	putative eukaryotic initiation factor-5	-4.08
TGGT1_244840	zinc knuckle domain-containing protein	-3.58
TGGT1_244910	MIZ/SP-RING zinc finger domain-containing protein	1.64
TGGT1_245620	ribosomal-ubiquitin protein RPS27A	-4.61
TGGT1_245660	hypothetical protein	-2.59
TGGT1_246160	hypothetical protein	-1.2
TGGT1_246200	zinc finger (CCCH type) motif-containing protein	-1.04
TGGT1_246220	hypothetical protein	0.29
TGGT1_246650	DHHC zinc finger domain-containing protein	-0.07

## ANNEXES

Gene ID	Product Description	<i>T. gondii</i> RH CRISPR score
TGGT1_247450	hypothetical protein	-3.03
TGGT1_247485	zinc finger, C3HC4 type (RING finger) domain-containing protein	-3.05
TGGT1_247652	hypothetical protein	-0.73
TGGT1_248270	zinc finger (CCCH type) motif-containing protein	0.28
TGGT1_248330	zinc finger, C3HC4 type (RING finger) domain-containing protein	0.73
TGGT1_248450	zinc finger, C3HC4 type (RING finger) domain-containing protein	0.28
TGGT1_248850	methionine aminopeptidase	-3.81
TGGT1_248940	hypothetical protein	2.18
TGGT1_249380	DHHC zinc finger domain-containing protein	-0.22
TGGT1_249410	hypothetical protein	1.54
TGGT1_250060	DNA-directed RNA polymerase I RPA12	-3.75
TGGT1_250690	zinc finger (CCCH type) motif-containing protein	-1.4
TGGT1_250780	Zn-finger in ubiquitin-hydrolases domain-containing protein	-2.58
TGGT1_250870	DHHC zinc finger domain-containing protein	1.55
TGGT1_252200	cell cycle regulator with zn-finger domain-containing protein	-4.09
TGGT1_252400	HIT zinc finger protein	-4.14
TGGT1_252420	histone arginine methyltransferase PRMT3	-0.53
TGGT1_253650	DnaJ C terminal region domain-containing protein	0.44
TGGT1_253790	zinc finger (CCCH type) motif-containing protein	0.34
TGGT1_253850	hypothetical protein	-2.46
TGGT1_254030	zinc finger CDGSH-type domain-containing protein	-4.26
TGGT1_254140	DNA-directed RNA polymerase II RPABC4	-4.69
TGGT1_254610	Tim10/DDP family zinc finger superfamily protein	0.1
TGGT1_254650	zinc finger protein	-3.31
TGGT1_255310	zinc finger (CCCH type) motif-containing protein	0.7
TGGT1_255650	DHHC zinc finger domain-containing protein	0.26
TGGT1_255740	hypothetical protein	-4.47
TGGT1_255910	putative PfmNL-2 CISD1 family iron-sulfur protein	1.64
TGGT1_255940	hypothetical protein	-2.38
TGGT1_256820	zinc finger (CCCH type) motif-containing protein	-4.96
TGGT1_256960	FYVE zinc finger domain-containing protein	-3.32
TGGT1_257070	hypothetical protein	-3.79
TGGT1_257130	zinc finger (CCCH type) motif-containing protein	0.79
TGGT1_257770	histone lysine methyltransferase SET2	-3.33
TGGT1_258030	DNA polymerase	-4.45
TGGT1_258790	zinc finger, C3HC4 type (RING finger) domain-containing protein	-3.52
TGGT1_259250	ATP-dependent DNA helicase, RecQ family protein	-1.46
TGGT1_259650	hypothetical protein	-1.59
TGGT1_259965	putative Bardet-Biedl syndrome 5	0.41
TGGT1_260340	DNL zinc finger protein	-0.36
TGGT1_260410	hypothetical protein	-3.85
TGGT1_260850	putative mitochondrial import inner membrane translocase subunit TIM10	0.97
TGGT1_260870	zinc finger cdgsh type protein	0.92

## ANNEXES

Gene ID	Product Description	<i>T. gondii</i> RH CRISPR score
TGGT1_261220	transcription elongation factor SPT4	-4.78
TGGT1_261960	hypothetical protein	-4.39
TGGT1_261990	zinc finger, C3HC4 type (RING finger) domain-containing protein	-1.3
TGGT1_262420	AP2 domain transcription factor APVIIb-1/ADA2-B	-0.05
TGGT1_262740	hypothetical protein	1.08
TGGT1_262970	hypothetical protein	1.7
TGGT1_263010	hypothetical protein	1.04
TGGT1_263020	putative 50S ribosomal protein L33	-0.24
TGGT1_263085	hypothetical protein	1.56
TGGT1_264840	ATP-dependent DNA helicase, RecQ family protein	-1.11
TGGT1_264860	zinc finger, C3HC4 type (RING finger) domain-containing protein	-2.12
TGGT1_265320	hypothetical protein	2.34
TGGT1_265380	tetratricopeptide repeat (TPR)-/ U-box domain-containing protein	0.77
TGGT1_266785	zinc finger (CCCH type) motif-containing protein	0.96
TGGT1_266860	BTB/POZ domain-containing protein	0.77
TGGT1_266940	DHHC zinc finger domain-containing protein	-0.38
TGGT1_267440	RING zinc finger protein	-0.35
TGGT1_267520	putative anaphase promoting complex subunit 11	-1.75
TGGT1_268570	zinc finger (CCCH type) motif-containing protein	-4.23
TGGT1_268900	dense granular protein GRA10	-4.56
TGGT1_268940	hypothetical protein	0.96
TGGT1_269150	DHHC zinc finger domain-containing protein	0.66
TGGT1_269310	hypothetical protein	-1.07
TGGT1_269420	hypothetical protein	0.36
TGGT1_269740	R3H domain-containing protein	-0.97
TGGT1_269910	putative transcription factor C2H2	1.87
TGGT1_269940	zinc finger motif, C2HC5-type protein	-2.28
TGGT1_270300	hypothetical protein	0.78
TGGT1_270340	BTB/POZ domain-containing protein	0.05
TGGT1_270540	Trm112p family domain-containing protein	-4.71
TGGT1_270840	poly(ADP-ribose) polymerase catalytic domain-containing protein	0.1
TGGT1_271315	hypothetical protein	1.47
TGGT1_271440	NPL4 family protein	-4.16
TGGT1_271740	hypothetical protein	0.36
TGGT1_271880	B-box zinc finger domain-containing protein	-0.3
TGGT1_272320	DHHC zinc finger domain-containing protein	-0.83
TGGT1_273070	putative GTPase activating protein for adp ribosylation factor	-3.81
TGGT1_273150	zinc finger, C3HC4 type (RING finger) domain-containing protein	-2.1
TGGT1_273780	SWI2/SNF2-containing protein	-0.76
TGGT1_274090	hypothetical protein	1.88
TGGT1_274140	hypothetical protein	0.22
TGGT1_275310	hypothetical protein	-3.21

## ANNEXES

Gene ID	Product Description	<i>T. gondii</i> RH CRISPR score
TGGT1_275420	histone lysine-specific demethylase	-2.47
TGGT1_276120	putative histone lysine methyltransferase, SET	-0.38
TGGT1_277000	putative transport protein Sec24	-4.58
TGGT1_277530	DNA topoisomerase domain-containing protein	-2.24
TGGT1_277740	zinc finger, C3HC4 type (RING finger) domain-containing protein	-2.11
TGGT1_277770	hypothetical protein	-0.82
TGGT1_278240	Zn-finger in Ran binding protein and others domain-containing protein	-1.17
TGGT1_278490	Zn-finger, RING domain containing protein	-0.01
TGGT1_278640	MIZ/SP-RING zinc finger domain-containing protein	-0.71
TGGT1_278850	DHHC zinc finger domain-containing protein	-4.36
TGGT1_280435	hypothetical protein	1.33
TGGT1_280490	U-box domain-containing protein	-2.72
TGGT1_281520	zinc finger, C3HC4 type (RING finger) domain-containing protein	-0.02
TGGT1_283840	GATA zinc finger domain-containing protein	-4.72
TGGT1_284170	DHHC zinc finger domain-containing protein	-1.02
TGGT1_284630	hypothetical protein	0.48
TGGT1_285190	zinc finger, C3HC4 type (RING finger) domain-containing protein	1.09
TGGT1_285810	MYND finger domain-containing protein	-0.17
TGGT1_286240	putative kelch repeat protein	0.28
TGGT1_286690	DNA/RNA-binding protein KIN17 domain-containing protein	-4.14
TGGT1_286710	TgZFN2, zinc finger, c2h2 type domain-containing protein	-1.94
TGGT1_287980	FHA domain-containing protein	-3.15
TGGT1_289750	ribosomal-ubiquitin protein RPL40	-4.59
TGGT1_291000	PHD-finger domain-containing protein	-1.34
TGGT1_291030	zinc finger, C3HC4 type (RING finger) domain-containing protein	0.03
TGGT1_291150	hypothetical protein	0
TGGT1_291590	hypothetical protein	-0.13
TGGT1_291680	Sec23/Sec24 trunk domain-containing protein	-5.46
TGGT1_292010	transcription initiation factor IIB	-4.82
TGGT1_292160	hypothetical protein	-4.06
TGGT1_292235	hypothetical protein	-1.79
TGGT1_292340	zinc finger, C3HC4 type (RING finger) domain-containing protein	0.75
TGGT1_293220	DHHC zinc finger domain-containing protein	-2.06
TGGT1_293510	poly(ADP-ribose) polymerase and DNA-Ligase Zn-finger region domain-containing protein	1.42
TGGT1_293630	hypothetical protein	-6.17
TGGT1_293670	transcription elongation factor A TFIIS	-5.68
TGGT1_293710	Zn-finger in Ran binding protein and others domain-containing protein	0.06
TGGT1_293730	DHHC zinc finger domain-containing protein	-3.21
TGGT1_294020	zinc finger, C3HC4 type (RING finger) domain-containing protein	-2.09
TGGT1_294220	hypothetical protein	0.25
TGGT1_294360	putative ubiquitin specific protease 39 isoform 2	-4.82
TGGT1_294380	PP-loop domain-containing protein	-1.11

## ANNEXES

Gene ID	Product Description	<i>T. gondii</i> RH CRISPR score
TGGT1_294720	hypothetical protein	-0.93
TGGT1_294785	zinc finger (CCCH type) motif-containing protein	0.86
TGGT1_294840	zinc finger (CCCH type) motif-containing protein	0.69
TGGT1_295620	hypothetical protein	-2.26
TGGT1_295658	zinc finger in N-recognin protein	-1.25
TGGT1_297730	putative transcription elongation factor 1	-0.49
TGGT1_298600	leucine zipper-like transcriptional regulator	0.57
TGGT1_299190	B-box zinc finger domain-containing protein	-2.58
TGGT1_300190	ribosomal protein RPL37A	-4.82
TGGT1_301340	DnaJ domain-containing protein	-2.96
TGGT1_301370	DHHC zinc finger domain-containing protein	0.69
TGGT1_304460	zinc finger, C3HC4 type (RING finger) domain-containing protein	-4.44
TGGT1_304720	hypothetical protein	-4.99
TGGT1_304750	zinc finger, C3HC4 type (RING finger) domain-containing protein	0.33
TGGT1_305760	hypothetical protein	-1.63
TGGT1_305780	putative 5'-3' exoribonuclease	-5.1
TGGT1_305940	peptidyl-prolyl cis-trans isomerase, cyclophilin-type domain-containing protein	-4.26
TGGT1_306040	CHY zinc finger protein	0.85
TGGT1_306080	ATP-dependent DNA helicase, RecQ family protein	-0.52
TGGT1_306380	U1 zinc finger protein	-0.91
TGGT1_306400	hypothetical protein	0.51
TGGT1_306510	hypothetical protein	0.89
TGGT1_308040	ZPR1 zinc finger domain-containing protein	-4.58
TGGT1_308870	hypothetical protein	-1.73
TGGT1_308930	putative 50S ribosomal protein L33	-1.69
TGGT1_309200	zinc finger (CCCH type) motif-containing protein	0.41
TGGT1_309220	GTPase activating protein for Arf protein	-4.23
TGGT1_309280	zinc finger, C3HC4 type (RING finger) domain-containing protein	-1.9
TGGT1_310530	SNF2 family N-terminal domain-containing protein	-1.68
TGGT1_310820	putative SLU7 splicing factor	-0.29
TGGT1_310850	MYND finger domain-containing protein	-2.81
TGGT1_311100	zinc finger (CCCH type) motif-containing protein	2.38
TGGT1_311240	putative DnaJ family chaperone	-3.96
TGGT1_311250	hypothetical protein	-2.04
TGGT1_311450	zinc finger, c2h2 type domain-containing protein	-4.64
TGGT1_311625	WD domain, G-beta repeat-containing protein	-3.31
TGGT1_312250	DNA-directed RNA polymerase III RPC11	-0.9
TGGT1_312520	tRNA dimethylallyltransferase	-0.48
TGGT1_313740	zinc finger (CCCH type) motif-containing protein	1.11
TGGT1_313760	hypothetical protein	0.24
TGGT1_313870	zinc finger, C3HC4 type (RING finger) domain-containing protein	-3.33
TGGT1_314860	zinc knuckle domain-containing protein	-1.53
TGGT1_315950	zinc finger, C3HC4 type (RING finger) domain-containing protein	-1.1

## ANNEXES

Gene ID	Product Description	<i>T. gondii</i> RH CRISPR score
TGGT1_316510	hypothetical protein	-1.05
TGGT1_318450	zinc finger, C3HC4 type (RING finger) domain-containing protein	0.96
TGGT1_318480	SWI2/SNF2-containing protein RAD5	-0.12
TGGT1_319730	YOU2 family C2C2 zinc finger protein	0.02
TGGT1_320070	CDK-activating kinase assembly factor MAT1 protein	-4.21
TGGT1_321310	16S rRNA processing protein RimM domain-containing protein	-1.46
TGGT1_321560	zinc knuckle domain-containing protein	-3.33
TGGT1_362290	hypothetical protein	1.85
TGGT1_410770	histone deacetylase SIR2-like protein	-3.05

***Annexe 3. List of oligonucleotides used in TgZFP2 characterisation study***

Primer name	Sequence	Application
ML841	ATGTTCCGTGGTCGCATGT	RT PCT Tubulin Fwd
ML842	TTCATGTTGTTGGGAATCCAC	RT PCR Tubulin Rev
ML1923	TACTTCCAATCCAATTTAATGCGAGTCACGCGGCGATGCACTC	LIC TgZFP2 3xHA tag Fwd
ML1924	TCCTCCACTTCCAATTTTAGCCGACAGCGCGTCCAGAGTTTC	LIC TgZFP2 3xHA tag Rev
ML2377	AACAGATCTATGAGTGGCCTCTCGTCT	cKD TgZFP2 Fwd
ML2378	TTAGCGGCCGCTTTTCCGACGGCTGGTTC	cKD TgZFP2 Rev
ML2379	CGCTTAACGGACTCAGTTCT	integr cKD TgZFP2 Fwd
ML2380	ACGCTTTGTCTCTCTCTTCG	integr cKD TgZFP2 Rev
ML2628	TTAAGGCCTATGAGTGGCCTCTCGTCTG	cDNA TgZFP2 Fwd
ML2629	AAACCCGGGTCACGACAGCGGTCCAGAG	cDNA TgZFP2 Rev
ML2630	TTAGCGGCCGCGGGAAAACGGAAAAAATGCAGATCG	TgZFP2 promoter Fwd
ML2631	AAAAGGCCTTTTTTCGGTGACGGTGACAGC	TgZFP2 promoter Rev
ML2821	CACAGCAGCTTTTCgGCGTCGCCgGTCAAACCTTTTTGC	Zn finger mutation Fwd
ML2822	GCAAAAAGGTTTGACCGGCGACGCCGAAAAGCTGCTGTG	Zn finger mutation Rev
ML2877	AATCATCTGAGCGAGCTGTC	RT PCR TgZFP2 Fwd
ML2878	TTGAACCGTGTGCATGGTG	RT PCR TgZFP2 Rev
ML4165	TACTTCCAATCCAATTTAATGCTGGGGACGCTCGACCGCAGC	LIC TgCEP250-L1 myc tag Fwd
ML4166	TCCTCCACTTCCAATTTAGCTCGCCCCGAAAGCGACGAC	LIC TgCEP250-L1 myc tag Rev

***Annexe 4. List of oligonucleotides used in study of TgZFP2 potential binding partners***

Primer name	Sequence	Application
ML2933	TACTTCCAATCCAATTTAATGCCTCAGAATCTGTTGGTAGATTC	LIC TgGSK 3xmyc tag Fwd
ML2934	TCCTCCACTTCCAATTTTAGCGCCACGGTTGTTGCACTGGC	LIC TgGSK 3xmyc tag Rev
ML2949	TACTTCCAATCCAATTTAATGCAGAACGCGTCATGGAAGTGC	LIC TgCyclin2 3xmyc tag Fwd
ML2938	TCCTCCACTTCCAATTTTAGCCGAGCACGGACCGAAGGAG	LIC TgCyclin2 3xmyc tag Rev
ML2989	TACTTCCAATCCAATTTAATGCGAAGAAGTTTACGAGGAGCGC	LIC TgCCT1 3xmyc tag Fwd
ML2990	TCCTCCACTTCCAATTTTAGCGTCATCCTGTTGGCCCCGTTT	LIC TgCCT1 3xmyc tag Rev
ML2991	TACTTCCAATCCAATTTAATGCTACGTAATATCGTAGCTTTTTG	LIC TgCCT2 3xmyc tag Fwd
ML2992	TCCTCCACTTCCAATTTTAGCCATTCCTGATCTCTCACGAG	LIC TgCCT2 3xmyc tag Rev
ML2993	TACTTCCAATCCAATTTAATGCACATGTTTGGATCCCTCAGC	LIC TgCCT5 3xmyc tag Fwd
ML2994	TCCTCCACTTCCAATTTTAGCCTGGTAGTCATTTGGCGCAATG	LIC TgCCT5 3xmyc tag Rev
ML3092	GCCAAGCTTATGAGTGGCCTCTCGTC	BACTH TgZFP2 Fwd
ML3093	CGGGGATCCCTCGACAACGCGTCCAGAG	BACTH TgZFP2 Rev
ML3094	GCCAAGCTTATGGCACTCGCAATCTTC	BACTH TgCCT1 Fwd
ML3095	TTTGGATCCATGTCATCCTGTTGGCCCCG	BACTH TgCCT1 Rev
ML3096	GCCAAGCTTATGATCTCCGAAGGTGG	BACTH TgCCT2 Fwd
ML3097	CAAGGATCCCTCATTCTGATCTCTCACG	BACTH TgCCT2 Rev
ML3098	GCCAAGCTTATGAATATCGCGACTGAC	BACTH TgCCT5 Fwd
ML3099	TTCGGATCCCTCTGGTAGTCATTTGGCGC	BACTH TgCCT5 Rev

## Summary

The phylum Apicomplexa encompasses parasitic protists with a complex life cycle that alternates between sexual and asexual replication in different hosts. Apicomplexa are obligate intracellular parasites that display a peculiar organisation of their cell cycle. It consists of a nuclear phase (DNA replication) and a budding phase (daughter cells assembly) that can be uncoupled or coordinated differently, resulting in four distinctive modes of division in the phylum. The simplest of them, endodyogeny, is characteristic for the rapidly proliferating tachyzoite asexual stage of *Toxoplasma gondii* and comprises a single round of DNA replication and subsequent formation of two daughter cells within the mother cell. The regulatory system of endodyogeny is suggested to be physically linked to the parasite's unusual bipartite centrosome, but remains largely unexplored. During this research project I characterized a novel *T. gondii* zinc finger protein named TgZFP2, whose knockdown led to a striking arrest of the parasite cell cycle. While DNA replication proceeded as normally, the budding was affected, resulting in appearance of immature daughters that failed to emerge from the mother cell and often failed to incorporate nuclear material. We have shown that, at the onset of daughter cells assembly, TgZFP2 re-localises from cytoplasmic puncta to the peri-centrosomal region where it persists until the completion of division. TgZFP2 also behaves as a cytoskeleton-associated protein. Though we were unable to identify TgZFP2 molecular partners to decipher the precise molecular mechanisms it is involved in, our data show TgZFP2 is an important regulator of the cell cycle that may have a pleiotropic function.

**Key words:** Apicomplexa, cell division, centrosome, *Toxoplasma gondii*, zinc finger protein

## Résumé

Le phylum des Apicomplexes regroupe des parasites protozoaires avec un cycle de vie complexe alternant des réplifications sexuée et asexuée chez différents hôtes. Ce sont des parasites intracellulaires obligatoires qui ont une l'organisation particulière de leur cycle cellulaire. Celui-ci consiste en une phase nucléaire (la réplication de l'ADN) et en une phase de bourgeonnement (l'assemblage des cellules filles) qui peuvent être découplées ou coordonnées différemment, générant quatre modes de division distincts au sein du phylum. Le plus simple d'entre eux, l'endodyogénie, est caractéristique de la forme tachyzoite de *Toxoplasma gondii*, un stade asexué et fortement prolifératif. Lors de ce type de division, il y a un seul tour de réplication de l'ADN avec une formation ultérieure de deux cellules filles dans la cellule mère. Le système de régulation de l'endodyogénie est physiquement lié à un centrosome atypique biparti, cependant il reste largement inexploré. Lors de ce projet de recherche, j'ai caractérisé chez *T. gondii* une nouvelle protéine à motif en doigt de zinc appelée TgZFP2. Interférer avec sa fonction résulte en l'arrêt du cycle cellulaire du parasite. Bien que la réplication de l'ADN se déroule normalement, le bourgeonnement des cellules filles est impacté, donnant naissance à des cellules filles immatures qui ne peuvent pas émerger de la cellule mère et ne parviennent souvent pas à incorporer le matériel nucléaire. Nous avons montré qu'au début de l'assemblage des cellules filles, la protéine TgZFP2 se re-localise depuis des puncta cytoplasmiques vers la région péri-centrosomale, où elle persiste jusqu'à l'achèvement de la division et l'émergence des cellules filles. TgZFP2 présente également des propriétés de protéine associée au cytosquelette. Bien que nous n'ayons pas été en mesure d'identifier les partenaires moléculaires de TgZFP2 pour identifier les mécanismes moléculaires dans lesquels elle est impliquée, nos données montrent que TgZFP2 est un régulateur important de la division cellulaire, potentiellement avec des fonctions multiples.

**Mots-clés:** Apicomplexes, division cellulaire, centrosome, *Toxoplasma gondii*, protéine à doigt de zinc